UNIVERSITÉ LIBRE DE BRUXELLES

DEPARTMENT OF PHYSICS
Mathematical Physics of Fundamental Interactions

DOCTORAL THESIS

Applications of space-time symmetries to black holes and gravitational radiation

Author
Roberto OLIVERI

Supervisor
Prof. Geoffrey COMPÈRE

A thesis submitted in partial fulfilment of the requirements for the degree of Doctor of Philosophy

Declaration of Authorship

I, Roberto OLIVERI, declare that this thesis titled "Applications of space-time symmetries to black holes and gravitational radiation" and the work presented in it are the result of my own work and of the scientific collaborations listed below, except where specific reference is made to the work of others. This thesis is based on the following research papers published in peer reviewed journals and listed in chronological order. They are the outcome of research conducted at Université Libre de Bruxelles, Belgium, between October 2014 and September 2018, and financially supported by the ERC Starting Grant 335146 "HoloBHC".

- Compère and Oliveri (2016),
  Near-horizon extreme Kerr magnetospheres
  Phys. Rev. D93 (2016) no. 2, 024035;

- Astorino, Compère, Oliveri, and Vandevoorde (2016),
  Mass of Kerr-Newman black holes in an external magnetic field
  Phys. Rev. D94 (2016) no. 2, 024019;

- Compère and Oliveri (2017),
  Self-similar accretion in thin discs around near-extremal black holes
  Mon. Not. Roy. Astron. Soc. 468 (2017) no. 4, 4351-4361;

- Compère, Oliveri, and Seraj (2018),
  Gravitational multipole moments from Noether charges
  J. High Energ. Phys. (2018) 2018: 54.

During the course of my doctoral studies, I also worked on the following paper:

- de Cesare, Oliveri, and van Holten (2017),
  Field theoretical approach to gravitational waves
  Fortsch. Phys. 65 (2017) no. 5, 1700012.

However, it is beyond the scope of this thesis and will not be discussed here.

This thesis was defended behind closed doors on the 3rd of August 2018, and publicly on the 31st of August 2018, at Université Libre de Bruxelles (ULB) in front of the following jury:

President: Prof. Marc Henneaux (ULB)
Secretary: Prof. Riccardo Argurio (ULB)
Supervisor: Prof. Geoffrey Compère (ULB)

Prof. Vitor Cardoso
Instituto Superior Técnico, Universidade de Lisboa
Perimeter Institute for Theoretical Physics
Prof. Constantinos Skordis
CEICO, Institute of Physics of the Czech Academy of Sciences
University of Cyprus
Prof. Jan-Willem van Holten
Nikhef
Lorentz Institute, Leiden University

"*We live on an island surrounded by a sea of ignorance.*
As our island of knowledge grows, so does the shore of our ignorance."

John Archibald Wheeler

UNIVERSITÉ LIBRE DE BRUXELLES

Faculty of Sciences
Department of Physics

Abstract

Applications of space-time symmetries to black holes and gravitational radiation

by Roberto OLIVERI

This thesis deals with two classes of space-time symmetries: emergent symmetries in the near-horizon region of rapidly rotating Kerr black holes and residual gauge symmetries. The main aim of the thesis is to investigate consequences and effects of these symmetries on black holes and gravitational radiation.

The first class of symmetries is exploited to address questions of astrophysical relevance for force-free magnetospheres, thin accretion discs, and strong magnetic fields around Kerr black holes. We investigate how the dynamics of electromagnetic and matter fields is constrained by global conformal symmetries of the near-horizon geometry. In the context of force-free electrodynamics, we find exact solutions and classify them according to the highest weight representation of the isometry group. We introduce novel criteria to distinguish physical solutions and deduce bounds on conformal weights of electromagnetic fields. For thin accretion discs, within the Novikov-Thorne model, new properties arise in the high spin regime of the Kerr black hole. We find a novel self-similar solution and we explain the critical behaviour of the observables by symmetry arguments. Afterwards, we study an exact analytic solution to the Einstein-Maxwell theory. It describes a black hole immersed in a strong magnetic field and it shares the same near-horizon geometry of extreme Kerr black holes. We compute its total conserved mass by means of the covariant phase space formalism and study its thermodynamics.

The second class of symmetries is considered in order to provide a new definition of gravitational multipole moments by means of Noether charges and by adopting the covariant phase space formalism. We show that such a definition in terms of Noether charges reproduces multipole moments in General Relativity. We propose to apply it to an arbitrary generally covariant metric theory of gravity.

Acknowledgements

I would like to express my sincere gratitude to my advisor, Geoffrey, for his constant and everyday guidance during my doctoral studies, for his technical advice during our collaborations, for transmitting me his passion in the scientific research and for teaching me how to be a researcher with his example. Thanks!

I also would like to thank my collaborators: Marco Astorino, Marco de Cesare, Ali Seraj, Jan-Willem van Holten, and Noé Vandevoorde. It has been a pleasure to work with all of you and share common research interests.

I thank the members of my Ph.D. jury for useful comments and interesting remarks on the thesis.

I am also grateful to Marek Abramowicz, Jiri Bicak, Luc Blanchet, Robert Beig, Marco Celoria, Horng Sheng Chia, Heino Falcke, Norman Guerlebeck, Filip Hejda, Edoardo Lauria, Alex Lupsasca, Achilleas Porfyriadis, Marco Scalisi, Alberto Sesana, Yichen Shi. I deeply benefitted from discussions with all of you.

I will have a great memory of these four years in Brussels thanks to my colleagues and friends at ULB/VUB. A special mention also goes to my friends in Munich and to the MCC group. I cannot forget my old friends in Sicily: going back home is always wonderful with you guys.

I am indebted to Avgustina V., Fabrizio F., Marco d.C., Marco S., Stefano D. for their careful reading of the thesis and for having spotted many typos.

Thanks to Silvana for her hospitality during the first weeks in Brussels and for never-ending discussions about Italian politics. I also thank De Bilio family for its kindness during my stay in Brussels. My thoughts go to Silvia for having been at my side for a significant part of this journey.

Finally, I am thankful to my family for supporting me every day wherever I am.

Contents

Introduction and main results

This thesis aims to address the following questions:

- *What is the behaviour of accreting matter and electromagnetic fields close to the horizon of rapidly rotating Kerr black holes?*
- *How to exploit the emergent global conformal symmetries in the near-horizon region of extreme Kerr black holes to address questions of astrophysical relevance?*
- *How to exploit large gauge transformations to compute multipole moments in theories of gravity?*

The motivation to pursue answers to these research questions is not only strongly supported by theoretical reasons but also motivated by ongoing and upcoming experimental missions. Continuous efforts to improve the accuracy of astrophysical observations, both in the electromagnetic and gravitational-wave spectrum, are underway by the scientific community. It is worth mentioning, among many others, the Event Horizon Telescope (EHT), GRAVITY, the Advanced Telescope for High ENergy Astrophysics (ATHENA), the Fermi Gamma-ray Space Telescope, the Square Kilometre Array (SKA), the LIGO/Virgo and LISA collaborations. Special attention is paid to the supermassive black hole at the centre of our galaxy, Sagittarius A* (see, *e.g.*, Broderick and Loeb, 2006; Doeleman, 2008; Doeleman et al., 2009; Johnson, 2015), and the supermassive black hole hosted in the galaxy M87 (Doeleman et al., 2009; Doeleman et al., 2012).

Recent astronomical observations suggest that rapidly rotating black holes exist in Nature (see, *e.g.*, McClintock et al., 2006; Gou et al., 2011; Brenneman, 2013; Gou et al., 2014; Reynolds, 2014). Assuming that astrophysical black holes are described by the Kerr solution (the so-called Kerr black hole hypothesis), it becomes of particular relevance for astrophysical purposes. Moreover, the near-horizon region of maximally rotating Kerr black holes exhibits an enhanced isometry group (Bardeen and Horowitz, 1999), containing the emergent global conformal group $SO(2,1)$. Such a unique feature has important consequences: it provides a connection between astrophysics and computational techniques used in theories with conformal symmetries, and it allows to analytically explore physical

phenomena occurring in the surroundings of these objects. The current state-of-the-art developments include gravitational waves, force-free magnetospheres, electromagnetic emission, and thin accretion discs.

One aim of this thesis is to investigate the effects of conformal symmetries on the dynamics of matter and electromagnetic fields in the region close to the event horizon of near-extreme Kerr black holes. We study force-free magnetospheres and thin accretion discs around near-extreme Kerr black holes. In the first case, the presence of symmetries helps us to solve force-free electrodynamics and classify solutions. In the second case, we show that the presence of conformal symmetries, and in particular the scaling symmetry near the horizon, implies a critical-like behaviour of the fields, whose critical exponents are related to their conformal weights.

The other aim of the thesis is to apply the covariant phase space formalism, developed by Regge and Teitelboim (1974), Iyer and Wald (1994), Barnich and Brandt (2002) and Barnich and Compère (2008), to two concrete examples in General Relativity. In the first case, we consider gravitational multipole moments. We propose a definition of multipole moments based on Noether charges associated to certain residual symmetries of the harmonic gauge. A new class of symmetries, called multipole symmetries, generates the multipole moments of the gravitational field. In the second case, instead, we consider an exact solution to Einstein-Maxwell field equations describing black holes interacting with external magnetic fields. This solution can be thought of as an analytical toy model to describe an astrophysical black hole within a certain length-scale, depending on the magnetic field strength. We address the problem to compute the total conserved mass and to study the thermodynamics of this space-time.

Thesis outline and main results

The thesis consists of two main parts.

Part I is thought of as an introduction to the main topics of research of the thesis. It is a brief review on the background material, as seen from the point of view of the author and for the purposes of this thesis, with a constant reference to the literature. In chapter 1, we introduce Kerr black holes, their near-horizon geometry and those properties of the isometry group to be exploited to address questions of astrophysical relevance. Chapter 2 deals with force-free electrodynamics. It is adopted to describe magnetospheres of black holes and to explain the Blandford-Znajek mechanism of energy extraction from rotating black holes. In chapter 3, we introduce the Novikov-Thorne model for thin accretion disc and particular care is

devoted to its derivation. To conclude the background part, chapter 4 introduces the reader to gravitational multipole moments in General Relativity.

Part II consists of original contributions of the author to the literature.

Chapter 5 addresses the problem of solving force-free electrodynamics around extreme Kerr black holes. To this aim, near-horizon global conformal symmetries are used to find exact solutions and to classify them according to the highest weight representation of the isometry group. Novel physical criteria are introduced to discriminate between formal mathematical solutions and potentially physical solutions describing force-free magnetospheres around extreme Kerr black holes. Among these criteria for the electromagnetic field strength, we require finite energy and angular momentum extraction as measured by an asymptotically flat observer. Such criteria imply bounds on the conformal weights of the solutions and, thus, highlight the importance of emergent symmetries on the dynamics of electromagnetic fields around extreme Kerr black holes.

In chapter 6, we introduce and study an exact analytical solution to Einstein-Maxwell theory describing a Kerr-Newman black hole immersed in an external magnetic field. Strong magnetic fields around Kerr-Newman black holes distort the geometry and the back-reaction affects the conserved charges (mass, angular momentum, electric charge). We compute the total mass by means of the covariant phase space formalism and study the resulting thermodynamics. We show that the total conserved mass, thermodynamic potentials and variables for the magnetised Kerr-Newman can be implicitly written as those of the usual Kerr-Newman black hole. This non-trivial property implies that magnetised Kerr-Newman and Kerr-Newman black holes share the same thermodynamics away from the extreme bound. Such a result extends away from extremality the property that both space-times share the same near-horizon geometry.

Chapter 7 deals with thin accretion discs around a rapidly rotating Kerr black hole. Thin accretion discs, within the Novikov-Thorne model, are studied with a particular boundary condition imposed at the physical edge of the disc. We construct piecewisely the global solution from the local solutions to the Novikov-Thorne model. Then, we explicitly show the phase diagrams of thin accretion discs for stellar-mass and supermassive black holes. We comment on the physical consequences of the boundary condition and show new features when the rotating Kerr black hole is in the high-spin regime. Such new features open up the possibility to investigate the model in the near-horizon region of rapidly spinning black holes, where a novel self-similar solution is obtained. The observables show a critical-like behaviour governed by the underlying symmetries of the background space-time. A quantitative analysis is performed to show the range of validity of

the self-similar solution.

In chapter 8, we define gravitational multipole moments from Noether charges. Such a definition relies on the novel concept of multipole symmetries, which extends the Poincaré Killing symmetries to higher multipole terms. They are specific residual gauge transformations preserving the harmonic gauge. We then show that source multipole moments can be expressed in terms of Noether charges associated to multipole symmetries, both for non-linear stationary solutions and for linearised radiating solutions. In the latter case, from the multipole charges, we extract the conserved multipole charges at spatial infinity, the source multipole moments in the near-zone, and the multipole charges at future null infinity. We also comment on the conservation law expressing the time variation of the source multipole moments in the near-zone in terms of the multipole charges at future null infinity. Our definition of gravitational multipole moments reproduces well-known results in General Relativity with the advantage that it can be applied to an arbitrary generally covariant metric theory of gravity.

The architecture of the thesis is summarised in the figure below:

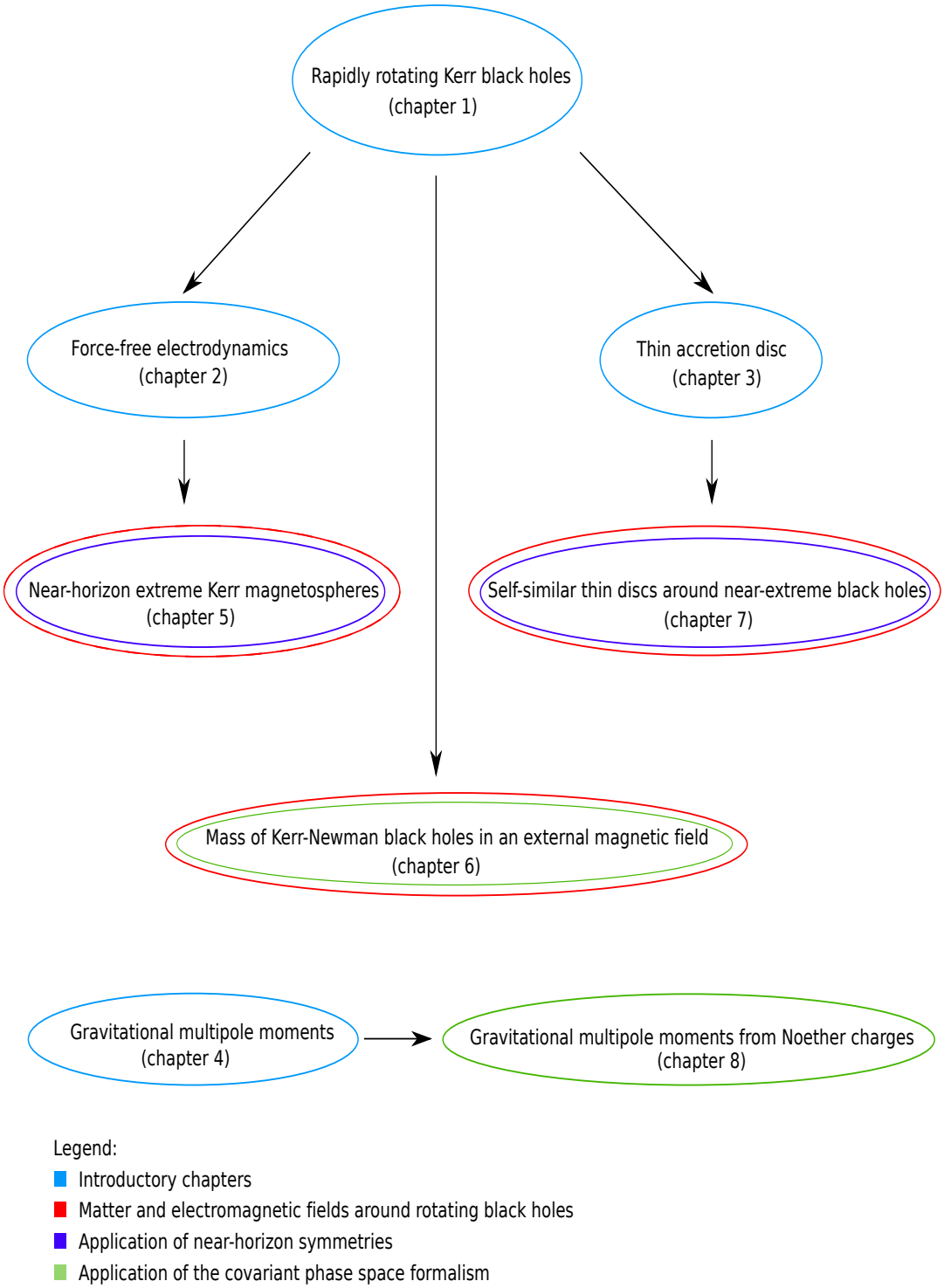

Part I

Background material

Chapter 1

Rapidly rotating Kerr black holes

Contents

In this first chapter, we introduce the main properties of Kerr black holes. In section 1.1, we write down the metric of the Kerr solution and study some basics of its kinematics. We motivate our study for extreme and near-extreme Kerr black holes by both theoretical and astrophysical reasons in section 1.2. Finally, in section 1.3, we derive and study the near-horizon region of the extreme Kerr black hole in order to analytically address questions of astrophysical relevance in the next chapters of the thesis.

1.1 Kerr black hole

The Kerr black hole is the asymptotically flat stationary solution to the four dimensional vacuum Einstein's field equations (Kerr, 1963). It describes the stationary and axisymmetric exterior gravitational field of a rotating black hole. According to the Kerr black hole hypothesis, it models the final state of the gravitational collapse of a star. It has been shown that Kerr space-time is stable against linear perturbations (Whiting, 1989; Dafermos, Rodnianski, and Shlapentokh-Rothman, 2014; Dias, Godazgar, and Santos, 2015). Therefore, the phenomenology of astrophysical black holes rely on the properties of the Kerr solution (Bardeen, Press, and Teukolsky, 1972).

The Kerr line element in Boyer-Lindquist coordinates (t, r, θ, ϕ) is given by[1]

$$ds^2_{Kerr} = -\frac{\Sigma\Delta}{A}dt^2 + \frac{\Sigma}{\Delta}dr^2 + \Sigma d\theta^2 + \sin^2(\theta)\frac{A}{\Sigma}\left(d\phi - \omega dt\right)^2, \tag{1.1}$$

where the metric functions read as

$$\Delta(r) = r^2 - 2Mr + a^2, \tag{1.2a}$$

$$\Sigma(r,\theta) = r^2 + a^2\cos^2(\theta), \tag{1.2b}$$

$$A(r,\theta) = \left(r^2 + a^2\right)^2 - a^2\Delta\sin^2(\theta), \tag{1.2c}$$

$$\omega(r,\theta) = \frac{2Mar}{A}. \tag{1.2d}$$

The Kerr black hole is parametrised by its mass M and its angular momentum per unit mass $a = J/M$. According to the cosmic censorship conjecture proposed by Penrose (1969), the specific angular momentum must satisfy the bound $a \leq |M|$. For $a = 0$, the line element (1.1) describes the Schwarzschild black hole space-time; whereas for $a = M$, it describes the maximally rotating or extreme Kerr black hole. The latter, and its near-extreme version, will be considered in section 1.3.

The Kerr black hole space-time is stationary and axisymmetric. The Killing vectors generating the time and axial symmetries are, respectively, $\eta = \delta^\mu_{\ t}\partial_\mu$ and $\xi = \delta^\mu_{\ \phi}\partial_\mu$. The conserved quantities along the geodesic world-line $x^\mu = x^\mu(\lambda)$ are the rest mass, the total energy $E = -g_{t\mu}\dot{x}^\mu$, and the component of the angular momentum parallel to the symmetry axis $L = -g_{\phi\mu}\dot{x}^\mu$. In addition to these obvious symmetries, the Kerr space-time possesses a Killing tensor (Carter, 1968). The corresponding conserved quantity, the Carter's constant, provides the fourth integral of the motion to analytically integrate the geodesic equation in closed form.

The Kerr line element (1.1) is singular for $\Sigma(r,\theta) = 0$ and for $\Delta(r,\theta) = 0$. The former represents the curvature singularity when $M \neq 0$, while the latter gives the radial location of the coordinate singularities. The event horizon is located at the outer root of $\Delta(r) = 0$,

$$r_+ = M + \sqrt{M^2 - a^2}. \tag{1.3}$$

The outer boundary of the ergo-sphere is located where the time Killing vector η is spacelike. This occurs at the outer root of $\Sigma(r,\theta) = 2Mr$,

$$r_0(\theta) = M + \sqrt{M^2 - a^2\cos^2(\theta)}. \tag{1.4}$$

The region between the event horizon and the ergo-sphere is the ergo-region.

[1] We adopt natural units where $G = c = 1$. Properties of the Kerr space-time are discussed in appendix B.

The existence of such a region permits the extraction of energy and angular momentum from Kerr black holes. Notable mechanisms describing this viable astrophysical phenomenon are the Penrose-Floyd process for point particles (Penrose and Floyd, 1971), the superradiant effect (or Misner (1972) process) for waves (Zel'Dovich, 1971; Bekenstein, 1973) and the Blandford-Znajek process for force-free magnetospheres (Blandford and Znajek, 1977).

For future reference, we focus our attention to circular orbits in the equatorial plane. From the radial component of the geodesic equation,

$$\Sigma(r,\theta)\frac{dr}{d\lambda} = \pm V_r^{1/2}(r), \tag{1.5}$$

where $V_r(r)$ is the effective potential governing the radial motion, one obtains three classes of orbits:

- the photon orbit, describing an orbit whose energy per unit rest mass is infinite,
$$r_{ph} = 2M\left\{1+\cos\left[\frac{2}{3}\arccos\left(\mp\frac{a}{M}\right)\right]\right\}, \tag{1.6}$$
- the marginally bound orbit or innermost bound circular orbit (IBCO),
$$r_{IBCO} = 2M \mp a + 2\sqrt{M(M\mp a)}, \tag{1.7}$$
- the marginally stable orbit or innermost stable circular orbit (ISCO),
$$r_{ISCO} = M\left(3+Z_2 \mp \sqrt{(3-Z_1)(3+Z_1+2Z_2)}\right), \tag{1.8}$$
where
$$Z_1 = 1+\left(1-\frac{a^2}{M^2}\right)^{1/3}\left[\left(1+\frac{a}{M}\right)^{1/3}+\left(1-\frac{a}{M}\right)^{1/3}\right], \tag{1.9a}$$
$$Z_2 = \sqrt{3\frac{a^2}{M^2}+Z_1^2}. \tag{1.9b}$$

The upper signs refer to orbits co-rotating with the Kerr black hole, while the lower signs refer to counter-rotating orbits. The Fig. 1.1 shows the circular co-rotating equatorial orbits as functions of the specific angular momentum parameter. It is evident that the Boyer-Lindquist radial locations of the horizon r_+, the photon orbit r_{ph}, the IBCO r_{IBCO}, and ISCO r_{ISCO} are coincident for $a = M$. Of course this is a deception of the Boyer-Lindquist coordinate system, because timelike surfaces, like the IBCO or the ISCO, cannot coincide with null sufaces, like the horizon. This

feature motives us to study in more detail the extreme Kerr black hole in the next section.

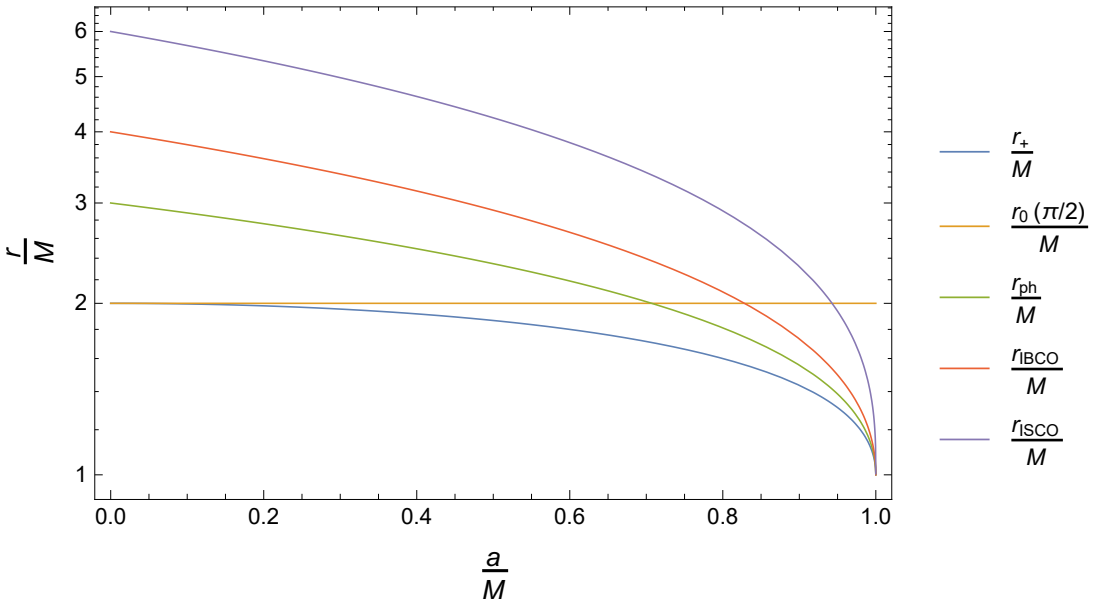

FIGURE 1.1: Circular co-rotating equatorial orbits around a Kerr black hole as functions of the specific angular momentum parameter a/M.

1.2 Extreme and near-extreme Kerr black hole

The Kerr black holes family contains a special class in its parameter space: the extreme case characterized by $a = M$. Extreme Kerr black holes rotate at the maximal angular momentum allowed by the cosmic censorship conjecture. According to the third law of black-hole mechanics, Israel (1986) showed that it is not possible to spin up a Kerr black hole to the extreme value within a finite (advanced) time. Moreover, extreme Kerr black holes suffer from instabilities against linear perturbations at the event horizon (Aretakis, 2012; Aretakis, 2015). Nevertheless, they serve as theoretical laboratories to investigate aspects of classical gravity (see, *e.g.*, Banados, Silk, and West, 2009) and, as we shall briefly comment in the next section 1.3, to study properties of the quantum nature of gravity.

For astrophysical purposes, it is better to consider near-extreme Kerr black holes as argued for the first time by Bardeen (1970), Bardeen and Wagoner (1971) and later by Thorne (1974), where he computed the well-known limit $a/M = 0.998$ within the thin accretion disc model. In addition to theoretical reasons, there is observational evidence about the existence of near-extreme black holes in Nature (see, *e.g.*, McClintock et al., 2006; Gou et al., 2011; Brenneman, 2013; Gou et al., 2014; Reynolds, 2014).

Since we would like to focus our attention on the limit $a \to M$, we introduce the near-extreme parameter σ that measures the deviation from the extreme case

$$\sigma = \sqrt{1 - \frac{a^2}{M^2}}. \tag{1.10}$$

By performing a Taylor expansion around $\sigma = 0$, we get the following leading behaviour for the circular co-rotating equatorial orbits around a near-extreme Kerr black hole:

$$\frac{r_+}{M} = 1 + \sigma, \tag{1.11a}$$
$$\frac{r_0(\pi/2)}{M} = 2, \tag{1.11b}$$
$$\frac{r_{ph}}{M} = 1 + \frac{2}{\sqrt{3}}\sigma + \mathcal{O}\left(\sigma^2\right), \tag{1.11c}$$
$$\frac{r_{IBCO}}{M} = 1 + \sqrt{2}\sigma + \mathcal{O}\left(\sigma^2\right), \tag{1.11d}$$
$$\frac{r_{ISCO}}{M} = 1 + 2^{1/3}\sigma^{2/3} + \mathcal{O}\left(\sigma^{4/3}\right). \tag{1.11e}$$

It is then clear that the ISCO radial location scales differently and it approaches M much slower than the horizon, the photon orbit and the IBCO radii. In particular, the proper radial distance,

$$d(r_f, r_i) = \int_{r_i}^{r_f} \sqrt{g_{rr}}\, dr, \tag{1.12}$$

between the horizon and the photon orbit as well as that between the photon orbit and the IBCO remain finite and non-zero for $\sigma \to 0$, whereas the proper radial distance between the ISCO and both the IBCO and the outer boundary of the ergosphere r_0 diverges for $\sigma \to 0$. This characteristic property of extreme Kerr black holes is diagrammatically summarized by the embedding diagrams for $\theta = \pi/2$ and $t = \text{const}$ in Fig. 1.2.

At the extreme value $a = M$, the Kerr space-time is divided into three regions. It would be better to say that Kerr space-time has three distinct limits (see Geroch, 1969, for a well-posed definition of limit of a space-time):

a) the extreme Kerr, obtained by keeping fixed the Boyer-Lindquist coordinates and sending $a \to M$. This limit does not alter the asymptotically flat region, but the manifold for $r \leq r_{ISCO}$ is singularly projected into the event horizon at $r_+|_{a=M} = M$, according to Eqs. (1.11)

b) the intermediate region, also known as near-horizon extreme Kerr geometry (NHEK), obtained by keeping fixed suitable co-rotating coordinates and

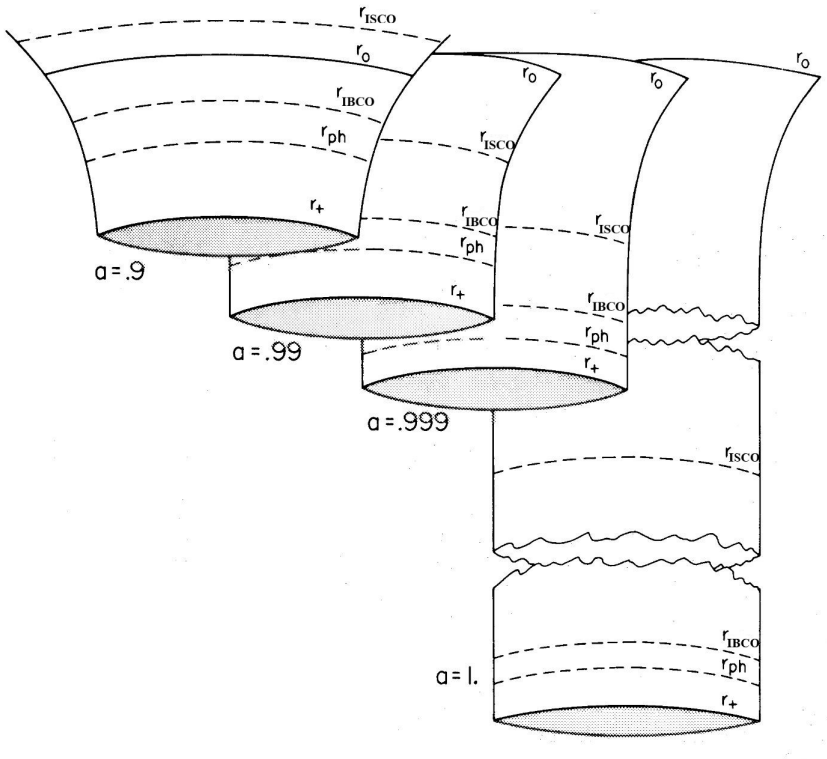

FIGURE 1.2: Embedding diagrams for $\theta = \pi/2$ and t = const of rapidly rotating Kerr black holes of unit mass $M = 1$. The cracks stand for infinite proper radial distance (Bardeen, Press, and Teukolsky, 1972).

sending $a \to M$. This space-time is no longer asymptotically flat: it has a timelike boundary. We shall provide its derivation in section 1.3.

c) the deepest region, known as near-NHEK, obtained by keeping fixed coordinates adapted to the event horizon and sending $a \to M$. It is diffeomorphic to NHEK.

1.3 Near-horizon extreme Kerr

The theoretical importance of the extreme Kerr space-time lies in the presence of an enhanced isometry group containing global conformal symmetries in its near-horizon region (Bardeen and Horowitz, 1999). Such a unique feature has important consequences: it provides a connection between astrophysics and computational techniques used in theories with conformal symmetries, and it allows to analytically investigate phenomena occurring in the surroundings of these objects. In fact, these symmetries have been exploited to analytically address astrophysical questions concerning gravitational waves (Gralla, Porfyriadis, and Warburton, 2015; Gralla, Hughes, and Warburton, 2016; Hadar and Porfyriadis, 2017; Compère

et al., 2017), force-free magnetospheres (Zhang, Yang, and Lehner, 2014; Lupsasca, Rodriguez, and Strominger, 2014; Lupsasca and Rodriguez, 2015; Compère and Oliveri, 2016; Gralla, Lupsasca, and Strominger, 2016), electromagnetic emission (Porfyriadis, Shi, and Strominger, 2017; Gralla, Lupsasca, and Strominger, 2017; Lupsasca, Porfyriadis, and Shi, 2018), and thin accretion discs (Compère and Oliveri, 2017).

The additional presence of infinite-dimensional conformal symmetries leds to the proposal that NHEK space-time may be dual to a conformal field theory (CFT) (Guica et al., 2009). Such putative correspondence takes the name of Kerr/CFT correspondence (see, *e.g.*, Bredberg et al., 2011; Compère, 2012). It turned out however not to be a duality as the celebrated AdS/CFT duality. Despite the fact that the Kerr/CFT correspondence is far to be a duality, there exist examples showing common mathematical features between the extreme Kerr and the dual CFT through explicit computation for gravitational waves (Porfyriadis and Strominger, 2014; Hadar, Porfyriadis, and Strominger, 2014; Hadar, Porfyriadis, and Strominger, 2015), superradiant effect (Bredberg et al., 2010), and wave scattering amplitudes (Hartman, Song, and Strominger, 2010; Castro, Maloney, and Strominger, 2010).

1.3.1 The NHEK space-time and its derivation

We now derive the NHEK space-time by a limiting procedure from Kerr line element in Boyer-Lindquist coordinates (t, r, θ, ϕ) in Eq. (1.1). Let us define the co-rotating coordinates (T, R, θ, Φ) as

$$T = \frac{t}{\tilde{r}_0}\lambda^n, \quad R = \frac{r - r_+}{\tilde{r}_0}\frac{1}{\lambda^n}, \quad \Phi = \phi - \Omega_+^{ext} t, \quad \text{and} \quad \sigma = \sqrt{1 - \frac{a^2}{M^2}} = \bar{\sigma}\lambda, \tag{1.13}$$

where $\Omega_+^{ext} = 1/(2M)$ is the extreme angular velocity of the event horizon, $\tilde{r}_0$ is a dimensional factor, $\bar{\sigma}$ is an arbitrary real number, and n is a positive and real exponent. By performing a Taylor expansion around $\lambda = 0$, one gets a formal series of the form

$$ds^2_{Kerr}(\lambda) = \sum_{p=p_0}^{\infty} ds^2_{(p)}\, \lambda^p. \tag{1.14}$$

The exponent n must be chosen in such a way that we get a well-defined limit for $\lambda \to 0$ at fixed co-rotating coordinates. This result is achieved by approaching the extreme value of the angular momentum faster than the zooming in the near-horizon region. In formulæ,

$$\frac{\sigma}{r - r_+} \propto \lambda^{1-n} \to 0 \quad \text{as} \quad \lambda \to 0 \tag{1.15}$$

implies that $n \in (0,1)$. This range of n selects the intermediate region in Fig. 1.2 between the extreme Kerr (for $n = 0$) and the near-NHEK (for $n = 1$). By keeping fixed the co-rotating coordinates (T, R, θ, Φ) and sending $\lambda \to 0$ with $n \in (0,1)$, one gets the NHEK line element at the leading order in λ

$$ds^2_{Kerr}(\lambda) = ds^2_{NHEK} + \mathcal{O}(\lambda^n), \tag{1.16a}$$

$$ds^2_{NHEK} = \tilde{r}_0^2\,\Gamma(\theta)\left[-R^2 dT^2 + \frac{dR^2}{R^2} + d\theta^2 + \gamma^2(\theta)\,(d\Phi + R dT)^2\right], \tag{1.16b}$$

where $\Gamma(\theta) = \left(1 + \cos^2(\theta)\right)/2$, $\gamma(\theta) = \sin(\theta)/\Gamma(\theta)$, and $\tilde{r}_0 = \sqrt{2}M$.

The $n = 1$ case adapts the co-rotating coordinates (1.13) to the event horizon. The limit $\lambda \to 0$ gives the near-NHEK line element which is diffeomorphic to the NHEK space-time (Amsel et al., 2009) and we will not consider it anymore in this thesis.

The NHEK line element (1.16b) is a solution to the vacuum Einstein's field equations and it is geodesically complete with a timelike boundary (Bardeen and Horowitz, 1999). Along the axis of rotation, *i.e.*, for $\theta = 0$ and $\theta = \pi$, Eq. (1.16b) is AdS_2 in Poincaré coordinates with the horizon located at $R = 0$. At fixed polar angle, the three-dimensional geometry is a quotient of warped AdS_3 (Anninos et al., 2009). In general, the NHEK line element is a warped and twisted product of $AdS_2 \times S^2$.

The NHEK space-time is manifestly scale invariant: the rescaling of the radial and time coordinates, $R \to cR$ and $T \to T/c$, leaves the line element (1.16b) invariant for arbitrary c. This is the dilation symmetry of AdS_2, whose generator is part of the $SL(2,\mathbb{R})$ algebra. Indeed, the isometry group of NHEK space-time is enhanced from the isometry group $\mathbb{R} \times U(1)$ of Kerr space-time to $SL(2,\mathbb{R}) \times U(1)$, in agreement with a general result proved by Kunduri, Lucietti, and Reall (2007) in a broad class of theories. The Killing vectors of NHEK space-time are

$$H_+ = \sqrt{2}\partial_T, \tag{1.17a}$$

$$H_0 = T\partial_T - R\partial_R, \tag{1.17b}$$

$$H_- = \sqrt{2}\left[\frac{1}{2}\left(T^2 + \frac{1}{R^2}\right)\partial_T - TR\partial_R - \frac{1}{R}\partial_\Phi\right], \tag{1.17c}$$

$$Q_0 = \partial_\Phi. \tag{1.17d}$$

The Killing vector H_+ is the generator of the (Poincaré) time translations, H_0 is

the generator of the scale invariance mentioned above, and Q_0 generates the azimuthal rotations. They obey the $SL(2,\mathbb{R}) \times U(1)$ commutation relations given by

$$[H_0, H_\pm] = \mp H_\pm, \quad [H_+, H_-] = 2H_0, \quad [Q_0, H_\pm] = 0 = [Q_0, H_0]. \tag{1.18}$$

One relevant property of NHEK space-time is the absence of any global timelike Killing vector (Amsel et al., 2009). This feature has the consequence that there is no unique definition of vacuum of a quantum field theory (DeWitt, 1975; Kay and Wald, 1991), as already known for the Kerr space-time (Ottewill and Winstanley, 2000a; Ottewill and Winstanley, 2000b). In particular, the Poincaré time translation generator H_+ is spacelike for $\gamma(\theta) > 1$, *i.e.*, in the region around the equator where $\theta \in [\theta_*, \pi - \theta_*]$ with $\theta_* = \arcsin[\sqrt{3} - 1] \approx 47°$. In other words, H_+ is timelike only in the region where $\theta \in [0, \theta_*] \cup [\pi - \theta_*, \pi]$, and therefore this region represents the physical region in the NHEK space-time. Such a characteristic property originates by the fact that the horizon-generating Killing vector of the non-extreme Kerr is timelike just outside the event horizon, then it becomes lightlike at the velocity of light surface, beyond which it is spacelike. At the extreme case and upon performing the near-horizon limit, the velocity of light surface asymptotically approaches the event horizon and the horizon-generating Killing vector is no longer timelike near the horizon around the equator.

1.3.2 The isometry group and critical phenomena

The presence of the global conformal group $SL(2,\mathbb{R}) \sim SO(2,1)$ in the isometry group of NHEK space-time allows us to classify fields defined on NHEK space-time. Moreover, these symmetries indicate the presence of critical behaviours of certain physical observables. Very recently, critical phenomena have been discovered in magnetospheres (Gralla, Lupsasca, and Strominger, 2017), thin accretion discs (Compère and Oliveri, 2017), scalar, electromagnetic and gravitational perturbations (Gralla and Zimmerman, 2017), electromagnetic line emission (Lupsasca, Porfyriadis, and Shi, 2018), and gravitational waves (Compère et al., 2017). As noticed for the first time in Gralla, Lupsasca, and Strominger (2017), the extreme Kerr space-time can be thought of as a critical point in the Kerr family. The origin of this interpretation stems from the seminal paper by Bardeen, Press, and Teukolsky (1972) and from the meaning of Fig. 1.2. From this perspective, the result of Bardeen and Horowitz (1999) can be viewed as the emergence of conformal symmetries near the critical point. As a consequence, extreme and near-extreme Kerr black holes admit critical phenomena in their near-horizon region.

In order to make this interpretation manifest and rigorous, let us consider a smooth tensor field F on extreme Kerr space-time. After transforming the field F to the co-rotating coordinates (1.13) and performing a Taylor expansion around $\lambda = 0$, one gets

$$F(\lambda) = \lambda^{-h} \sum_{p=0}^{\infty} \mathscr{F}_{(p)}(T,R,\theta,\Phi)\, \lambda^p. \tag{1.19}$$

Here h is a real number and it depends on the rank of the field F. The leading term

$$\mathscr{F}_{(0)}(T,R,\theta,\Phi) = \lim_{\lambda\to 0} \lambda^h F(\lambda) \tag{1.20}$$

is the near-horizon field whenever it exists. We should notice that the near-horizon limit in Eq. (1.13) is invariant under an arbitrary rescaling of the limiting parameter $\lambda \to c\lambda$ and under the simultaneous rescaling of the time and radial coordinates $t \to t/c^n$ and $r \to c^n r$ (or, equivalently, the simultaneous rescaling of the near-horizon time and radial coordinates $T \to T/c^n$ and $R \to c^n R$). After performing the limit in Eq. (1.20), the near-horizon field does not depend any longer by λ and it scales like $\mathscr{F}_{(0)} \to c^h \mathscr{F}_{(0)}$ under $T \to T/c^n$ and $R \to c^n R$. Infinitesimally, the near-horizon field must obey the self-similarity condition given by

$$\mathscr{L}_{H_0} \mathscr{F}_{(0)} = h \mathscr{F}_{(0)}, \tag{1.21}$$

where $\mathscr{L}_{H_0}$ is the Lie derivative operator with respect to the dilation generator H_0 which generates the finite rescaling $T \to T/c$ and $R \to cR$. As an example, the NHEK metric field in Eq. (1.16b) obeys Eq. (1.21) with $h = 0$, *i.e.*, it is scale invariant.

In order to classify tensor fields defined in NHEK space-time, we might use representations of $SL(2,\mathbb{R}) \times U(1)$. Among all the representations of $SL(2,\mathbb{R})$, one can consider the highest or lowest weight representations. Both of them are infinite-dimensional (Barut and Raczka, 1986). A given tensor field F falls into the highest weight representation labelled by $\{h,q,k\}$ if

$$\begin{cases} \mathscr{L}_{H_+} F_{(h,q,0)} = 0, \\ \mathscr{L}_{H_0} F_{(h,q,0)} = h F_{(h,q,0)}, \\ \mathscr{L}_{Q_0} F_{(h,q,0)} = i q F_{(h,q,0)}, \end{cases} \tag{1.22}$$

with descendants given by $\left(\mathscr{L}_{H_-}\right)^k F_{(h,q,0)} = F_{(h,q,k)}$. In physical terms (and in Poincaré coordinates), the first condition imposes the stationarity of the field, the second gives the self-similarity condition with respect to the dilation generator H_0

with weight h ($h = 0$ being a scale-invariant field), and the third condition introduces the $U(1)$ charge q of the field ($q = 0$ meaning an axisymmetric field). Explicit examples of highest-weight classification of force-free electromagnetic fields have been derived in Lupsasca, Rodriguez, and Strominger (2014), Lupsasca and Rodriguez (2015), and Compère and Oliveri (2016). A systematic approach for scalar, vector and symmetric tensor fields is found in Chen and Stein (2017).

Chapter 2

Force-free electrodynamics

Contents

This chapter is devoted to force-free electrodynamics and it is conceived as a quick introduction to the topic. We first motivate and introduce the reader to the subject in section 2.1. Then, in section 2.2, we write down the equations governing force-free electrodynamics. In section 2.3, we explicit certain properties of force-free fields and, in section 2.4, we give a field-theoretical description of the force-free electrodynamics in terms of Euler potentials. Section 2.5 specialises to force-free magnetospheres that are stationary and axial symmetric. This is a necessary step to introduce the celebrated Blandford-Znajek mechanism of energy extraction in section 2.6.

2.1 Astrophysical motivations

Force-free electrodynamics (FFE) was first introduced in astrophysics by Lüst and Schlüter (1954) in the context of the solar magnetosphere. This application motivated the search for exact solutions to FFE by Chandrasekhar (1956) and Chandrasekhar and Kendall (1957). Goldreich and Julian (1969) applied FFE to magnetospheres of pulsars[1], observed one year earlier by Hewish et al. (1968) and identified with rapidly rotating and highly magnetized neutron stars (Gold, 1968; Pacini, 1968). Goldreich and Julian (1969) restricted their study to stationary and axisymmetric electromagnetic field configurations that are solutions to the Maxwell's electrodynamics. They estimated that, though the pulsar magnetosphere is populated by electron-positron plasma, the plasma rest-mass density is negligible with respect to the electromagnetic field energy density. This implies that one may neglect the exchange of energy-momentum between the plasma and the electromagnetic field, *i.e.*, one may impose the constraint of vanishing Lorentz force density, from which the name force-free electrodynamics. For many years, the solution obtained by Michel (1973) has been the only analytical solution to investigate pulsar magnetospheres.

The range of applicability of force-free electrodynamics is not only limited to pulsar magnetospheres. It plays a fundamental role in the physics of the active galactic nuclei (AGN), discovered more than fifty years ago by Schmidt (1963), where a supermassive and rotating black hole is surrounded by an accretion disc, sourcing magnetic fields, and a plasma. These objects are observed at the centre of galaxies and they are the brightest object in our observable universe (see, *e.g.*, Fabian, 2012). The most viable mechanism of energy extraction has been proposed by Blandford and Znajek (1977) and it involves force-free electrodynamics. General relativistic magneto-hydro-dynamics simulations confirm the force-free approximation (McKinney, Tchekhovskoy, and Blandford, 2012; Penna, Narayan, and Sadowski, 2013), and suggest that the Blandford-Znajek process is responsible for the jets observed in the AGN (Tchekhovskoy, Narayan, and McKinney, 2011).

2.2 Equations of motion

Let $g_{\mu\nu}$ be the background space-time metric and A_μ be the gauge potential. The Maxwell field is $F_{\mu\nu} = \nabla_\mu A_\nu - \nabla_\nu A_\mu$. It obeys Maxwell's equations

$$\nabla_{[\sigma} F_{\mu\nu]} = 0, \quad \nabla_\nu F^{\mu\nu} = j^\mu, \tag{2.1}$$

[1] See the reviews (Michel, 1982; Beskin, Gurevich, and Istomin, 1993) for a complete account on the topic.

with j^μ being the electric current density. The corresponding energy-momentum tensor of the electromagnetic field reads as

$$T^{\mu\nu}_{em} = F^{\mu\alpha}F^{\nu}_{\ \alpha} - \frac{1}{4}g^{\mu\nu}F^{\alpha\beta}F_{\alpha\beta}. \tag{2.2}$$

The total energy-momentum tensor is the sum of the contribution of the electromagnetic field and of that of the matter content:

$$T^{\mu\nu} = T^{\mu\nu}_{em} + T^{\mu\nu}_{matter}. \tag{2.3}$$

The conservation of the total energy-momentum implies that

$$0 = \nabla_\nu T^{\mu\nu}_{em} + \nabla_\nu T^{\mu\nu}_{matter} = -F^{\mu\nu}j_\nu + \nabla_\nu T^{\mu\nu}_{matter}. \tag{2.4}$$

The above equation governs the transfer of energy and momentum between the electromagnetic field and the matter content. Under the simplifying assumption that inertial forces are negligible with respect to the Lorentz force density, *i.e.*, neglecting any exchange of energy and momentum from the electromagnetic field to the matter content, one obtains the so-called force-free condition

$$F_{\mu\nu}j^\nu = 0. \tag{2.5}$$

This constraint decouples the dynamics of the electromagnetic field from that of the plasma. Therefore, the FFE equations are

$$\nabla_{[\sigma}F_{\mu\nu]} = 0, \qquad \nabla_\nu F^{\mu\nu} = j^\mu, \qquad F_{\mu\nu}j^\nu = 0, \tag{2.6}$$

or, eliminating j^μ,

$$\nabla_{[\sigma}F_{\mu\nu]} = 0, \qquad F_{\mu\nu}\nabla_\sigma F^{\nu\sigma} = 0. \tag{2.7}$$

FFE equations (2.6) are non-linear and, therefore, exact analytical solutions are hard to find. Only a few exact analytical solutions are known: in Schwarzschild space-time (Michel, 1973; Lyutikov, 2011), Kerr space-time (Blandford and Znajek, 1977; Menon and Dermer, 2005; Menon and Dermer, 2007; Menon and Dermer, 2011; Brennan, Gralla, and Jacobson, 2013; Menon, 2015), and near-horizon extreme Kerr space-time (Lupsasca, Rodriguez, and Strominger, 2014; Zhang, Yang, and Lehner, 2014; Lupsasca and Rodriguez, 2015; Compère and Oliveri, 2016).

However, despite the non-linearity, FFE equations show interesting and non-trivial geometric properties. A force-free field defines a space-time foliation (Carter,

1979) and it is described by Euler potentials (Uchida, 1997a; Uchida, 1997b). Recently, diverse attempts have been made to understand the analytical properties of FFE equations and to find new exact analytical solutions (Tanabe and Nagataki, 2008; Pan and Yu, 2015a; Pan and Yu, 2015b; Pan and Yu, 2016; Compère, Gralla, and Lupsasca, 2016; Pan, Yu, and Huang, 2017; Harte, 2017; Kinoshita and Igata, 2017; Li and Wang, 2017; Grignani, Harmark, and Orselli, 2018).

For a detailed covariant treatment of FFE theory and its implications for pulsar and black hole magnetospheres, we refer the reader to the review by Gralla and Jacobson (2014), that we shall closely follow in this chapter.

2.3 Degenerate electromagnetic fields

From now on, we prefer adopting the language of differential forms for the ease of notation and to make manifest properties of force-free fields that are metric-independent. Our conventions on differential forms are summarised in appendix A.

FFE equations (2.6) can be rewritten, respectively, as

$$dF = 0, \quad d\star F = \star J, \quad J \wedge \star F = 0. \tag{2.8}$$

The first equation is the Bianchi identity: it is independent of the metric field and reproduces the homogeneous Maxwell's equations. The second equation gives the inhomogeneous Maxwell's equations, while the third equation is the force-free constraint equivalent to the inner product between J and F, $i_J F = 0$.[2] The conservation of the current 1-form J follows directly from the property that $d^2 = 0$.

We first notice that any source-free solution to Maxwell's electrodynamics is also a trivial solution to force-free electrodynamics. We shall consider solutions with non-vanishing current 1-form J in the rest of the chapter. Another observation worth of mention is that the current J plays no role in the dynamics of the field: indeed, it can be eliminated as shown in Eq. (2.7).

2.3.1 Degeneracy and field sheets

An important property obeyed by force-free fields is the degeneracy condition. From the force-free condition $i_J F = 0$, one has that

$$i_J (F \wedge F) = i_J F \wedge F + F \wedge i_J F = 0. \tag{2.9}$$

[2] Here, we used the property that $i_X \star\omega = \star(\omega \wedge X)$, with $X = J$, $\star\omega = F$ and $\omega = -\star(\star\omega) = -\star F$.

Since $F \wedge F$ is a 4-form in four dimensions (and $J \neq 0$), it follows that F must be degenerate

$$F \wedge F = 0. \tag{2.10}$$

This is a necessary, but not sufficient, condition for an electromagnetic field to be force-free. The degeneracy of the Maxwell field occurs when there exists a given vector field v such that $i_v F = 0$, as it is clear from Eq. (2.9). In physical terms, if v is a unit time-like observer, $i_v F = 0$ is the ideal Ohm' law – stating that the electric field in the local rest frame of the plasma is vanishing – and by no means the degenerate electromagnetic field is force-free.

A direct consequence of the degeneracy condition (2.10) is that the Maxwell field F can be written as the wedge product of two 1-forms, *i.e.*, F is a simple 2-form

$$F = \alpha \wedge \beta. \tag{2.11}$$

This is readily showed by considering two arbitrary vector fields v and w such that their contraction with the electromagnetic field, $i_v i_w F \neq 0$, is non zero. Then

$$0 = i_w i_v (F \wedge F) = i_w (i_v F \wedge F + F \wedge i_v F) = 2 i_v i_w F \, F + 2 i_w F \wedge i_v F. \tag{2.12}$$

Hence, $\alpha \propto i_v F$ and $\beta \propto i_w F$.

The Frobenius' theorem guarantees that a degenerate field $F = \alpha \wedge \beta$, obeying the Bianchi identity $dF = 0$, has integrable kernels. In other words, the Pfaffian system $\alpha = 0 = \beta$ is completely integrable because the integrability conditions $\alpha \wedge F = 0 = \beta \wedge F$ are obeyed (Choquet-Bruhat, DeWitt-Morette, and Dillard-Bleick, 1982). The vector fields annihilating the degenerate electromagnetic field span a two-dimensional sub-manifold in the four-dimensional space-time. These integral surfaces are called field sheets (Carter, 1979; Uchida, 1997a). The existence of field sheets can be visualised by a simpler geometrical argument (Gralla and Jacobson, 2014). Assume that v is a vector in the kernel of F, that is $i_v F = 0$ everywhere in space-time. Then, by using the Cartan's formula and the Bianchi identity, one has that $\mathcal{L}_v F = 0$, *i.e.*, the electromagnetic field F is preserved along the flow of v. Now, consider a second vector field w such that $\mathcal{L}_v w = 0$ and $i_w F = 0$ on the three-dimensional surface transverse to the flow of v. It follows that the contraction of w with F is preserved along the flow of v because $\mathcal{L}_v (i_w F) = 0$. Thus, $i_w F = 0$ everywhere and w is in the kernel of F. In conclusion, the electromagnetic field F is preserved along the flow of v and w or, in different words, it is "frozen" on the field sheet.

Force-free configurations have current vectors J tangent to the field sheets and

force-free fields induce a foliation of space-times. This property will be important for the existence of the Euler-potential formulation of the force-free electrodynamics in section 2.4.

2.3.2 Lorentz invariants

In classical electrodynamics, we have two Lorentz invariants: $\star(F\wedge F)$ and $\star(F\wedge\star F)$.

The first invariant is explicitly given by

$$\star(F\wedge F)=\frac{1}{4}\varepsilon^{\alpha\beta\gamma\delta}F_{\alpha\beta}F_{\gamma\delta}\propto\sqrt{\det(F)}. \tag{2.13}$$

Force-free fields are degenerate and, therefore, $\det(F)=0$ implies that F is a matrix of rank two and its kernel is two-dimensional, as already stated above.

The second invariant is the Hodge dual of the Lagrangian density. It reads as

$$\star(F\wedge\star F)=-\frac{1}{2}F_{\mu\nu}F^{\mu\nu}=-\frac{1}{2}F^2. \tag{2.14}$$

It is useful to introduce the electric and magnetic fields as measured by a (not normalized) time-like observer v

$$E_\mu=F_{\mu\nu}v^\nu,\quad B_\mu=(\star F)_{\mu\nu}v^\nu. \tag{2.15}$$

The electromagnetic field $F_{\mu\nu}$ can be decomposed in terms of E_μ and B_μ as

$$F_{\mu\nu}=\frac{1}{v^2}\left(2E_{[\mu}v_{\nu]}-\epsilon_{\mu\nu\gamma\delta}B^\gamma v^\delta\right). \tag{2.16}$$

The first Lorentz invariant reads as

$$\star(F\wedge F)=\frac{1}{4}\epsilon^{\alpha\beta\gamma\delta}F_{\alpha\beta}F_{\gamma\delta}=\frac{2}{v^2}E_\mu B^\mu. \tag{2.17}$$

Thus, the force-free condition implies that the electric and magnetic fields are orthogonal to each other. The second Lorentz invariant reads as

$$\star(F\wedge\star F)=-\frac{1}{2}F^2=-\frac{1}{v^2}\left(E^2-B^2\right). \tag{2.18}$$

We can classify degenerate fields into three classes by looking at the sign of $\star(F\wedge\star F)$. We call F to be magnetically dominated if F^2 is positive, electrically dominated if F^2 is negative, and null otherwise. Magnetically dominated configurations are considered of physical relevance because the kernel of F is time-like and so is the current four-vector ($i_J F=0$) and there always exists an observer four-velocity who

measures only the magnetic field in his frame ($i_v F = 0$). Null configurations are also relevant because they describe the radiation field.

2.4 Euler potentials formulation

Uchida, in a series of papers (Uchida, 1997a; Uchida, 1997b), introduced a new formulation of FFE based on Euler potentials as field variables. Motivated by the degeneracy condition (2.11), one can introduce two scalar fields, the Euler potentials ϕ_1 and ϕ_2, such that

$$F = d\phi_1 \wedge d\phi_2. \tag{2.19}$$

The force-free condition $0 = i_J F = -(i_J d\phi_2) d\phi_1 + (i_J d\phi_1) d\phi_2$ becomes equivalent to the system [3]

$$0 = d\phi_i \wedge \star J = d\phi_i \wedge d \star F = -d\left(d\phi_i \wedge \star F\right), \quad i = 1,2. \tag{2.20}$$

The two expressions $d\phi_i \wedge \star F$ are called Euler currents (Gralla and Jacobson, 2014). We will show that the conservation of energy and angular momentum amount to the conservation of the first Euler current (see Eq. (2.44)), and the stream equation is equivalent to the conservation of the second Euler current (see Eq. (2.46)).

The Euler potentials give a description of closed and degenerate 2-form fields which is equivalent to the usual one in terms of gauge potential. However, Euler potentials are not unique. Indeed, we might introduce a new pair of Euler potentials $\tilde{\phi_1} = \tilde{\phi_1}(\phi_1, \phi_2)$ and $\tilde{\phi_2} = \tilde{\phi_2}(\phi_1, \phi_2)$ and the electromagnetic field strength becomes

$$\tilde{F} = d\tilde{\phi_1} \wedge d\tilde{\phi_2} = \left(\frac{\partial\tilde{\phi_1}}{\partial\phi_1}\frac{\partial\tilde{\phi_2}}{\partial\phi_2} - \frac{\partial\tilde{\phi_1}}{\partial\phi_2}\frac{\partial\tilde{\phi_2}}{\partial\phi_1}\right) d\phi_1 \wedge d\phi_2 = \frac{\partial(\tilde{\phi_1}, \tilde{\phi_2})}{\partial(\phi_1, \phi_2)} F. \tag{2.21}$$

The invariance of the field strength F under an arbitrary Euler potentials redefinition implies that the Jacobian of the transformation must be unitary. In geometrical terms, the unitary of the Jacobian means that the area element of the field sheets remains invariant under a field redefinition. It is worth mentioning that this arbitrariness is equivalent to the gauge freedom of the gauge potential (Uchida, 1997a).

[3] For two p-forms α and β, $\alpha \wedge \star\beta = (i_\beta \alpha)\varepsilon$ where ε is the volume element. Eq. (2.20) follows for $\alpha = d\phi_i$, $\beta = J$.

2.4.1 Euler potentials with one symmetry

Assume that F is invariant under the flow of the vector field s. By using the Cartan's formula and the Bianchi identity, one obtains that

$$0 = \mathscr{L}_s F = d i_s F. \tag{2.22}$$

By the Poincaré's lemma, there exists a function f such that

$$df = i_s F = i_s(d\phi_1 \wedge d\phi_2) = -(i_s d\phi_2) d\phi_1 + (i_s d\phi_1) d\phi_2. \tag{2.23}$$

In particular, $f = f(\phi_1, \phi_2)$. There are two cases: either $df = 0$ and both Euler potentials are invariant under the symmetry s, or $df \neq 0$. In the latter case, we can redefine the Euler potentials such that $f = -\tilde{\phi}_1$. The unitary of the Jacobian guarantees the existence of $\tilde{\phi}_2$. Thus,

$$-d\tilde{\phi}_1 = -(i_s d\tilde{\phi}_2) d\tilde{\phi}_1 + (i_s d\tilde{\phi}_1) d\tilde{\phi}_2, \tag{2.24}$$

and we conclude that

$$i_s d\tilde{\phi}_1 = 0, \quad i_s d\tilde{\phi}_2 = 1. \tag{2.25}$$

2.4.2 Euler potentials with two commuting symmetries

Assume that F is invariant under the flow of two commuting vector fields s_1 and s_2. Then, we have

$$i_{s_1} F = df, \quad i_{s_2} F = dg, \tag{2.26}$$

for some functions f and g. From $F \wedge i_{s_2} F = 0$, one has

$$0 = i_{s_1}(F \wedge i_{s_2} F) = i_{s_1} F \wedge i_{s_2} F + (i_{s_1} i_{s_2} F) F = df \wedge dg - (i_{s_2} i_{s_1} F) F. \tag{2.27}$$

This means that $F \propto df \wedge dg$. The scalar $i_{s_2} i_{s_1} F$ is a real constant, since $d(i_{s_2} i_{s_1} F) = \mathscr{L}_{s_2}(i_{s_1} F) - i_{s_2} d i_{s_1} F = i_{[s_2, s_1]} F + i_{s_1} \mathscr{L}_{s_2} F - i_{s_2} \mathscr{L}_{s_1} F = 0$ by assumptions. As before, there are two cases: either $i_{s_2} i_{s_1} F = 0$ or $i_{s_2} i_{s_1} F \neq 0$, respectively, case I and case II studied in Uchida (1997b).

Let us analyse the case I. We have two subcases. In the first subcase Ia, $df = 0 = dg$, and thus the Euler potentials are invariant under both symmetries s_1 and s_2. In the second subcase Ib, where $df \neq 0$, we redefine the Euler potentials such that $f = -\tilde{\phi}_1$. Because $i_{s_2} i_{s_1} F = 0$, Eq. (2.27) implies that $df \wedge dg = 0$ and thus

$g = g(\tilde{\phi}_1)$. Then,

$$df = i_{s_1} F = -(i_{s_1} d\tilde{\phi}_2) d\tilde{\phi}_1 + (i_{s_1} d\tilde{\phi}_1) d\tilde{\phi}_2 = -d\tilde{\phi}_1, \tag{2.28a}$$

$$dg = i_{s_2} F = -(i_{s_2} d\tilde{\phi}_2) d\tilde{\phi}_1 + (i_{s_2} d\tilde{\phi}_1) d\tilde{\phi}_2 = \frac{\partial g(\tilde{\phi}_1)}{\partial \tilde{\phi}_1} d\tilde{\phi}_1, \tag{2.28b}$$

and we conclude that

$$i_{s_1} d\tilde{\phi}_1 = 0, \qquad i_{s_1} d\tilde{\phi}_2 = 1, \tag{2.29a}$$

$$i_{s_2} d\tilde{\phi}_1 = 0, \qquad i_{s_2} d\tilde{\phi}_2 = -\frac{\partial g(\tilde{\phi}_1)}{\partial \tilde{\phi}_1} \equiv \Omega(\tilde{\phi}_1). \tag{2.29b}$$

Notice that the Euler potentials are invariant under the flow of $s_3 = s_2 - \Omega(\tilde{\phi}_1) s_1$. It is not a Killing vector, except when $\Omega(\tilde{\phi}_1)$ is constant. In particular, since $\tilde{\phi}_1$ is always constant on the field sheet, the vector field s_3 deserves the name of field sheet Killing vector.

In the case II, by choosing the Euler potentials such that $f = -\tilde{\phi}_1$ and $g = (i_{s_2} i_{s_1} F)\tilde{\phi}_2$, one has

$$i_{s_1} d\tilde{\phi}_1 = 0, \qquad i_{s_1} d\tilde{\phi}_2 = 1, \tag{2.30a}$$

$$i_{s_2} d\tilde{\phi}_1 = -i_{s_2} i_{s_1} F, \qquad i_{s_2} d\tilde{\phi}_2 = 0. \tag{2.30b}$$

In the next section, we are going to study stationary and axisymmetric force-free magnetospheres. Later, in Part II, we will relax the assumption of axial symmetry $\mathcal{L}_{\partial_\phi} F = 0$ in favour of axial eigenvalue $\mathcal{L}_{\partial_\phi} F = iqF$. Generalization on the functional form of the Euler potentials can be found in section 5.3.

2.5 Stationary and axisymmetric force-free magnetospheres

Let ∂_ϕ and ∂_t be the two commuting Killing vectors, where ϕ and t are Killing coordinates in a given coordinate system (t, r, θ, ϕ). Moreover, we restrict our considerations to background geometries that are asymptotically flat solutions to Einstein's equations in vacuum, so that we deal with circular space-times (Wald, 1984). In a circular space-time, the Killing vector fields are orthogonal to two-dimensional surfaces. As a consequence, the four-dimensional space-time is split into poloidal

subspaces described by (r,θ) and toroidal subspaces described by (t,ϕ). In particular, the full volume element can be split into poloidal and toroidal volume elements

$$\varepsilon = \sqrt{-g}\,dt\wedge dr\wedge d\theta\wedge d\phi = \left(\sqrt{-g^T}\,dt\wedge d\phi\right)\wedge\left(\sqrt{g^P}\,dr\wedge d\theta\right) = \varepsilon^T\wedge\varepsilon^P, \quad (2.31)$$

obeying the identities $\star\varepsilon^T = -\varepsilon^P$ and $\star\varepsilon^P = \varepsilon^T$.

By considering two commuting symmetries, we fall into the case I discussed before, since the constant $i_{\partial_\phi} i_{\partial_t} F$ vanishes on the axis of rotation.
We have three different scenarios.

- First scenario: $i_{\partial_\phi} F \neq 0$

Let $s_1 = \partial_\phi$ and $s_2 = \partial_t$ be the two commuting vector fields. In the case in which $i_{s_1} F \neq 0$, Eqs. (2.29) implies that

$$i_{s_1} d\phi_1 = \partial_\phi \phi_1 = 0, \qquad i_{s_1} d\phi_2 = \partial_\phi \phi_2 = 1, \quad (2.32a)$$

$$i_{s_2} d\phi_1 = \partial_t \phi_1 = 0, \qquad i_{s_2} d\phi_2 = \partial_t \phi_2 = -\Omega(\phi_1). \quad (2.32b)$$

Thus, the Euler potentials take the following functional form

$$\phi_1 = \psi_1(r,\theta), \quad \phi_2 = \psi_2(r,\theta) + \phi - \Omega(\psi_1)\,t. \quad (2.33)$$

The electromagnetic field strength reads as

$$F = d\psi_1\wedge d\psi_2 + d\psi_1\wedge\left(d\phi - \Omega(\psi_1)\,dt\right). \quad (2.34)$$

Notice that we might write $F = d\left(\psi_1 d\phi_2\right)$ and the quantity $\psi_1 d\phi_2$ plays the role of the gauge potential. Then $i_{\partial_t}(\psi_1 d\phi_2) = -\psi_1\Omega(\psi_1)$ can be interpreted as the electrostatic potential between magnetic field lines. Moreover, there is no (toroidal) electric field component proportional to $dt\wedge d\phi$ because of the Faraday's law (Gralla and Jacobson, 2014).

In order to interpret the physical meaning of the Euler potentials, it is instructive to compute some observables. Let us compute the magnetic flux through the surface $\mathscr{S}$ bounded by the closed line obtained by flowing a poloidal point (r,θ) along the azimuthal vector field ∂_ϕ at t fixed. The surface $\mathscr{S}$ is a two-dimensional surface in the poloidal space. One has

$$\frac{1}{2\pi}\int_{\mathscr{S}} F = \frac{1}{2\pi}\int_{\mathscr{S}} d\psi_1\wedge d\phi_2 = \frac{1}{2\pi}\int_{\mathscr{S}} d\left(\psi_1 d\phi_2\right) = \frac{1}{2\pi}\int_{\partial\mathscr{S}} \psi_1 d\phi_2 = \psi_1(r,\theta). \quad (2.35)$$

Since $\psi_1(r,\theta)$ describes the magnetic flux through a given surface spanned by the poloidal coordinates, it deserves the name of magnetic flux function.
Another enlightening computation is the integration of the 3-form current over the volume generated by the flowing of $\mathscr{S}$ along the vector field ∂_t, which is by definition the electric current along the flow of the Killing time

$$\frac{1}{2\pi\Delta t}\int_{\mathscr{S}\times\Delta t} d\star F = \frac{1}{2\pi\Delta t}\int_{\partial\mathscr{S}\times\Delta t}\star F = \frac{1}{2\pi\Delta t}\int_{\partial\mathscr{S}\times\Delta t}\star\left(d\psi_1\wedge d\psi_2\right)\equiv I(r,\theta). \tag{2.36}$$

In the first step, we have used the Stokes' theorem and we have neglected the two contributions from the top and bottom surfaces of $\mathscr{S}\times\Delta t$ because the field is stationary. In the second step, we have computed the Hodge dual of the field strength F. Since $d\psi_1\wedge d\psi_2 \propto dr\wedge d\theta$, it turns out that $\star\left(d\psi_1\wedge d\psi_2\right)\propto dt\wedge d\phi$, and we have defined $\star\left(d\psi_1\wedge d\psi_2\right) = (I/2\pi)dt\wedge d\phi$. The function $I = I(r,\theta)$ is called the polar current and it generates the toroidal magnetic field in the azimuthal direction. The second term, namely, $\star\left[d\psi_1\wedge\left(d\phi-\Omega(\psi_1)dt\right)\right] = -\star_P d\psi_1\wedge\star_T\left(d\phi-\Omega(\psi_1)dt\right)$ does not contribute to the integral because we are integrating $\star F$ over a surface of constant r and θ.

The third function which characterises the Euler potentials is $\Omega(\psi_1)$. It can be interpreted as the angular velocity of the magnetic field lines. If the angular velocity Ω vanishes, there is no electric field in Eq. (2.34).

- Second scenario: $i_{\partial_\phi}F = 0$ and $i_{\partial_t}F \neq 0$

Let $s_1 = \partial_t$ and $s_2 = \partial_\phi$ be the two commuting vector fields. In the case in which $i_{s_2}F = 0$, Eqs. (2.29) implies that

$$i_{s_1}d\phi_1 = \partial_t\phi_1 = 0, \qquad i_{s_1}d\phi_2 = \partial_t\phi_2 = 1, \tag{2.37a}$$

$$i_{s_2}d\phi_1 = \partial_\phi\phi_1 = 0, \qquad i_{s_2}d\phi_2 = \partial_\phi\phi_2 = 0. \tag{2.37b}$$

Thus, the Euler potentials take the following functional form

$$\phi_1 = \chi_1(r,\theta), \quad \phi_2 = \chi_2(r,\theta) + t. \tag{2.38}$$

The electromagnetic field strength reads as

$$F = d\chi_1\wedge d\chi_2 + d\chi_1\wedge dt. \tag{2.39}$$

In this scenario, there are no terms proportional to $dr\wedge d\phi$ and $d\theta\wedge d\phi$. In other words, the only non-vanishing component of the magnetic field is proportional to

$dr \wedge d\theta$. According to the nomenclature in the literature, this is equivalent to say that there are no poloidal magnetic fields.

- Third scenario: $i_{\partial_\phi} F = 0$ and $i_{\partial_t} F = 0$

This is the simplest scenario. The Euler potentials do not depend on t and ϕ, therefore

$$\phi_1 = \xi_1(r,\theta), \quad \phi_2 = \xi_2(r,\theta), \tag{2.40}$$

and the electromagnetic field strength is simply given by

$$F = d\xi_1 \wedge d\xi_2. \tag{2.41}$$

The 2-form F is proportional to $dr \wedge d\theta$, *i.e.*, there are no poloidal magnetic fields and no electric fields. In other words, F describes only purely toroidal magnetic fields.

2.5.1 Force-free condition

The three scenarios presented above concern generic degenerate, stationary and axisymmetric electromagnetic fields F. Now, we want to make explicit the physical meaning of the force-free condition (2.20) for the first scenario (2.34), which is the most general one.

The first of the two equations in (2.20) is $d\left(d\psi_1 \wedge \star F\right) = 0$. As noticed earlier, the 3-form in parenthesis is the Euler current and it is conserved. It can be shown that the Euler current conservation amounts to the conservation of energy and angular momentum (Gralla and Jacobson, 2014). To see this, let J_ξ be the Noether current associated to the Killing vector ξ

$$J_\xi = -i_\xi F \wedge \star F + \frac{1}{2} i_\xi \left(F \wedge \star F\right) = -i_\xi F \wedge \star F + \frac{1}{4} F^2 i_\xi \varepsilon. \tag{2.42}$$

In the case of $\xi = \{\partial_t, \partial_\phi\}$ and using Eqs. (2.32), one gets

$$i_{\partial_t} F = i_{\partial_t}\left(d\phi_1 \wedge d\phi_2\right) = -(i_{\partial_t} d\phi_2) d\phi_1 + (i_{\partial_t} d\phi_1) d\phi_2 = \Omega(\psi_1) d\psi_1, \tag{2.43a}$$

$$i_{\partial_\phi} F = i_{\partial_\phi}\left(d\phi_1 \wedge d\phi_2\right) = -(i_{\partial_\phi} d\phi_2) d\phi_1 + (i_{\partial_\phi} d\phi_1) d\phi_2 = -d\psi_1. \tag{2.43b}$$

The Noether currents are then

$$J_{\partial_t} = -\Omega(\psi_1) d\psi_1 \wedge \star F + \frac{1}{4} F^2 i_{\partial_t} \varepsilon, \tag{2.44a}$$

$$J_{-\partial_\phi} = -d\psi_1 \wedge \star F - \frac{1}{4} F^2 i_{\partial_\phi} \varepsilon. \tag{2.44b}$$

By computing the exterior derivative of Eqs. (2.44), the second term in both expressions is conserved by itself.[4] Thus, both the conservation of energy and the conservation of angular momentum follow from the first constraint $d\left(d\psi_1 \wedge \star F\right) = 0$. It is interesting to explicit the constraint:

$$\begin{aligned} 0 = d\psi_1 \wedge d\star F = d\psi_1 \wedge d\left\{\frac{I}{2\pi} dt \wedge d\phi + \star\left[d\psi_1 \wedge \left(d\phi - \Omega(\psi_1) dt\right)\right]\right\}, \\ = \frac{1}{2\pi} d\psi_1 \wedge dI \wedge dt \wedge d\phi + d\psi_1 \wedge d\star\left[d\psi_1 \wedge \left(d\phi - \Omega(\psi_1) dt\right)\right]. \end{aligned} \tag{2.45}$$

The second term contains necessarily three poloidal 1-forms: one from the $d\psi_1$ and two from $d\star\left[d\psi_1 \wedge \left(d\phi - \Omega(\psi_1) dt\right)\right]$, as can be checked by explicit computations. Therefore, since the poloidal subspace is two-dimensional, it must vanish identically. Thus, we conclude that the polar current must be a function of the magnetic flux function, *i.e.*, $I = I(\psi_1)$. We want to emphasise that all the results obtained so far are valid for a generic stationary, axisymmetric field such that it conserves the energy and angular momentum. Force-free magnetospheres must obey also the second constraint, that we are going to discuss now.

The second of the two equations in (2.20), $d\left(d\phi_2 \wedge \star F\right) = 0$, gives a non-linear partial differential equation for the magnetic flux function ψ_1 known as stream equation (sometimes also dubbed as Grad-Shafranov equation). Expanding the constraint, one has (Gralla and Jacobson, 2014)

$$d\star\left(i_\eta \eta\, d\psi_1\right) = \left[\frac{I(\psi_1) I'(\psi_1)}{4\pi^2 g^T} - \Omega'(\psi_1) i_{d\psi_1} d\psi_1 i_\eta dt\right] \varepsilon, \tag{2.46}$$

where $\eta = d\phi - \Omega(\psi_1) dt$ is the co-rotation 1-form and the prime denotes derivation with respect to the flux function ψ_1. Hence, the stream equation (2.46) also constrains the magnetic flux function ψ_1 in terms of the unknown polar current $I(\psi_1)$ and the unknown angular velocity $\Omega(\psi_1)$. This highlights the difficulties to find exact analytical solutions in Kerr space-time much better than any word. Known classes of solutions have been found by restricting the dependence of ψ_1 to only one poloidal coordinate. This approach converts the stream equation to an ordinary differential equation. The two notable examples in literature are the class of solutions of null type ($F^2 = 0$) where ψ, I and Ω do not depend on the radial coordinate (Menon and Dermer, 2005; Menon and Dermer, 2007; Menon and Dermer, 2011) and the class of solutions of magnetic type ($F^2 > 0$) where ψ, I and Ω do not depend on the polar coordinate (Menon, 2015). These exact analytical solutions share the property that the current is null. By making the ansatz of null

[4] This is readily seen because $\frac{1}{4} F^2 i_\xi \varepsilon = -i_\xi L$, where $L = -\frac{1}{2}(F \wedge \star F)$ is the Lagrangian density. Then, $d i_\xi L = \mathscr{L}_\xi L - i_\xi dL = \mathscr{L}_\xi L = 0$ if ξ is a symmetry of the theory.

current, Brennan, Gralla, and Jacobson (2013) discovered a larger class of exact solutions of null type. Another way to find exact analytical solutions is to convert the stream equation (2.46) in an equation for the foliation of the field lines (Compère, Gralla, and Lupsasca, 2016). Despite of this effort, no other new solutions have been found in Kerr space-time.

2.5.2 Energy and angular momentum extraction

We might make use of the Noether currents (2.44) to investigate the flux of energy and angular momentum through a given three-surface. We first notice that the integral of (the pullback of) the currents on surfaces where $\psi_1(r,\theta) = \text{const}$ vanish; this is equivalent to say that there is no flux of energy or angular momentum through a poloidal two-surface and the fluxes flow along these poloidal surfaces in the toroidal directions. Let us define the three-surface $\Sigma = \mathscr{P} \times S^1 \times \Delta t$ generated by a curve $\mathscr{P}$ in the poloidal space rotated around the axis of symmetry and evolved along the Killing time Δt. Then

$$\int_\Sigma J_{\partial_t} = -\int_\Sigma \Omega(\psi_1) d\psi_1 \wedge \star F + \frac{1}{4}\int_\Sigma F^2 i_{\partial_t}\varepsilon = -\int_\Sigma \Omega(\psi_1) d\psi_1 \wedge \frac{I(\psi_1)}{2\pi} dt \wedge d\phi, \tag{2.47a}$$

$$\int_\Sigma J_{-\partial_\phi} = -\int_\Sigma d\psi_1 \wedge \star F - \frac{1}{4}\int_\Sigma F^2 i_{\partial_\phi}\varepsilon = -\int_\Sigma d\psi_1 \wedge \frac{I(\psi_1)}{2\pi} dt \wedge d\phi. \tag{2.47b}$$

In the first step, the second integrals vanish because so does the pullback of the interior product $i_{\partial_t}\varepsilon$ (respectively, $i_{\partial_\phi}\varepsilon$) to a surface including the ∂_t (respectively, ∂_ϕ) direction. In the second step, we just considered the toroidal part of the integrand because the integration is performed over a 3-surface extending in the time and azimuthal directions. Performing the integration after the last step, one obtains the flux of energy and angular momentum, respectively, given by the following line integrals

$$\frac{d\mathscr{E}}{dt} = -\int_{\mathscr{P}} \Omega(\psi_1) I(\psi_1) d\psi_1, \tag{2.48a}$$

$$\frac{d\mathscr{L}}{dt} = -\int_{\mathscr{P}} I(\psi_1) d\psi_1. \tag{2.48b}$$

Notice that, for constant angular velocity Ω, we have $d\mathscr{E}/dt = \Omega\, d\mathscr{L}/dt$ and an outflow of energy is always accompanied by an outflow of angular momentum.

2.6 The Blandford-Znajek mechanism

In this section, we consider Kerr black hole as fixed background geometry and we investigate force-free electrodynamics on such a space-time. The presence of the ergo-region and the event horizon plays a fundamental physical role in the description of force-free magnetospheres. The former allows the extraction of rotational energy of Kerr black hole via force-free electromagnetic fields (Blandford and Znajek, 1977), the latter acts as a surface where to impose the boundary condition[5] (Znajek, 1977).

2.6.1 The Blandford-Znajek monopole solution

Blandford and Znajek (1977) found a perturbative solution, to the second order in the angular momentum parameter a, describing the stationary and axisymmetric force-free magnetosphere around Kerr space-time. Before 1977, the only exact solution to force-free electrodynamics was the Michel (1973) solution, which can be thought of as a particular superposition of the vacuum monopole solution and the Poynting flux solution.

To illustrate the basic idea, we start with the vacuum magnetic monopole solution to source-free Maxwell equations on Schwarzschild space-time

$$F^{mon} = q\sin(\theta)d\theta\wedge d\phi = d\left(-q\cos(\theta)\right)\wedge d\phi, \tag{2.49}$$

where q is the (magnetic) monopole charge. This solution is also a trivial solution to force-free electrodynamics in the sense that it has no current $d\star F^{mon}=0$. The Poynting flux solution to force-free electrodynamics on Schwarzschild space-time is

$$F^{flux} = d\zeta(u,\theta,\phi)\wedge du, \tag{2.50}$$

where $\zeta(u,\theta,\phi)$ is an arbitrary function of the retarded time u and the spherical coordinates (Brennan, Gralla, and Jacobson, 2013). It turns out that the linear superposition of F^{mon} and F^{flux} gives rise to a new solution to force-free electrodynamics. This is not true in general, because force-free electrodynamics is non-linear. Then

$$F = q\sin(\theta)d\theta\wedge d\phi + d\zeta(u,\theta,\phi)\wedge du. \tag{2.51}$$

[5]The Znajek's horizon boundary condition follows from the stream equation (2.46) and corresponds to the regularity condition of the electromagnetic field on the future event horizon (MacDonald and Thorne, 1982).

This class of solutions has been proved to be the general force-free solution with radial and null current in Schwarzschild space-time (Brennan, Gralla, and Jacobson, 2013; Gralla and Jacobson, 2014). The celebrated Michel's monopole solution is recovered by choosing the Euler potential in the Poynting flux solution as $\zeta = q\Omega\cos(\theta)$

$$F^{Michel} = q\sin(\theta)d\theta\wedge\left(d\phi-\Omega du\right). \tag{2.52}$$

Blandford and Znajek (1977) noticed that the Michel's field strength remains solution to force-free electrodynamics in Schwarzschild when the angular velocity is promoted to an arbitrary function of the polar angle $\Omega=\Omega(\theta)$ and $\zeta=-q\int\sin(\theta)\Omega(\theta)d\theta$. Another generalisation of the Michel's solution was found by Lyutikov (2011), who realised that Ω can also be a function of the retarded time and $\zeta=-q\int\sin(\theta)\Omega(u,\theta)d\theta$.

In Kerr space-time, the superposition procedure fails. Nevertheless, up to the first order in the angular momentum parameter, the Blandford-Znajek solution is nothing but the Michel's solution with $\Omega\sim\mathcal{O}(a)$ (Gralla and Jacobson, 2014). Thus,

$$F^{BZ} = q\sin(\theta)d\theta\wedge\left(d\phi-\Omega du\right). \tag{2.53}$$

Of course, the coordinate u is the outgoing Kerr coordinate. The co-rotating 1-form $d\phi-\Omega du$ in outgoing Kerr coordinates must be regular on the event horizon. To this end, we transform the 1-form to ingoing Kerr coordinates, v and $\tilde{\phi}$, that are regular on the future event horizon, and are defined by

$$du = dv - 2\frac{r^2+a^2}{\Delta(r)}dr, \tag{2.54a}$$

$$d\phi = d\tilde{\phi} - \frac{a}{\Delta(r)}dr, \tag{2.54b}$$

where $\Delta(r)$ is defined in Eqs. (1.2). One has that

$$d\phi-\Omega du = d\tilde{\phi}-\Omega dv + \frac{2\Omega(r^2+a^2)-\Omega_+(r_+^2+a^2)}{\Delta(r)}dr. \tag{2.55}$$

The coefficient of dr must vanish at the horizon $r=r_+$ in order to guarantee regularity of the 1-form. This implies that $\Omega=\frac{1}{2}\Omega_+=\frac{1}{2}\frac{a}{2Mr_+}\sim\mathcal{O}(a)$, that is consistent with the ansatz (2.53).

Of course, the monopole solution (2.53) is not realised in Nature. Nevertheless, it is possible to build a more realistic solution, as done by Blandford and Znajek in their original paper, by splitting the monopole solution in the equatorial plane and by gluing the upper and lower monopole solutions to cancel the total magnetic monopole charge. The splitting procedure implies the presence of a surface charge and a surface current localised in the equatorial plane. In other words, the

split monopole solution is a crude model for (force-free) electromagnetic fields sourced by accretion discs in the equatorial plane.

2.6.2 The Blandford-Znajek energy extraction

The Blandford-Znajek mechanism is a Penrose-like process (see, *e.g.*, Komissarov, 2009; Ruiz et al., 2012; Lasota et al., 2014; Koide and Baba, 2014). In order to evaluate the explicit expressions of the flux of energy and angular momentum in Eqs. (2.48), we have to compute the expression of the polar current $I(\psi_1)$ defined in Eq. (2.36) in the case of the Kerr space-time. Let $\chi = \partial_t + \Omega_+ \partial_\phi$ be the horizon-generating Killing vector field and Ω_+ be the angular velocity of the event horizon. We first notice that, by using the expression (2.34) for the electromagnetic field, one obtains

$$i_\chi F = \big(\Omega(\psi_1) - \Omega_+\big)\, d\psi_1, \tag{2.56}$$

which can be interpreted as the variation of the electrostatic potential between the event horizon and the magnetic field line in the context of the membrane paradigm (Thorne, Price, and Macdonald, 1986). The polar current is, by definition (see discussion below Eq. (2.36)), proportional to the toroidal component of $\star F$. Hence, as shown in Gralla and Jacobson (2014), it is given by

$$\frac{I}{2\pi} = i_{\partial_\phi} i_\chi\, (\star F) = \big(\Omega(\psi_1) - \Omega_+\big)\, (\partial_\theta \psi_1) \sqrt{\frac{g_{\phi\phi}}{g_{\theta\theta}}}. \tag{2.57}$$

This expression, when evaluated on the future event horizon, is the Znajek's horizon boundary condition (Znajek, 1977). Actually, it is better to say that the Znajek's boundary condition is simply a consistency condition. MacDonald and Thorne (1982) showed that it directly comes from the stream equation (2.46) evaluated on the horizon. This condition guarantees the force-free electromagnetic field to be regular there. Substituting the polar current into the expressions for the fluxes (2.48), one gets

$$\frac{d\mathscr{E}}{dt} = 2\pi \int_0^\pi \Omega(\psi_1)\, \big(\Omega_+ - \Omega(\psi_1)\big)\, (\partial_\theta \psi_1)^2 \sqrt{\frac{g_{\phi\phi}}{g_{\theta\theta}}}\, d\theta, \tag{2.58a}$$

$$\frac{d\mathscr{L}}{dt} = 2\pi \int_0^\pi \big(\Omega_+ - \Omega(\psi_1)\big)\, (\partial_\theta \psi_1)^2 \sqrt{\frac{g_{\phi\phi}}{g_{\theta\theta}}}\, d\theta. \tag{2.58b}$$

Notice that the outflow of energy comes along the outflow of angular momentum. In order to have a positive outflow of energy, the angular velocity of the magnetic

field lines must be bounded from above by the angular velocity of the event horizon, $0 \leq \Omega(\psi_1) \leq \Omega_+$. Indeed, there exists a thermodynamical argument for the existence of an upper bound of the energy extracted (Gralla and Jacobson, 2014). From the null energy condition, the electromagnetic energy-momentum tensor obeys the inequality

$$0 \leq T_{\mu\nu}\chi^\mu\chi^\nu = T_{\mu\nu}\left(\partial_t\right)^\mu\chi^\nu - \Omega_+ T_{\mu\nu}\left(-\partial_\phi\right)^\mu\chi^\nu = -\delta\mathscr{E} + \Omega_+\delta\mathscr{L}. \tag{2.59}$$

The ratio between the two angular velocities $\Omega(\psi_1)/\Omega_+$ is the efficiency of the energy extraction process. In the framework of the membrane paradigm, such a ratio represents the circuit efficiency (see Fig. 38 in Thorne, Price, and Macdonald, 1986). The maximum efficiency at fixed magnetic flux is reached for $\Omega(\psi_1) = 1/2\ \Omega_+$, which is the value for which the electromagnetic field of the Blandford-Znajek solution is regular on the horizon, as shown below Eq. (2.55). Another reason for which $\Omega(\psi_1) = 1/2\ \Omega_+$ is that it maximizes the power of energy emission. Indeed, from the flux of energy (2.48), the power (per unit length) is proportional to $\Omega(\psi_1)\left(\Omega_+ - \Omega(\psi_1)\right)$ and it is maximum for $\Omega(\psi_1) = 1/2\ \Omega_+$. This result is confirmed by numerical simulations of jets dynamics (Penna, 2015).

Chapter 3

Thin accretion disc

Contents

In this chapter, we introduce the reader to the physics of accretion discs and, in particular, of thin accretion discs. We provide some astrophysical motivations to the subject to motivate the reader with this fascinating topic in section 3.1. In section 3.2, we write down the most fundamental equations governing the accretion phenomenon: the energy balance equation and the relativistic Navier-Stokes equations. Then, in section 3.3, we first introduce the approximations characterising the thin accretion disc and then we provide a step-by-step derivation of the fundamental equations governing the dynamics of the disc. Section 3.4 is devoted to the well-known Novikov-Thorne model of thin accretion discs and section 3.5

lists the local solutions of the model in certain particular regimes of interest for our later purposes.

3.1 Astrophysical motivations

The first indirect observational evidence of an astrophysical black hole is dated back to the paper of Schmidt (1963) with the identification of the quasar[1] 3C 273 located at redshift $z = 0.158$ with luminosity $L \approx 10^{46}$ erg s^{-1}. In order to explain the total luminosity, Lynden-Bell (1969) proposed a model consisting of a massive black hole, located at the centre of the host galaxy, accreting the surrounding matter. The model describes a mechanism, the accretion process onto the black hole, in which the accreting matter forms a disc-like object - the accretion disc - where loss of angular momentum due to viscosity effects heats the gas that radiates away efficiently its gravitational energy.

First attempts to describe accretion of interstellar gas by stars have been proposed by Hoyle, Lyttleton and Bondi in the 1940s. One very crude approximation in these models was to neglect the effects of pressure with respect to dynamical effects. The reason of this approximation lies in the fact that the heat generated during the accretion process would be radiated away very efficiently. In 1952, Bondi introduced his model (Bondi, 1952), where the pressure effects were considered. The model assumes a black hole surrounded by a cloud of gas, accreting with stationary and spherically symmetric motion. The model neglects any self-gravity effects of the cloud, magnetic fields, angular momentum and viscosity due to the accretion mechanism.

Several analytical models of accretion discs have been proposed after the seminal paper of Bondi. Each of them describes different types of accretion discs (see, *e.g.*, the review of Abramowicz and Fragile, 2013), based on certain relevant physical parameters like, *e.g.*, the geometrical thickness, the optical depth, the accretion rate and efficiency. The most important scale in the accretion process is the so-called Eddington accretion rate $\dot{M}_{Edd}$ (Eddington, 1988). It is defined as a fraction, denoted by η, of the maximum luminosity $L_{Edd} = \eta \dot{M}_{Edd} c^2$ produced during the accretion process of a spherically distributed cloud of fully ionised hydrogen (where electrons and photons interact via Thomson scattering). By equating

[1] A quasar, or quasi-stellar-object (QSO), is an active galactic nucleus (AGN) consisting of a massive black hole surrounded by an accretion disc of gas.

the radiation force (acting outward) and the gravitational force (acting inward) exerted on a single electron, it is easy to show that

$$\dot{M}_{Edd} = \frac{L_{Edd}}{\eta c^2} = \frac{4\pi G}{c\bar{\kappa}_{es}}\frac{M}{\eta} = 2.2\times 10^{-8}\left(\frac{\eta}{0.1}\right)^{-1}\left(\frac{M}{M_\odot}\right) M_\odot \text{ yr}^{-1}. \tag{3.1}$$

Here $\bar{\kappa}_{es}$ is the electron-scattering Thomson opacity. Thin accretion discs describe accretion flows with $\dot{M} < \dot{M}_{Edd}$, slim accretion discs describe accretion flows at roughly the Eddington rate $\dot{M} \approx \dot{M}_{Edd}$ and thick accretion discs are consistent with super-Eddington accretion rates $\dot{M} \gg \dot{M}_{Edd}$ (Abramowicz et al., 1988).

In this chapter, we will derive the Novikov-Thorne model of thin accretion disc, originally presented in Novikov and Thorne (1973). It describes a geometrically thin and optically thick accretion disc and it extends the non-relativistic version of Shakura and Sunyaev (1973). Further extensions and refinements of the model have been published in Page and Thorne (1974) for the equations governing the radial structure of the disc, in Lightman and Eardley (1974) for the introduction of the magnetic viscosity, in Riffert and Herold (1995) and in Abramowicz, Lanza, and Percival (1997) for corrections about the vertical equilibrium equation, and in Li (2002) for the introduction of the magnetic coupling between the disc and the black hole.

For sake of completeness, we also mention other well-established accretion disc models. The slim accretion disc model, firstly introduced by Abramowicz et al. (1988), describes a geometrically slim and optically thick disc, where advection effects and radial pressure gradients are taken into account. Geometrically thick accretion disc models were introduced by Jaroszynski, Abramowicz, and Paczynski (1980), Paczyński and Wiita (1980) and Paczynski and Abramowicz (1982). They describe optically thick discs with negligible accretion efficiency. There also exist analytical models constructed by Abramowicz et al. (1996) and Gammie and Popham (1998) describing optically thin accretion discs with sub-Eddington accretion rate and dominated by the advection mechanism: the advection-dominated accretion flow (ADAF) models.

The plethora of models needs to understand observational data and to test our theoretical knowledge of the topic. Indeed, these models – along with numerical simulations – serve to fit both thermal and non-thermal emissions from AGN and to estimate the black hole parameters. We would like to recall the main efforts in this direction. Accretion models are tested via the continuum X-ray spectra observed during the thermally-dominant state of the accretion disc emission (see, *e.g.*, Miller, Fabian, and Miller, 2004; Shafee et al., 2006; Davis, Done, and Blaes, 2006; McClintock et al., 2006). Another interesting applications of accretion

disc models is the fitting of the Iron $K\alpha$ line profiles (see, *e.g.*, Karas et al., 2000; Reynolds and Fabian, 2008), the quasi-periodic oscillations (QPOs) (see, *e.g.*, Cui, Zhang, and Chen, 1998; Abramowicz and Kluzniak, 2001; Török, G. et al., 2005), and the black hole's shadow (Falcke, Melia, and Agol, 2000; Takahashi, 2004; Johannsen et al., 2016; Fish et al., 2016).

One important theoretical aspect, that is not yet fully understood at the present, is the stability of the analytical models mentioned above. It is well-known that the magneto-rotational instability (MRI) (Balbus and Hawley, 1991; Balbus and Hawley, 1998) plays a fundamental role in the accretion mechanism. Indeed, it explains how turbulence arises, transports angular momentum in the disc with weak magnetic fields, and enhances the effective viscosity of the disc. Another aspect to analyse is the thermal-viscosity instability of the model. It arises when the radiative cooling varies slower than the heating due to viscosity. For instance, it is known that radiation-dominated regions of thin accretion discs are both thermally and viscously unstable (Lightman and Eardley, 1974; Shibazaki and Hoshi, 1975; Shakura and Sunyaev, 1976). At present, there are no stabilisation mechanisms to avoid these instabilities and, therefore, disc models suffering from these instabilities are not expected to occur in Nature and to exist in steady-state configurations.

3.2 Fundamental equations

Let $T^{\mu\nu}$ be the energy-momentum tensor of a single component relativistic viscous fluid. Without any loss of generality, we can algebraically decompose $T^{\mu\nu}$ with respect to the four-velocity vector u^μ. The decomposition reads as

$$T^{\mu\nu} = \epsilon u^\mu u^\nu + t^{\mu\nu} + u^\mu q^\nu + q^\mu u^\nu. \tag{3.2}$$

Here $\epsilon = \rho + \Pi$ is the total energy density, with ρ being the rest-mass density and Π being the internal energy density, $t^{\mu\nu}$ represents the (symmetric) transverse stress-tensor, and q^μ is the transverse heat flux. All the quantities in Eq. (3.2) are referred to the local rest frame (LRF; see appendix B.3 for details) and all the indices are raised with $g^{\mu\nu}$. We adopt $g_{\mu\nu}$ to be the Kerr space-time metric. Hence, the background geometry is asymptotically flat, stationary, axisymmetric, and reflection-symmetric with respect to the equatorial plane. The disc is assumed not to self-gravitate and not to self-irradiate. Magnetic fields are ignored except for their contribution to the stresses. We also neglect neutrinos and dark matter. It is useful to

factor out the isotropic pressure in Eq. (3.2) and write the energy-momentum tensor as

$$T^{\mu\nu} = \rho\eta u^\mu u^\nu + p g^{\mu\nu} + S^{\mu\nu} + u^\mu q^\nu + q^\mu u^\nu, \tag{3.3}$$

where we have defined the relativistic enthalpy $\eta = (\epsilon + p)/\rho$. The symmetric, transverse and traceless tensor $S^{\mu\nu}$ is the anisotropic stress-tensor responsible, for instance, of viscous and magnetic stresses. From the four-velocity u^μ, we can construct the projector operator $h^{\mu\nu} = u^\mu u^\nu + g^{\mu\nu}$ and define the following kinematical quantities

$$\theta \equiv u^\mu_{\ ;\mu}, \quad a^\mu \equiv u^\nu u^\mu_{\ ;\nu}, \tag{3.4}$$

$$\omega_{\mu\nu} \equiv h^\alpha_{\ \mu} h^\beta_{\ \nu} u_{[\alpha;\beta]}, \quad \theta_{\mu\nu} \equiv h^\alpha_{\ \mu} h^\beta_{\ \nu} u_{(\alpha;\beta)}, \quad \sigma_{\mu\nu} \equiv \theta_{\mu\nu} - \frac{1}{3} h_{\mu\nu}\theta, \tag{3.5}$$

respectively, the expansion scalar, the acceleration, the vorticity tensor, the expansion tensor and the shear tensor. The covariant derivative of the four-velocity vector is, therefore, decomposed as $u_{\mu;\nu} = \theta_{\mu\nu} + \omega_{\mu\nu} - a_\mu u_\nu$.

The vanishing covariant divergence $T^{\mu\nu}_{\ \ ;\nu} = 0$, expressing the energy-momentum conservation, is equivalent to

$$(\epsilon u^\nu)_{;\nu} = -(S^{\nu\sigma}\sigma_{\nu\sigma} + q^\nu a_\nu + q^\nu_{\ ;\nu} + p\theta), \tag{3.6}$$

$$(\epsilon + p) a^\mu + h^\mu_{\ \rho}\left(g^{\rho\nu} p_{,\nu} + S^{\rho\nu}_{\ \ ;\nu} + u^\nu q^\rho_{\ ;\nu}\right) + \left(\sigma^\mu_{\ \nu} + \omega^\mu_{\ \nu} + \frac{4}{3}\theta h^\mu_{\ \nu}\right) q^\nu = 0. \tag{3.7}$$

The first equation is the component of $T^{\mu\nu}_{\ \ ;\nu} = 0$ along the four-velocity u^μ and it is often referred to as the energy balance equation, because it takes into account all the forms of energies involved in the accretion process. The second equation is the projection of $T^{\mu\nu}_{\ \ ;\nu} = 0$ onto the three-dimensional space orthogonal to u^μ and we refer to it as the relativistic Navier-Stokes equations or momentum balance equations. Indeed, these equations can be interpreted as balance equations for the force densities in the three dimensional space orthogonal to the four-velocity u^μ. These fundamental equations must be supplemented by the equation of state, the radiative energy transport law and prescriptions about the nature of the viscous stresses and opacity, as we shall discuss below.

Before introducing the working assumptions and the approximations that we need to treat these equations on the analytical ground, it is instructive to have a closer look at them and exploit the physical meaning of the terms appearing in the energy balance equation (3.6) and in the three relativistic Navier-Stokes equations (3.7).

3.2.1 Energy balance equation

The left-hand-side of Eq. (3.6) gives the total energy density production rate (per unit time and unit volume) along the four-vector u^μ of the fluid. From the definition of the total energy density, we have $(\epsilon u^\mu)_{;\mu} = (\rho u^\mu)_{;\mu} + (\Pi u^\mu)_{;\mu} = (\Pi u^\mu)_{;\mu}$, because of the rest-mass conservation $(\rho u^\mu)_{;\mu} = 0$. Then, the energy equation (3.6) reads

$$(\Pi u^\mu)_{;\mu} = -(S^{\mu\nu}\sigma_{\mu\nu} + q^\mu a_\mu + q^\mu_{;\mu} + p\theta). \tag{3.8}$$

In words, the production of internal energy in the fluid frame is due to the energy generated by viscous shear stresses $S^{\mu\nu}\sigma_{\mu\nu}$, by the inertia of the heat flux $q^\mu a_\mu$,[2] by radiative losses $q^\mu_{;\mu}$ and by compression $p\theta$. To maintain contact with the literature, it easy to check that Eq. (3.8) might be written as (see, *e.g.*, Gammie and Popham, 1998; Ellis, 2009)

$$u^\mu\left[\partial_\mu\Pi - \frac{\Pi + p}{\rho}\partial_\mu\rho\right] = Q_{diss} - Q_{cool}, \tag{3.9}$$

where $Q_{diss} = -S^{\mu\nu}\sigma_{\mu\nu}$ is the dissipative term due to viscous stresses and $Q_{cool} = q^\mu_{;\mu} + q^\mu a_\mu$ is the cooling term due to radiation losses. The physical interpretation of the left-hand-side is manifest if we introduce the specific entropy: it is the advection term. To this aim, we write the energy equation (3.6) in an equivalent form by using the first law of thermodynamics and assuming thermal equilibrium. We define the specific total energy density $u = \epsilon/\rho$, the specific volume $v = 1/\rho$ and the specific entropy s. The first law of thermodynamics $Tds = du + pdv$ becomes $\rho Tds = d\epsilon - \eta d\rho$ and the energy balance equation (3.6) takes the form

$$\rho Tu^\mu s_{,\mu} + \eta(\rho u^\mu)_{;\mu} = -(S^{\mu\nu}\sigma_{\mu\nu} + q^\mu a_\mu + q^\mu_{;\mu}). \tag{3.10}$$

After imposing rest mass conservation $(\rho u^\mu)_{;\mu} = 0$, we obtain the rate of change of the specific entropy along the four-velocity u^μ (see, *e.g.*, Peitz and Appl, 1997; Ellis, 2009)

$$\rho Tu^\mu s_{,\mu} = -(S^{\mu\nu}\sigma_{\mu\nu} + q^\mu a_\mu + q^\mu_{;\mu}). \tag{3.11}$$

The quantity on the left-hand-side is the advection term, $Q_{adv} = \rho Tu^\mu s_{,\mu}$, that takes into account the rate of change of the specific entropy along the four-velocity. Thus, Eq. (3.11) might be written as

$$Q_{adv} = Q_{diss} - Q_{cool}. \tag{3.12}$$

[2] This term is a purely relativistic correction and we will neglect it in the non-relativistic regime.

Therefore, the dissipation of energy involves both the advection and cooling effects.

More generally, the entropy must obey the second law of thermodynamics. We define the entropy four-current $J_s^\mu = s\rho u^\mu + q^\mu/T$ and the entropy production must be always non-negative, *i.e.*,

$$0 \leq J^\mu_{s\ ;\mu} = -\frac{1}{T} S^{\mu\nu}\sigma_{\mu\nu} - \frac{1}{T^2} q^\mu (T_{,\mu} + T a_\mu), \tag{3.13}$$

where, in the second step, we used the rest-mass conservation law and Eq. (3.11). Thus, the second law of thermodynamics implies the two constitutive equations

$$S^{\mu\nu} = -\xi\sigma^{\mu\nu}, \qquad q^\mu = -\lambda h^{\mu\nu}(T_{,\nu} + T a_\nu) \qquad \text{with} \qquad \xi, \lambda \geq 0, \tag{3.14}$$

with ξ and λ being the shear viscosity and heat conduction coefficients, respectively. We neglect bulk viscosity in our discussion by following the traditional assumption in the literature.[3]

3.2.2 Relativistic Navier-Stokes equations

The relativistic Navier-Stokes equations (3.7) can be rewritten in a more compact form as

$$(\epsilon + p)a^\mu + h^\mu_{\ \rho} g^{\rho\nu} p_{,\nu} + S^\mu + Q^\mu = 0. \tag{3.15}$$

The first term is proportional to the four-acceleration a^μ and it takes into account the gravitational acceleration due to the presence of the black hole; the second term describes the acceleration due to pressure gradients in the fluid flow. The contributions to the acceleration due to anisotropic viscous stresses S^μ and the heat flux Q^μ are, respectively, written as

$$S^\mu = h^\mu_{\ \rho} S^{\rho\nu}_{\ \ ;\nu}, \tag{3.16}$$

$$Q^\mu = h^\mu_{\ \rho}\left(u^\nu q^\rho + u^\rho q^\nu\right)_{;\nu} = h^\mu_{\ \rho} u^\nu q^\rho_{\ ;\nu} + \left(\sigma^\mu_{\ \nu} + \omega^\mu_{\ \nu} + \frac{4}{3}\theta h^\mu_{\ \nu}\right) q^\nu. \tag{3.17}$$

The aim of the next section is to introduce physically meaningful approximations to analytically deal with the energy balance and relativistic Navier-Stokes equations. This programme will be explicitly presented for the case of geometrically thin accretion discs. The outcome is the celebrated Novikov-Thorne model of a thin accretion disc (Novikov and Thorne, 1973; Page and Thorne, 1974).

[3] However, in an optically thick disc in the pressure-dominated phase, the presence of a shear viscosity gives rise to a bulk viscosity of comparable magnitude (Papaloizou and Pringle, 1977). See also the recent work by Moeen Moghaddas (2016).

3.3 The thin disc approximation

From the fundamental equations (3.6) and (3.7), we shall derive the explicit expressions of the rest-mass, energy and angular momentum conservation laws and the radial and vertical equilibrium equations. This goal is achieved by implementing certain working assumptions and averaging approximations (see, *e.g.*, Novikov and Thorne, 1973; Page and Thorne, 1974). We will explicitly state those assumptions in order to simplify the physical description of the accretion flow and to keep our discussion on the analytical ground.

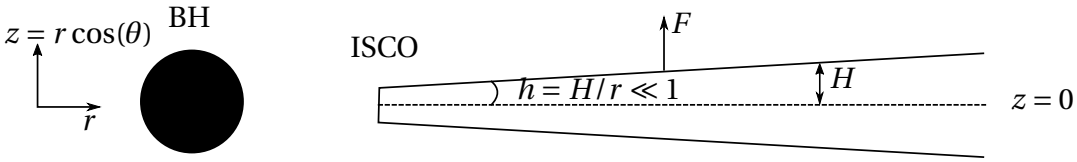

FIGURE 3.1: Schematic representation of thin accretion disc. Here $h \ll 1$ is the opening angle, H is the half-thickness of the disc and F is the flux of radiant energy off the upper surface

We assume that the angular momentum of the accreting flow is parallel to the angular momentum of the black hole. This alignment is due to the Lense-Thirring effect which causes the gradual transition of the tilted disc into the equatorial plane, also known as Bardeen-Petterson effect (Bardeen and Petterson, 1975). The Kerr metric near the equatorial plane, where the disc lies, is written in Eq. (B.3) in coordinates $(t, r, z = r\cos\theta, \phi)$ up to $\mathcal{O}(z/r)$. The disc is assumed to be geometrically thin, *i.e.*, there exists a characteristic angular scale $h(r) = \sin(H(r)/r) \approx H(r)/r \ll 1$, where $H(r)$ is the half-thickness of the disc about the equatorial plane, located at $z = 0$ (or equivalently at $\theta = \pi/2$).

On general ground, the accretion process is a complicated ensemble of different physical phenomena with different characteristic time-scales. We might identify three time-scales: the characteristic times of the fluid orbital motion, of the thermal processes and that of the viscous mechanisms, respectively, defined by (see, *e.g.*, Lasota, 2016)

$$t_{orb} = \frac{1}{\Omega_c}, \quad t_{th} = \frac{1}{\alpha}\frac{1}{\Omega_c} = \frac{1}{\alpha}t_{orb}, \quad t_{vis} = \frac{1}{\alpha}\left(\frac{H}{r}\right)^{-2} t_{orb}. \tag{3.18}$$

Here Ω_c is the angular velocity of circular equatorial orbits in the Kerr space-time and H is the vertical depth of the disc with respect to the equatorial plane. The effective parameter α, originally introduced by Shakura and Sunyaev (1973), describes magnetic and turbulent stresses in the disc by assuming that the shear stresses (in the LRF) are proportional to the total pressure $S_{\hat{r}\hat{\phi}} = \alpha p$. Moreover, it

obeys the bound $\alpha < 1$, because the characteristic speed of the turbulent motion is bound from above by the speed of sound (Shakura and Sunyaev, 1973; Novikov and Thorne, 1973). The characteristic times in Eq. (3.18) obey the following hierarchy

$$t_{orb} < t_{th} \ll t_{vis}, \tag{3.19}$$

because $\alpha < 1$ and, for geometrically thin discs, $H \ll r$. The hierarchical relation (3.19) implies that the time-scale of the viscous mechanisms is much longer than the time-scales of the fluid dynamics and thermal processes and, as a consequence, we are allowed to consider the disc in hydrostatic equilibrium in its vertical structure.

In the following, we write the fundamental equations in a suitable form by first averaging the physical quantities over the time coordinate t and the azimuthal coordinate ϕ, and then by integrating the averaged quantities over the height of the disc. As an illustrative example, let $f = f(t, r, z, \phi)$ be a function of the space-time coordinates. Then, the averaged function $\bar{f}$ is given by

$$\bar{f}(r, z) = \frac{1}{\Delta t}\frac{1}{2\pi}\int_t^{t+\Delta t}\int_0^{2\pi} f(t', r, z, \phi')\, dt'\, d\phi'. \tag{3.20}$$

A given physical quantity, that is symmetric with respect to the equatorial plane, admits a Taylor expansion as

$$\bar{f}(r, z) = \sum_{n=0}^{\infty} \bar{f}_{2n}(r)\left(\frac{z}{r}\right)^{2n}, \tag{3.21}$$

and the vertically integrated quantity then reads as

$$F(r) = \int_{-H}^{+H} \bar{f}(r, z)\, dz = 2H\bar{f}_0(r) + \mathcal{O}\left(\frac{H}{r}\right)^2, \tag{3.22}$$

where $\bar{f}_0$ is the averaged quantity evaluated at the equatorial plane $z = 0$. We shall see that the equations governing the dynamics of the thin accretion disc are derived by approximating all the physical quantities at the equatorial plane. The only exception is represented by the vertical equilibrium equation, where we have to assume a certain vertical profile for the total pressure.

3.3.1 Rest-mass and mass-energy conservation

We assume that the baryon number is conserved along the fluid flow, *i.e.*, we impose that $(\rho u^\mu)_{;\mu} = 0$. This assumption is valid for energies below $2m_b$, where m_b is the rest-mass of the baryon species or, equivalently, for temperatures below 10^{10}

K for electrons and 10^{13} K for protons and neutrons. The rest-mass conservation $(\rho u^{\mu})_{;\mu} = 0$, after the averaging approximation over t and ϕ, gives

$$\partial_r \left(2\pi r \Delta t \bar{\rho} u^r\right) + r\partial_z \left(2\pi \Delta t \bar{\rho} u^z\right) = 0. \tag{3.23}$$

After integrating over the vertical coordinate $z \in [-H, +H]$, one finds

$$\partial_r \left(2\pi r \Delta t \Sigma u^r\right) + 2\pi r \Delta t \left(\bar{\rho} u^z\right)\Big|_{z=-H}^{z=+H} = 0, \tag{3.24}$$

where we defined the surface density of the disc

$$\Sigma(r) = \int_{-H}^{H} \bar{\rho}(r,z)dz. \tag{3.25}$$

We require the additional assumption that the mass (per unit time and unit area) $\bar{\rho} u^z$ leaving the disc surface at $z = \pm H$ is negligible with respect to the mass accreted along the radial direction. Therefore the second term can be neglected and integration over r gives the amount of mass accreting onto the black hole during the time interval Δt, the mass accretion rate $\dot{M}$, given by

$$\dot{M} = -2\pi r \Sigma u^r = -2\pi r \Sigma \frac{V\mathscr{D}^{1/2}}{\sqrt{1-V^2}}, \tag{3.26}$$

where the minus sign has been chosen to have positive accretion mass. Note that $\dot{M}$ is constant (independent of r) and it will be a parameter of the Novikov-Thorne model.

For future reference, we notice that the rest-mass conservation law can be written in differential form as

$$\left(\frac{1}{r} + \frac{1}{\rho}\frac{d\rho}{dr} + \frac{1}{u^r}\frac{du^r}{dr}\right) + r\left(\frac{u^z}{u^r}\frac{1}{\rho}\frac{d\rho}{dz} + \frac{1}{u^r}\frac{du^z}{dz}\right) = 0. \tag{3.27}$$

In addition, we assume that the vertical component of the four-velocity and its derivative with respect to the vertical coordinate z are negligible with respect to the radial flow. This approximation leads us to consider only the terms in the first bracket. Therefore, the differential form of the rest-mass conservation equation is given by

$$\frac{1}{r} + \frac{1}{\rho}\frac{d\rho}{dr} + \frac{1}{u^r}\frac{du^r}{dr} = 0. \tag{3.28}$$

This last equation, when integrated, gives the rest-mass conservation law (3.26).

Let us conclude the discussion with the closely related mass-energy conservation equation derived by exploiting the time Killing vector η. The conserved

current associated to η is given by

$$J^{\mu}_{\eta} = T^{\mu}_{\ \nu}\eta^{\nu} = \left[-\eta\rho E + q_t\right] u^{\mu} + p\eta^{\mu} + S^{\mu}_{\ t} - Eq^{\mu}, \tag{3.29}$$

where $E = -u_t$ is the specific energy of the fluid particle. We first assume that the fluid is non-relativistic, *i.e.*, the relativistic enthalpy is $\eta = 1$.[4] Following the same steps that we outlined to obtain the rest-mass conservation (3.26), and assuming that $\bar{\rho}u^z = 0$, $\bar{q}_t = 0 = \bar{q}_r$ and $\bar{S}^z_{\ t} = 0$ at $z = \pm H$, the law of conservation of energy reads as

$$\partial_r\left(\dot{M}E + 2\pi r W^r_{\ t}\right) = 4\pi r EF, \tag{3.30}$$

where $F(r) = \bar{q}^z(r,+H) = -\bar{q}^z(r,-H)$ is the flux of radiant energy[5] off the upper and lower surfaces of the disc and $W^r_{\ t}(r) = \int_{-H}^{+H}\bar{S}^r_{\ t}(r,z)dz$ is the vertically integrated shear stress. We notice that, since $S^{\mu}_{\ \nu}u^{\nu} = 0$, after averaging we have $W^r_{\ t}(r) = -\left(u^{\phi}/u^t\right)W^r_{\ \phi}(r) = -\Omega W^r_{\ \phi}(r)$. Thus, the law of conservation of energy equivalently reads as

$$\partial_r\left(\dot{M}E - 2\pi r\Omega W^r_{\ \phi}(r)\right) = 4\pi r EF. \tag{3.31}$$

3.3.2 Angular momentum conservation

The angular momentum conservation can be derived by computing the conserved current J_{ξ} associated to the azimuthal Killing vector ξ

$$J^{\mu}_{\xi} = \left[\eta\rho L + q_{\phi}\right] u^{\mu} + p\xi^{\mu} + S^{\mu}_{\ \phi} + Lq^{\mu}, \tag{3.32}$$

where $L = u_{\phi}$ is the specific angular momentum of the fluid particle. We again assume that the fluid is non-relativistic, *i.e.*, the relativistic enthalpy is $\eta = 1$. Following the usual averaging and vertically integration approximations, and assuming that $\bar{\rho}u^z = 0$, $\bar{q}_r = 0 = \bar{q}_{\phi}$ and $\bar{S}^z_{\ \phi} = 0$ at $z = \pm H$, the law of conservation of angular momentum is given by

$$\partial_r\left(\dot{M}L - 2\pi r W^r_{\ \phi}\right) = 4\pi r LF, \tag{3.33}$$

where $F(r) = \bar{q}^z(r,+H) = -\bar{q}^z(r,-H)$ is the flux of radiant energy off the upper and lower surfaces of the disc and $W^r_{\ \phi}(r) = \int_{-H}^{+H}\bar{S}^r_{\ \phi}(r,z)dz$ is the vertically integrated

[4] This is equivalent to $\Pi \ll \rho$ and $p \ll \rho$, *i.e.*, the specific internal energy and the total pressure are negligible with respect to the rest-mass density. This is an assumption of the Novikov-Thorne model.

[5] Notice that the heat flux q^{μ} is assumed to be antisymmetric with respect to the equatorial plane.

shear stress.

3.3.3 Radial equation

Let us write the radial component of Eq. (3.7) in its explicit form. The radial component of the acceleration, after substituting the four-velocity profile (B.22) for general near-equatorial orbits, reads as

$$a^r = \frac{\mathscr{D}}{1-V^2}\left(\frac{V}{1-V^2}\frac{dV}{dr} - f_r\right), \qquad f_r \equiv -M\frac{\gamma_\phi^2}{r^2}\frac{\mathscr{A}}{\mathscr{D}}\left(1-\frac{\Omega}{\Omega_c^+}\right)\left(1-\frac{\Omega}{\Omega_c^-}\right), \tag{3.34}$$

where V is the rescaled radial velocity defined in Eq. (B.21), $\gamma_\phi = \left(1-(\mathcal{V}^{(\phi)})^2\right)^{-1/2}$ is the gamma factor with respect to the azimuthal velocity as measure by the locally non-rotating frame (LNRF), and $\Omega_c^\pm$ are the angular velocity of the prograde (+) and retrograde (−) circular equatorial orbits computed in Eqs. (B.9). The f_r contribution to the radial acceleration vanishes for circular equatorial orbits. The radial pressure gradient becomes

$$h^{r\mu}p_{,\mu} = h^{rr}\frac{dp}{dr} = \frac{\mathscr{D}}{1-V^2}\frac{dp}{dr}. \tag{3.35}$$

Thus, the radial momentum conservation is equivalent to the expression

$$\frac{\mathscr{D}}{1-V^2}\left[(\epsilon+p)\left(\frac{V}{1-V^2}\frac{dV}{dr} - f_r\right) + \frac{dp}{dr}\right] + S^r + Q^r = 0. \tag{3.36}$$

An equivalent expression for the radial momentum equation, in terms of u^r rather than V, has been derived in Peitz and Appl (1997).

It is common to assume that the radial acceleration due to viscous stresses S^r and the heat flux Q^r are negligible when compared with the radial acceleration due to the pressure. Under these simplifying assumptions, the radial momentum conservation takes the simpler form

$$\frac{V}{1-V^2}\frac{dV}{dr} = f_r - \frac{1}{\epsilon+p}\frac{dp}{dr}. \tag{3.37}$$

This is the radial momentum equation derived for advection-dominated accretion discs in Gammie and Popham (1998), which generalises that first presented for slim discs in Abramowicz et al. (1996) for non-relativistic fluid with $\eta = 1$. It is nothing but the radial Euler equation for a perfect fluid.

When considering thin accretion discs, one assumes that the averaged and vertically integrated orbital motion of the fluid is approximated by circular equatorial

geodesics. The assumption that the averaged motion is nearly circular automatically implies that the radial pressure gradient and the radial velocity gradient are negligible with respect to the gravitational acceleration. Thus, from Eq. (3.37), the term f_r must vanish, which implies that the orbital motion is Keplerian $\Omega = \Omega_c^{\pm}$. Therefore, the radial equilibrium equation is trivially satisfied in the thin disc approximation.

Let us conclude the discussion of the radial momentum equation with one interesting observation. We define the adiabatic sound speed by

$$c_{ad}^2 \equiv \left.\frac{dp}{d\epsilon}\right|_{ad} = \frac{1}{\eta}\frac{dp}{d\rho} = \frac{\rho}{\epsilon+p}\frac{dp}{d\rho} = \frac{1}{\epsilon+p}\frac{dp}{dr}\left(\frac{1}{\rho}\frac{d\rho}{dr}\right)^{-1}. \tag{3.38}$$

By using the rest-mass conservation law in its differential form (3.28) and substituting the definition of adiabatic sound speed, the radial Euler equation can be written as

$$\frac{1}{V}\frac{dV}{dr} = -\frac{1-V^2}{c_{ad}^2 - V^2}\left\{f_r + c_{ad}^2\left[\frac{1}{r} + \frac{M}{r^2\mathscr{D}}\left(1 - \frac{a^2}{Mr}\right)\right]\right\}. \tag{3.39}$$

The accretion flow is subsonic ($V < c_{ad}$) for large radii, then it approaches the speed of sound at a certain radius location and it becomes transonic ($V > c_{ad}$). The above equation has a critical point for $V = c_{ad}$: this defines the so-called sonic surface and it depends on the mass accretion rate and the α parameter. Thus, in order to have a regular global solution, the factor in brackets must vanish at the same radial location. This regularity condition amounts to an eigenvalue problem for angular momentum values. For more details, see Abramowicz et al. (1996) and Gammie and Popham (1998) in the context of slim accretion discs, Peitz and Appl (1997) for more general disc-like accretion flows, and the recent review by Abramowicz and Fragile (2013). In Abramowicz et al. (2010) (see their Fig. 7), it has been shown that, for small accretion rates $\dot{M} < 0.3\dot{M}_{Edd}$, the sonic-surface is located at ISCO independently of the α parameter. For thin accretion discs, where the physical edge is the ISCO by construction, one can consistently make the assumption that the sonic-surface coincides with the ISCO. As we will see in section 7.2, this assumption amounts to impose non-vanishing viscous stresses at ISCO (Penna, Sadowski, and McKinney, 2012).

3.3.4 Vertical equilibrium equation

In the following, and only to derive the vertical equilibrium equation, we consider those terms linear in $\cos\theta$, *i.e.*, terms of $\mathscr{O}(z/r)$. We neglect higher orders terms.

The polar component of the acceleration is explicitly given by

$$a_\theta = \cos\theta\left(u^r\frac{d(\gamma r U)}{dr} - \gamma^2 U^2 - \frac{\mathscr{L}_\star^2}{r^2}\right), \tag{3.40}$$

where $\mathscr{L}_\star^2 = L^2 - a^2(E^2-1)$, being $L = u_\phi$ and $E = -u_t$ the specific angular momentum and the specific energy, respectively, and U is related to the polar component of the four-velocity by $u_\theta = \gamma r U\cos\theta$. Following the work of Abramowicz, Lanza, and Percival (1997), we assume the following pressure profile

$$p(r,\theta) = p_0(r)\left[1 - \frac{r^2\cos^2\theta}{H^2}\right] = p_0(r)\left[1 - \frac{\cos^2\theta}{\cos^2\theta_H}\right], \tag{3.41}$$

where $p_0(r) = p(r,\theta=\pi/2)$ and $H = r\cos\theta_H$ The polar gradient of the pressure is given by

$$h_\theta^\rho p_{,\rho} = \cos\theta\left(u^r\gamma r U\frac{\partial p_0}{\partial r} + 2\frac{r^2}{H^2}p_0\right). \tag{3.42}$$

The contribution of viscous stresses $h_{\theta\rho}S^{\rho\nu}_{\ ;\nu}$ is proportional to the vertical velocity U. As done for the radial equilibrium equation, we neglect contributions from viscous stresses and from the heat flux. In other words, we consider the Euler vertical equation for a perfect fluid, instead of the more complicated Navier-Stokes vertical equation. Moreover, from Eqs. (3.40) and (3.42), we consider only those terms not involving the polar component U and its radial derivative. By adopting this approximation, we obtain the final form of the vertical equilibrium equation, originally derived by Abramowicz, Lanza, and Percival (1997). It reads as

$$-2\frac{p_0}{\rho_0} + \frac{H^2}{r^2}\frac{\mathscr{L}_\star^2}{r^2} = 0, \tag{3.43}$$

where we have used the non-relativistic fluid approximation $\epsilon + p \approx \rho$.

3.4 The Novikov-Thorne model

As already said, one of the main assumptions made by Novikov and Thorne (1973) is that the fluid particles move on nearly circular equatorial geodesics. In different words, the motion in the t-ϕ plane is geodesic with a small radial (and non-geodesic) component, u^r, produced by viscous stresses, responsible for the accretion process onto the black hole. Such an assumption implies that we can use the kinematic quantities of circular equatorial geodesics listed in appendix B.2 and B.3. In particular, in the LRF, the shear tensor $\sigma_{\hat\mu\hat\nu}$ of circular equatorial geodesics

has only one non-vanishing component

$$\sigma_{\hat{r}\hat{\phi}} = \sigma_{\hat{\phi}\hat{r}} = \frac{1}{2}\frac{A}{r^3}\gamma^2\Omega_{,r} = -\frac{3}{4}M^{-1}x^{-3}\mathscr{C}^{-1}\mathscr{D}. \tag{3.44}$$

This is an important observation to express the thin disc equations in an appropriate form for our purposes. Indeed, according to the first constitutive equation (3.14), one can write the vertically integrated shear tensor, already defined below the angular momentum conservation law (3.33), as

$$W(r) \equiv \int_{-H}^{H} \bar{S}_{\hat{r}\hat{\phi}}(r,z)dz = 2H\bar{S}_{\hat{r}\hat{\phi}}. \tag{3.45}$$

We assume the α-viscosity prescription of Shakura and Sunyaev (1973)

$$\bar{S}_{\hat{r}\hat{\phi}} = \alpha p, \tag{3.46}$$

where α is a free parameter and p is total pressure. It is a crude effective description of viscous mechanisms involved in the accretion process. In words, the Shakura-Sunyaev prescription states that, in the LRF, the vertically integrated shear stress is proportional to the total pressure.[6]

3.4.1 Energy balance equation

We recall that the energy balance (3.12) states that the energy dissipated is given by the energy generated by advection and the energy radiated away

$$Q_{diss} = Q_{adv} + Q_{cool}. \tag{3.47}$$

We neglect the advection term and, therefore, the energy balance equation implies that the energy dissipated equals the energy radiated away. In formulæ, after averaging and vertically integrating, one gets

$$F(r) = -\sigma_{\hat{r}\hat{\phi}}W(r). \tag{3.48}$$

This equation determines the radiated flux $F(r)$ once we know the integrated shear stress $W(r)$.

[6] Some specific MHD turbulent discs might be modelled by this prescription (Balbus and Papaloizou, 1999). The modification of αp to αp_{gas} was argued in Lightman and Eardley (1974) and further developed in Bisnovatyi-Kogan and Blinnikov (1977) and Sakimoto and Coroniti (1981). Such models, later called βp models, do not suffer from thermal instabilities. However, MHD simulations do not conclude on their validity (Hirose, Krolik, and Blaes, 2009; Ohsuga et al., 2009; Ross, Latter, and Guilet, 2016). More elaborated prescriptions have been developed by Ogilvie (2003) and Pessah, Chan, and Psaltis (2006).

3.4.2 Conservation laws

The rest-mass conservation law (3.26) is given by

$$\dot{M} = -2\pi r \Sigma(r) u^r. \tag{3.49}$$

The mass-energy conservation law (3.31) and the angular momentum conservation law (3.33) can be integrated to obtain (Page and Thorne, 1974)

$$-4\pi r \frac{(E-\Omega L)^2}{\Omega_{,r}} \frac{F}{\dot{M}} = \int_{r_0}^{r} (E-\Omega L) L_{,r'} dr' + M\mathscr{P}_0. \tag{3.50}$$

The constant of integration $\dot{M}$ is the accretion rate, while E, L, Ω and $\sigma_{\hat{r}\hat{\phi}}$ are kinematic quantities of circular equatorial geodesics (see appendix B.2 for their expressions). The right-hand side of Eq. (3.50) is nothing else than $M\mathscr{P}$ defined in (B.10). The dimensionless integration constant $\mathscr{P}_0$ is fixed by the boundary conditions, which are discussed in section 7.2.

From the conservation laws, we can explicitly compute $F(r)$ (and then $W(r)$) and the product $\Sigma(r)u^r$. To calculate $\Sigma(r)$ and u^r we need equations governing the vertical equilibrium and describing the equation of state of the fluid and other physical features of the disc.

3.4.3 Vertical equilibrium equation

The vertical equilibrium equation, after the approximations discussed above (see Eq. (3.43)), reads as (Abramowicz, Lanza, and Percival, 1997)[7]

$$2\frac{p}{\rho} = \frac{H^2}{r^2}\frac{\mathscr{L}_\star^2}{r^2}, \tag{3.51}$$

where p is the total pressure, *i.e.*, it is the sum of the radiation pressure and the gas pressure $p = p^{(gas)} + p^{(rad)}$.

3.4.4 Equation of state and energy transport law

We express the equation of state for the ideal gas and the radiation pressure as

$$p^{(gas)} = \frac{k_B \rho}{m_p} T, \tag{3.52a}$$

$$p^{(rad)} = \frac{1}{3} b T^4, \tag{3.52b}$$

[7] Note the factor 2 typo in Eq. (B12) of Penna, Sadowski, and McKinney (2012).

where $b = 4\sigma_{SB}/c$ is the radiation constant density, k_B Boltzmann's constant, σ_{SB} Stefan-Boltzmann's constant and m_p the rest-mass of the proton.

We also impose the energy transport law

$$bT^4 = \bar{\kappa}\Sigma F, \tag{3.53}$$

where $\bar{\kappa}$ is the optical opacity of the disc

$$\bar{\kappa} = \bar{\kappa}_{ff} + \bar{\kappa}_{es}, \tag{3.54a}$$

$$\bar{\kappa}_{ff} = \left(0.64 \times 10^{23} cm^2 g^{-1}\right)\left(\frac{\rho}{g/cm^3}\right)\left(\frac{T}{K}\right)^{-7/2}, \tag{3.54b}$$

$$\bar{\kappa}_{es} = 0.40\, cm^2 g^{-1}, \tag{3.54c}$$

originating from the free-free (ff) absorption and the electron scattering (es).

3.5 Local solutions to the Novikov-Thorne model

The Novikov-Thorne model consists of eight equations, (3.25), (3.45), (3.48), (3.49), (3.50), (3.51), (3.52), (3.53) and eight unknown functions F, Σ, W, h, u^r, p, ρ, T of the radial coordinate. The system of equations is algebraic and admits a single solution upon imposing the physical conditions that $T > 0$, $p > 0$. The solution depends upon four free parameters. The solution can be patched by local solutions where either the gas pressure or radiation pressure dominates, and opacity is either dominated by electron scattering or free-free absorption. The three relevant local solutions are detailed below and are denoted as

Gas-es: Gas pressure-electron scattering dominated: $p = p^{(gas)}$ and $\bar{\kappa} = \bar{\kappa}_{es}$;

Rad-es: Radiation pressure-electron scattering dominated: $p = p^{(rad)}$ and $\bar{\kappa} = \bar{\kappa}_{es}$;

Gas-ff: Gas pressure-free free absorption dominated: $p = p^{(gas)}$ and $\bar{\kappa} = \bar{\kappa}_{ff}$.

The numerical values in cgs units of all physical constants used in the solutions are

$$G = 6.67 \times 10^{-8} cm^3/(sec^2 g), \quad c = 3.00 \times 10^{10} cm/sec, \quad k_B = 1.38 \times 10^{-16} erg/K,$$
$$m_p = 1.67 \times 10^{-24} g, \quad b = 7.56 \times 10^{-15} erg/(cm^3 K^4), \quad M_\odot = 1.99 \times 10^{33} g.$$

We took particular care to correct various algebraic errors and typos found in the literature. The Novikov-Thorne local solutions (with typos fixed) can be recovered by substituting $x \to \sqrt{r_*}$, $\mathscr{P} \to r_*^{1/2}\mathscr{B}^{-1}\mathscr{C}^{1/2}\mathscr{Q}$ and using the boundary condition

at the ISCO $\mathscr{Q}(r_0) = 0$. The curly functions $\mathscr{B}, \mathscr{C}, \mathscr{D}, \mathscr{R}$ are defined in Eqs. (B.6) and the function $\mathscr{P}$ is defined in Eq. (B.10) (see also Eq. (3.50)).

[Gas-es] Gas pressure-electron scattering dominated solution

In this region, the gas pressure $p^{(gas)}$ is predominant with respect to the radiation pressure $p^{(rad)}$ and the electron scattering contributes mainly to the opacity of the disc.

$$F = \left(5.5 \times 10^{25} erg/(cm^2 sec)\right)\left(M_\star^{-2}\dot{M}_\star\right) x^{-7}\mathscr{C}^{-1}\mathscr{P}, \tag{3.55a}$$

$$\Sigma = \left(5.0 \times 10^{4} g/cm^2\right)\left(\alpha^{-4/5} M_\star^{-2/5}\dot{M}_\star^{3/5}\right) x^{-9/5}\mathscr{C}^{1/5}\mathscr{D}^{-4/5}\mathscr{P}^{3/5}, \tag{3.55b}$$

$$W = \left(1.1 \times 10^{21} dyn/cm\right)\left(M_\star^{-1}\dot{M}_\star\right) x^{-4}\mathscr{D}^{-1}\mathscr{P}, \tag{3.55c}$$

$$h = \left(7.0 \times 10^{-3}\right)\left(\alpha^{-1/10} M_\star^{-3/10}\dot{M}_\star^{1/5}\right) x^{-1/10}\mathscr{C}^{-1/10}\mathscr{D}^{-1/10}\mathscr{R}^{-1/2}\mathscr{P}^{1/5}, \tag{3.55d}$$

$$u^r = \left(-7.3 \times 10^{5} cm/sec\right)\left(\alpha^{4/5} M_\star^{-3/5}\dot{M}_\star^{2/5}\right) x^{-1/5}\mathscr{C}^{-1/5}\mathscr{D}^{4/5}\mathscr{P}^{-3/5}, \tag{3.55e}$$

$$p^{(gas)} = \left(1.8 \times 10^{17} dyn/cm^2\right)\left(\alpha^{-9/10} M_\star^{-17/10}\dot{M}_\star^{4/5}\right) x^{-59/10}\mathscr{C}^{1/10}\mathscr{D}^{-9/10}\mathscr{R}^{1/2}\mathscr{P}^{4/5}, \tag{3.55f}$$

$$\rho = \left(8.1 g/cm^3\right)\left(\alpha^{-7/10} M_\star^{-11/10}\dot{M}_\star^{2/5}\right) x^{-37/10}\mathscr{C}^{3/10}\mathscr{D}^{-7/10}\mathscr{R}^{1/2}\mathscr{P}^{2/5}, \tag{3.55g}$$

$$T = \left(2.6 \times 10^{8} K\right)\left(\alpha^{-1/5} M_\star^{-3/5}\dot{M}_\star^{2/5}\right) x^{-11/5}\mathscr{C}^{-1/5}\mathscr{D}^{-1/5}\mathscr{P}^{2/5}. \tag{3.55h}$$

For consistency, this solution is valid where $h \ll 1$, $u^r \ll 1$ and

$$\frac{p^{(rad)}}{p^{(gas)}} = (69.)\left(\alpha^{1/10} M_\star^{-7/10}\dot{M}_\star^{4/5}\right) x^{-29/10}\mathscr{C}^{-9/10}\mathscr{D}^{1/10}\mathscr{R}^{-1/2}\mathscr{P}^{4/5} \ll 1, \tag{3.56a}$$

$$\frac{\bar{\kappa}_{ff}}{\bar{\kappa}_{es}} = \left(4.4 \times 10^{-6}\right)\left(M_\star \dot{M}_\star^{-1}\right) x^{4}\mathscr{C}\mathscr{R}^{1/2}\mathscr{P}^{-1} \ll 1. \tag{3.56b}$$

[Rad-es] Radiation pressure-electron scattering dominated solution

In this region, the radiation pressure $p = p^{(rad)}$ is dominant, but still the electrons scattering is the main mechanism for the opacity in the disc.

$$F = \left(5.5\times10^{25} erg/(cm^2 sec)\right)\left(M_\star^{-2}\dot{M}_\star\right) x^{-7}\mathscr{C}^{-1}\mathscr{P}, \tag{3.57a}$$

$$\Sigma = \left(10. g/cm^2\right)\left(\alpha^{-1}M_\star\dot{M}_\star^{-1}\right) x^{4}\mathscr{C}^{2}\mathscr{D}^{-1}\mathscr{R}\mathscr{P}^{-1}, \tag{3.57b}$$

$$W = \left(1.1\times10^{21} dyn/cm\right)\left(M_\star^{-1}\dot{M}_\star\right) x^{-4}\mathscr{D}^{-1}\mathscr{P}, \tag{3.57c}$$

$$h = (0.5)\left(M_\star^{-1}\dot{M}_\star\right) x^{-3}\mathscr{C}^{-1}\mathscr{R}^{-1}\mathscr{P}, \tag{3.57d}$$

$$u^r = \left(-3.5\times10^{9} cm/sec\right)\left(\alpha M_\star^{-2}\dot{M}_\star^{2}\right) x^{-6}\mathscr{C}^{-2}\mathscr{D}\mathscr{R}^{-1}\mathscr{P}, \tag{3.57e}$$

$$p^{(rad)} = \left(2.6\times10^{15} dyn/cm^2\right)\left(\alpha^{-1}M_\star^{-1}\right) x^{-3}\mathscr{C}\mathscr{D}^{-1}\mathscr{R}, \tag{3.57f}$$

$$\rho = \left(2.5\times10^{-5} g/cm^3\right)\left(\alpha^{-1}M_\star\dot{M}_\star^{-2}\right) x^{5}\mathscr{C}^{3}\mathscr{D}^{-1}\mathscr{R}^{2}\mathscr{P}^{-2}, \tag{3.57g}$$

$$T = \left(3.2\times10^{7} K\right)\left(\alpha^{-1/4}M_\star^{-1/4}\right) x^{-3/4}\mathscr{C}^{1/4}\mathscr{D}^{-1/4}\mathscr{R}^{1/4}. \tag{3.57h}$$

For consistency, this solution is valid where $h \ll 1$, $u^r \ll 1$ and

$$\frac{p^{(gas)}}{p^{(rad)}} = \left(2.6\times10^{-5}\right)\left(\alpha^{-1/4}M_\star^{7/4}\dot{M}_\star^{-2}\right) x^{29/4}\mathscr{C}^{9/4}\mathscr{D}^{-1/4}\mathscr{R}^{5/4}\mathscr{P}^{-2} \ll 1, \tag{3.58a}$$

$$\frac{\bar{\kappa}_{ff}}{\bar{\kappa}_{es}} = \left(2.2\times10^{-8}\right)\left(\alpha^{-1/8}M_\star^{15/8}\dot{M}_\star^{-2}\right) x^{61/8}\mathscr{C}^{17/8}\mathscr{D}^{-1/8}\mathscr{R}^{9/8}\mathscr{P}^{-2} \ll 1. \tag{3.58b}$$

[Gas-ff] Gas pressure-free free absorption dominated solution

In this region, the gas pressure $p = p^{(gas)}$ and the free-free term contribution in the opacity law are dominant. Then, we find

$$F = \left(5.5 \times 10^{25} erg/(cm^2 sec)\right)\left(M_\star^{-2}\dot{M}_\star\right) x^{-7}\mathscr{C}^{-1}\mathscr{P}, \tag{3.59a}$$

$$\Sigma = \left(1.70 \times 10^5 g/cm^2\right)\left(\alpha^{-4/5} M_\star^{-1/2}\dot{M}_\star^{7/10}\right) x^{-11/5}\mathscr{C}^{1/10}\mathscr{D}^{-4/5}\mathscr{R}^{-1/20}\mathscr{P}^{7/10}, \tag{3.59b}$$

$$W = \left(1.1 \times 10^{21} dyn/cm\right)\left(M_\star^{-1}\dot{M}_\star\right) x^{-4}\mathscr{D}^{-1}\mathscr{P}, \tag{3.59c}$$

$$h = \left(3.8 \times 10^{-3}\right)\left(\alpha^{-1/10} M_\star^{-1/4}\dot{M}_\star^{3/20}\right) x^{1/10}\mathscr{C}^{-1/20}\mathscr{D}^{-1/10}\mathscr{R}^{-19/40}\mathscr{P}^{3/20}, \tag{3.59d}$$

$$u^r = \left(-2.1 \times 10^5 cm/sec\right)\left(\alpha^{4/5} M_\star^{-1/2}\dot{M}_\star^{3/10}\right) x^{1/5}\mathscr{C}^{-1/10}\mathscr{D}^{4/5}\mathscr{R}^{1/20}\mathscr{P}^{-7/10}, \tag{3.59e}$$

$$p^{(gas)} = \left(3.3 \times 10^{17} dyn/cm^2\right)\left(\alpha^{-9/10} M_\star^{-7/4}\dot{M}_\star^{17/20}\right) x^{-61/10}\mathscr{C}^{1/20}\mathscr{D}^{-9/10}\mathscr{R}^{19/40}\mathscr{P}^{17/20}, \tag{3.59f}$$

$$\rho = \left(51. g/cm^3\right)\left(\alpha^{-7/10} M_\star^{-5/4}\dot{M}_\star^{11/20}\right) x^{-43/10}\mathscr{C}^{3/20}\mathscr{D}^{-7/10}\mathscr{R}^{17/40}\mathscr{P}^{11/20}, \tag{3.59g}$$

$$T = \left(7.7 \times 10^7 K\right)\left(\alpha^{-1/5} M_\star^{-1/2}\dot{M}_\star^{3/10}\right) x^{-9/5}\mathscr{C}^{-1/10}\mathscr{D}^{-1/5}\mathscr{R}^{1/20}\mathscr{P}^{3/10}. \tag{3.59h}$$

For consistency, this solution is valid where $h \ll 1$, $u^r \ll 1$ and

$$\frac{p^{(rad)}}{p^{(gas)}} = (0.27)\left(\alpha^{1/10} M_\star^{-1/4}\dot{M}_\star^{7/20}\right) x^{-11/10}\mathscr{C}^{-9/20}\mathscr{D}^{1/10}\mathscr{R}^{-11/40}\mathscr{P}^{7/20} \ll 1, \tag{3.60a}$$

$$\frac{\bar{\kappa}_{es}}{\bar{\kappa}_{ff}} = \left(4.8 \times 10^2\right)\left(M_\star^{-1/2}\dot{M}_\star^{1/2}\right) x^{-2}\mathscr{C}^{-1/2}\mathscr{R}^{-1/4}\mathscr{P}^{1/2} \ll 1. \tag{3.60b}$$

Chapter 4

Gravitational multipole moments

Contents

Multipole moments in the theory of General Relativity are introduced in this chapter. After stating motivations in section 4.1, we introduce the common nomenclature to define regions around a gravitational wave source in section 4.2. Then, in section 4.3, we introduce the harmonic gauge and we define the so-called canonical harmonic gauge, where gravitational multipole moments can be read off from the multipolar expansion of the metric field. Finally, section 4.4 provides the definition of source multipole moments and radiation multipole moments.

4.1 Astrophysical motivations

Multipole moments, and multipole expansion, are ubiquitous in theoretical physics wherever one deals with fields (electromagnetic, gravitational, hydrodynamical, *etc.*...). The idea that multipole moments are in connection with the coefficients of the multipole expansion of the given field is meaningful whenever the theory is linear. General Relativity is not and this feature, together with the tensorial nature of the gravitational interaction, makes the definition of the gravitational multipole moments more involved (see Box. 1 in Thorne, 1980, for a historical overview of

the literature on multipole expansion in General Relativity). In addition, in general curved space-times there is no a natural choice of the origin with respect to which one can perform the harmonic expansion.

The gravitational field, in General Relativity, is characterized by two and only two sets of multipole moments: the mass multipole moments and the current multipole moments. The former moments are already defined in Newtonian theory (see, *e.g.*, Poisson and Will, 2014), while the current multipole moments are only defined in General Relativity (Geroch, 1970; Hansen, 1974; Thorne, 1980; Fodor, Hoenselaers, and Perjés, 1989).

The gravitational field surrounding a stationary body in General Relativity is entirely described by its mass and current multipole moments, determined by the expansion of the metric at spatial infinity (Geroch, 1970; Hansen, 1974; Simon and Beig, 1983), up to a diffeomorphism (Beig and Simon, 1980; Beig and Simon, 1981; Kundu, 1981a; Kundu, 1981b). Any stationary and axisymmetric metric in General Relativity can be reconstructed from given multipole moments under certain assumptions (Backdahl and Herberthson, 2005; Backdahl, 2007). The gravitational field of a non-stationary body in the wave-zone region, assuming no incoming radiation and asymptotically flatness, is also entirely described by its mass and current multipole moments, determined by the expansion of the metric at future null infinity, up to a diffeomorphism (Blanchet and Damour, 1986).

For a Kerr black hole, the mass multipole moments I^{lm} and the current multipole moments S^{lm} are completely determined by its mass M and angular momentum $J = Ma$. Since the Kerr black hole is axisymmetric, $I^{lm} = I_l \delta_{m,0}$ and $S^{lm} = S_l \delta_{m,0}$. Since it is reflection-symmetric (*i.e.*, symmetric under reflection with respect to the equatorial plane), odd mass multipole moments and even current multipole moments vanish, $I_{2l+1} = S_{2l} = 0$. The non-vanishing multipole moments are given by the Geroch-Hansen formulæ (Geroch, 1970; Hansen, 1974)

$$I_{2l} = (-1)^l M a^{2l}, \qquad S_{2l+1} = (-1)^l M a^{2l+1}, \tag{4.1}$$

where $I_0 = M$ is the mass, $S_1 = J$ is the angular momentum and $I_2 = -J^2/M$ is the mass quadrupole moment. Kerr black hole is generally accepted to be the final stationary state in General Relativity. Thus, measuring more than two multipole moments of the gravitational field surrounding a stationary black hole is a direct test of General Relativity, or more precisely, of its no-hair theorems (see, *e.g.*, Collins and Hughes, 2004; Cardoso and Gualtieri, 2016). The gravitational wave detector LISA might be able to measure the mass quadrupole moment of merging black holes with good accuracy (Ryan, 1997; Barack and Cutler, 2007). This would

allow to constrain alternative gravitational theories that predict a different mass quadrupole moment (see, *e.g.*, Berti (2015) for a status report and Yagi, Yunes, and Tanaka (2012); Ayzenberg and Yunes (2014); Collins and Hughes (2004); Herdeiro and Radu (2015) for specific models).

Another potential application of gravitational multipole moments is in the rich physics of neutron stars (Baiotti and Rezzolla, 2017; Fernández and Metzger, 2016) and in the long-standing open problem of their equation of state (Lattimer, 2012). For neutron stars or other types of stars, the two sets of multipole moments are determined by the matter distribution. The multipole moments of a stationary neutron star also characterize the equation of state of the matter it consists of (see, *e.g.*, Datta, 1988; Salgado et al., 1994; Laarakkers and Poisson, 1999). Indeed, it has been proposed that the equation of state can be constrained by the gravitational waveform of a binary neutron stars system (Bauswein and Janka, 2012) and of a black hole-neutron star system (Lackey et al., 2012), because the imprinting of the equation of state in the waveform is due to the quadrupole-monopole interaction (Poisson, 1998) and to tidal deformations of the neutron stars in the binary system (Hinderer et al., 2010; Damour, Nagar, and Villain, 2012). Gravitational wave emission from binary neutron star mergers, such as the one recently observed (Abbott, 2017a; Abbott, 2017b), or black hole-neutron star mergers, therefore, contains signatures of the equation of state of neutron stars. Another aspect of neutron stars concerns the universal relations among certain multipole moments (see, *e.g.*, Yagi and Yunes, 2017, and references therein) and their origin for this universality (Yagi et al., 2014).

4.2 Regions around an isolated source

Before defining source and radiative multipole moments, it is much instructive to introduce all the characteristic length-scales involved in the process of gravitational radiation.

Let us consider a given isolated source of mass M described by an energy-momentum tensor that is defined inside a compact region of size a. Such a source emits gravitational radiation with a characteristic wavelength λ. We define the following regions defined by the above characteristic lengths (Thorne, 1980):

1. the source region defined by $r \leq a$ where the source lies,

2. the strong-field region characterised by $r \leq 5r_S$[1] if $a/M \leq 10$. The strong-field regime typically does not exist if the ratio of compactness a/M is much

[1] We define $r_S = 2M$ as the radius of influence or the Schwarzschild radius of the source.

bigger than 10,

3. the weak-field near zone, where $r > a$ and defined by $2r_S \ll r \ll \lambda$.

In addition to these regions, we define the

- the local wave zone defined between two characteristic radii: the inner radius r_I and the outer radius r_O. The former is located where one or more of the following instances take place: a) the waves become a near-zone field, *i.e.*, $r \leq \lambda$, b) one has to consider the red-shift effect of the source, *i.e.*, $r \approx r_S$, c) the source distorts the wave fronts and produces the back-scattering of the waves, *i.e.*, $\left(r^3/M\right)^{1/2} \approx \lambda$, d) one enters the source region. The outer radius is located where either a) the Newtonian potential M/r of the source produces a significant phase-shift in the wave or b) the presence of nearby masses perturbs the propagation of the waves. We also demand that $r_O - r_I \gg \lambda.$, so that the local wave zone is very large with respect to the characteristic wavelength of the gravitational radiation.

- the distant wave zone is defined as $r > r_O$.

The wave generation and the wave propagation regions overlap in the local wave zone, where one has to match the source multipole moments and the radiation multipole moments (see, *e.g.*, the recent review of Blanchet, 2014). In other words, source multipole moments parametrise the source, while the radiative multipole moments parametrise the radiation field. These two kinds of moments must be related to each other by means of the matching asymptotic expansion technique. This is a necessary step when one wants to compare theoretical predictions with experimental observations by gravitational waves detectors.

4.3 Harmonic gauge

We consider an asymptotically flat space-time with dynamical metric $g_{\mu\nu}$. We denote the inverse metric as $g^{\mu\nu}$ and the Minkowski metric as $\eta_{\mu\nu}$, whose inverse is $\eta^{\mu\nu}$. We define the field $\mathfrak{g}^{\mu\nu} \equiv \eta^{\mu\nu} - \sqrt{-g}g^{\mu\nu}$ and impose the *de Donder* or *harmonic gauge*

$$\partial_\mu \mathfrak{g}^{\mu\nu} = 0. \tag{4.2}$$

The exact equations of General Relativity are written in this gauge as (see, *e.g.*, Blanchet, 2014))

$$\Box_\eta \mathfrak{g}^{\mu\nu} = -16\pi\tau^{\mu\nu} \equiv 16\pi|g|T^{\mu\nu} + \Lambda^{\mu\nu}, \tag{4.3}$$

where $\Lambda^{\mu\nu}$ is the effective stress tensor of the gravitational field and is quadratic or higher order in powers of $\mathfrak{g}^{\mu\nu}$ and $\Box_\eta = \eta^{\mu\nu}\partial_\mu\partial_\nu = -\partial_t^2 + \bar{\nabla}^2$ is the D'Alembertian operator with respect to the background flat metric. Due to the de Donder gauge, the stress-energy *pseudo-tensor* $\tau^{\mu\nu}$ is conserved $\partial_\mu\tau^{\mu\nu} = 0$.

4.3.1 Canonical harmonic gauge in General Relativity

As claimed in the section 4.1, the definition of multipole moments is ambiguous in harmonic gauge. It is, therefore, necessary to further fix the gauge. For outgoing-wave linearised configurations and for stationary non-linear configurations in General Relativity, Thorne (1980) provided a unique and well-defined definition of multipole moments for asymptotically flat space-times. His definition is stated in the so-called Asymptotically Cartesian Mass Centered (ACMC_∞) gauge, also known as *canonical harmonic gauge* (Blanchet, 1998), obtained from the usual *de Donder gauge* after further gauge fixing.

Here, we outline, following the section VIII of Thorne (1980), the main steps to reach the canonical harmonic gauge in the linearised theory.[2]

Consider the linearised metric field $g_{\mu\nu} = \eta_{\mu\nu} + h_{\mu\nu}$ around Minkowski space-time. At the linearised level, the field $\mathfrak{g}^{\mu\nu}$ is given by $\mathfrak{g}^{\mu\nu} = \gamma^{\mu\nu} + \mathcal{O}(\gamma^2)$ where

$$\gamma^{\mu\nu} = \eta^{\mu\alpha}\eta^{\nu\beta}h_{\alpha\beta} - \frac{1}{2}\eta^{\mu\nu}\eta^{\alpha\beta}h_{\alpha\beta} = h^{\mu\nu} - \frac{1}{2}\eta^{\mu\nu}h \tag{4.4}$$

is the trace-reversed perturbation. The harmonic gauge, $\partial_\mu\gamma^{\mu\nu} = 0$, and the linearised equations of motion in vacuum read as

$$\dot{\gamma}_{\mu 0} = \partial_i\gamma_{\mu i}, \quad \Box_\eta\gamma_{\mu\nu} = 0, \tag{4.5}$$

where the dot stands for the derivative with respect to time. The most general symmetric gravitational field satisfying the above equations and describing outgoing waves has the following form

$$\begin{aligned}
\gamma_{00} &= \partial_{A_l}\left(r^{-1}\mathcal{A}_{A_l}(u)\right) \\
\gamma_{0i} &= \partial_{A_{l-1}}\left(r^{-1}\mathcal{B}_{iA_{l-1}}(u)\right) + \partial_{pA_{l-1}}\left(r^{-1}\epsilon_{ipq}\mathcal{C}_{qA_{l-1}}(u)\right) + \partial_{iA_l}\left(r^{-1}\mathcal{D}_{A_l}(u)\right) \qquad (4.6a) \\
\gamma_{ij} &= \delta_{ij}\partial_{A_l}\left(r^{-1}\mathcal{E}_{A_l}(u)\right) + \partial_{A_{l-2}}\left(r^{-1}\mathcal{F}_{ijA_{l-2}}(u)\right) + \partial_{pA_{l-2}}\left(r^{-1}\epsilon_{pq(i}\mathcal{G}_{j)qA_{l-2}}(u)\right) + \\
&\quad + \left[\partial_{jA_{l-1}}\left(r^{-1}\mathcal{H}_{iA_{l-1}}(u)\right) + \partial_{jpA_{l-1}}\left(r^{-1}\epsilon_{ipq}\mathcal{N}_{qA_{l-1}}(u)\right)\right]^S + \partial_{ijA_l}\left(r^{-1}\mathcal{K}_{A_l}(u)\right),
\end{aligned}$$

[2] We refer the reader to section IX and section X of Thorne (1980) and references therein, respectively, for the explicit construction of the canonical harmonic coordinates in radiating and stationary space-times in the full non-linear theory.

where all coefficients are functions of the retarded time $u = t - r$. The functions $\mathcal{A}, \mathcal{B}, \ldots$ are symmetric and trace-free (STF) tensors (see appendix E). The harmonic or de Donder gauge fixes the constraints

$$\mathcal{B}_{A_l} = \dot{\mathcal{A}}_{A_l} - \ddot{\mathcal{D}}_{A_l}, \tag{4.7a}$$

$$\mathcal{E}_{A_l} = \dot{\mathcal{D}}_{A_l} - \frac{1}{2}\mathcal{H}_{A_l} - \ddot{\mathcal{K}}_{A_l}, \tag{4.7b}$$

$$\mathcal{F}_{A_l} = \ddot{\mathcal{A}}_{A_l} - \dddot{\mathcal{D}}_{A_l} - \frac{1}{2}\ddot{\mathcal{H}}_{A_l}, \tag{4.7c}$$

$$\mathcal{G}_{A_l} = 2\dot{\mathcal{C}}_{A_l} - \ddot{\mathcal{N}}_{A_l}. \tag{4.7d}$$

From Eqs. (4.6), it is immediate to notice that the STF coefficients $\mathcal{B}, \mathcal{C}, \mathcal{H}, \mathcal{N}$ appear from the dipole term $l \geq 1$ and $\mathcal{F}, \mathcal{G}$ appear from quadrupole term $l \geq 2$. Thus, the harmonic gauge conditions (4.7) imply for the monopole and dipole terms the following constraints

$$0 = \dot{\mathcal{A}} - \ddot{\mathcal{D}}, \tag{4.8a}$$

$$\mathcal{E} = \dot{\mathcal{D}} - \ddot{\mathcal{K}}, \tag{4.8b}$$

$$0 = \ddot{\mathcal{A}}_i - \dddot{\mathcal{D}}_i - \frac{1}{2}\ddot{\mathcal{H}}_i, \tag{4.8c}$$

$$0 = 2\dot{\mathcal{C}}_i - \ddot{\mathcal{N}}_i. \tag{4.8d}$$

The first and third equations of (4.8) are equivalent to the four-momentum conservation law, being

$$P^0 = \frac{1}{4}\left(\mathcal{A} - \dot{\mathcal{D}}\right), \quad P_i = -\frac{1}{4}\left(\dot{\mathcal{A}}_i - \ddot{\mathcal{D}}_i - \frac{1}{2}\dot{\mathcal{H}}_i\right) \tag{4.9}$$

the total four-momentum of the source, according to Eq. (20.6) of Misner, Thorne, and Wheeler (1973). Now, we perform a Lorentz boost to go to the rest-mass frame of the source and we set the centre of mass at the origin of our coordinates. These last two requirements are equivalent, respectively, to

$$\dot{\mathcal{A}}_i - \ddot{\mathcal{D}}_i - \frac{1}{2}\dot{\mathcal{H}}_i = 0, \quad \mathcal{A}_i - \dot{\mathcal{D}}_i - \frac{1}{2}\mathcal{H}_i = 0. \tag{4.10}$$

The next step is to use the gauge freedom to bring to zero four of the aforementioned STF coefficients. To this aim, we recall that a gauge transformation acts on the linearised metric perturbation as $h_{\mu\nu} \mapsto h_{\mu\nu} + \partial_\mu \xi_\nu + \partial_\nu \xi_\mu$ and therefore as

$$\gamma_{\mu\nu} \mapsto \gamma_{\mu\nu} + \partial_\mu \xi_\nu + \partial_\nu \xi_\mu - \eta_{\mu\nu}\partial_\alpha \xi^\alpha, \tag{4.11}$$

on the trace-reversed field, where all indices are lowered with the flat metric. The explicit form of the vector field ξ_μ, preserving the harmonic gauge, can be written as[3]

$$\xi_0 = -\partial_{A_l}\left(r^{-1}\mathcal{D}_{A_l}(u)\right) + \frac{1}{2}\partial_{A_l}\left(r^{-1}\dot{\mathcal{K}}_{A_l}(u)\right), \tag{4.12a}$$

$$\xi_i = -\frac{1}{2}\partial_{iA_l}\left(r^{-1}\mathcal{K}_{A_l}(u)\right) - \frac{1}{2}\partial_{A_{l-1}}\left(r^{-1}\mathcal{H}_{iA_{l-1}}(u)\right) - \frac{1}{2}\partial_{pA_{l-1}}\left(r^{-1}\epsilon_{ipq}\mathcal{N}_{qA_{l-1}}(u)\right). \tag{4.12b}$$

Thus, we use the gauge freedom to set to zero $\mathcal{D}_{A_l}, \mathcal{H}_{A_l}, \mathcal{N}_{A_l}, \mathcal{K}_{A_l}$. This defines the canonical harmonic gauge, *i.e.*, the harmonic gauge in the rest-frame of the source with the centre of mass at the origin of the coordinates and with the only two independent STF coefficients $\mathcal{A}$ and $\mathcal{C}$ in Eq. (4.6) parametrising the linearised metric perturbation.

4.4 Multipole moments

The definitions of mass and current multipole moments require a background structure involving Minkowski space-time and either a choice of gauge (in the Thorne's approach with canonical harmonic gauge) or a choice of conformal completion (in the Geroch-Hansen's formalism).

Source multipole moments are defined in canonical harmonic gauge at spatial infinity from the spherical harmonic decomposition of the metric field. Thorne's source moments agree with the Geroch-Hansen's definition for stationary space-times (Geroch, 1970; Hansen, 1974), up to a choice of normalization, after calibrating appropriately the ambiguity in the definition of the conformal factor in the Geroch-Hansen formalism (Gürsel, 1983).

Independently, *radiative multipole moments* are defined in radiative (Bondi) gauge at future null infinity from the spherical harmonic decomposition of the Bondi news tensor (Bondi, van der Burg, and Metzner, 1962; Sachs, 1962).

4.4.1 Source multipole moments

Multipole moments are generated by sources. In linearised General Relativity, source multipole moments can be expressed as volume integrals depending on

[3] see section VIII, Eq. (8.9) of Thorne (1980) and the equivalent expression in terms of vector spherical harmonics in Eq. (E.52).

the source stress-tensor (Campbell and Morgan, 1971; Campbell, Macek, and Morgan, 1977; Damour and Iyer, 1991). In full General Relativity, the problem of defining source multipole moments is more involved as it has been already said at the beginning of the introduction of this chapter. The reason is that source multipole moments mix with each other and it is not obvious at first sight how to define a consistent multipole expansion. However, for slow moving sources ($v \ll c$), the post-Newtonian (PN) expansion of General Relativity is applicable and multipole moments can still be expressed as volume integrals over the sources (Burke, 1971; Epstein and Wagoner, 1975; Thorne, 1980; Blanchet, 1998). These volume integrals can be expressed as surface integrals in the outer or weak-field near-zone, *i.e.*, far from the source but at radii negligible with respect to the radiation wavelength (Blanchet, Damour, and Iyer, 2005).

In the following, we introduce source multipole moments from the expansion at spatial infinity ($r \to \infty$ and t = constant) of the metric field in canonical harmonic gauge. We first consider the case of radiating space-times within the linearised theory and then we discuss the case of stationary space-times within the full General Relativity.

Phase space for linearised radiating space-times

Recall that $g_{\mu\nu} = \eta_{\mu\nu} + h_{\mu\nu}$ is the linearised metric describing the external gravitational field of an arbitrary isolated system with no incoming wave boundary conditions, and further excluding NUT or acceleration parameters which are not considered physical.

In the canonical harmonic gauge (also called $ACMC_\infty$ coordinates in Thorne, 1980), $h_{\mu\nu}$ takes the following form

$$
\begin{aligned}
h_{00} &= \frac{2\mathcal{I}}{r} + \sum_{l=2}^{\infty} (-1)^l \frac{2}{l!} \partial_{A_l} \left(\frac{\mathcal{I}_{A_l}(u)}{r} \right), \\
h_{0j} &= -\sum_{l=1}^{\infty} (-1)^l \frac{4l}{(l+1)!} \partial_{qA_{l-1}} \left(\frac{\epsilon_{jpq} \mathcal{S}_{pA_{l-1}}(u)}{r} \right) + \sum_{l=2}^{\infty} (-1)^l \frac{4}{l!} \partial_{A_{l-1}} \left(\frac{\dot{\mathcal{I}}_{jA_{l-1}}(u)}{r} \right), \\
h_{ij} &= h_{00}\delta_{ij} + \sum_{l=2}^{\infty} (-1)^l \left[\frac{4}{l!} \partial_{A_{l-2}} \left(\frac{\ddot{\mathcal{I}}_{ijA_{l-2}}(u)}{r} \right) - \frac{8l}{(l+1)!} \partial_{qA_{l-2}} \left(\frac{\epsilon_{pq(i} \dot{\mathcal{S}}_{j)pA_{l-2}}(u)}{r} \right) \right].
\end{aligned}
\tag{4.13}
$$

The linearised metric is expressed in terms of symmetric trace-free (STF) tensors $\mathcal{I}_{A_l}(u)$, $\mathcal{S}_{A_l}(u)$ that are respectively the *mass* and *current* gravitational multipole moments. This is Thorne's definition in terms of metric components. The mass monopole $\mathcal{I}$ is constant and is interpreted as the mass of the source. The current dipole $\mathcal{S}_i$ is also constant and is interpreted as the angular momentum of the

source. Because we are in the centre of mass frame, no mass dipole moment $\mathcal{I}_i$ is present.

Phase space for stationary space-times

Let $g_{\mu\nu} = \eta_{\mu\nu} + \mathcal{O}(1/r)$ be an asymptotically flat stationary metric in de Donder coordinates. We restrict our analysis to those metrics that are solutions to General Relativity, where the metric coefficients $g_{\mu\nu}$ are analytic functions of the de Donder coordinates (Hagen, 1970). In canonical harmonic coordinates, the resulting metric reads as (see section X and Eqs. (10.6) in Thorne (1980))

$$
\begin{aligned}
g_{00} &= -1 + \frac{2\mathcal{I}}{r} + \frac{(0)\text{pole}}{r^2} + \sum_{l=2}^{\infty} \frac{1}{r^{l+1}} \left(\frac{2(2l-1)!!}{l!} \mathcal{I}_{A_l} N_{A_l} + (l-1)\text{pole} + \cdots + (0)\text{pole} \right), \\
g_{0j} &= \sum_{l=1}^{\infty} \frac{1}{r^{l+1}} \left(-\frac{4l(2l-1)!!}{(l+1)!} \epsilon_{jpa_l} \mathcal{S}_{pA_{l-1}} N_{A_l} + (l-1)\text{pole} + \cdots + (0)\text{pole} \right), \qquad (4.14) \\
g_{ij} &= \delta_{ij} \left(1 + \frac{2\mathcal{I}}{r} \right) + \frac{(0)\text{pole}}{r^2} + \sum_{l=2}^{\infty} \frac{1}{r^{l+1}} \left(\frac{2(2l-1)!!}{l!} \mathcal{I}_{A_l} N_{A_l} \delta_{ij} + (l-1)\text{pole} + \cdots + (0)\text{pole} \right).
\end{aligned}
$$

Here (0)pole is a constant monopole, (1)pole a combination of $l = 1$ spherical harmonics, *etc.* The tensors N_{A_l} are defined in appendix E.1. The coefficients $\mathcal{I}_{A_l}$ and $\mathcal{S}_{A_l}$ are defined as the mass multipole moments and the current multipole moments, respectively (Thorne, 1980). In such canonical harmonic coordinates there is no mass dipole moment $\mathcal{I}_i$. The mass and angular momentum are respectively $\mathcal{I}$ and $\mathcal{S}_i$. The STF version of the multipole moments $\mathcal{I}_{A_l}$, $\mathcal{S}_{A_l}$ can be translated in harmonic coefficients I^{lm} and S^{lm} (see, *e.g.*, Eq. (E.33)).

4.4.2 Radiative multipole moments

The radiative multipole moments parametrize the radiation field. Throughout the local wave zone, by definition, the gravitational waves can be described as linearised perturbation of the metric around the Minkowski background.

We introduce radiative multipole moments from the expansion at future null infinity ($R \to \infty$ and u = constant) of the metric field in radiative (Bondi) gauge (U, R, θ, ϕ), where $R = r$ and $U = u - 2M\log(r)$. In radiative coordinates and under the assumption of no incoming radiation, the metric admits an expansion at future null infinity in powers of $1/R$ without logarithmic terms (Blanchet, 1987). In this coordinate system, the gravitational radiation is fully determined by the transverse and traceless (TT) part of the spatial part of linearised metric perturbation (see, *e.g.*, Misner, Thorne, and Wheeler, 1973). Mathews (1962) proved that

the linearised radiation field must have the following form

$$h_{ij}^{TT} = \frac{1}{R}\sum_{l=2}^{\infty}\sum_{m=-l}^{l}\left[{}^{(l)}I^{lm}(U)\,T_{ij}^{E2\,lm} + {}^{(l)}S^{lm}(U)\,T_{ij}^{B2\,lm}\right], \tag{4.15}$$

where $T_{ij}^{E2\,lm}$ and $T_{ij}^{B2\,lm}$ are the transverse and traceless tensor spherical harmonics of spin-2 defined in appendix E.2.3. The gravitational radiation field in (4.15) is the most general outgoing-wave TT solution of the equation $\Box_\eta h_{ij}^{TT} = 0$. It is manifest that the radiation field contains multipole moments from the quadrupole term ($l = 2$) and higher: this is another way to highlight the tensorial nature of the gravitational radiation within General Relativity.

The equivalent expression in terms of STF tensors reads as (Sachs, 1961; Thorne, 1980)

$$\begin{aligned} h_{ij}^{TT} &= \frac{1}{R}\sum_{l=2}^{\infty}\left[\frac{4}{l!}\,{}^{(l)}\mathcal{I}_{ijA_{l-2}}(U)N_{A_{l-2}} + \frac{8}{(l+1)!}\epsilon_{pq(i}\,{}^{(l)}\mathcal{S}_{j)pA_{l-2}}(U)n_q N_{A_{l-2}}\right]^{TT}, \\ &= \frac{1}{R}\sum_{l=2}^{\infty}\left[\frac{4}{l!}U_{ijA_{l-2}}(U)N_{A_{l-2}} + \frac{8}{(l+1)!}\epsilon_{pq(i}V_{j)pA_{l-2}}(U)n_q N_{A_{l-2}}\right]^{TT}. \end{aligned} \tag{4.16}$$

The radiative multipole moments U_{A_l} and V_{A_l} characterize the radiation field. We notice that the radiative multipole moments are the l-th derivatives of the source multipole moments at the linearised order in the gravitational coupling. For example, the quadrupole formula as derived by Einstein (1918) is simply given by

$$U_{ij}(U) = {}^{(2)}\mathcal{I}_{ij}(U) + \mathcal{O}(G). \tag{4.17}$$

The expression of radiative multipole moments in terms of source multipole moments can be established perturbatively to all orders in the gravitational coupling under certain hypotheses including no incoming radiation (Blanchet, 1987). Such expressions involve time integrals, known as *tails*, and further non-linear terms including the non-linear memory (see, *e.g.*, the review of Blanchet, 2014).

In chapter 8, we shall discuss how to directly extract the source multipole moments (without derivative) close to future null infinity by means of Noether charges.

Part II

Original contributions

Chapter 5

Near-horizon extreme Kerr magnetospheres

Contents

In the first two chapters of Part I, we have introduced the Near-Horizon Extreme Kerr (NHEK) space-time and Force-Free Electrodynamics (FFE). In this chapter, we will proceed in a systematic study of FFE around NHEK. The content of this chapter is mainly based on Compère and Oliveri (2016).

After a brief introduction in section 5.1, we define the problem we want to address in section 5.2, namely, to solve the FFE equations around NHEK space-time and to classify the solutions using the highest weight representation of the isometry group of NHEK space-time. We introduce the language of canonical Euler potential in section 5.3. Then, we find the maximally symmetric solutions to the above problem in section 5.4. Later, in section 5.5, we outline the strategy to solve the equations. Having found a list of mathematical solutions to the equations, in section 5.6, we introduce certain physical requirements to discriminate the physically relevant ones describing the extreme Kerr force-free magnetospheres. Finally, section 5.7 concludes the chapter with the discussion of the main results.

5.1 Introduction

The study of FFE around (near-) NHEK space-time started with the paper of Li et al. (2015) and continued with Lupsasca, Rodriguez, and Strominger (2014), Zhang, Yang, and Lehner (2014), Lupsasca and Rodriguez (2015), and Compère and Oliveri (2016). In Li et al. (2015), it has been realised that (near-) NHEK space-time allows to analytically investigate force-free magnetospheres around rapidly rotating (astrophysical) black holes. In this earlier attempt, no use of conformal symmetries has been made. Lupsasca, Rodriguez, and Strominger (2014) and subsequent papers mentioned above, instead, exploit the symmetries of the NHEK isometry group to solve FFE and to find classes of exact analytical solutions.

In this context, we build on previous works and extend their preceding results in several directions. First of all, we extend the list of exact solutions to FFE around NHEK and classify them in seven independent classes. Second, we provide new insights into the physical properties of force-free magnetospheres by introducing criteria to select potentially physical solutions. Among such criteria, the solutions must admit finite extraction of energy and angular momentum with respect to an asymptotically flat observer. As a consequence, the criteria impose tight constraints on the conformal weights of the solutions, in agreement with the analysis of Gralla, Lupsasca, and Strominger (2016). Another result is to have highlighted the presence and the role of the velocity of light surface, where potentially physical solutions have a logarithmic divergence.[1]

[1] See the discussion below Eq. (1.18) for the definition of the velocity of light surface. Moreover, the velocity of light surface changes the order of the differential equations describing the magnetospheres (Zhang, Yang, and Lehner, 2014).

5.2 Set-up of the problem

The basic problem is to find solutions to FFE

$$dF_{(h,q,0)} = 0, \quad d\star F_{(h,q,0)} = \star J_{(h,q,0)}, \quad J_{(h,q,0)} \wedge \star F_{(h,q,0)} = 0, \tag{5.1}$$

falling into the highest weight representation[2] of $SL(2,\mathbb{R})\times U(1)$ labelled by $\{h,q,k\}$, where k labels descendants given by $\left(\mathscr{L}_{H_-}\right)^k F_{(h,q,0)} = F_{(h,q,k)}$,

$$\begin{cases} \mathscr{L}_{H_+} F_{(h,q,0)} = 0, \\ \mathscr{L}_{H_0} F_{(h,q,0)} = h F_{(h,q,0)}, \\ \mathscr{L}_{Q_0} F_{(h,q,0)} = i q F_{(h,q,0)}, \end{cases} \tag{5.2}$$

around the NHEK space-time

$$ds^2_{NHEK} = 2M^2\,\Gamma(\theta)\left[-R^2 dT^2 + \frac{dR^2}{R^2} + d\theta^2 + \gamma^2(\theta)\,(d\Phi + R dT)^2\right], \tag{5.3}$$

where $\Gamma(\theta) = \left(1+\cos^2(\theta)\right)/2$ and $\gamma(\theta) = \sin(\theta)/\Gamma(\theta)$. Notice that the metric in Poincaré coordinates can be decomposed into the toroidal part spanned by (T,Φ) with volume form $\epsilon^T = \Gamma\gamma R dT \wedge d\Phi$, and the poloidal part spanned by (R,θ) with volume form $\epsilon^P = \frac{\Gamma}{R} dR \wedge d\theta$. We have $\epsilon = \epsilon^T \wedge \epsilon^P$, $\star\epsilon^T = -\epsilon^P$, $\star\epsilon^P = \epsilon^T$.

Once classes of solutions have been found, it is natural to ask whether they are physical or not. First of all, the electromagnetic field F must be real and its character must be either magnetically dominated or null. Then, we demand that they should have finite and computable energy and angular momentum flux with respect to an asymptotically flat observer. In addition, we would like to select those solutions that come from the near-horizon limit of regular solutions to FFE around (near-) extreme Kerr. In different words, we want to have a criterion to select genuine NHEK solutions from solutions that are originated as limit (in the sense defined at the end of chapter 1) of solutions existing on (near-) extreme Kerr.

5.3 Canonical Euler potentials

5.3.1 Stationary and axisymmetric case

Let us first summarise the stationary and axisymmetric case as analysed in section 2.5. There is no toroidal electric field (and therefore no components of the

[2] The physical motivation behind this strategy is to find stationary, self-similar and $U(1)$-charged solutions. See also the discussion below Eq. (1.22).

field strength proportional to $dT \wedge d\Phi$) for axisymmetric configurations as a simple consequence of Faraday's law. We distinguish three scenarios:

generic case $i_{\partial_\Phi} F \neq 0$. One can choose

$$\phi_1 = \psi(R,\theta), \qquad \phi_2 = \Phi + \psi_2(R,\theta) - \Omega(\psi)T. \tag{5.4}$$

The polar current $I(R,\theta)$ is defined as

$$\star(d\psi \wedge d\psi_2) = \frac{I(R,\theta)}{\sqrt{-g^T}}\epsilon^T. \tag{5.5}$$

It is equal to the electric current with respect to time T flowing in the upward direction through the loop of revolution defined by the poloidal point (R,θ). Note that this interpretation breaks down beyond the velocity of light surface where ∂_T is spacelike. The force-free equations imply that $I = I(\psi)$. We therefore have

$$F = d\psi \wedge \big(d\Phi - \Omega(\psi)\,dT\big) + I(\psi)\frac{dR\wedge d\theta}{\gamma R^2}. \tag{5.6}$$

In particular, if $\Omega(\psi) = 0$, there is no electric field, $i_{\partial_T} F = 0$.

No poloidal magnetic field $i_{\partial_\Phi} F = 0$, $i_{\partial_T} F \neq 0$. One can choose instead

$$\phi_1 = \chi(R,\theta), \qquad \phi_2 = T + \chi_2(R,\theta). \tag{5.7}$$

We then define the polar current as $\star(d\chi \wedge d\chi_2) = \frac{I(R,\theta)}{\sqrt{-g^T}}\epsilon^T$ which has the same interpretation as above. The force-free equations imply $I = I(\chi)$. The corresponding field strength takes the form

$$F = d\chi \wedge dT + I(\chi)\frac{dR\wedge d\theta}{\gamma R^2}. \tag{5.8}$$

Only toroidal magnetic field $i_{\partial_T} F = 0$, $i_{\partial_\Phi} F = 0$. In that case,

$$\phi_1 = \chi(R,\theta), \qquad \phi_2 = \chi_2(R,\theta), \qquad F = I(\chi)\frac{dR\wedge d\theta}{\gamma R^2}. \tag{5.9}$$

There is no electric field and no poloidal magnetic field.

5.3.2 Stationary and ∂_Φ-eigenvalue case

Let us now consider a complex force-free field strength which is stationary, $\mathscr{L}_{\partial_T} F = 0$, and which is an iq ∂_Φ-eigenvalue, $\mathscr{L}_{\partial_\Phi} F = iqF$. Stationarity implies

$$0 = \mathscr{L}_{\partial_T} F = d\, i_{\partial_T} F = d\left(-\partial_T \phi_2 d\phi_1 + \partial_T \phi_1 d\phi_2\right), \tag{5.10}$$

where we used Cartan's formula, Bianchi's identity and the degeneracy of F. By Poincaré's lemma, there exists a function $f = f(\phi_1, \phi_2)$ such that:

$$-\partial_T \phi_2 d\phi_1 + \partial_T \phi_1 d\phi_2 = df. \tag{5.11}$$

We distinguish here two cases: (i) $i_{\partial_T} F = df = 0$ which implies that both Euler potentials are time independent and (ii) $i_{\partial_T} F = df \neq 0$ to which we now turn our attention. Euler potentials are defined up to the following arbitrariness: we may choose any other pair of potentials $(\tilde{\phi}_1, \tilde{\phi}_2)$, leaving the electromagnetic 2-form invariant, provided the map $(\phi_1, \phi_2) \to (\tilde{\phi}_1, \tilde{\phi}_2)$ has unit Jacobian determinant. Using this freedom, we choose $\tilde{\phi}_1 = -f$. Let us check the existence of $\tilde{\phi}_2(\phi_1, \phi_2)$. The Jacobian of the transformation reads as

$$1 = \frac{\partial \tilde{\phi}_1}{\partial \phi_1}\frac{\partial \tilde{\phi}_2}{\partial \phi_2} - \frac{\partial \tilde{\phi}_1}{\partial \phi_2}\frac{\partial \tilde{\phi}_2}{\partial \phi_1} = -\frac{\partial f}{\partial \phi_1}\frac{\partial \tilde{\phi}_2}{\partial \phi_2} + \frac{\partial f}{\partial \phi_2}\frac{\partial \tilde{\phi}_2}{\partial \phi_1}, \tag{5.12}$$

which is a first order partial differential equation (PDE) for $\tilde{\phi}_2(\phi_1, \phi_2)$ and can be integrated with respect to ϕ_2 if $\frac{\partial f}{\partial \phi_1} \neq 0$ or with respect to ϕ_1 if $\frac{\partial f}{\partial \phi_2} \neq 0$. With this new pair of Euler potentials, Eq. (5.11) becomes

$$-\partial_T \tilde{\phi}_2 d\tilde{\phi}_1 + \partial_T \tilde{\phi}_1 d\tilde{\phi}_2 = -d\tilde{\phi}_1, \tag{5.13}$$

from which we read off the conditions

$$\partial_T \tilde{\phi}_1 = 0, \qquad \partial_T \tilde{\phi}_2 = 1, \tag{5.14}$$

whose solutions are

$$\tilde{\phi}_1 = \chi_1(R, \theta, \Phi), \qquad \tilde{\phi}_2 = T + \chi_2(R, \theta, \Phi). \tag{5.15}$$

Finally, merging cases (i) and (ii) and dropping tildes, Euler potentials for stationary solutions can be fixed to

$$\phi_1 = \chi_1(R, \theta, \Phi), \qquad \phi_2 = \epsilon\, T + \chi_2(R, \theta, \Phi), \tag{5.16}$$

where $\epsilon = 1$ if $i_{\partial_T} F \neq 0$ and $\epsilon = 0$ if $i_{\partial_T} F = 0$.

Let us now turn our attention to the second condition $\mathscr{L}_{\partial_\Phi} F = iqF$. We have

$$\begin{aligned} 0 &= d i_{\partial_\Phi} F - iqF \\ &= d i_{\partial_\Phi}(d\phi_1 \wedge d\phi_2) - iq d\phi_1 \wedge d\phi_2 \\ &= d\left[(i_{\partial_\Phi} d\phi_1) d\phi_2 - (i_{\partial_\Phi} d\phi_2) d\phi_1\right] - iq d\phi_1 \wedge d\phi_2 \\ &= d\left[(\partial_\Phi \phi_1 - iq\phi_1) d\phi_2 - (\partial_\Phi \phi_2) d\phi_1\right] \\ &= d\left[(\partial_\Phi \chi_1 - iq\chi_1)(\epsilon dT + d\chi_2) - (\partial_\Phi \chi_2) d\chi_1\right], \end{aligned} \tag{5.17}$$

where we used Bianchi identity in the first step and stationarity in the last one. Let us first discuss the case $\epsilon = 1$. Since χ_1, χ_2 have no time dependence, from the identity

$$0 = d(\partial_\Phi \chi_1 - iq\chi_1) \wedge (dT + d\chi_2) - d(\partial_\Phi \chi_2) \wedge d\chi_1, \tag{5.18}$$

we infer that

$$\partial_\Phi \chi_1 - iq\chi_1 = \text{const}, \qquad \partial_\Phi \chi_2 = \kappa(\chi_1), \tag{5.19}$$

where $\kappa(\chi_1)$ is an arbitrary function of the Euler potential χ_1 and where the arbitrary constant can be set to zero by shifting χ_1.
From the first differential equation we have

$$\chi_1(R,\theta,\Phi) = e^{iq\Phi} \tilde{\chi}_1(R,\theta). \tag{5.20}$$

From the second differential equation, we infer

$$\chi_2(R,\theta,\Phi) = \int^\Phi \kappa\left(e^{iq\Phi'} \tilde{\chi}_1\right) d\Phi' + \tilde{\chi}_2(R,\theta). \tag{5.21}$$

In conclusion, dropping the tildes for simplicity, the Euler potentials in the case $i_{\partial_T} F \neq 0$ can be taken as

$$\phi_1 = e^{iq\Phi} \chi_1(R,\theta), \qquad \phi_2 = T + \chi_2(R,\theta) + \int^\Phi \kappa\left(e^{iq\Phi'} \chi_1(R,\theta)\right) d\Phi'. \tag{5.22}$$

Let us compute the field strength. We define $h(R,\theta,\Phi) = \int^\Phi \kappa\left(e^{iq\Phi'} \chi_1(R,\theta)\right) d\Phi'$, then

$$dh(R,\theta,\Phi) = \frac{\partial h}{\partial R} dR + \frac{\partial h}{\partial \theta} d\theta + \frac{\partial h}{\partial \Phi} d\Phi, \tag{5.23}$$

where

$$\frac{\partial h}{\partial R} = \int^{\Phi} \frac{\partial \kappa(\phi_1)}{\partial \phi_1}\Big|_{\Phi\to\Phi'} e^{iq\Phi'}\partial_R\chi_1 d\Phi', \tag{5.24}$$

$$\frac{\partial h}{\partial \theta} = \int^{\Phi} \frac{\partial \kappa(\phi_1)}{\partial \phi_1}\Big|_{\Phi\to\Phi'} e^{iq\Phi'}\partial_\theta\chi_1 d\Phi', \tag{5.25}$$

$$\frac{\partial h}{\partial \Phi} = \kappa(\phi_1). \tag{5.26}$$

The exterior derivative of ϕ_2 is

$$d\phi_2 = dT + d\chi_2 + \kappa(\phi_1)d\Phi + \left(\int^{\Phi} \frac{\partial \kappa(\phi_1)}{\partial \phi_1}\Big|_{\Phi\to\Phi'} e^{iq\Phi'} d\Phi'\right) d\chi_1, \tag{5.27}$$

and the field strength takes the following form

$$F = d\phi_1 \wedge (dT + d\chi_2) + e^{iq\Phi}\left[\kappa(\phi_1) - iq\chi_1 \int^{\Phi} \frac{\partial \kappa(\phi_1)}{\partial \phi_1}\Big|_{\Phi\to\Phi'} e^{iq\Phi'} d\Phi'\right] d\chi_1 \wedge d\Phi. \tag{5.28}$$

Let us now return to the case $\epsilon = 0$ ($i_{\partial_T} F = 0$). We restart from Eq. (5.17). By Poincaré's lemma there exists a function f such that

$$\left[(\partial_\Phi\chi_1 - iq\chi_1)(d\chi_2) - (\partial_\Phi\chi_2)d\chi_1\right] = df. \tag{5.29}$$

If $df = 0$ we find directly

$$\partial_\Phi\chi_2 = 0, \qquad \partial_\Phi\chi_1 - iq\chi_1 = 0, \tag{5.30}$$

and we find the Euler potentials in the case $\partial_T F = 0$ with $df = 0$,

$$\phi_1 = e^{iq\Phi}\chi_1(R,\theta), \qquad \phi_2 = \chi_2(R,\theta). \tag{5.31}$$

In that case, the field strength is

$$F = e^{iq\Phi}\Big(d\chi_1 \wedge d\chi_2 - iq\chi_1 d\chi_2 \wedge d\Phi\Big). \tag{5.32}$$

If $df \neq 0$, one can use again the ambiguity in the definition of Euler potentials to choose $\chi_1 = -f$. Then

$$\partial_\Phi\chi_2 = 1, \qquad \partial_\Phi\chi_1 - iq\chi_1 = 0, \tag{5.33}$$

and we find the Euler potentials $\phi_1 = e^{iq\Phi}\chi_1(R,\theta)$, $\phi_2 = \Phi + \chi_2(R,\theta)$. Since these potentials generalise (5.4) when $\Omega = 0$, we find it convenient to align the notations

so that finally we get in the case $\partial_T F = 0$ with $df \neq 0$,

$$\phi_1 = e^{iq\Phi}\psi(R,\theta), \qquad \phi_2 = \Phi + \psi_2(R,\theta). \tag{5.34}$$

In that case, the field strength is

$$F = e^{iq\Phi}\Big(d\psi \wedge d\psi_2 + (d\psi - iq\psi d\psi_2) \wedge d\Phi\Big). \tag{5.35}$$

5.4 Maximally symmetric solutions

To warm up, we begin by deriving the maximally symmetric solutions to FFE, *i.e.*, those solutions invariant under the full isometry group $SL(2,\mathbb{R}) \times U(1)$. We first want to exploit the symmetries and find solutions to the system $\mathscr{L}_X F = 0$, where $X = \{H_\pm, H_0, Q_0\}$. We notice that $0 = \mathscr{L}_X F = \mathscr{L}_X dA = d\mathscr{L}_X A$. Therefore, $\mathscr{L}_X A = 0$ implies $\mathscr{L}_X F = 0$. The invariance of the gauge potential A under the generators $H_\pm$, H_0 and Q_0 constrains the potential to be

$$A = A_0(\theta)\hat{Q}_0 + A_1(\theta)d\theta, \tag{5.36}$$

where A_0 and A_1 are two arbitrary real-valued function of the polar angle and $\hat{Q}_0 = Q_0/|Q_0| = d\Phi + RdT$. We impose the gauge $A_1 = 0$ and we get

$$F = -A_0(\theta)dT \wedge dR + \partial_\theta A_0(\theta)d\theta \wedge \hat{Q}_0, \tag{5.37a}$$

$$J = -\frac{\gamma(\theta)}{\Gamma(\theta)}\left[\partial_\theta\left(\frac{\partial_\theta A_0(\theta)}{\gamma(\theta)}\right) + \gamma(\theta)A_0(\theta)\right]\hat{Q}_0. \tag{5.37b}$$

The force-free condition amounts to

$$0 = J \wedge \star F = -\frac{\partial_\theta A_0(\theta)}{\Gamma(\theta)}\left[\partial_\theta\left(\frac{\partial_\theta A_0(\theta)}{\gamma(\theta)}\right) + \gamma(\theta)A_0(\theta)\right] dT \wedge dR \wedge d\theta. \tag{5.38}$$

There are two branches:

- the non-trivial force-free solution for constant $A_0 = -E_0$ and

$$A = -E_0\hat{Q}_0, \quad F = -E_0 d\hat{Q}_0, \quad J = -\frac{\gamma^2(\theta)}{\Gamma(\theta)}A. \tag{5.39}$$

  This solution is electrically dominated, because $\star(F\wedge\star F) = -1/2\,F^2 = E_0^2/\Gamma^2(\theta) > 0$. This solution is also understood to be the $h = 0$ universal near-horizon limit of force-free magnetospheres defined on extreme Kerr (see Eqs. (23) in Gralla, Lupsasca, and Strominger, 2016). In other words, this solution is the unique electromagnetic field with conformal weight $h = 0$ originating from

a stationary, axisymmetric and regular (on the future horizon) solution to FFE on extreme Kerr space-time. We shall review the reasoning leading to this conclusion in section 5.6.5.

- the trivial force-free solution (or source-free Maxwell solution) obeying

$$\partial_\theta \left(\frac{\partial_\theta A_0(\theta)}{\gamma(\theta)} \right) + \gamma(\theta) A_0(\theta) = 0. \tag{5.40}$$

The general solution reads as

$$A_0(\theta) = M_0 \cos\left[\theta_0 + 2 \arctan\cos(\theta)\right], \tag{5.41}$$

where M_0 and θ_0 are the two constants of integration. The electromagnetic field is regular both at the north and at south pole since $A_0'(0) = 0 = A_0'(\pi)$. The character of the solution is given by the expression

$$\star\,(F \wedge \star F) = -1/2\; F^2 = \frac{1}{\gamma^2(\theta)\Gamma^2(\theta)} \left[-\left(\partial_\theta A_0(\theta)\right)^2 + \gamma^2(\theta) A_0^2(\theta) \right]. \tag{5.42}$$

It is possible to make this solution magnetically dominated in the physical region beyond the velocity of light surface upon choosing the constant of integration $\theta_0 \leq |2 \arctan \sqrt{2\sqrt{3}-3} - \pi/4| \approx 23.5°$.

The same solution to the source-free Maxwell's equations has been found in Gralla, Lupsasca, and Strominger (2016); see their Eq. (15). The two constants are identified with the electric and magnetic charges associated to the solution:

$$A_0(\theta) = -Q_e \cos[G(\theta)] + Q_m \sin[G(\theta)], \quad G(\theta) = -\int^\theta \gamma(\theta')\, d\theta'. \tag{5.43}$$

Astrophysical black holes have no net electric and magnetic charge, therefore we have to set $Q_e = 0 = Q_m$. Thus the electromagnetic field F entirely vanishes in the near-horizon geometry as a consequence of the $SL(2,\mathbb{R})$ symmetry. This statement is stronger than the so-called Meissner effect where the magnetic flux through the upper hemisphere of the event horizon vanishes in the extreme Kerr case (see section 6.2 for a discussion about the Meissner-like effect).

5.5 Highest weight classification of solutions

5.5.1 Solving the force-free condition

In order to classify highest weight solutions, we first choose a $SL(2,\mathbb{R})$ covariant basis for 1-forms $\{\mu^i\}_{i=1,\dots,4}$ and 2-forms $\{w^j\}_{j=1,\dots,6}$, whose explicit expressions can be found in appendix C.3. The electromagnetic field can be written in the $\{w^j\}$ basis as

$$F_{(h,q)} = F_{(h,q),i}\, w^i, \tag{5.44}$$

where $F_{(h,q),i}$ are functions of the space-time coordinates. Then, the system (5.2) is equivalent to the following conditions on the coefficients of $F_{(h,q)}$

$$\begin{cases} H_+ F_{(h,q),i} = 0, \\ H_0 F_{(h,q),i} = (h-1) F_{(h,q),i}, \\ Q_0 F_{(h,q),i} = i q F_{(h,q),i}, \end{cases} \tag{5.45}$$

where, *e.g.*, $H_+ F_{(h,q),i} = H_+^\mu \partial_\mu F_{(h,q),i}$. The most general solution is expressed by

$$F_{(h,q)} = \Phi_{(h-1,q)}\, f_i(\theta)\, w^i, \tag{5.46}$$

where $\Phi_{(h,q)}$ are the highest weight scalars[3] defined in Eq. (C.4) and $f_i(\theta)$ are six arbitrary functions of the polar angle. In other words, the symmetries of $F_{(h,q)}$ imply that the space-time dependence of $F_{(h,q),i}$ is factorised into the functions $\Phi_{(h,q)}$, carrying the conformal weight and the $U(1)$ charge of the field, and $f_i(\theta)$, expressing the polar angle dependence.

The most general vector potential $A_{(h,q)}$ such that $F_{(h,q)} = dA_{(h,q)}$ can be written in terms of four arbitrary functions of the polar angle $a_i(\theta)$ as

$$A_{(h,q)} = \Phi_{(h,q)}\, a_i(\theta)\, \mu^i. \tag{5.47}$$

[3] Do not confuse the azimuthal coordinate Φ with the highest weight scalar $\Phi_{(h,q)}$. All Φ's appearing in the expressions of A, F and J hereafter are the highest weight scalars.

Simple algebra shows that f_i's can be written in terms of a_i's functions as follows

$$\begin{cases} f_1(\theta) & = h a_3(\theta) - \gamma(\theta) a_4'(\theta), \\ f_2(\theta) & = -iq a_3(\theta) + \gamma(\theta)\left(-a_1'(\theta) + a_2'(\theta)\right), \\ \gamma^2(\theta) f_3(\theta) & = iq a_3(\theta) - \gamma(\theta) a_2'(\theta), \\ f_4(\theta) & = (1-h) a_1(\theta) + h a_2(\theta) - iq a_4(\theta), \\ f_5(\theta) & = -h a_2(\theta) + iq a_4(\theta), \\ f_6(\theta) & = iq a_1(\theta). \end{cases} \tag{5.48}$$

Of course Bianchi identity $dF_{(h,q)} = 0$ is automatically satisfied. It reduces the number of independent components $f_i(\theta)$ to three. Upon choosing a gauge, *e.g.*, $a_4(\theta) = 0$, we are left with only three functions of the polar angle $a_i(\theta)$. The non-linear force-free condition will fix them, as we shall discuss. From the inhomogeneous Maxwell's equation, $d \star F_{(h,q)} = \star J_{(h,q)}$, the current takes the form

$$J_{(h,q)} = \Phi_{(h,q)} j_i(\theta) \mu^i, \tag{5.49}$$

where the j_i's are expressed in terms of f_i's functions

$$\begin{cases} \gamma^2(\theta)\Gamma(\theta) j_1(\theta) & = \gamma(\theta) f_2'(\theta) + iq f_6(\theta)\left(\gamma^2(\theta) - 1\right) + \\ & \quad + \gamma^2(\theta)\left[\gamma(\theta) f_3'(\theta) + \left(h - \gamma^2(\theta)\right) f_4(\theta) + (h-1) f_5(\theta)\right], \\ \Gamma(\theta) j_2(\theta) & = (h-1) f_5(\theta) + iq f_6(\theta) - \gamma(\theta)\left(\gamma(\theta) f_4(\theta) - f_3'(\theta)\right), \\ \Gamma(\theta) j_3(\theta) & = -(h-1) f_1(\theta) - iq(f_2(\theta) + f_3(\theta)), \\ \gamma^2(\theta)\Gamma(\theta) j_4(\theta) & = \gamma(\theta) f_1'(\theta) - iq\left(\gamma^2(\theta) f_4(\theta) + f_5(\theta)\right). \end{cases} \tag{5.50}$$

Up to this point, we have only used the Maxwell's equations. The force-free condition, $J_{(h,q)} \wedge \star F_{(h,q)} = 0$, is equivalent to the following relations between f_i's and j_i's:

$$\begin{cases} \left(f_2(\theta) + f_3(\theta)\right) j_3(\theta) + \left(f_5(\theta) + \gamma^2(\theta) f_4(\theta)\right) j_4(\theta) = f_6(\theta) j_1(\theta), \\ f_2(\theta) j_3(\theta) + \gamma^2(\theta) f_4(\theta) j_4(\theta) = f_6(\theta) j_2(\theta), \\ -\gamma^2(\theta) f_4(\theta) j_1(\theta) + \left(f_5(\theta) + \gamma^2(\theta) f_4(\theta)\right) j_2(\theta) = f_1(\theta) j_3(\theta), \\ f_2(\theta) j_1(\theta) - \left(f_2(\theta) + f_3(\theta)\right) j_2(\theta) = f_1(\theta) j_4(\theta). \end{cases} \tag{5.51}$$

By substituting the expressions of $f_i = f_i[a_j]$ from Eqs. (5.48) and $j_i = j_i[a_j]$ from Eqs. (5.50), the force-free condition (5.51) becomes a system of three highly non-linear ordinary differential equations (ODEs). It is then obvious that such a system

is computationally hard to solve in terms of the three functions a_i's. However, the system (5.51) is linear in f_i's and j_i's. Hence, we can recast this system of equations in the matrix form

$$\begin{bmatrix} \mathbb{A} & -f_6(\theta)\,\mathbb{1} \\ -f_1(\theta)\,\mathbb{1} & \mathbb{B} \end{bmatrix} \begin{bmatrix} \mathbf{x} \\ \mathbf{y} \end{bmatrix} = \begin{bmatrix} 0 \\ 0 \end{bmatrix}, \tag{5.52}$$

where the 2×2 matrices $\mathbb{A}$ and $\mathbb{B}$ are given by

$$\mathbb{A} = \begin{bmatrix} f_2(\theta)+f_3(\theta) & f_5(\theta)+\gamma^2(\theta)f_4(\theta) \\ f_2(\theta) & \gamma^2(\theta)f_4(\theta) \end{bmatrix}, \quad \mathbb{B} = \sigma\mathbb{A}^T\sigma, \quad \sigma = \begin{bmatrix} 0 & 1 \\ -1 & 0 \end{bmatrix}, \tag{5.53}$$

and the two 2-dimensional vectors $\mathbf{x}$ and $\mathbf{y}$ are

$$\mathbf{x} = \begin{bmatrix} j_3(\theta) \\ j_4(\theta) \end{bmatrix}, \quad \mathbf{y} = \begin{bmatrix} j_1(\theta) \\ j_2(\theta) \end{bmatrix}. \tag{5.54}$$

The linear system (5.52) has non-trivial solutions if its determinant is vanishing, *i.e.*,

$$0 = \det \begin{bmatrix} \mathbb{A} & -f_6\,\mathbb{1} \\ -f_1\,\mathbb{1} & \mathbb{B} \end{bmatrix} = \left[\det(\mathbb{A}) + f_1 f_6\right]^2, \tag{5.55}$$

which turns out to be equivalent to the degeneracy condition of the field strength $F_{(h,q)}$. For definiteness, we work in the gauge

$$a_4(\theta) = 0 \quad \forall h \qquad \text{and} \qquad a_3(\theta) = a_4(\theta) = 0 \quad \text{for } h = 0. \tag{5.56}$$

The degeneracy condition (see Eq. (2.13)) can then be written as

$$(h-1)\,a_1(\theta)\,a_2'(\theta) - h\,a_1'(\theta)\,a_2(\theta) + i\,q\,\frac{a_1(\theta)\,a_3(\theta)}{\gamma(\theta)} = 0. \tag{5.57}$$

The degeneracy condition (5.57) is one of the three non-linear coupled ODEs in terms of the gauge potential functions a_1, a_2, a_3. This is consistent with the fact the a force-free field must be degenerate, as discussed in section 2.3. The two other equations are lengthy and unenlightening and we omit them. Given the difficulty to find solutions to the system of coupled ODEs, it is useful to organize them in independent classes characterised by conditions on the components of the field strength and the current vector. It is possible to identify seven independent and complete cases

1. $f_1 = f_2 = f_3 = f_4 = f_6 = 0$, $f_5 \neq 0$, $j_2 = j_4 = 0$,
2. $f_1 = f_2 = f_3 = f_6 = 0$, $f_4 \neq 0$, $j_4 = 0$, $j_1 = j_2 + \frac{f_5 j_2}{f_4 \gamma^2}$,

3. $f_1 = f_2 = f_4 = f_6 = 0$, $f_3 \neq 0$, $j_2 = 0$, $j_3 = -\frac{f_5 j_4}{f_3}$,

4. $f_1 = 0$, $f_2 \neq 0$, $f_5 = \frac{\gamma^2 f_3 f_4}{f_2}$, $j_1 = j_2 + \frac{f_3 j_2}{f_2}$, $j_3 = \frac{f_6 j_2 - \gamma^2 f_4 j_4}{f_2}$,

5. $f_1 = f_2 = f_3 = 0$, $f_6 \neq 0$, $j_1 = \frac{j_4(f_5+\gamma^2 f_4)}{f_6}$, $j_2 = \frac{\gamma^2 f_4 j_4}{f_6}$,

6. $f_1 = f_2 = f_4 = 0$, $f_6 \neq 0$, $j_2 = 0$, $j_1 = \frac{f_3 j_3 + f_5 j_4}{f_6}$,

7. $f_1 \neq 0$, $f_6 = \frac{f_2 f_5 - \gamma^2 f_3 f_4}{f_1}$, $j_3 = \frac{f_5 j_2 + \gamma^2 f_4(-j_1+j_2)}{f_1}$, $j_4 = \frac{-f_3 j_2 + f_2(j_1-j_2)}{f_1}$.

The cases from 1 to 6 are entirely solved and all solutions have been found and classified. However, the general solution in case 7 eluded us, because the remaining two ODEs are strongly non-linear and it is not clear whether we have obtained all possible solutions. The full list of solutions is presented in section 5.5.4.

5.5.2 Nomenclature for the classification

In order to better present the solutions, it is first instructive to get some intuition by concentrating on Poincaré coordinates (T, R, θ, Φ). The field strength then reads as

$$F = \frac{e^{iq\Phi}}{R^h} \begin{pmatrix} 0 & (h-1)a_1(\theta) & -Ra_1'(\theta) & -iqRa_1(\theta) \\ & 0 & -h\frac{a_3(\theta)}{\gamma R} & -h\frac{a_2(\theta)}{R} \\ & & 0 & a_2'(\theta) - iq\frac{a_3(\theta)}{\gamma} \\ & & & 0 \end{pmatrix}. \tag{5.58}$$

It is therefore natural to distinguish four (partially overlapping) qualitative classes of solutions types[4]:

Poincaré magnetic $\Leftrightarrow a_1 = 0$

Poincaré electric $\Leftrightarrow a_2 = a_3 = 0$

Poincaré nontoroidal $\Leftrightarrow a_2 = 0$, $q = 0$

Poincaré generic $\Leftrightarrow a_1 \neq 0$ and $a_2 \neq 0$ which obey (5.57).

A Poincaré magnetic solution has no electric field with respect to $\frac{\partial}{\partial T}$. Any such real solution is therefore magnetically dominated. For example, an axisymmetric configuration ($q = 0$) with real weight h and a_i's is real and magnetically dominated. (Other real solutions can be obtained by superposition as discussed in

[4]Poincaré magnetic was denoted as Type M in Lupsasca and Rodriguez (2015) while Poincaré electric was denoted as Type E and Poincaré generic was denoted as Type E-M. Our terminology emphasizes the role of the Poincaré time t in the $3+1$ decomposition.

section 5.6.) A Poincaré electric solution has no magnetic field with respect to the $3+1$ decomposition involving the Poincaré time T. Any such real solution is therefore electrically dominated. A Poincaré nontoroidal solution has no components of the electromagnetic field along $d\Phi$. This implies that the electric field has no toroidal components while the magnetic field (related to the dual of F) has no poloidal components. Since the toroidal and poloidal subspaces are orthogonal, it is indeed consistent with $E_\mu B^\mu = 0$. In general, there are still toroidal magnetic fields and poloidal electric fields but nothing prevents us from canceling one such field. The solution can then also be either Poincaré magnetic or Poincaré electric. The Poincaré generic solution has no particular electromagnetic property with respect to Killing time T. For real fields, there might however be another observer that identifies the solution as magnetically or electrically dominated or null.

5.5.3 Linear superposition

The FFE equations of motion (5.1) are non-linear. Hence, the principle of linear superposition of solutions does not apply in general. However, Lupsasca and Rodriguez (2015) provided sufficient conditions to superpose solutions. Here, we review these conditions and apply them to our programme.

$SL(2,\mathbb{R})$ descendants superposition

Let K be a Killing vector. Assume that F is a solution to FFE equations and that $\mathscr{L}_K J \propto J$.[5] Then $\mathscr{L}_K F$ is a solution to FFE. Indeed,

$$d\mathscr{L}_K F = \mathscr{L}_K dF = 0, \tag{5.59a}$$

$$d\star\mathscr{L}_K F = d\mathscr{L}_K \star F = \mathscr{L}_K d\star F = \mathscr{L}_K \star J = \star\mathscr{L}_K J, \tag{5.59b}$$

$$i_{\mathscr{L}_K J}\mathscr{L}_K F \propto i_J \mathscr{L}_K F = \left[i_J, \mathscr{L}_K\right] F + \mathscr{L}_K i_J F = i_{[J,K]}F = -i_{\mathscr{L}_K J}F \propto -i_J F = 0. \tag{5.59c}$$

$SL(2,\mathbb{R})$ descendants of the highest weight solution $F_{(h,q,0)}$ are defined by the operation $F_{(h,q,k)} = \left(\mathscr{L}_{H_-}\right)^k F_{(h,q,0)}$. Since H_- is a Killing vector, $F_{(h,q,k)}$ is a solution provided that $J_{(h,q,k)} = \left(\mathscr{L}_{H_-}\right)^k J_{(h,q,0)} \propto J_{(h,q,0)}$. This condition is met when the current $J_{(h,q,0)}$ is a linear combination of Q_0, H_- and ∂_θ, because all these three vector fields commute with H_-. This property allows us to linearly superpose a primary solution with its descendants. Such class of solutions are labelled as *admitting descendants*.

[5] The symbol $\propto$ stands for *proportional*. In other words, the two current vectors are collinear and the proportionality factor can be a function of space-time coordinates.

$SL(2,\mathbb{R})$ primaries superposition

Assume that F_1 and F_2 are two solutions to FFE equations and that the associated two currents $J_1 \propto J_2$. Then an arbitrary linear combination $F = \alpha F_1 + \beta F_2$, with α, β constants, is a solution to FFE.

$$dF = d\left(\alpha F_1 + \beta F_2\right) = \alpha dF_1 + \beta dF_2 = 0, \tag{5.60a}$$

$$d \star F = \alpha d \star F_1 + \beta d \star F_2 = \alpha \star J_1 + \beta \star J_2 = \star J, \tag{5.60b}$$

$$i_J F \propto i_{\alpha J_1 + \beta J_2}\left(\alpha F_1 + \beta F_2\right) = \alpha^2 i_{J_1} F_1 + \beta^2 i_{J_2} F_2 + \alpha\beta\left(i_{J_2} F_1 + i_{J_1} F_2\right) = 0. \tag{5.60c}$$

This property allows us to linearly superpose two different primary solutions.

5.5.4 List of all solutions

Here, we list all solutions to force-free electrodynamics with nonvanishing current that we found in our analysis starting from the highest-weight ansatz. We first classify the solutions according to their highest-weight representation labeled by the (complex) weight h and the (integer) $U(1)$-charge q and then by their Poincaré electromagnetic type. The functions $X_i(\theta)$, $i = 1,2,3,4,5$ obey ODEs in θ which are described in appendix D.1. More details on the solutions including the field strength, current and Euler potentials can be found in appendix D.2. We keep explicit k that for NHEK geometry is simply $k = 1$.

(h, q)-eigenstates Two classes of solutions with arbitrary weight h and $U(1)$-charge q:

- **Poincaré magnetic**

$$A = \int dh \sum_{q\in\mathbb{Z}} \Phi^h \lambda^q \left[X_5 \mu^2 - \frac{iq\gamma(1-k^2\gamma^2)}{q^2 - \Delta(h,q)\gamma^2} X_5' \mu^3 \right], \tag{5.61}$$

  where $X_5 = X_5(\theta; h, q)$ and $\Delta(h,q) = h(h-1) + k^2 q^2$. The solution is pure gauge for $h = 0$. When $q = 0$, $h \neq 0, 1$ the solution reduces to (5.65).

- **Poincaré generic**

$$A_{(h,q)} = \Phi^h \lambda^q \left[h(h-1) X_2 \mu^1 - kq^2 X_2 \mu^2 + ikq\gamma X_2' \mu^3 \right], \tag{5.62}$$

  where $X_2 = X_2(\theta; \Delta(h,q), c_1 = q^2)$. The solution is pure gauge for $h = 0$.

($h \neq 0, q = 0$)-eigenstates Four classes of axisymmetric solutions with arbitrary weight h and one special subcase:

- **Poincaré generic**

$$A_{(h,0)} = c_1^h \Phi^h \left[-X_3^{h-1} \mu^1 + X_3^h \mu^2 \pm \sqrt{\xi} X_3^{h-1} \mu^3 \right], \tag{5.63}$$

where $X_3 = X_3(\theta; h, \xi)$, $h, \xi \in \mathbb{C}$ and $c_1 \neq 0$.

- **Poincaré magnetic**

$$A_{(h,0)} = c_2^h \Phi^h \left[X_4 \mu^2 \pm X_4^{\frac{h-1}{h}} \mu^3 \right], \tag{5.64}$$

where $X_4 = X_4(\theta; \Delta(h))$ with $\Delta(h) = h(h-1)$ and $c_2 \neq 0$.

- **Poincaré magnetic**

$$A = \int dh \, \Phi^h X_1 \mu^2, \tag{5.65}$$

where $X_1 = X_1(\theta; \Delta(h))$.

- **Poincaré nontoroidal**

$$A_{(h,0)} = \Phi^h X_2 \left[h\mu^1 \pm \sqrt{c_1} \mu^3 \right], \tag{5.66}$$

where $X_2 = X_2(\theta, \Delta(h, q), c_1)$.

- **Poincaré electric and nontoroidal - admitting descendants**

$$A_{(h,0)} = \Phi^h X_2 \mu^1, \tag{5.67}$$

where $X_2 = X_2(\theta, \Delta(h, q), 0)$. It is the special case $c_1 = 0$ of (5.66).

($\mathbf{h = 0, q \neq 0}$)-eigenstates One weight 0 solution with arbitrary $U(1)$ charge q :

- **Poincaré electric**

$$A_{(0,q)} = \lambda^q e^{\pm \int \frac{q}{\gamma} d\theta} \mu^1. \tag{5.68}$$

($\mathbf{h = 1, q \neq 0}$)-eigenstates One weight 1 solution with arbitrary $U(1)$ charge q:

- **Poincaré electric - admitting descendants**

$$A = \sum_{q \in \mathbb{Z}} \Phi \lambda^q e^{\pm \int \frac{q}{\gamma} d\theta} \mu^1. \tag{5.69}$$

($\mathbf{h = \pm ikq, q \neq 0}$)-eigenstates Two weight $\pm ikq$ solutions with arbitrary $U(1)$ charge q:

- **Poincaré generic**

$$A_{(h=\pm ikq,q)} = \Phi^h \lambda^q e^{\pm\int \frac{d\theta}{\gamma}} \left[ikq\mu^1 + iq\mu^2 \pm \mu^3 \right], \tag{5.70}$$

$$A_{(h=\pm ikq,q)} = \Phi^h \lambda^q \left[k\mu^1 + \mu^2 \right]. \tag{5.71}$$

($h = 1 \pm ikq, q \neq 0$)-eigenstates One weight $1 \pm ikq$ solution with arbitrary $U(1)$ charge q:

- **Poincaré generic - null**

$$\sum_{q\in\mathbb{Z}} A_{(h(q)=1\pm ikq,q)} = \sum_{q\in\mathbb{Z}} \Phi^h \lambda^q \left[h(q) a_1(\theta)\mu^1 \pm iq a_1(\theta)\mu^2 \pm \gamma a_1'(\theta)\mu^3 \right]. \tag{5.72}$$

($h = 1, q = 0$)-eigenstates Two weight 1 axisymmetric solutions:

- **Poincaré nontoroidal - null**

$$A_{(1,0)} = \Phi \left[a_1(\theta)\mu^1 \pm \sqrt{c_3 + [\gamma a_1'(\theta)]^2}\mu^3 \right], \tag{5.73}$$

  where a_1 is an arbitrary function.

- **Poincaré magnetic**

$$A_{(1,0)} = \Phi(c_2\mu^2 + c_3\mu^3). \tag{5.74}$$

($h = 0, q = 0$)-eigenstates One weight 0 axisymmetric solution:

- **Poincaré electric and nontoroidal - admitting descendants**

$$A_{(0,0)} = -E_0 \left(\mu^1 + \frac{1}{k}\mu^2 \right). \tag{5.75}$$

  This solution is just the $SL(2,\mathbb{R})$ invariant solution (5.39) with $k = 1$ (for the near-horizon geometry of the extreme Kerr).

In comparison with Lupsasca and Rodriguez, 2015, the solutions (5.64), (5.66), (5.70), (5.71), (5.72), (5.73) are new and the solutions (5.68), (5.69) are given with two branches distinguished by a sign.

5.6 Physical requirements

So far, we have classified the solutions to force-free electrodynamics around NHEK according to their highest weight representation labelled by the (complex) conformal weight h and the (integer) $U(1)$ charge q. These solutions are, in general, complex and it is not obvious a priori which of them are physically relevant to describe stationary and axisymmetric magnetospheres of rapidly rotating Kerr black holes. To this aim, we introduce certain physical requirements to discriminate potentially physical solutions from the list of all mathematical solutions. We demand that potentially physical solutions are real, either magnetically dominated or null, admit finite extraction of energy and angular momentum as measured by an asymptotically flat observer, and are limiting solution of a regular solution defined on (near-) extreme Kerr.

5.6.1 Reality condition

The sufficient condition for linearly superpose primary solutions is used to build real solutions from complex ones. Given a complex solution to FFE, $F_{(h,q)}$, and its associated current $J_{(h,q)}$, we can build the real solution by linearly superpose $F_{(h,q)}$ and its complex conjugate $F^*_{(h,q)}$ provided that $J_{(h,q)} \propto J^*_{(h,q)}$. We scrutinised the list of solutions to FFE to build the largest class of real solutions that are magnetically dominated or null dominated.

5.6.2 List of near-horizon solutions

Let us now list all real magnetically dominated or null solutions that we could build from the complex solutions enumerated in section 5.5.4. At this stage, we list these solutions with arbitrary highest-weight h.

- Nonaxisymmetric, magnetic:

$$A^M = \int dh \sum_{q\in\mathbb{Z}} \Phi^h \lambda^q \left[X_5 \mu^2 - \frac{iq\gamma(1-k^2\gamma^2)}{q^2-\Delta(h,q)\gamma^2} X_5' \mu^3 \right] + c.c. \tag{5.76}$$

  where $X_5 = X_5(\theta; h, q)$ and $\Delta(h,q) = h(h-1) + k^2 q^2$. The axisymmetric case $q = 0$ is listed below and we have then $X_5(\theta, h, 0) = X_1(\theta, \Delta(h))$.

- Nonaxisymmetric, magnetic:

$$\begin{aligned} A^{EM}_{(h=1+i\mu,q)} &= \Phi^{1+i\mu}\lambda^q \left[h(h-1) X_2 \mu^1 - kq^2 X_2 \mu^2 + ikq\gamma X_2' \mu^3 \right] \\ &\quad + \Phi^{1-i\mu}\lambda^{*q} \left[h^*(h^*-1) X_2^* \mu^1 - kq^2 X_2^* \mu^2 - ikq\gamma X_2^{*\prime} \mu^3 \right], \end{aligned} \tag{5.77}$$

where $X_2 = X_2(\theta; \Delta(h,q), c_1 = q^2)$. The solution is magnetically dominated in the range $-kq < \mu < kq$. The borderline case $\mu^2 = k^2 q^2$ is a null solution. (This is an example of Poincaré generic solution which is magnetically dominated.)

- Axisymmetric (magnetic dominance not checked):

$$A^{EM}_{(h,0)} = c_1^h \Phi^h \left[-X_3^{h-1} \mu^1 + X_3^h \mu^2 \pm \sqrt{\xi} X_3^{h-1} \mu^3 \right], \tag{5.78}$$

where $h > 1$, c_1 is real, and $\xi > 0$. (In the case $h = 1$, X_3 becomes X_1 and the solution is not smooth at the velocity of light surface; see appendix D.2). It has been observed that for $h = -1$ this solution is magnetically dominated (Zhang, Yang, and Lehner, 2014). We did not check if it is the case for $h \geq 1$. The solution to the non-linear equation for $X_3(\theta)$ is required which we did not obtain here.

- Axisymmetric, magnetic:

$$A^{M}_{(h,0)} = c_2^h \Phi^h \left[X_4 \mu^2 \pm X_4^{\frac{h-1}{h}} \mu^3 \right], \tag{5.79}$$

where $X_4 = X_4(\theta; \Delta(h))$, c_2 is real and arbitrary and $h \geq 2$. It is magnetically dominated since it is Poincaré magnetic.

- Axisymmetric, magnetic:

$$\int dh A^{M}_{(h,0)} = \int dh \Phi^h X_1 \mu^2 + c.c. \tag{5.80}$$

where $X_1 = X_1(\theta, \Delta(h))$ and h is complex. For h real we observed that the spectrum of h is discrete and the lowest value is greater than 4 in appendix D.1.

- Axisymmetric, magnetic, nontoroidal:

$$A^{NT}_{(h,0)} = \Phi^h X_2 \left[h\mu^1 \pm \sqrt{c_1} \mu^3 \right], \tag{5.81}$$

where $X_2 = X_2(\theta, \Delta(h), c_1)$, h is real. After a numerical check involving X_2, it turns out that for all $c_1 > 0$ there exists a range of $1 \leq h \leq h_{max}(c_1)$ where the solution is magnetically dominated for all values of θ. The function h_{max} tends to 1 in the limit $c_1 \to 0$ and tends to infinity in the limit $c_1 \to \infty$. It is a solution with no toroidal electric field and no poloidal magnetic field.

- Nonaxisymmetric, null:

$$\sum_{q\in\mathbb{Z}} A^{EM}_{(h=1\pm ikq,q)} = \sum_{q\in\mathbb{Z}} \Phi^h \lambda^q \left[h a_1(\theta)\mu^1 \pm i q a_1(\theta)\mu^2 \pm \gamma a_1'(\theta)\mu^3 \right] + c.c. \quad (5.82)$$

  Here $a_1(\theta)$ can be complex. We require that $a_1(\theta)$ and $a_1'(\theta)$ vanish at the poles.

- Axisymmetric, null

$$A^{EM}_{(1,0)} = \Phi(a_1(\theta)\mu^1 \pm \gamma a_1'(\theta)\mu^3), \quad (5.83)$$

  where $a_1(\theta)$ and $a_1'(\theta)$ vanish at the poles but $a_1(\theta)$ is otherwise arbitrary. This is a special case of the solution (5.82) for $q = 0$.

5.6.3 Finite energy and angular momentum fluxes

Additional constraints on the conformal weight can be obtained by demanding that a given solution have a finite extraction of energy and angular momentum. We want to compute the energy and angular momentum fluxes in Poincaré coordinates for definiteness. Let $\mathscr{E}$ and $\mathscr{L}$ be the energy and angular momentum, respectively, with respect to the ∂_T and $-\partial_\Phi$. The fluxes per unit time and per solid angle are given by

$$\dot{\mathscr{E}} = \sqrt{-\sigma} T^\mu_{\ \nu}[F] (\partial_T)^\nu n_\mu \propto E(\theta) R^{2-2h}, \quad (5.84a)$$

$$\dot{\mathscr{L}} = \sqrt{-\sigma} T^\mu_{\ \nu}[F] (-\partial_\Phi)^\nu n_\mu \propto J(\theta) R^{1-2h}. \quad (5.84b)$$

Here the dot stands for derivative with respect to the Poincaré time T, σ is the induced metric on surfaces of constant radius R, n^μ is the unit normal vector to these surfaces and $T_{\mu\nu}[F]$ is the electromagnetic energy-momentum tensor. The explicit expressions of the functions $E(\theta)$ and $J(\theta)$ are written in section 5.3 of Compère and Oliveri (2016) and we omit them, because they are not important for the following discussion.

We have two different limits to consider: either we study the fluxes at the boundary of NHEK located at $R \to \infty$ or we study the fluxes from the Poincaré horizon located at $R = 0$. In the former case, by requiring no energy and angular momentum flux at the boundary and assuming that both $E(\theta)$ and $J(\theta)$ are non-vanishing, we have that the real part of h must obey the condition $\Re(h) > 1$. This conclusion is in contradiction with the regularity condition derived later. Moreover, the fluxes diverge at the Poincaré horizon, where we have to require $\Re(h) < 1/2$ to have finite quantities. These two classes of solutions, namely those with

$\Re(h) < 1/2$ and with $\Re(h) > 1$, might be useful for discussing holographic duality in near-horizon geometries in the framework of Kerr/CFT correspondence.[6] We neglect them, because we are more interested in those solutions with finite extraction of energy as measured by an asymptotic observer.

Let us now define the energy and angular momentum with respect to an asymptotically flat observer, *i.e.*, with respect to ∂_t and $-\partial_\phi$, respectively. From the scaling co-rotating coordinates (1.13), one finds that $\partial_t + \Omega_+^{ext}\partial_\phi = (\lambda/r_0)\,\partial_T$ and $\partial_\phi = \partial_\Phi$. Thus, the definitions of angular momentum in the near-horizon and far-region agree, whereas the definition of energy in the near-horizon is the linear combination of energy and angular momentum of the co-rotating observer. From Eqs. (5.84), substituting to each power of R a power of λ (because $r = r_+ + \lambda r_0 R$), we can deduce the scaling between far-region and near-horizon fluxes

$$\mathscr{E}' - \Omega_+^{ext}\mathscr{L}' \sim \lambda^{2-2h}\dot{\mathscr{E}}, \tag{5.85a}$$

$$\mathscr{L}' \sim \lambda^{1-2h}\dot{\mathscr{L}}. \tag{5.85b}$$

The prime stands for derivative with respect to the asymptotic time t. In the near-horizon limit, $\lambda \to 0$, the flux of energy and angular momentum should remain finite. There are five scenarios (see also appendix B of Gralla, Lupsasca, and Strominger (2016)):

1. for $\Re(h) < 1/2$, one has $\mathscr{E}' = 0 = \mathscr{L}'$. The far-region fluxes both vanish and the asymptotic observer does not measure any extraction of energy and angular momentum, whatever the near-horizon fluxes $\dot{\mathscr{E}}$, $\dot{\mathscr{L}}$ are;

2. for $\Re(h) = 1/2$, one has $\mathscr{E}' = \Omega_+^{ext}\mathscr{L}'$ and $\mathscr{L}' \sim \dot{\mathscr{L}}$. The electromagnetic field saturates the superradiant bound;

3. for $1/2 < \Re(h) < 1$ and $J(\theta) = 0$, one has $\mathscr{E}' = \Omega_+^{ext}\mathscr{L}'$ and $\mathscr{L}'$ is not determined from the near-horizon flux. Once again, the electromagnetic field saturates the superradiant bound. The far-region flux of the angular momentum is not determined, and so is also the far-region flux of the energy as measured by the asymptotic observer;

4. for $\Re(h) = 1$ and $J(\theta) = 0$, one has $\mathscr{E}' - \Omega_+^{ext}\mathscr{L}' \sim \dot{\mathscr{E}}$ and $\mathscr{L}'$ undetermined. Using the thermodynamic argument, and Eq. (2.59), one finds that $\mathscr{E}' - \Omega_+^{ext}\mathscr{L}' \sim \dot{\mathscr{E}} \leq 0$; this result is equivalent to assume the first and second law of thermodynamics $\delta M - \Omega_+\delta J = \kappa/(8\pi)\delta A \geq 0$ with $\delta M = -\delta\mathscr{E}$ and $\delta J = -\delta\mathscr{L}$;

[6] See Jacobson and Rodriguez, 2017 for an earlier attempt of an holographic dual to the Blandford-Znajek mechanism.

5. for $\Re(h) > 1$ and $E(\theta) = 0 = J(\theta)$, both far-region fluxes $\mathscr{E}'$ and $\mathscr{L}'$ are not determined from the near-horizon fluxes.

We want to select those solutions with finite fluxes of energy and angular momentum with respect to an asymptotic observer. Finiteness implies that $\Re(h) \geq 1/2$. In addition, according to regularity condition, $\Re(h) \leq 1$. Thus, the window of conformal weights h for potentially physical solutions is

$$\frac{1}{2} \leq \Re(h) \leq 1 \qquad \text{and} \qquad \left(\Re(h) - \frac{1}{2}\right) J(\theta) = 0. \tag{5.86}$$

The list of potentially physical solutions is presented in the next section.

5.6.4 List of potentially physical solutions

In the following we list the real, magnetically dominated or null force-free solutions with nontrivial current and $\Re(h) = \frac{1}{2}$ or $\frac{1}{2} < \Re(h) \leq 1$ and $J(\theta) = 0$, which lead to finite asymptotically flat energy and angular momentum fluxes. We also do consider linear superposition.

- Nonaxisymmetric, magnetic

  We have two classes of solutions from Eq. (5.76). The first one for $h(\eta) = \frac{1}{2} + i\eta$, $\eta \in \mathbb{R}$:

$$A = \int d\eta \sum_{q\in\mathbb{Z}} \left\{ \Phi^{h(\eta)} \lambda^q \left[X_5 \mu^2 - \frac{iq\gamma(1-k^2\gamma^2)}{q^2 - \Delta(h(\eta),q)\gamma^2} X_5' \mu^3 \right] + c.c. \right\}, \tag{5.87}$$

  where $X_5 = X_5(\theta; h(\eta), q)$ and $\Delta(h(\eta), q) = k^2 q^2 - \eta^2 - \frac{1}{4}$. When $q = 0$, the solution reduces to Eq. (5.90).

  When $\mathrm{Re}(h) \neq \frac{1}{2}$, the constraint $J(\theta) = 0$ imposes $h = 1$. The solution is

$$A = \sum_{q\in\mathbb{Z}} \left\{ \Phi \lambda^q \left[X_2 \mu^2 - \frac{i\gamma}{q} X_2' \mu^3 \right] + c.c. \right\}, \tag{5.88}$$

  after using (D.26), where $X_2 = X_2(\theta; k^2 q^2, q^2)$.

- Nonaxisymmetric, null

  The solution (5.77) has $J(\theta) = 0$ for $\mu = \pm kq$. This leads to the null solution

$$A_{(q)} = \Phi^{1\pm ikq} \lambda^q \left[(ikq \pm 1) X_2 \mu^1 + iq X_2 \mu^2 + \gamma X_2' \mu^3 \right] + c.c. \tag{5.89}$$

  where $X_2 = X_2(\theta; \pm ikq, c_1 = q^2)$.

- Axisymmetric, magnetic

$$A = \int dh \Phi^h X_1 \mu^2 + c.c. \tag{5.90}$$

where $X_1 = X_1(\theta; \Delta(h))$ and h is complex in the range $\frac{1}{2} \leq \Re(h) \leq 1$. It is not clear whether regular solutions exist in that range. Indeed, at least for h real, the spectrum of h is discrete for regular solutions and the lowest value is greater than 4; see appendix D.1. Since the solution is axisymmetric, we can check the Znajek's condition

$$I(\psi) = (\Omega(\psi) - \Omega_H)\partial_\theta \psi \sqrt{\frac{g_{\phi\phi}}{g_{\theta\theta}}}. \tag{5.91}$$

After taking the near-horizon limit, the generator of the black hole horizon is ∂_T so the angular velocity at the Poincaré horizon of the near-horizon geometry is $\Omega_H = 0$. We also have $I(\psi) = \Omega(\psi) = 0$ as shown in (D.33), and therefore (5.91) holds. The second regularity condition that should be obeyed for extremal black holes only, as described in Gralla and Jacobson (2014), is also trivially satisfied.

- Axisymmetric, magnetic
The solution (5.81) has $J(\theta) = 0$. For $h = 1$, it is magnetically dominated and therefore admissible. It reads as

$$A = \Phi X_2 \left[\mu^1 \pm \sqrt{c_1} \mu^3 \right], \tag{5.92}$$

where $X_2 = X_2(\theta, 0, c_1)$ and $c_1 > 0$. Znajek's condition does not apply because the field is non-toroidal, $i_{\partial_\Phi} F = 0$.

- Nonaxisymmetric, null
Solutions (5.82) with $h(q) = 1 \pm ikq$ have $J(\theta) = 0$:

$$A = \sum_{q \in \mathbb{Z}} \Phi^{h(q)} \lambda^q \left[h(q) a_1(\theta) \mu^1 \pm i q a_1(\theta) \mu^2 \pm \gamma a_1'(\theta) \mu^3 \right] + c.c \tag{5.93}$$

We require a_1 to vanish at the poles. For $q = 0$, we obtain the axisymmetric null solution:

- Axisymmetric, null

$$A_{(1,0)} = \Phi \left(a_1(\theta) \mu^1 \pm \gamma a_1'(\theta) \mu^3 \right). \tag{5.94}$$

As discussed in appendix D.1, solutions to the ODEs for X_1, X_2 and X_5 exist which are regular at the north and south poles. However, the functions X_1 and X_5 are generically logarithmically divergent at the velocity of light surface. Since the fate of the velocity of light surface is unclear when extending these solutions to the asymptotically flat region, we do not exclude them and consider them as potentially physical. A more complete analysis of the extension of these solutions to the asymptotically flat region would however be necessary to fully settle the issue.

Generically, highest weight solutions with non-zero weight have a singular field strength at the Poincaré horizon. However, the energy and angular momentum fluxes are regular at the Poincaré horizon as a consequence of the restriction (5.86). One exception is the negative branch of (5.94) which is, up to a gauge transformation, $A_{(1,0)} = a_1(\theta)d\left(T - \frac{1}{R}\right)$. This solution is regular at the future horizon but singular at the past horizon (see Eq. (5.101) later).

The solutions are written in a $SL(2,\mathbb{R})$ covariant manner and one can choose any $SL(2,\mathbb{R})$ generators related by isomorphisms of the algebra, as discussed around (C.14).

5.6.5 Regularity conditions

Among all the real solutions, one aims to have those that come from solutions to FFE around (near-) extreme Kerr and are regular on the future event horizon. The first condition is imposed to avoid those solutions that are genuine solutions in NHEK and do not have a continuation from the throat geometry all the way to the asymptotic region. This approach has been pursued in Gralla, Lupsasca, and Strominger (2016). Here, we outline the reasoning.[7]

Let F be the electromagnetic field strength defined on (near-) extreme Kerr in a given coordinates system. By transforming the field to the co-rotating coordinates (1.13) and performing a Taylor expansion around $\lambda = 0$, one gets

$$F = \lambda^{-h} \sum_{p=0}^{\infty} \mathscr{F}_{(p)}\, \lambda^p = \lambda^{-h}\left(\mathscr{F}_{(0)} + \mathscr{F}_{(1)}\lambda + \mathscr{O}(\lambda^2)\right). \tag{5.95}$$

The leading field $\mathscr{F}_{(0)} = \lim_{\lambda\to 0}\lambda^h F$ is the near-horizon field and it is self-similar with respect to the dilation operator $\mathscr{L}_{H_0}\mathscr{F}_{(0)} = h\mathscr{F}_{(0)}$. Though the conformal weight h is a complex number, its real part is bounded by the rank of the field

[7] See also the discussion at the end of chapter 1 about the isometry group and critical phenomena in NHEK space-time.

F. Indeed, by considering F to be a smooth field on extreme Kerr in ingoing coordinates (v,r,θ,ϕ), its transformation to the co-rotating coordinates (1.13) gives

$$F_{\mu\nu}(T,R,\theta,\Phi) = J_{\mu}^{\ \alpha} F_{\alpha\beta}(v,r,\theta,\phi) J^{\beta}_{\ \nu}, \tag{5.96}$$

where $J^{\mu}_{\ \nu}$ is the Jacobian, whose elements can be read from

$$dv = \frac{2M}{\lambda}\left[dT + \left(\frac{1}{R^2} + \frac{\lambda}{R} + \frac{\lambda^2}{2}\right)dR\right], \tag{5.97a}$$

$$dr = \lambda M dR, \tag{5.97b}$$

$$d\phi = \frac{1}{\lambda}\left(dT + \frac{dR}{R^2}\right) + d\Phi. \tag{5.97c}$$

Since the elements of the Jacobian have leading terms of $\mathscr{O}(\lambda^{-1})$, the transformation law introduces at most two factors of $\mathscr{O}(\lambda^{-1})$. In addition, because F is an antisymmetric tensor of rank-two, the transformation law implies that the leading term is of $\mathscr{O}(\lambda^{-1})$. In terms of the conformal weight, this reasoning implies that the conformal weight h is $h \leq 1$. Therefore, we conclude that for electromagnetic fields one has

$$F = \frac{1}{\lambda}\left(\mathscr{F}_{(0)} + \mathscr{F}_{(1)}\lambda + \mathscr{O}(\lambda^2)\right). \tag{5.98}$$

Moreover, for fields with positive conformal weight, the norm (taken with respect to the NHEK metric) must vanish. Indeed, by computing the norm of F (with respect the extreme Kerr metric), one obtains that

$$F^2 = \frac{1}{\lambda^2}\left(\mathscr{F}^2_{(0)} + 2\lambda\mathscr{F}_{(0)}\cdot\mathscr{F}_{(1)} + \mathscr{O}(\lambda^2)\right). \tag{5.99}$$

Since F^2 is a scalar quantity (*i.e.*, it has weight $h = 0$), upon taking the near-horizon limit it should be finite. Therefore, we infer that $\mathscr{F}_{(0)}$ must be null.

By imposing that $\mathscr{F}_{(0)}$ is stationary, axisymmetric, null, self-similar with conformal weigh $h = 1$ and obeys the FFE equations, one finds that

$$\mathscr{F}_{(0)} = F_{(1,0)} = A(\theta)\gamma(\theta)\left(w^2 - w^1\right). \tag{5.100}$$

This solution has been originally found in Lupsasca and Rodriguez (2015).
In Poincaré coordinates, it reads as

$$\mathscr{F}_{(0)} = F_{(1,0)} = A(\theta) d\left(T - \frac{1}{R}\right) \wedge d\theta, \tag{5.101}$$

where $A(\theta)$ is an arbitrary function of the polar angle. This solution is the unique electromagnetic field with conformal weight $h = 1$ (and the properties mentioned

above) to be regular on the future event horizon and to be the near-horizon limit of a solution in extreme Kerr. Notice that this solution is the axisymmetric null solution obtained in Eq. (5.94).

If instead the arbitrary function $A(\theta)$ vanishes, then the next to leading order $\mathscr{F}_{(1)}$ in Eq. (5.98) is nothing but the maximally symmetric solution obtained in Eq. (5.39).

5.7 Discussion and conclusions

In this chapter, we have outlined the strategy to solve force-free electrodynamics (FFE) around near-horizon extreme Kerr (NHEK) space-time We have exploited the isometry group and the presence of global conformal symmetries to solve FFE equations and to classify the solutions using the highest weight representation.

We found a plethora of solutions and we organized them in seven independent classes. As in each solution generating technique, one has to distinguish between the set of formal solutions and the set of physical solutions. In order to discriminate the latter, we have introduced criteria for the electromagnetic field strengths: reality and regularity conditions, and finite energy and angular momentum extraction measured by an asymptotically flat observer. All these conditions imply bounds on the conformal weight. The set of potentially physical solutions for which $1/2 \leq \Re(h) \leq 1$ does not overlap with the set of near-horizon solutions for which either $\Re(h) < 1/2$ (finite flux at the Poincaré horizon) or $\Re(h) > 1$ (no outward flux at the boundary of NHEK).

Among the potentially physical solutions, there are two notable solutions:

1. the maximally symmetric one, discussed earlier in Eq. (5.39),

$$F_{(0,0)} = E_0 \, dT \wedge dR. \tag{5.102}$$

   Though this solution is electrically dominated, it deserves further investigation. Indeed, as pointed out in Gralla, Lupsasca, and Strominger (2016), the presence of gravitational fields might prevent charged particles of the plasma to travel faster than the speed of light as happens in Minkowski space-time (see. *e.g.*, Komissarov, 2004). This is still an open question and we leave it for future work.

2. the $h = 1$ and axisymmetric solution, discussed in Eqs. (5.94) and (5.101),

$$F_{(1,0)} = A(\theta) d\left(T - \frac{1}{R}\right) \wedge d\theta. \tag{5.103}$$

This solution is null and it is the only one to be regular on the future event horizon.

These two notable solutions should descend from smooth solutions defined on extreme Kerr, according to the discussion below Eq. (5.95). Solving analytically FFE around (extreme) Kerr is a hard computational task and, therefore, except few exceptions mentioned earlier in chapter 2, we do not know the analytical expressions of the original solutions. However, we know the near-horizon limits and we can attempt to reconstruct the full original solutions by using the matched asymptotic expansion. In other words, we may glue the near-horizon solutions to the asymptotically flat region which has been decoupled by the near-horizon limit.[8] Such programme has not been yet realized in the context of force-free magnetospheres. That is another open question that requires further study.

Another interesting point that comes to light is the role of the velocity of light surface. It marks the boundary of the physical region in NHEK. The potentially physical solutions have a logarithmic divergence at the velocity of light surface and it is not clear whether such a divergence is physical or it disappears upon gluing the near-horizon solution with the asymptotic region. This is yet another aspect that is remained unsolved.

[8] Recall the Fig. 1.2.

Chapter 6

Mass of Kerr-Newman black holes in an external magnetic field

Contents

In this chapter, we are going to investigate the thermodynamics of Kerr-Newman black holes immersed in an external back-reacting magnetic field, sometimes known as Melvin-Kerr-Newman or Magnetised-Kerr-Newman (MKN) black holes. The content of this chapter is based on Astorino, Compère, Oliveri, and Vandevoorde (2016). In section 6.1, we introduce the research literature on the topic. Then, in section 6.2 and section 6.3, we discuss how to embed a rotating black hole in test and back-reacting external magnetic field, respectively. Section 6.4 addresses

the problem to compute the total conserved mass of the MKN black hole. In section 6.5, we study the canonical thermodynamics and, in section 6.6, we comment about alternative thermodynamic description of the MKN solution and make contact between our results and those already present in the literature. We conclude with a discussion in section 6.7.

6.1 Introduction

According to the black hole no-hair theorems of General Relativity (Israel, 1967; Israel, 1968; Carter, 1971; Hawking, 1972; Robinson, 1974), an isolated rotating black hole is completely described by its mass M, angular momentum J, and if any, by its net electric charge Q. However, astrophysical black holes are not isolated objects and they are usually surrounded by electromagnetic fields produced by external sources like, *e.g.*, plasma, accretion discs, and stars (Eatough, 2013). Few exact analytical models, which describe black holes interacting with their surroundings, are known in the literature.

The first attempt to construct an analytical model, describing Kerr black holes immersed in a magnetic field, is due to Wald (1974) and it is reviewed in section 6.2. Though Wald's solution was a great first achievement, it was a perturbative approach valid in the weak field regime. Several attempts to find exact solutions to Einstein-Maxwell equations, describing black holes immersed in external magnetic fields, received attention since the Wald's paper. In 1976, Ernst (1976a), Ernst (1976b), and Ernst and Wild (1976), in a series of three papers, were able to build an exact and regular solution by using the solution generating technique originally presented by Harrison (1968) and reformulated by Ernst (1968a); Ernst (1968b). The Ernst-Wild solution is a stationary and axisymmetric solution to the Einstein-Maxwell equations. In section 6.3 we will introduce this solution and comment about its main properties. Since this solution can be interpreted as a Kerr-Newman black hole immersed in an external back-reacting magnetic field, it is often dubbed as Magnetised-Kerr-Newman or Melvin-Kerr-Newman black hole, because it reduces to the Bonnor-Melvin solution (Bonnor, 1954; Melvin, 1964) when the mass, angular momentum and electric charge vanish. The asymptotics, the ergo-sphere and the motion of test charged particles around MKN black hole have been investigated in Gal'tsov and Petukhov (1978), Aliev, Gal'tsov, and Sokolov (1980), Hiscock (1981), Aliev and Gal'tsov (1988), Aliev and Gal'tsov (1989a), Aliev and Gal'tsov (1989b), and Karas and Vokrouhlický (1991) and in the two reviews by Dokuchaev et al. (1987) and Aliev and Gal'tsov (1989c).

Recently, MKN solution received a renewed attention. Gibbons, Mujtaba, and Pope (2013) studied the causal and asymptotic structure of MKN solution. For certain values of the parameters of the solution, the ergo-region forms around the axis of rotation and it extends all the way to infinity. Moreover, despite the common phrasing in the literature that MKN is asymptotically Melvin, it is not true in general. These features make the MKN black hole unphysical and its role unclear for an astrophysical perspective. The fact that the asymptotic region of MKN space-time is not conventional amounts to serious difficulties in defining global charges like its mass and angular momentum and, in turn, its thermodynamics. Several attempts have been made in that direction by using different theoretical methods, but there has been no general agreement. The thermodynamics of MKN black hole has been studied in Gibbons, Pang, and Pope (2014) and Booth et al. (2015) by making use of two different approaches: the former used an approach based on dimensional reduction, while the latter adopted the isolated horizon formalism. However, the definitions of mass proposed do not coincide. To resolve this tension, Astorino et al. (2016) used the covariant phase space formalism (Regge and Teitelboim, 1974; Iyer and Wald, 1994; Barnich and Brandt, 2002; Barnich, 2003; Barnich and Compère, 2008). This formalism was already applied previously to black holes with unusual asymptotics (Barnich and Compère, 2005; Banados et al., 2006; Compère, 2007b). It is especially well adapted to the problem at hand since the asymptotic region has no role to play. The lack of known boundary conditions for Melvin universes is, therefore, not an obstacle for defining the mass. The procedure amounts to first define the infinitesimal change of mass due to infinitesimal changes of phase space parameters by considering the integral of a uniquely defined surface charge form on an arbitrary sphere surrounding the black hole. One then writes the conditions for the existence of a finite mass known as integrability conditions. The definition of the mass amounts to solving these integrability conditions, as we will show in section 6.4.

Interestingly, Astorino (2015) and Bičák and Hejda (2015) showed that the extreme MKN shares the same near-horizon geometry with the extreme Kerr-Newman black hole by providing a map among the parameters of the two solutions. This conclusion, based on explicit computations, is implied by more general results obtained by Lewandowski and Pawlowski (2003) and Kunduri and Lucietti (2013). Though the definition of the mass of MKN has been controversial until our proposal, its extreme limit was known and matched with the definition proposed in Booth et al. (2015) by means of the isolated horizon formalism. Same agreement is found for the mass computed in Astorino et al. (2016) by means of covariant phase space formalism. In addition, Astorino et al. (2016) establishes a relationship away

from the extreme case: both the MKN and the Kerr-Newman black holes share the same thermodynamics. This aspect will be discussed in section 6.5.

6.2 Black holes with external magnetic test fields

In this section, we work in the weak field regime, *i.e.*, we do not consider any back-reaction of the electromagnetic field on the Kerr black hole geometry, and we treat all the fields as test fields. More formally, the Einstein-Maxwell equations are

$$\begin{cases} R_{\mu\nu} - \frac{1}{2} R g_{\mu\nu} = 2 T^{EM}_{\mu\nu}, \\ F^{\mu\nu}{}_{;\nu} = 0, \end{cases} \tag{6.1}$$

where $F_{\mu\nu}$ is the electromagnetic field and $T^{EM}_{\mu\nu}$ the associated energy-momentum tensor. We assume that the contribution of the external electromagnetic fields on the geometry is negligible, therefore $T^{EM}_{\mu\nu} \approx 0$ and it does not alter the geometry of the space-time. In other words, we want to consider electromagnetic perturbations around the Kerr black holes space-time. In particular, we are going to construct two different kinds of electromagnetic test perturbations: one giving a negligible electric charge Q to the Kerr black hole, the other embedding the Kerr black hole in a (asymptotically uniform) magnetic test field B. In natural units, the mass of the Kerr black hole determines the characteristic scale of the system. Therefore, if both $Q/M \ll 1$ and $B \ll 1/M$, we might neglect any back-reaction and consider the electromagnetic field as a test field on the fixed background geometry.

6.2.1 Wald's solution

Wald (1974) showed the existence of a mechanism to charge up the Kerr black hole when it is immersed in an external magnetic test field. The argument of Wald, as we shall review below, is based on a well-known result by Papapetrou (1966).

Assume that ξ is a Killing vector field. Then, $\mathscr{L}_\xi g_{\mu\nu} = \xi_{\mu;\nu} + \xi_{\nu;\mu} = 0$ where $g_{\mu\nu}$ is the metric field and the semicolon stands for the operation of covariant derivation. The Papapetrou's result states that a Killing vector generates a solution to Maxwell's equations in vacuum space-times. Let us define the antisymmetric rank-two tensor as

$$F_{\mu\nu} = \xi_{\nu;\mu} - \xi_{\mu;\nu} = -2\xi_{\mu;\nu}. \tag{6.2}$$

Its covariant derivative is

$$F^{\mu\nu}{}_{;\nu} = -2\xi^{\mu;\nu}{}_{;\nu} = -2R^{\mu}{}_{\lambda}\xi^{\lambda} = 0. \tag{6.3}$$

In the second step, we have used the property that the double covariant derivative of a Killing vector is $\xi_{\mu;\nu;\sigma} = \xi^{\lambda}R_{\lambda\sigma\mu\nu}$, while in the last step we have used the assumption of vacuum space-time $R_{\mu\nu} = 0$. Therefore, the electromagnetic test field $F_{\mu\nu}$ satisfies the source-free Maxwell's equations.

In Minkowski space-time, there are ten independent Killing vectors. The electromagnetic field generated by the four translation Killing vectors vanish, those generated by the three rotational Killing vectors reproduce uniform magnetic fields, and those generated by the three boost Killing vectors reproduce uniform electric fields.

In Kerr space-time, there are two independent Killing vectors: the time Killing vector $\eta^{\mu}\partial_{\mu} = \partial_t$ and the axial Killing vector $\psi^{\mu}\partial_{\mu} = \partial_{\phi}$. We denote the electromagnetic test field generated by η as $F_{\eta} = d\eta$.[1] The 1-form corresponding to the Killing vector, $\eta_{\mu} = g_{\mu\nu}\eta^{\nu}$, serves as gauge potential for the electromagnetic field F_{η}. Analogously for the axial Killing vector ψ. Both F_{η} and F_{ψ} are stationary and axisymmetric fields

$$\mathscr{L}_{\eta}F_{\eta} = 0 = \mathscr{L}_{\psi}F_{\eta}, \qquad \mathscr{L}_{\eta}F_{\psi} = 0 = \mathscr{L}_{\psi}F_{\psi}. \tag{6.4}$$

The electromagnetic field generated by the time Killing vector vanishes asymptotically. When integrated over a topological two-sphere, one has

$$\frac{1}{4\pi}\int_{S^2} F_{\eta} = 0, \qquad \frac{1}{4\pi}\int_{S^2} \star F_{\eta} = -2M. \tag{6.5}$$

Instead, the electromagnetic field generated by the axial Killing vector approaches the uniform magnetic field asymptotically. Integrations over a two-sphere give

$$\frac{1}{4\pi}\int_{S^2} F_{\psi} = 0, \qquad \frac{1}{4\pi}\int_{S^2} \star F_{\psi} = 4J. \tag{6.6}$$

Thus, the two Killing vectors generate stationary and axisymmetric electromagnetic (test) fields, F_{η} and F_{ψ}, carrying charges $-2M$ and $4J$, respectively.

At this stage, one may wonder if it is possible to perturb the Kerr black hole by introducing a perturbation to add a net electric charge Q or to place the Kerr black hole in a (asymptotically uniform) magnetic field. The answer to both questions is positive and the uniqueness relies on a theorem proved by Carter (see, *e.g.*,

[1] Here, $F_{\eta} = \frac{1}{2}F_{\eta\ \mu\nu}dx^{\mu}\wedge dx^{\nu} = \frac{1}{2}(d\eta)_{\mu\nu}dx^{\mu}\wedge dx^{\nu} = \frac{1}{2}\left(\partial_{\mu}\eta_{\nu} - \partial_{\nu}\eta_{\mu}\right)_{\mu\nu}dx^{\mu}\wedge dx^{\nu}$.

the republication of his Les Houches lecture notes in Carter, 2009; Carter, 2010), stating that if the electromagnetic test field F is a) stationary and axisymmetric, b) regular on the horizon and in the exterior region of the black hole, c) asymptotically vanishing and d) without magnetic monopole and charge, then $F = 0$. Thus, in order to have a non-trivial perturbation, we need to relax one of the hypothesis. For the aim to add a net electric charge Q, we relax hypothesis d). From Eqs. (6.5), we might define the electromagnetic field to be

$$F_Q = -(Q/2M)\, F_\eta. \tag{6.7}$$

Notice that if F'_Q is another field carrying the same charge Q, the theorem above implies that $F'_Q - F_Q = 0$. Moreover, as it should be, $F_Q = -(Q/2M)\, F_\eta$ is exactly the Kerr-Newman electromagnetic field.

Now, let us focus on the second aim: embedding the Kerr black hole in an asymptotically uniform magnetic field. To this aim, we have to relax the hypothesis c) in favour of having an asymptotically uniform magnetic field. From Eqs. (6.5) and Eqs. (6.6), it is clear that

$$F_B = \frac{1}{2} B_0 \left(F_\psi + \frac{2J}{M} F_\eta \right) \tag{6.8}$$

is the only combination with vanishing charges. The uniqueness is again guaranteed by the theorem mentioned above. Asymptotically, F_B behaves like F_ψ and B_0 is a real number equal to the magnitude of the asymptotic uniform magnetic field.

These two results, Eqs. (6.7) and (6.8), can be linearly superposed to describe the electromagnetic test field for a Kerr black hole perturbed by an electric charge Q and immersed in a magnetic field

$$F_{Wald} = F_Q + F_B = -(Q/2M)\, F_\eta + \frac{1}{2} B_0 \left(F_\psi + \frac{2J}{M} F_\eta \right) = \frac{1}{2M} (2B_0 J - Q)\, F_\eta + \frac{1}{2} B_0 F_\psi. \tag{6.9}$$

Such a field is generated by the gauge potential

$$A_{Wald} = \frac{1}{2M} (2B_0 J - Q)\, \eta + \frac{1}{2} B_0 \psi. \tag{6.10}$$

The time Killing vector generates the Coulomb part of the electromagnetic field and it contributes to the electric field and magnetic field for $J \neq 0$ [2]. In other words, the rotation of the charged black hole immersed in the magnetic field induces an electric field and contributes further to the magnetic field.

In order to unveil the charging mechanism, we restrict our discussion only to

[2] It is easy to check that, in coordinates, both F_η and F_ψ contribute to the electric field in the $dt \wedge dr$ and $dt \wedge d\theta$ components and to the magnetic field in the $dr \wedge d\phi$ and $d\theta \wedge d\phi$ components

particles along the axis of rotation at $\theta = 0$. For a particle of mass m, charge q and four-momentum $p^\mu = mu^\mu - qA^\mu$, the variation of the electrostatic potential $U = -p_\mu \eta^\mu$ between infinity ($r \to \infty$) and the event horizon ($r = r_+$) reads as

$$\Delta U = U_{r=r_+} - U_\infty = q A_{Wald\ \mu} \eta^\mu \Big|_\infty^{r=r_+} = -q A_{Wald\ \mu} \eta^\mu \Big|_\infty = -\frac{q}{2M}(Q - 2B_0 J), \tag{6.11}$$

where, in the second step, we have used the fact that $\eta_\mu \eta^\mu|_{\theta=0} = 0$ on the horizon, $\psi_\mu \eta^\mu|_{\theta=0} = 0$, and $\eta_\mu \eta^\mu \to -1$ as $r \to \infty$. Fixed the sign of the charge q, for $\Delta U < 0$ the accretion mechanism of such charged particles is energetically favourable till $\Delta U = 0$. Therefore, regardless of the sign of q, the equilibrium charge is given by $Q_{Wald} = 2B_0 J$. Moreover, assuming that $J \leq M^2$, the charge-to-mass ratio of the black hole is

$$\frac{Q_{Wald}}{M} = \frac{2B_0 J}{M} \leq 2B_0 M \approx 1.7 \times 10^{-20} \left(\frac{M}{M_\odot}\right)\left(\frac{B_0}{1\text{Gauss}}\right). \tag{6.12}$$

The ratio Q_{Wald}/M, or equivalently the product $B_0 M$, is well below the unity for astrophysically realistic black hole masses and magnetic field strengths (Dokuchaev et al., 1987).

6.2.2 Meissner-like effect for rotating black holes

One year after Wald published his solution, King, Lasota, and Kundt (1975) computed the flux of the magnetic field through the upper hemisphere of the event horizon. Given the electromagnetic test field in (6.8), the magnetic flux across the upper hemisphere H^2_+ is

$$\Phi_B = \frac{1}{2\pi}\int_{H^2_+} F_B = \frac{1}{2\pi}\int_{\partial H^2_+} A_B = A_\phi\Big|_{\substack{\theta=\pi/2 \\ r=r_+}} = \frac{1}{2} B_0 r_+^2 \left(1 + \frac{a^2}{r_+^2}\right)\left(1 - \frac{a^2}{r_+^2}\right), \tag{6.13}$$

where we used the Stokes' theorem. The magnetic flux $\Phi_B = \Phi_B(a; B_0)$ is a function of the spin parameter a and of the magnetic field strength at infinity B_0. It is a monotonic function of a: its maximum is for Schwarzschild black hole ($a = 0$) and it vanishes for extreme Kerr black hole ($a = M$). The expulsion of magnetic field lines from the upper hemisphere of extreme Kerr black hole is known as Meissner-like effect.[3] Here, we have shown it for magnetic test field on Kerr black hole background. Ten years later, Bičák and Janiš (1985) confirmed this effect for all axisymmetric stationary test fields, by explicitly solving the vacuum Maxwell's

[3] The Meissner effect, originally discovered by Meissner and Ochsenfeld (1933), describes the expulsion of magnetic fields from a superconductor when it is cooled below a critical temperature T_c, marking the transition to the superconducting state.

equations around Kerr space-time. Actually, the effect has been also checked for back-reacting magnetic field for uncharged MKN solution (Karas and Vokrouhlickỳ, 1991). More recently, the Meissner-like effect has been shown to operate also in more general settings, *e.g.*, where Kerr black hole is surrounded by accretion disc (Guerlebeck and Scholtz, 2017; Guerlebeck and Scholtz, 2018). The Meissner-like effect has astrophysical relevance because it might affect the efficiency of the extraction of energy from rotating black holes. Indeed, further studies on the Meissner-like effect have been pursued by Penna (2014a) and Penna (2014b) to highlight feasible conditions to evade this effect. However, there is no total consensus whether this effect realistically quenches the jet creation efficiency (see, *e.g.*, Ruiz et al., 2012; Kinoshita and Igata, 2017).

A similar computation with the Wald's solution (6.9) leads to a more general expression accounting for the charge of the black hole (see, *e.g.*, Kim, Lee, and Lee, 2001)

$$\Phi_W = \frac{1}{2\pi}\int_{H_+^2} F_W = \frac{1}{2}B_0 r_+^2\left(1+\frac{a^2}{r_+^2}\right)\left[1-\frac{a^2}{r_+^2}\left(1-\frac{Q}{B_0 J}\right)\right]. \tag{6.14}$$

For $Q=0$, we recover the result in Eq. (6.13). For finite values of Q in the range $0<Q<Q_{Wald}=2B_0J$, the magnetic flux never reaches zero, as shown in Fig. 6.1 for some values of the electric charge. At extremality, its value equals the electric charge. Therefore charged black holes immersed in an external magnetic field do not experience the Meissner-like effect at the extremal bound. For the limiting value of the Wald's charge, the flux becomes $\Phi_W = 1/2B_0 r_+^2\left(1+a^2/r_+^2\right)^2$. Surprisingly, an extreme black hole with the Wald's charge has the same magnetic flux as in the Schwarzschild case (Dokuchaev et al., 1987). In other words, the Wald's charge can be thought of as that equilibrium charge to match the magnetic flux for both cases of slightly charged Kerr and Schwarzschild black holes.

6.3 Black holes with external magnetic back-reacting fields

6.3.1 Magnetised-Kerr-Newman black hole

We begin with the Kerr-Newman (KN) solution, describing an electrically charged and rotating black hole, parametrised by the mass M, the angular momentum per unit mass a, the electric charge q and the magnetic charge p. The line element of KN space-time can be recast in the same form of the Kerr line element in Eq. (1.1)

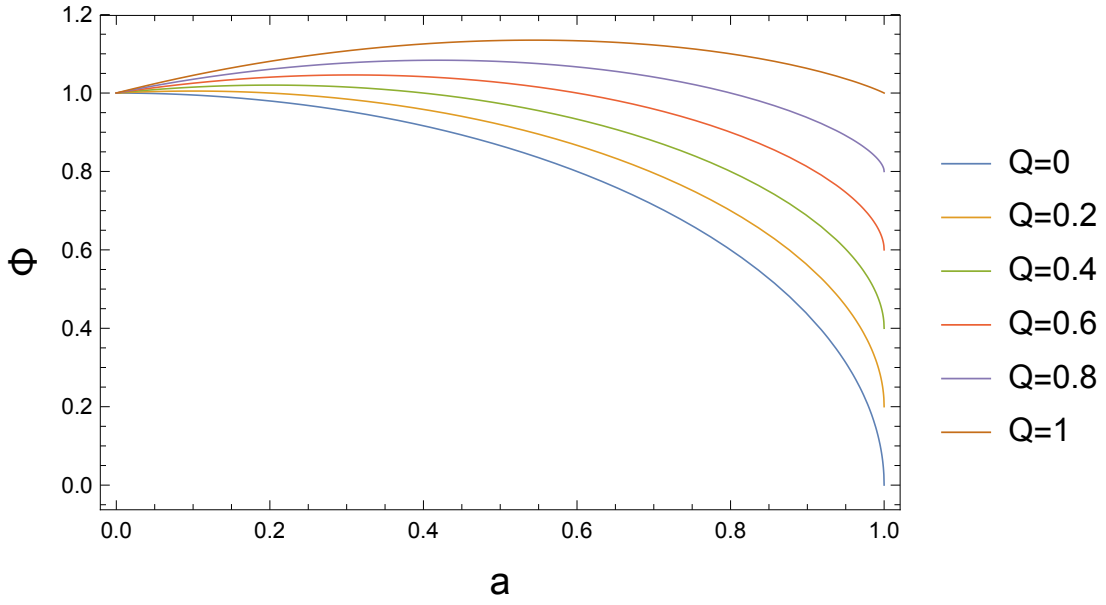

FIGURE 6.1: Magnetic flux for different values of the electric charge Q as function of the angular momentum parameter a. We have set $m = 1$ and $B_0 = 1/2$ to normalize the flux to the unity for the Schwarzschild case.

as follows (see, *e.g.*, appendix B of Gibbons, Mujtaba, and Pope, 2013)

$$ds^2_{KN} = -\frac{\Sigma\bar{\Delta}}{\bar{A}}dt^2 + \frac{\Sigma}{\bar{\Delta}}dr^2 + \Sigma d\theta^2 + \sin^2(\theta)\frac{\bar{A}}{\Sigma}\left(d\phi - \bar{\omega}dt\right)^2, \tag{6.15a}$$

$$A_{KN} = \bar{A}_t dt + \bar{A}_\phi d\phi, \tag{6.15b}$$

where the metric and gauge potential functions read as

$$\bar{\Delta}(r) = r^2 - 2Mr + a^2 + q^2 + p^2, \tag{6.16a}$$

$$\Sigma(r,\theta) = r^2 + a^2\cos^2(\theta), \tag{6.16b}$$

$$\bar{A}(r,\theta) = \left(r^2 + a^2\right)^2 - a^2\bar{\Delta}\sin^2(\theta), \tag{6.16c}$$

$$\bar{\omega}(r,\theta) = \frac{a\left(2Mr - q^2 - p^2\right)}{\bar{A}}, \tag{6.16d}$$

$$\bar{A}_t(r,\theta) = \bar{\Phi}_0(r,\theta) - \bar{\omega}(r,\theta)\bar{\Phi}_3(r,\theta), \tag{6.16e}$$

$$\bar{A}_\phi(r,\theta) = \bar{\Phi}_3(r,\theta), \tag{6.16f}$$

and where the functions $\bar{\Phi}_0$ and $\bar{\Phi}_0$ read as

$$\bar{\Phi}_0(r,\theta) = \frac{1}{\bar{A}}\left[ap\bar{\Delta}\cos(\theta) - qr\left(r^2 + a^2\right)\right], \tag{6.17a}$$

$$\bar{\Phi}_3(r,\theta) = \frac{1}{\Sigma}\left[aqr\sin^2(\theta) - p\left(r^2 + a^2\right)\cos(\theta)\right]. \tag{6.17b}$$

The MKN solution is obtained by applying the Harrison transformation to the

KN solution (Harrison, 1968). The transformation appends an external magnetic field, parametrised by the real number B, to the seed KN solution. The result has been nicely written in appendix B of Gibbons, Mujtaba, and Pope (2013). The MKN line element takes the form

$$ds^2_{MKN} = H(r,\theta)\left[-\frac{\Sigma\bar{\Delta}}{\bar{A}}dt^2 + \frac{\Sigma}{\bar{\Delta}}dr^2 + \Sigma d\theta^2\right] + \frac{1}{H(r,\theta)}\left[\sin^2(\theta)\frac{\bar{A}}{\Sigma}\left(d\phi - \omega dt\right)^2\right], \tag{6.18a}$$

$$A_{MKN} = A_t dt + A_\phi d\phi. \tag{6.18b}$$

The KN line element is modified by the presence of the Harrison function $H(r,\theta)$ and the angular velocity $\omega(r,\theta)$, both expressed by a finite expansion in powers of the magnetic field parameter B

$$H(r,\theta) = 1 + \frac{H_{(1)}B + H_{(2)}B^2 + H_{(3)}B^3 + H_{(4)}B^4}{\Sigma}, \tag{6.19a}$$

$$\omega(r,\theta) = \bar{\omega}(r,\theta) + \frac{\omega_{(1)}B + \omega_{(2)}B^2 + \omega_{(3)}B^3 + \omega_{(4)}B^4}{\bar{A}}. \tag{6.19b}$$

The gauge potential components, given by $A_t(r,\theta) = \Phi_0 - \omega\Phi_3$ and $A_\phi(r,\theta) = \Phi_3$, are, instead, deformed as

$$\Phi_0(r,\theta) = \bar{\Phi}_0 + \frac{\Phi_0^{(1)}B + \Phi_0^{(2)}B^2 + \Phi_0^{(3)}B^3}{4\bar{A}}, \tag{6.20a}$$

$$\Phi_3(r,\theta) = \frac{\bar{\Phi}_3}{H} + \frac{\Phi_3^{(1)}B + \Phi_3^{(2)}B^2 + \Phi_3^{(3)}B^3}{\Sigma H}. \tag{6.20b}$$

The explicit expressions of the functions $H_{(i)}(r,\theta)$, $\omega_{(i)}(r,\theta)$, $\Phi_0^{(i)}(r,\theta)$, and $\Phi_3^{(i)}(r,\theta)$ can be found in appendix B of Gibbons, Mujtaba, and Pope (2013).

The MKN black hole depends upon five parameters: the mass parameter M, the angular momentum parameter $j = aM$ or the angular momentum per unit mass a, the electric charge parameter q, the magnetic charge parameter q, and the magnetic field B. In order to cancel the magnetic monopole charge, we set the parameter $p = 0$. It is easy to verify that the MKN metric smoothly reduces to the KN metric for $B = 0$, to the Kerr metric for $B = 0$ and $q = 0$, to the Schwarzschild metric for $B = 0$, $q = 0$ and $j = 0$, to the Minkowski metric for $B = 0$, $q = 0$, $j = 0$ and $M = 0$ and to the Melvin metric (sometimes called magnetised Minkowski) for $q = 0$, $j = 0$ and $M = 0$. As claimed in the Introduction, this exact solution to Einstein-Maxwell equations has not a clear physical interpretation in general, because of its unconventional asymptotic region and because the ergo-region extends all the way to infinity along the axis of rotation for a certain range of the

parameter B. However, it has a well-defined weak field approximation in agreement with the Wald's solution discussed before. When $Q/M \ll 1$ and $BM \ll 1$ (see Eq. (6.12)), MKN metric approaches the Kerr metric in the linear approximation and the gauge potential is given by a linear combination of the two Killing vectors, according to the Wald's construction in Eq. (6.10) (Gibbons, Mujtaba, and Pope, 2013). The weak field approximation guarantees that the magnetic field does not affect the geometry of the Kerr or Kerr-Newman black hole up to the so-called Melvin radius $r_{Melvin} = B^{-1}$, beyond which the magnetic field distorts the metric in the far asymptotic region. Therefore, MKN solution can be used as a toy model in the surroundings of the black hole in the radial range $r_+ \ll r \ll r_{Melvin} = B^{-1}$ with $BM \ll 1$ (Aliev and Gal'tsov, 1989c).

To ensure that the MKN metric does not admit any conical deficit at the North and South poles of the sphere, the azimuthal angle ϕ must have a period equals to (Hiscock, 1981)

$$\Delta\phi = 2\pi H(r,0) = 2\pi H(r,\pi) = 2\pi\left[1+\frac{3}{2}q^2B^2+2jqB^3+\left(j^2+\frac{q^4}{16}\right)B^4\right] \equiv 2\pi\Xi. \tag{6.21}$$

We rescale the azimuthal angle ϕ by Ξ, so that its period is equal to 2π. Moreover, we add a space-time constant $A^{(0)}_\phi$ to the azimuthal component of the gauge potential to have regularity along the axis of rotation. The regularity condition at both the North and South poles is $A_\phi(r,0) = 0 = A_\phi(r,\pi)$ and it amounts to the expression

$$A^{(0)}_\phi = -\left[\frac{3}{2}q^2+3jqB+\frac{1}{8}\left(q^4+16j^2\right)B^2\right]B. \tag{6.22}$$

For future reference, we compute other physical quantities to discuss the thermodynamics of the MKN black hole. The inner and outer horizons are located at $r_\pm = M \pm \sqrt{M^2-a^2-q^2}$ and their expressions are not affected by the magnetic field parameter. Therefore, also the Hawking temperature given by

$$T_H = \frac{\kappa_+}{2\pi} = \frac{1}{4\pi}\frac{r_+-r_-}{r_+^2+a^2}, \tag{6.23}$$

does not depend upon the magnetic field parameter B. However, the other thermodynamic potentials, namely, the angular velocity and the Coulomb electrostatic potential do depend on the four parameters of the solution. Indeed, the angular velocity of the event horizon r_+ is given by (after having rescaled the azimuthal coordinate $\phi \to \phi/\Xi$)

$$\Omega_+ = -\left.\frac{g_{t\phi}}{g_{\phi\phi}}\right|_{r=r_+} = \omega(r_+,\theta), \tag{6.24}$$

while the Coulomb electrostatic potential measured at the event horizon is

$$\Phi_+ = -A_\mu \xi^\mu \Big|_{r=r_+} = -A_\phi^{(0)} \Omega_+ - \Phi_0(r_+), \tag{6.25}$$

where ξ is the horizon-generating Killing vector $\xi = \partial_t + \Omega_+ \partial_\phi$. Finally, the area of the event horizon is given by $A_+ = 4\pi\Xi\left(r_+^2 + a^2\right)$ and the Bekenstein-Hawking entropy is $S = A_+/4$.

6.3.2 Near-horizon geometry of the MKN black hole

The near-horizon geometry of the extreme MKN black hole (abbreviated in NH-EMKN) can be cast in the same form as in the case of extreme Kerr (see Eq. (1.16b)). More precisely, one first goes to the extreme case, defined by the constraint $M = \sqrt{a^2+q^2}$ on the parameters. Then one performs a gauge transformation of the form $A_t \to A_t + \Phi_e$ to guarantee the finiteness of the near-horizon limit of the gauge potential (Compère, 2012). Finally, one changes the coordinates from the (t, r, θ, ϕ) of the EMKN black hole (6.18) to the scaling coordinates (T, R, θ, Φ) defined in Eq. (1.13)

$$T = \frac{t}{\tilde{r}_0}\lambda, \quad R = \frac{r - r_+}{\tilde{r}_0}\frac{1}{\lambda}, \quad \Phi = \phi - \Omega_+^{ext} t, \tag{6.26}$$

and one gets

$$ds^2_{NH-EMKN} = \tilde{r}_0^2\, \Gamma(\theta) \left[-R^2 dT^2 + \frac{dR^2}{R^2} + d\theta^2 + \gamma^2(\theta)\left(d\Phi + kR dT\right)^2 \right], \tag{6.27a}$$

$$A_{NH-EMKN} = l(\theta)\left(d\Phi + kR dT\right) - \frac{e}{k} d\Phi. \tag{6.27b}$$

The functions $\Gamma(\theta)$, $\gamma(\theta)$, $l(\theta)$ and the constants $\tilde{r}_0$, k, e in the metric tensor and in the gauge potential are written in appendix A of Astorino (2015).

In Astorino (2015) and in Bičák and Hejda (2015), an explicit map have been derived between the parameters of the near-horizon geometry of the extreme Kerr-Newman (a_{KN}, q_{KN}) and the parameters of the near-horizon geometry of the extreme Magnetised-Kerr-Newman (a_{MKN}, q_{MKN}, B)

$$a_{MKN} = a_{KN} - q_{KN}\sqrt{a_{KN}^2 + q_{KN}^2}B - \frac{a_{KN}}{4}\left(4a_{KN}^2 + 3q_{KN}^2\right)B^2, \tag{6.28a}$$

$$q_{MKN} = q_{KN} + 2a_{KN}\sqrt{a_{KN}^2 + q_{KN}^2}B - \frac{q_{KN}^3}{4}B^2. \tag{6.28b}$$

As we will show in Eqs. (6.34) and (6.35), both a_{MKN} and q_{MKN} coincide, respectively, with the angular momentum (per unit mass) and the physical electric charge

of the extreme MKN black hole. Therefore, by assuming that also the mass can be mapped according to the above parameter redefinition, one can infer the extreme mass of MKN black hole to be

$$M_{MKN} = \sqrt{a_{MKN}^2 + q_{MKN}^2} = \sqrt{a_{KN}^2 + q_{KN}^2} + a_{KN} q_{KN} B + \frac{1}{4}\sqrt{a_{KN}^2 + q_{KN}^2}(4a_{KN}^2 + q_{KN}^2)B^2. \tag{6.29}$$

It is worth noticing that this last expression can be recovered as the extreme value of the mass of MKN black hole computed by the isolated horizon formalism in Booth et al., 2015 and does not agree with the extreme value of the mass of MKN black hole computed by dimensional reduction in Gibbons, Pang, and Pope, 2014. In the following, we resolve this tension by using the covariant phase space formalism and, in addition, we will clarify the relation between the two different definitions of mass by studying the respective thermodynamics.

6.4 Mass of Magnetised-Kerr-Newman black holes

In the strong field regime, where the magnetic field back-reacts with the geometry and the space-time is described by the MKN line element (6.18), the conserved charges of the MKN black hole are affected by the presence of the electromagnetic field.

The unconventional asymptotic region of the metric introduces subtleties and ambiguities in the calculation of conserved charges. While the conserved angular momentum J and the electric charge Q do not raise any obstacle in their computation, such problems are manifest in the definition of the mass. Several attempts have been made since the publication of the MKN solution. The first attempts performed in Dokuchaev et al. (1987), and later in Aliev and Gal'tsov (1989c) and Karas and Vokrouhlickỳ (1991), consisted in computing the following integrals at spatial infinity $r \to \infty$

$$\mathscr{M} = \frac{1}{8\pi}\int_{S^2} \eta^{\mu;\nu} d^2\Sigma_{\mu\nu}, \tag{6.30a}$$

$$J = -\frac{1}{16\pi}\int_{S^2} \psi^{\mu;\nu} d^2\Sigma_{\mu\nu}, \tag{6.30b}$$

$$Q = \frac{1}{8\pi}\int_{S^2} F^{\mu\nu} d^2\Sigma_{\mu\nu}, \tag{6.30c}$$

where η and ψ are, respectively, the time and axial Killing vectors and the 2-form $d^2\Sigma_{\mu\nu} = 1/2\varepsilon_{\mu\nu\alpha\beta} dx^\alpha \wedge dx^\beta$ is the differential area element of the two-sphere. For asymptotically flat space-times, the definitions above give the total conserved mass, angular momentum and electric charge (Bardeen, Carter, and Hawking,

1973). For MKN space-time, that is not asymptotically flat, the total mass is formally divergent as an immediate computation can show. Therefore, a change of strategy to compute the conserved charges is needed. Such new ideas come with the recent attempts by Gibbons, Pang, and Pope (2014) and Booth et al. (2015), using Kaluza-Klein reduction to three-dimensional gravity and isolated horizon formalism, respectively. Their results totally agree for the angular momentum and the electric charge expressions, but these two approaches give two different expressions for the total mass. Astorino et al. (2016) resolved the tension between the two definitions by adopting the covariant phase space formalism and provided a detailed analysis of the thermodynamics of MKN space-time.

6.4.1 Covariant phase space formalism

Before starting the computation of the conserved charges, we have to mention the notation and the nomenclature of the covariant phase space formalism used in the following (see, *e.g.*, the review Compère, 2006). In the context of Einstein-Maxwell theory, the generalised Killing equations for the metric field $g_{\mu\nu}$ and the gauge field A_μ are

$$\mathscr{L}_\xi g_{\mu\nu} = 0, \qquad \mathscr{L}_\xi A_\mu + \partial_\mu \lambda = 0, \tag{6.31}$$

where $\xi = \xi^\mu \partial_\mu$ is a Killing vector field and λ is a real constant. We call symmetry parameter the pair (ξ, λ), which is solution to the generalised Killing equations. It can be shown that a surface charge $k_{(\xi,\lambda)}[\delta g, \delta A; g, A]$ is associated with the symmetry parameter (ξ, λ) and it is uniquely fixed as a functional of the Lagrangian, up to an irrelevant total derivative (Barnich and Brandt, 2002). The surface charges $k_{(\xi,\lambda)}$ are space-time 2-forms and 1-forms in the field space. The explicit formula for the surface charge that we will use in this chapter can be found in Eq. (4.22) of Compère, Murata, and Nishioka (2009) (where one sets the scalar field to zero, $\chi = 0$, $h_{IJ} = 0$ and $k_{IJ} = 1$).

The total conserved charge $\mathscr{Q}_{(\xi,\lambda)}$ associated to (ξ, λ) is defined by

$$\mathscr{Q}_{(\xi,\lambda)}[g, A; \bar{g}, \bar{A}] = \int_{S^2} \int_{\bar{g}}^{g} \int_{\bar{A}}^{A} k_{(\xi,\lambda)}[\delta g', \delta A'; g', A'], \tag{6.32}$$

where S^2 is a space-time two-surface. Such a definition is meaningful provided that the surface charge does not depend on the path in the field space. This requirement is called the integrability condition and reads as

$$\int_{S^2} \delta_1 k_{(\xi,\lambda)}[\delta_2 g, \delta_2 A; g', A'] - \int_{S^2} \delta_2 k_{(\xi,\lambda)}[\delta_1 g, \delta_1 A; g', A'] = 0. \tag{6.33}$$

Since the surface charge is closed on-shell (Barnich and Brandt, 2002), the charge (6.32) is conserved under any deformation of the surface. It is, therefore, radius and time independent.

The integrability condition depends on the choice of the symmetry parameters (ξ, λ). One can introduce a prefactor α (which is a function of the phase space parameters) in front of the symmetry parameters and solve the integrability of the total conserved charge over the phase space (Barnich and Compère, 2008). In other words, the prefactor α serves as an integrating factor for Eq. (6.33). As an example, let us consider the total energy of Schwarzschild or Kerr black holes. It is the total conserved charge associated to the Killing vector $\xi = \partial_t$. It is integrable and equals to the mass parameter m. However, for Kerr black holes in anti-de Sitter (AdS) space-time in Boyer-Lindquist coordinates, one needs to multiply the Killing vector $\xi = \partial_t$ by a prefactor $\xi' = \left(1 - a^2/l^2\right)^{-1} \partial_t$, where a is the spin parameter and l is the AdS radius, to get the canonical integrable mass $M = \left(1 - a^2/l^2\right)^{-2} m$ (see, *e.g.*, Caldarelli, Cognola, and Klemm, 2000; Gibbons, Perry, and Pope, 2005; Deruelle and Katz, 2005; Barnich and Compere, 2005). The integrating factor technique reproduces the mass obtained from consistent boundary conditions by Henneaux and Teitelboim (1985) and, in that sense, it is equivalent to requiring a differentiable generator in the Hamiltonian sense (Regge and Teitelboim, 1974).

In the following section, we will address the problem to compute the integrable mass of MKN black holes by allowing all the phase space parameters to vary.

6.4.2 Computation of conserved charges

Let us first obtain the angular momentum J and electric charge Q. By definition, the angular momentum and electric charge are the conserved charges associated with the symmetry parameters $(-\partial_\phi, 0)$ and $(0, -1)$, respectively. Using the Barnich-Brandt method (Barnich and Brandt, 2002), we directly note that the infinitesimal charges δQ and δJ obey the integrability conditions (6.33). Using the definition (6.32), we obtain

$$J \equiv \mathscr{Q}_{(-\partial_\phi,0)} = j - q^3 B - \frac{3}{2} j q^2 B^2 - \frac{1}{4} q(8j^2 + q^4) B^3 - \frac{1}{16} j(16j^2 + 3q^4) B^4, \quad (6.34)$$

$$Q \equiv \mathscr{Q}_{(0,-1)} = q + 2jB - \frac{1}{4} q^3 B^2, \quad (6.35)$$

Both the angular momentum and the total electric charge match with the results in the literature (Gibbons, Pang, and Pope, 2014; Astorino, 2015; Booth et al., 2015).

Let us now compute the infinitesimal change of energy caused by a change of all parameters of the solution $(\delta M, \delta j, \delta q, \delta B)$. Since it is not clear which canonical generator is associated with the conserved energy, let us first obtain the infinitesimal conserved charge $\not{\delta}\mathcal{Q}_{(\partial_t,0)} = \oint_{S^2} k_{(\partial_t,0)}$ associated with the symmetry parameter $(\partial_t, 0)$. Here S^2 is a sphere of integration around the black hole, *i.e.*, the integration is performed on a constant t and r surface. Using the definition of the surface charge and after a lengthy algebra, we obtain

$$\not{\delta}\mathcal{Q}_{(\partial_t,0)} = c_M \delta M + c_j \delta j + c_q \delta q + c_B \delta B, \tag{6.36}$$

where the coefficients read as

$$c_M = 1 + \frac{3}{2}q^2B^2 + 2jqB^3 + \left(j^2 + \frac{q^4}{16}\right)B^4, \tag{6.37a}$$

$$c_j = -5MqB^3 - \frac{1}{8}\frac{j}{M}\left(28M^2 + q^2\right)B^4, \tag{6.37b}$$

$$c_q = -3MqB^2 - \frac{1}{4}\frac{j}{M}\left(8M^2 + 5q^2\right)B^3, \tag{6.37c}$$

$$c_B = \frac{j}{M}q + \frac{3}{2}Mq^2B - 3jq\left(2M + \frac{q^2}{4M^2}\right)B^2 - \frac{1}{2}\left(\frac{5}{4}Mq^4 + \frac{j^2}{M}(8M^2 + q^2)\right)B^4. \tag{6.37d}$$

We have used the symbol $\not{\delta}$ to emphasize that the expression (6.36) is not integrable in the parameter space. Indeed, it is easy to check that $\delta_1(\not{\delta}_2\mathcal{Q}_{(\partial_t,0)}) - (1 \leftrightarrow 2) \neq 0$. Therefore, ∂_t is not associated with the energy. Note that the coefficient c_M exactly matches with the factor Ξ introduced in Eq. (6.21) to avoid conical deficits.

The goal of this section is now to define the mass from integration over the phase space of an integrable infinitesimal canonical charge $\delta\mathcal{M}$ and prove that the procedure is unique and, therefore, that the mass $\mathcal{M}$ is uniquely defined. The black hole admits exactly three generalised Killing vectors and the symmetry associated with the mass can be any combination thereof. We can parametrize it as $\alpha(\chi, \lambda) = \left(\alpha(\partial_t + \Omega_{int}\partial_\phi), \alpha\Phi_{int}\right)$. We have to determine the four following functions defined over the parameter space: the mass $\mathcal{M} = \mathcal{M}(M, j, q, B)$ and the three constants which fix the canonical generator: $\alpha = \alpha(M, j, q, B)$, $\Omega_{int} = \Omega_{int}(M, j, q, B)$ and $\Phi_{int} = \Phi_{int}(M, j, q, B)$. By definition, these four functions obey the following equality

$$\delta\mathcal{M} = \alpha\left(\not{\delta}\mathcal{Q}_{(\partial_t,0)} - \Omega_{int}\delta J - \Phi_{int}\delta Q\right). \tag{6.38}$$

Quite remarkably, these defining equations are four equations since there are four parameters to be varied: M, j, q, B. They read in detail as

$$\partial_M \mathscr{M} = \alpha \Xi, \tag{6.39}$$

$$\partial_q \mathscr{M} = \alpha \Big(c_q - \partial_q Q \Phi_{int} - \partial_q J \Omega_{int} \Big), \tag{6.40}$$

$$\partial_B \mathscr{M} = \alpha \Big(c_B - \partial_B Q \Phi_{int} - \partial_B J \Omega_{int} \Big), \tag{6.41}$$

$$\partial_j \mathscr{M} = \alpha \Big(c_j - \partial_j Q \Phi_{int} - \partial_j J \Omega_{int} \Big). \tag{6.42}$$

From the first equation, we algebraically solve for α and we obtain

$$\alpha = \frac{1}{\Xi} \partial_M \mathscr{M}. \tag{6.43}$$

By algebraically solving the second and third equation for Φ_{int} and Ω_{int}, we get

$$\Omega_{int} = \frac{1}{\alpha(\partial_q J \partial_B Q - \partial_B J \partial_q Q)} \Big[\alpha(c_q \partial_B Q - c_B \partial_q Q) + \partial_q Q \partial_B \mathscr{M} - \partial_B Q \partial_q \mathscr{M} \Big], \tag{6.44}$$

$$\Phi_{int} = \frac{1}{\alpha(\partial_q J \partial_B Q - \partial_B J \partial_q Q)} \Big[\alpha(c_B \partial_q J - c_q \partial_B J) + \partial_B J \partial_q \mathscr{M} - \partial_q J \partial_B \mathscr{M} \Big]. \tag{6.45}$$

One can check that the denominator $\partial_q J \partial_B Q - \partial_B J \partial_q Q$ only vanishes when the charge parameter $q = 0$ or $q = 3jB$. However both Ω_{int} and Φ_{int} shall be well defined, except for the trivial case $m = 0$, upon substituting α and the mass $\mathscr{M}$ into their expressions.

Finally, by substituting α, Ω_{int} and Φ_{int} in the last equation, we obtain a first-order linear homogeneous partial differential equation for the total mass $\mathscr{M}$

$$\big[\mathscr{D} - M(4 + 9q^2 B^2) \partial_B \big] \mathscr{M} = 0, \tag{6.46}$$

where we defined the differential operator

$$\mathscr{D} = 2q(2j + 3qM^2 B) \partial_M + 2M(4j + 3q^3 B) \partial_q - 4Mq^2 (q - 3jB) \partial_j. \tag{6.47}$$

We reduced the integrability requirement for defining the mass to a single partial differential equation for the mass (6.46). Let us now solve it. First note that $B = 0$ is a regular point of the differential operator. Therefore, one has an analytic solution around $B = 0$,

$$\mathscr{M}(M, j, q, B) = \sum_{n \geq 0} f_n(M, j, q) B^n. \tag{6.48}$$

The differential equation requires a boundary condition at $B = 0$. We now impose

the physical requirement that the mass should coincide with the Kerr-Newman mass M in the absence of a magnetic field. Thus, we set $f_0(M,j,q) = M$. It can be shown that the ansatz (6.48) leads to an infinite series in the B expansion which we can solve exactly to each order in B. It turns out to be simpler to consider the expansion of the mass squared:

$$\mathscr{M}^2(M,j,q,B) = M^2 + \sum_{n\geq 1} g_n(M,j,q)B^n \tag{6.49}$$

The functions $g_n(M,j,q)$ must satisfy the following differential equation:

$$M(4+9q^2B^2)\sum_{n\geq 1} n g_n(M,j,q)B^{n-1} - \sum_{n\geq 1}\mathscr{D}[g_n(M,j,q)]B^n = 4Mq(2j+3qM^2B) \tag{6.50}$$

By collecting the terms order by order in the above equation, we get

$$g_1 = 2jq, \tag{6.51}$$

$$g_2 = \frac{1}{2M}\left(3M^3q^2 + \mathscr{F}[g_1]\right) = 2j^2 + \frac{3}{2}M^2q^2 - q^4, \tag{6.52}$$

$$g_n = \frac{1}{4nM}\Big[3Mq^2\big(-3(n-2)g_{n-2} + 2\mathscr{G}[g_{n-2}]\big) + 4\mathscr{F}[g_{n-1}]\Big], \tag{6.53}$$

where the differential operators $\mathscr{F}$ and $\mathscr{G}$ are defined as

$$\mathscr{F} = qj\partial_M - Mq^3\partial_j + 2Mj\partial_q, \tag{6.54}$$

$$\mathscr{G} = M\partial_M + 2j\partial_j + q\partial_q. \tag{6.55}$$

We would like to stress that the coefficients are uniquely determined, so that the mass $\mathscr{M}$ is unique. We can solve explicitly for the coefficients g_n. We observe that $g_n = 0 \quad \forall n \geq 5$. Thus, the solution (6.49) has the remarkable advantage of admitting a finite B expansion up to the fourth power in the parameter B

$$\begin{aligned}\mathscr{M}^2(M,j,q,B) = M^2 + 2jqB + \left(2j^2 + \frac{3}{2}M^2q^2 - q^4\right)B^2 + \\ + jq\left(2M^2 - \frac{3}{2}q^2\right)B^3 + \left(j^2M^2 - \frac{1}{2}j^2q^2 + \frac{1}{16}M^2q^4\right)B^4.\end{aligned} \tag{6.56}$$

This is, therefore, the unique mass of the Kerr-Newman black hole immersed in a back-reacting magnetic field. This answer agrees with the mass computed in Booth et al., 2015 by using the isolated-horizon formalism.[4] It disagrees with the other proposals in the literature.

[4] The published version of Booth et al. (2015) does not contain the explicit expression of the total mass. It is written in the unpublished second version of the preprint posted on ArXiv.

We checked that our total mass (6.56) reproduces the putative extreme limit in Eq. (6.29) proposed by Astorino (2015) and Bičák and Hejda (2015).

We conclude this section with another interesting observation about the total mass in Eq. (6.56). It is nothing but the Christodoulou-Ruffini mass originally derived for the Kerr-Newman black hole by Christodoulou and Ruffini, 1971 and given by

$$\mathscr{M}^2(S,J,Q) = \frac{S}{4\pi} + \frac{Q^2}{2} + \frac{\pi(Q^4+4J^2)}{4S}. \tag{6.57}$$

When expressed in terms of extensive quantities, the entropy S, the angular momentum J and the total electric charge Q, the total mass does not depend explicitly on the magnetic field parameter B.[5] This result is in agreement with the general proof of the first law that we shall give in section 6.5, where no additional δB term is present.

6.5 Thermodynamics of Magnetised-Kerr-Newman black holes

In this section, we prove the first law of black hole mechanics for MKN black holes by considering the integrable mass computed before.[6] Our proof only relies on the geometrical derivation of the first law and the integrability of the mass. The original proof of the first law was done for asymptotically flat space-times by Bardeen, Carter, and Hawking (1973). However, one readily generalizes it to any asymptotics using the definition of infinitesimal charge associated with canonical generators as done by Iyer-Wald in pure gravity using covariant phase space methods (Iyer and Wald, 1994) (this derivation was extended in Einstein-Maxwell theory by Rogatko (2002) and Gao (2003). We want to emphasize that there are no subtleties related to the presence of the magnetic field. Indeed, the metric is smooth and the gauge field is regular outside the black hole. In particular, in the following derivation, we have assumed that no magnetic monopole is present and we have used a gauge potential regular at the poles. In the presence of magnetic monopoles or dipoles where the gauge field is singular, subtleties in the geometrical derivation

[5] Though the Christodoulou-Ruffini mass was originally derived for the asymptotically flat Kerr-Newman black hole, the robustness of the formula can be checked for Kerr-Newman-AdS black holes (Caldarelli, Cognola, and Klemm, 2000) and for accelerating Reissner-Nordstrom black holes (Astorino, 2017).

[6] However, we will discuss alternative thermodynamics description of MKN space-time in section 6.6, where the mass is not integrable because the magnetic field is considered as an external source (Gibbons, Pang, and Pope, 2014).

of the first law are present and lead to an additional term (Copsey and Horowitz, 2006).

6.5.1 First law and Smarr formula for MKN black holes

The first law of black hole mechanics is essentially the expansion of the following conservation law

$$\int_{H^2} k_{(\xi,0)} = \int_{S^2} k_{(\xi,0)}, \tag{6.58}$$

where $\xi = \partial_t + \Omega_H \partial_\phi$ is the Killing generator of the black hole horizon and Ω_H is the angular velocity of the horizon. The equivalence is between the surface charge integrated over the spacelike section of the black hole horizon H^2 and over the sphere at infinity S^2, even though any sphere enclosing the horizon is equally valid for the argument.

At the horizon, the standard derivation of Bardeen, Carter, and Hawking (1973) and Iyer and Wald (1994) leads to

$$\int_{H^2} k_{(\xi,0)} = T_H \delta S + \Phi_+ \delta Q, \tag{6.59}$$

where the chemical potential T_H, associated to the entropy S, is the Hawking temperature. The Coulomb electrostatic potential at the horizon is defined as $\Phi_+ = -A_\mu \xi^\mu|_{r=r_+}$ and Q is the electric charge. We have computed Φ_+ in Eq. (6.25) and Q in Eq. (6.35) for the MKN space-time.

In order to develop the right-hand side of Eq. (6.58), it is necessary to identify which is the canonical symmetry parameter associated with the energy. In general, it is not $(\partial_t, 0)$. In other words, one needs to consider the most general symmetry generator $\alpha\left(\chi, \Phi\right)$, where $\chi = \partial_t + \Omega \partial_\phi$ is a Killing vector field and Φ is a gauge transformation parameter. Here, α, Ω and Φ are space-time constants, but they are functions of the phase space parameters. We can use the linearity of the definition of symmetry parameters and write the symmetry parameter as follows:

$$\alpha\left(\partial_t + \Omega_+ \partial_\phi, 0\right) = \alpha\left(\partial_t + \Omega_{int}\partial_\phi, \Phi_{int}\right) + \alpha\left((\Omega_+ - \Omega_{int})\partial_\phi, -\Phi_{int}\right). \tag{6.60}$$

Since the surface charge is linear in the symmetry parameter, Eq. (6.58) becomes

$$\int_{H^2} k_{\alpha(\xi,0)} = \int_{S^2} k_{\alpha(\chi,\Phi_{int})} + \int_{S^2} k_{\alpha((\Omega_+ - \Omega_{int})\partial_\phi, -\Phi_{int})}. \tag{6.61}$$

Using the following definitions,

$$\delta\mathscr{M} = \int_{S^2} k_{\alpha(\chi,\Phi_{int})}, \qquad \delta J = \int_{S^2} k_{(-\partial_\phi,0)}, \qquad \delta Q = \int_{S^2} k_{(0,-1)}, \tag{6.62}$$

Eq. (6.61) becomes

$$\alpha\,(T_H\delta S + \Phi_+\delta Q) = \delta\mathscr{M} - \alpha(\Omega_+ - \Omega_{int})\delta J + \alpha\Phi_{int}\delta Q, \tag{6.63}$$

from which we obtain

$$\delta\mathscr{M} = \alpha\Big(T_H\delta S + (\Omega_+ - \Omega_{int})\delta J + (\Phi_+ - \Phi_{int})\delta Q\Big) \tag{6.64}$$

which is the first law of black hole mechanics.

Under a change of frame, $t \to \tilde{t} = \Delta_t\, t$, $\phi \to \tilde{\phi} = \phi + \Delta\Omega\, t$ and a change of gauge $A \to \tilde{A} = A + d\lambda$ with $\lambda = -(\Delta A_t)\,t$ (leading to the total transformation $A_t \to \tilde{A}_{\tilde{t}} = \Delta_t^{-1}(A_t - \Delta\Omega A_\phi - \Delta A_t)$) the potentials appearing in the first law transform as

$$\begin{aligned}
T_H &\to T_H\Delta_t^{-1}, & \alpha &\to \alpha\Delta_t,\\
\Omega_+ &\to (\Omega_+ + \Delta\Omega)\,\Delta_t^{-1}, & \Omega_{int} &\to (\Omega_{int} + \Delta\Omega)\,\Delta_t^{-1},\\
\Phi_+ &\to (\Phi_+ + \Delta A_t)\,\Delta_t^{-1}, & \Phi_{int} &\to (\Phi_{int} + \Delta A_t)\,\Delta_t^{-1}.
\end{aligned} \tag{6.65}$$

Here $\Delta\Omega$, Δ_t and ΔA_t are space-time constants, but functions of the phase space parameters.[7] The last transformation law follows from the fact that the surface charge $k_{(\partial_t,0)}$ transforms under the large gauge transformation $A \to A + d\lambda$ generated by $\lambda = -\Delta A_t\, t$ as $\oint_S k_{(\partial_t,0)} \to \oint_S k_{(\partial_t,0)} - (\Delta A_t)\oint_S k_{(0,-1)}$, as described in Compère, 2007b. Therefore, one needs a compensating shift of Φ_{int} to preserve the symmetry generator which defines the mass. Therefore, it is natural to define the frame independent thermodynamic potentials:

$$T = \alpha T_H, \tag{6.66a}$$

$$\Omega = \alpha(\Omega_+ - \Omega_{int}), \tag{6.66b}$$

$$\Phi = \alpha(\Phi_+ - \Phi_{int}). \tag{6.66c}$$

Then, the first law (6.64) takes the standard textbook form:

$$\delta\mathscr{M} = T\delta S + \Omega\delta J + \Phi\delta Q. \tag{6.67}$$

[7] It is easy to realise that the canonical frame, *i.e.*, that frame in which the mass $\mathscr{M}$ is associated with $(\partial_{t_{can}},0)$ is reached with $\Delta_t = \alpha^{-1}$, $\Delta\Omega = -\Omega_{int}$ and $\Delta A_t = -\Phi_{int}$.

We then recognize the thermodynamic quantities T, Ω and Φ as the chemical potentials associated to S, J and Q, respectively. The first law (6.67) differs from the one presented in Gibbons, Pang, and Pope (2014), where there is an additional δB term. The discrepancy arises from the fact that their mass is not integrable for arbitrary variations of the magnetic field parameter B. We will comment about this tension in section 6.6.

Another relation among the black hole conserved charges is the Smarr formula. Let us review that the Smarr formula follows from the first law and Euler's theorem for homogeneous functions (see, *e.g.*, the excellent lecture notes of Townsend, 1997)).[8] The main observation, from Eq. (6.57), is that the mass squared is an homogeneous function of S, J, Q^2, because its variables have the same dimension, $[S] = [J] = [Q^2] = [mass^2]$ in geometric units ($G = c = 1$). Therefore, the mass $\mathscr{M}$ must be homogeneous of degree $n = 1/2$ and it fulfils the relation

$$\frac{1}{2}\mathscr{M} = \frac{\partial \mathscr{M}}{\partial S} S + \frac{\partial \mathscr{M}}{\partial J} J + \frac{\partial \mathscr{M}}{\partial Q^2} Q^2 . \tag{6.68}$$

After using $\frac{\partial \mathscr{M}}{\partial Q^2} Q^2 = \frac{1}{2}\frac{\partial \mathscr{M}}{\partial Q} Q$ and the first law (6.67), we get the Smarr formula

$$\mathscr{M} = 2TS + 2\Omega J + \Phi Q . \tag{6.69}$$

6.5.2 Thermodynamic potentials of MKN black holes

With the unique mass at hand, we obtain the expression of α from Eq. (6.43). It is given by

$$\alpha = \frac{M}{\mathscr{M}} . \tag{6.70}$$

We can then derive Ω_{int} and Φ_{int} from Eqs. (6.44) and (6.45). Their expressions are well defined except for the trivial case $m = 0$. When the magnetic field is turned off, we can check that we get $\alpha = 1$, $\Omega_{int} = 0 = \Phi_{int}$ as expected in an asymptotically flat space-time. The thermodynamic quantities defined in Eqs. (6.66) are

[8] Euler's theorem states that any homogeneous function of degree n of N variables, *i.e.*, such that $f(t\mathbf{x}) = t^n \mathbf{x}$, satisfies the relation $\sum_{i=1}^{N} x^i \frac{\partial f}{\partial x^i} = n f(\mathbf{x})$.

then explicitly given by

$$T = \alpha T_H = \Xi \frac{M}{\mathscr{M}} \frac{2}{A_+}(r_+ - M), \tag{6.71a}$$

$$\Omega = \alpha(\Omega_+ - \Omega_{int}) = \frac{1}{\Xi}\frac{J}{\mathscr{M}}\frac{1}{r_+^2 + a^2}, \tag{6.71b}$$

$$\Phi = \alpha(\Phi_+ - \Phi_{int}) = \frac{1}{\Xi}\frac{M}{\mathscr{M}} Q\left[\frac{r_+}{r_+^2 + a^2}\left(\frac{Q}{q}\right)^2 + \frac{M}{q^2}\left(\Xi - \frac{\mathscr{M}^2}{M^2}\right)\right]. \tag{6.71c}$$

The quantities r_+, T_H, Ω_+, Φ_+, A_+ have been computed at the end of section 6.3. For $B = 0$, we recover the well-known expressions of the Kerr-Newman black hole. We can also check that the thermodynamic potentials coincide with the ones derived from the Christodoulou-Ruffini mass (6.57):

$$T = \frac{\partial \mathscr{M}}{\partial S} = \frac{1}{8\pi\mathscr{M}}\left[1 - \frac{4\pi^2}{S^2}\left(J^2 + \frac{Q^4}{4}\right)\right], \tag{6.72a}$$

$$\Omega = \frac{\partial \mathscr{M}}{\partial J} = \frac{\pi J}{\mathscr{M} S}, \tag{6.72b}$$

$$\Phi = \frac{\partial \mathscr{M}}{\partial Q} = \frac{Q}{2\mathscr{M} S}(S + \pi Q^2). \tag{6.72c}$$

By construction, the first law (6.67) and the Smarr relation (6.69) are verified.

The magnetic field parameter B only appears implicitly in the thermodynamic quantities T, Ω and Φ. That means that the study of the thermodynamic stability against thermal or electric fluctuations is unchanged with respect to the Kerr-Newman black hole (Davies, 1977). For example, the expressions for the heat capacity and electric permittivity are identical as in the Kerr-Newman case in terms of explicit thermodynamic variables. In Fig. 6.2, we schematically emphasize that the magnetised Kerr-Newman and the Kerr-Newman black holes share the same thermodynamics away from the extreme limit (see Eqs. (6.72)), while they share the same near-horizon geometry at extremality (see Eqs. (6.28)).

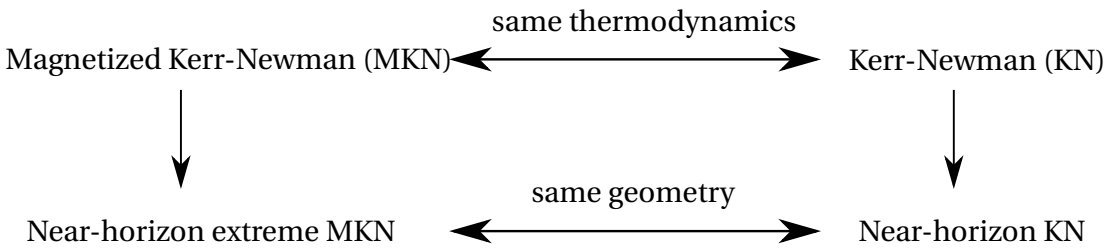

FIGURE 6.2: The magnetised Kerr-Newman and the Kerr-Newman share the same thermodynamics away from extremality and the same near-horizon geometry at extremality

6.6 Alternative thermodynamics: magnetic field as a source

If one allows for all physical quantities $(\mathscr{M}, Q, J, B)$ to be varied, the definition of mass is unique as we have shown. It matches with the mass computed using the isolated horizon formalism (Booth et al., 2015) and, at extremality, using the match with the near-horizon of the Kerr-Newman black hole (Astorino, 2015; Bičák and Hejda, 2015). This existence and uniqueness of the result suggests that the solution space of Melvin-Kerr-Newman metrics with arbitrary freely varying parameters constitutes a phase space with well-defined boundary conditions.

Now, alternative boundary conditions can lead to alternative definitions of the gravitational mass, as illustrated, *e.g.*, in the case of gravity coupled to scalar fields (Henneaux et al., 2007) with bare mass in the Breitenlohner-Freedman range which allows for various boundary conditions (Breitenlohner and Freedman, 1982). More precisely, one defines new quantities $\widetilde{\alpha}, \widetilde{\Omega}_{int}$ and $\widetilde{\Phi}_{int}$. The infinitesimal charge $\not{\delta}\mathscr{M}$ associated with the generator $\widetilde{\alpha}(\partial_t + \widetilde{\Omega}_{int}\partial_\phi, \widetilde{\Phi}_{int})$ is not integrable for arbitrary variations of the magnetic field B, but it can be written as

$$\not{\delta}\mathscr{M} = \delta\widetilde{\mathscr{M}} + \mu\delta B \tag{6.73}$$

The left-hand side of Eq. (6.73) is exactly the infinitesimal charge which can be deduced from Eqs. (6.34)-(6.35)-(6.36). Once $\widetilde{\mathscr{M}} = \widetilde{\mathscr{M}}(M, a, q, B)$ is fixed as a function of the parameters, μ is uniquely defined from Eq. (6.73). There are four unknown functions $\widetilde{\alpha}, \widetilde{\Omega}_{int}, \widetilde{\Phi}_{int}, \widetilde{\mathscr{M}}$ and three integrability conditions (6.39)-(6.40)-(6.42). There is, therefore, one free function, the mass, which should be fixed by independent considerations such as a boundary condition. A physical requirement is that the mass reduces to the Kerr mass in the absence of magnetic field, $\widetilde{\mathscr{M}} = M + \mathscr{O}(B)$. Otherwise, the mass is arbitrary with this method. Once the remaining function is fixed, one can compute μ from Eq. (6.73), which can be interpreted as a conjugate chemical potential for the magnetic field, *i.e.*, an induced magnetic dipole moment. Indeed, after using Eq. (6.73), the first law (6.67) reads as

$$\delta\widetilde{\mathscr{M}} + \mu\delta B = \widetilde{T}\delta S + \widetilde{\Omega}\delta J + \widetilde{\Phi}\delta Q, \tag{6.74}$$

where the tilded chemical potentials are defined as

$$\widetilde{T} = \widetilde{\alpha} T_H, \tag{6.75}$$

$$\widetilde{\Omega} = \widetilde{\alpha}(\Omega_+ - \widetilde{\Omega}_{int}), \tag{6.76}$$

$$\widetilde{\Phi} = \widetilde{\alpha}(\Phi_+ - \widetilde{\Phi}_{int}). \tag{6.77}$$

Since B has mass dimension $[mass]^{-1}$, the Smarr relation reads as

$$\widetilde{\mathscr{M}} = 2\widetilde{T}_H S + 2\widetilde{\Omega} J + \widetilde{\Phi} Q + \mu B. \tag{6.78}$$

As an intermediate summary, one can arbitrarily define the mass with the integrability procedure, up to the constraint of matching with M in the absence of magnetic field, and still get a consistent thermodynamics with first law and Smarr formula.

One such definition of mass was recently given in Gibbons, Pang, and Pope (2014) after using a Kaluza-Klein reduction to three dimensions. Its expression is given by

$$\mathscr{M}_{GPP} = \Xi M, \tag{6.79}$$

where the factor Ξ defined in Eq. (6.21) naturally appears in the regulation of the metric in order to avoid conical defects. Identifying $\widetilde{\mathscr{M}} = \mathscr{M}_{GPP}$ one can solve the three integrability conditions (6.39)-(6.40)-(6.42) with

$$\widetilde{\alpha} = 1, \tag{6.80}$$

$$\widetilde{\Omega}_{int} = \frac{B^3\left[160qM^2 + j(80M^2+76q^2)B + 8q(4j^2+31M^2q^2)B^2 + 3jq^2(44M^2+q^2)B^3\right]}{8\Xi M(4+9q^2B^2)}, \tag{6.81}$$

$$\begin{aligned}\widetilde{\Phi}_{int} = \frac{1}{16\Xi M(4+9q^2B^2)}\Big[&-384qM^2B^2 - 16j(16M^2+5q^2)B^3 - 16q(2j^2+53M^2q^2)B^4 \\ &+ 96jq^2(q^2-5M^2)B^5 + 8(-46M^2q^5 + qj^2(28M^2+43q^2))B^6 + \\ &+ j(-408M^2q^4 + 5q^6 + 32j^2(2M^2+11q^2))B^7 + 3q(32j^4 - 8j^2M^2q^2 + 5M^2q^6)B^8\Big].\end{aligned} \tag{6.82}$$

According to Eq. (6.73), this leads to the magnetic dipole moment

$$\mu = \Xi \frac{2q}{M}\frac{2j - 3BqM^2}{4+9B^2q^2}. \tag{6.83}$$

In the weak magnetic field approximation both $\widetilde{\Omega}_{int}$ and $\widetilde{\Phi}_{int}$ vanish, whereas μ approaches $\frac{jq}{M} \simeq \frac{JQ}{\mathscr{M}}$, which is the well-known magnetic dipole moment of a

charged stationary axisymmetric vacuum black hole space-time (Wald, 1974).

In summary, the mass proposed in Gibbons, Pang, and Pope (2014) leads to a consistent thermodynamics in the case where the magnetic field is considered as an external source. The definition $\mathscr{M}_{GPP}$ however does not match with the extremal mass (6.29) computed from the near-horizon matching (Astorino, 2015; Bičák and Hejda, 2015). We found that in all generality, integrability methods are ambiguous up to one arbitrary function which can be precisely identified with the mass. There is, therefore, a one-function family of consistent thermodynamics when the magnetic field is considered as an external source.

6.7 Discussion and conclusions

In this chapter, we have discussed the Kerr-Newman black hole immersed in an external magnetic field in the weak and strong regime. The exact analytical solution to the Einstein-Maxwell theory, known as Melvin-Kerr-Newman (MKN) space-time, has been presented and discussed. In particular, we focused on the effect of the external magnetic field on the conserved charges in the strong field regime. Though such a solution might not have a physical role in modelling an active galactic nucleus, we were motivated to study the MKN because of the open problem in defining its total mass and, consequently, its thermodynamics. Recent approaches have been made by means of dimensional reduction methods (Gibbons, Pang, and Pope, 2014), the isolated horizon formalism (Booth et al., 2015), and the covariant phase space formalism (Astorino et al., 2016). We extensively discussed the results presented in Astorino et al. (2016). We showed that the mass in Eq. (6.56), originally computed in Booth et al. (2015) (though not published in the final version of the paper), is the unique and integrable mass of the MKN black hole. To achieve this result, we first showed that the integrability condition leads to a partial differential equation of the first order in the parameters of the MKN solution. Then, by demanding that the mass is that of the Kerr-Newman when the magnetic field parameter vanishes, we obtained the unique solution to the integrability condition. Such an unique and integrable total mass correctly reproduces the extreme mass computed after matching the parameters of the near-horizon geometries of the extreme MKN and the extreme KN (Astorino, 2015; Bičák and Hejda, 2015). Additionally, we derived the first law of black hole thermodynamics for MKN (see Eq. (6.67)) when all the parameters of the phase space are allowed to vary. Consistently with the first law, we were able to write the total mass in terms of the thermodynamic variables (and without any explicit dependence on the magnetic field parameter) and we checked that it is equivalent to the the well-known

Christodoulou-Ruffini mass formula (6.57). Interestingly, we found that MKN and KN space-times share the same thermodynamics: this is a nontrivial relationship away from extremality, where the two space-times share the same near-horizon geometry. We also studied alternative thermodynamics, where the magnetic field is considered as an external source with no dynamics. Such alternative thermodynamics has a modified first law, given in Eq. (6.74), with an explicit term accounting for the variation of the external magnetic field. In this case, we found a consistent family of thermodynamics parametrised by an alternative mass. The latter is not anymore integrable. One such example is provided by the work of Gibbons, Pang, and Pope (2014).

We leave open the problem whether or not an alternative mass exists in this framework which matches with the Kerr mass in the absence of magnetic field and which also matches with the near-horizon extremal mass at extremality. The relationship between the mass formula and consistent boundary conditions for Melvin-Kerr-Newman space-times is also left open.

Chapter 7

Self-similar thin discs around near-extreme black holes

Contents

This chapter is based on Compère and Oliveri (2017), where a new research programme to investigate specific signatures of conformal symmetries in the high spin regime for accretion discs has been initiated. We start with an introduction in section 7.1. Then, we discuss a particular boundary condition imposed at the physical edge of the thin accretion disc; we comment the physical consequences of such a condition in the Novikov-Thorne model presented in chapter 3. In section 7.3, we study the Novikov-Thorne model with the above boundary condition and we derive new features of the accretion disc when the central black hole is rapidly rotating. Such new features open up the possibility to study the Novikov-Thorne accretion disc around the near-horizon region of a rapidly rotating black hole. The outcome of this analysis, discussed in section 7.4, is that the disc shows a critical-like behaviour dictated by the conformal symmetry of the underlying background geometry. We conclude the chapter with section 7.5.

7.1 Introduction

In this chapter, we exploit the emergent conformal symmetry of near-extreme black holes in their near-horizon region to find physical implications on thin accretion discs within the Novikov-Thorne model introduced in chapter 3. The model is analytical, based on falsifiable assumptions whose range of validity can be tested, and it only depends on four free parameters that include the phenomenological Shakura-Sunyaev α prescription for the viscosity. In particular, the model predicts a black-body thermal spectrum in the range $10^4 - 10^7$K which makes it suitable as a rough model of several classes of black hole binaries and luminous active galactic nuclei (see, *e.g.*, Koratkar and Blaes, 1999; McClintock, Narayan, and Steiner, 2014).

The original Novikov-Thorne model has the property that the torque vanishes at the ISCO (the physical edge of the accretion disc), which leads to an inconsistency of the model, because the radial fluid velocity diverges at the ISCO even though observables remain finite. This boundary condition has also been challenged by other considerations (Krolik, 1999; Gammie, 1999; Li, 2000; Noble, Krolik, and Hawley, 2010). Modelling physical boundary conditions at the ISCO is crucial in particular for highly spinning black holes in order to accurately calibrate their spin estimate (Li et al., 2005). In Penna, Sadowski, and McKinney (2012), a self-consistent boundary condition, hereafter called *"sonic-ISCO"*, was proposed, which consists in equating the radial co-moving fluid velocity at the ISCO with the sound speed. Two arguments were presented in its favour. First, in slim disc models around the Schwarzschild black hole analysed in Abramowicz et al. (2010), the sonic point asymptotes to the ISCO in the thin disc regime (where the accretion rate is sub-Eddington), independently of α. Secondly, the boundary condition implies that advection terms are negligible with respect to the stresses at the ISCO in the energy balance, in the limit where the disc height is negligible with respect to α. We will check that the latter assumption is self-consistent for typical stellar-mass black holes and luminous AGN parameters. A crucial consistency condition of thin discs is therefore satisfied. As we will discuss, the boundary condition also implies that the specific internal energy is negligible, which automatically enforces another hypothesis of the Novikov-Thorne model. In addition, we will show that the sonic-ISCO boundary condition allows for a well-defined near-horizon near-extreme scaling behaviour, in contrast to the no-torque boundary condition.

According to the cosmic censorship conjecture, the spin of the Kerr black hole

is bounded by its value at extremality. Extreme spinning black holes admit a near-horizon region with global conformal symmetry $SO(2,1)$, as has been discussed in chapter 1. Approaching the extreme bound by realistic accreting processes is, however, limited by the absorption cross-section of retrograde photons as shown by Thorne (1974), leading to the bound $J/M^2 < 99.8\%$. This bound is commonly accepted (see, *e.g.*, the recent work by Kesden, Lockhart, and Phinney, 2010), even though it can be lowered by magnetic fields (Gammie, Shapiro, and McKinney, 2004) or instead challenged (Sądowski et al., 2011). More fundamentally, for accretion disc models where the inner edge approaches the marginally bound orbit instead of the innermost stable orbit, the capture of retrograde photons asymptotes to zero, which allows spinning black hole to further approach extremality (Abramowicz and Lasota, 1980). Such scenarios have been shown to occur in slim disc models (Sądowski et al., 2011). It is therefore worthwhile to explore which specific signatures may arise in the extremely high spin regime, where conformal symmetry is only slightly broken.

A new feature emerges from our analysis. For highly spinning stellar-mass black holes, gas pressure at the ISCO becomes negligible with respect to radiation pressure. The sonic-ISCO boundary condition then implies that the accretion rate is not a free parameter of the model. Instead, the disc height at the ISCO is the fourth independent parameter. It allows us to infer a best-fitting value for the Shakura-Sunyaev parameter α in terms of the total luminosity, radiative efficiency and spin of the source. For example in the case of the X-ray binary source GRS 1915+105, recent estimates of the mass and spin, using the Very Long Baseline Array, give $M \sim 12 \pm 2\ \mathrm{M}_\odot$ and $J/M^2 = 0.98 \pm 0.01$ (Reid et al., 2014). Also, the best-fitting model of the *NuSTAR* observation of GRS 1915+105 in the plateau state gives a disc luminosity at $23\% \pm 4\%$ of the Eddington rate (Miller et al., 2013). Taking into account the torque contribution to the radiative efficiency of thin accretion discs (Li, 2002), we will infer that the best-fitting Novikov-Thorne model is a disc dominated by radiation around the ISCO with $\alpha = 0.43$ and $\dot{M} = 1.6 \times 10^{18} g\ sec^{-1}$.

7.2 Sonic-ISCO boundary condition

A physical system is determined by its equations of motion and its boundary conditions. In the original analysis of Novikov and Thorne (1973), it was assumed that there is no torque at the ISCO, located at $r = r_0$, which is equivalent to assume that there is no radiation at that point,

$$F(r_0) = 0, \tag{7.1}$$

which is also equivalent to fixing the integration constant $\mathscr{P}_0 = 0$ in Eq. (3.50).

Following Penna, Sadowski, and McKinney (2012), we impose instead that the radial fluid velocity in the frame co-rotating with the geodesic flow equals (minus) the sound speed at the ISCO,

$$c_s(r_0) = -u^{\hat{r}}(r_0). \tag{7.2}$$

This boundary condition has three important advantages that we will describe in what follows: firstly, it implies that the advection processes are negligible with respect to the dissipative and radiating effects; secondly, it reinforces the hypothesis that the specific internal energy can be neglected and, then, the boundary condition regularizes the original Novikov-Thorne model.

So far, we can rewrite the energy conservation equation as

$$Q_{diss} = Q_{cool} + Q_{adv}, \tag{7.3}$$

where $Q_{diss} = -S^{\mu\nu}\sigma_{\mu\nu}$ is the dissipation function, $Q_{cool} = q^{\mu}_{;\mu}$ is the cooling function and $Q_{adv} = \rho T u^{\mu} s_{,\mu}$ is the advection function that takes into account the rate of change of the specific entropy along the four-velocity. Now, as shown in Penna, Sadowski, and McKinney (2012), the boundary condition (7.2) implies the following scaling relations: $Q_{adv} \sim h^2$, $Q_{cool} \sim Q_{diss} \sim \alpha h$; so if $h \ll \alpha$, advection can indeed be neglected.

Thin disc models usually assume that the specific internal energy density is negligible $\Pi = 0$. This hypothesis is justified if the sound speed is non-relativistic, $c_s \ll 1$. Due to the gravitational potential, the sound speed is highest in the near-horizon region of the disc, where we will impose the boundary condition (7.2). The hypothesis $c_s \ll 1$ will therefore be obeyed as long as $|u^{\hat{r}}| \ll 1$ at the ISCO, which is already part of the hypotheses since we assumed that the fluid follows nearly circular geodesics. We will check that the solutions indeed obey $|u^{\hat{r}}| \ll 1$ and $c_s \ll 1$.

Finally, with the no-torque boundary condition, the disc model has no regular limit at the ISCO, as we will review below, while the boundary condition (7.2) regularizes the model.

Let us now fix the remaining integration constant $\mathscr{P}_0$ for the sonic-ISCO boundary condition. It will be fixed as a function of the disc height at the ISCO, h_0, as follows. The integral in the right-hand side of (3.50) is zero when evaluated at the ISCO. Thus, Eq. (3.50) reads as

$$\left(\frac{F}{\dot{M}}\right)_0 = -\frac{M\Omega_{,r}|_0 \mathscr{P}_0}{4\pi r_0 (E_0 - \Omega_0 L_0)^2}. \tag{7.4}$$

On the other hand, dividing equations (3.49) and (3.48), we get

$$\left(\frac{F}{\dot{M}}\right)_0 = \left(\frac{\sigma_{\hat{r}\hat{\phi}}W}{2\pi r\Sigma u^r}\right)_0 = -\frac{1}{\sqrt{2}}\frac{A_0}{4\pi r_0^4\Delta_0^{1/2}}\alpha h_0\gamma_0^2\mathscr{L}_{\star,0}\Omega_{,r}|_0. \tag{7.5}$$

In the second step, we have expressed the radial velocity component in the LRF, $u^r = (\Delta^{1/2}/r)u^{\hat{r}}$, we have substituted the definitions of Σ and W, we have used the Shakura-Sunyaev prescription and assumed the sonic-ISCO boundary condition (7.2), $u_0^{\hat{r}} = -\sqrt{p_0/\rho_0}$. Equating (7.4) and (7.5), we find

$$\mathscr{P}_0 = \frac{1}{\sqrt{2}}\frac{\alpha h_0}{M}\frac{A_0}{r_0^3\Delta_0^{1/2}}\gamma_0^2(E_0-\Omega_0 L_0)^2\mathscr{L}_{\star,0} = \frac{1}{\sqrt{2}}\alpha h_0 x_0\mathscr{D}_0^{1/2}\mathscr{R}_0^{1/2}, \tag{7.6}$$

after some algebra involving the functions defined in appendix B. Our final formula for $M\mathscr{P}_0$ disagrees with the constant C derived in Penna, Sadowski, and McKinney (2012), which is easily seen to be incorrect since it has the wrong dimension of length.

The physical meaning of the integration constant $\mathscr{P}_0$ is to introduce a torque at the ISCO. More precisely, the torque might be derived by comparison of Eq. (3.50) and Eq. (12) of Li (2002). The torque g_0 is then

$$g_0 = \frac{M\dot{M}\mathscr{P}_0}{E_0-\Omega_0 L_0}. \tag{7.7}$$

The total energy radiated per unit time as measured by an observer at infinity is therefore given by both an accretion and a torque contribution (Li, 2002)

$$\mathscr{L}_{tot} = \eta_0\dot{M} + g_0\Omega_0 \equiv \eta\dot{M}, \tag{7.8}$$

where $\eta_0 = 1 - E_0$ is the specific conserved energy of a particle orbiting along the ISCO (see Eqs. (B.9)) and η is the radiative efficiency of the disc

$$\eta = \eta_0 + \frac{g_0\Omega_0}{\dot{M}} = \eta_0\left(\frac{a}{M}\right) + \alpha h_0 g\left(\frac{a}{M}\right), \tag{7.9}$$

where

$$g\left(\frac{a}{M}\right) = 2^{-1/2}M\Omega_0(E_0-\Omega_0 L_0)^{-1}x_0\sqrt{\mathscr{D}_0\mathscr{R}_0} = 2^{-1/2}x_0^{-2}\mathscr{C}_0^{-1/2}\sqrt{\mathscr{D}_0\mathscr{R}_0}. \tag{7.10}$$

Here, we are ignoring the capture of radiation from the hole, which decreases the efficiency for high spin (Thorne, 1974).

7.3 Features of the general solution

We introduce the dimensionless mass and mass accretion rate

$$M_\star \equiv \frac{M}{3M_\odot}, \qquad \dot{M}_\star \equiv \frac{\dot{M}}{10^{17} g\, sec^{-1}}, \tag{7.11}$$

where $M_\odot$ is the mass of the Sun.

The global solution can be approximated by a piece-wise construction of three local solutions described in section 3.5, which are patched according to their range of validity. The qualitative features of the global solution depend upon the region that dominates at the ISCO. There are three possibilities depending which of the three relevant local solution is valid around the ISCO.

7.3.1 Gas-pressure-dominated ISCO

In the "standard" first two cases, the ISCO lies in the region dominated by gas pressure, either Region [Gas-es] or Region [Gas-ff] of section 3.5. The four free parameters of the model are $(M, a, \dot{M}, \alpha)$ and the disc height at the ISCO, h_0, is fixed. Indeed, if the ISCO lies in Region [Gas-es], we evaluate (3.55d) at the ISCO using Eq. (7.6). The result is

$$h_0 = \left(1.8\times 10^{-3}\right)\left(\alpha^{1/8} M_\star^{-3/8} \dot{M}_\star^{1/4}\right) x_0^{1/8} \mathscr{C}_0^{-1/8} \mathscr{R}_0^{-1/2}. \tag{7.12}$$

If the ISCO lies in Region [Gas-ff] instead, we evaluate (3.59d) at the ISCO using Eq. (7.6). The result is

$$h_0 = \left(1.3\times 10^{-3}\right)\left(\alpha^{1/17} M_\star^{-5/17} \dot{M}_\star^{3/17}\right) x_0^{5/17} \mathscr{C}_0^{-1/17} \mathscr{D}_0^{-1/34} \mathscr{R}_0^{-8/17}. \tag{7.13}$$

We checked that the hypothesis $h_0 \ll \alpha$ is obeyed at the ISCO in both cases (7.12) and (7.13) for the range $\alpha \sim 0.01 - 1$ and $a/M \sim 0 - 0.999$ and either $(M_\star, \dot{M}_\star) \sim (1,1)$ or $(M_\star, \dot{M}_\star) \sim (10^7, 10^5)$.

As explicit examples, the disc regions and their transitions are plotted in Figs 7.1 and 7.2 for the spin range $0 \le a \le 0.999M$ assuming $\alpha = 0.2$ for either $(M_\star, \dot{M}_\star) = (1,1)$ (modelling a stellar-mass black hole) and $(M_\star, \dot{M}_\star) = (10^7, 10^5)$ (modelling an AGN).

In Fig. 7.1, the first region in which the ISCO is located is called the *edge region*. There, the gas pressure overwhelms the radiation pressure and the opacity due to electron scattering is dominant over the free-free absorption. The disc height is given by Eq. (7.12). The transition to the *inner region* occurs when radiation pressure starts becoming predominant over the gas pressure. A new transition

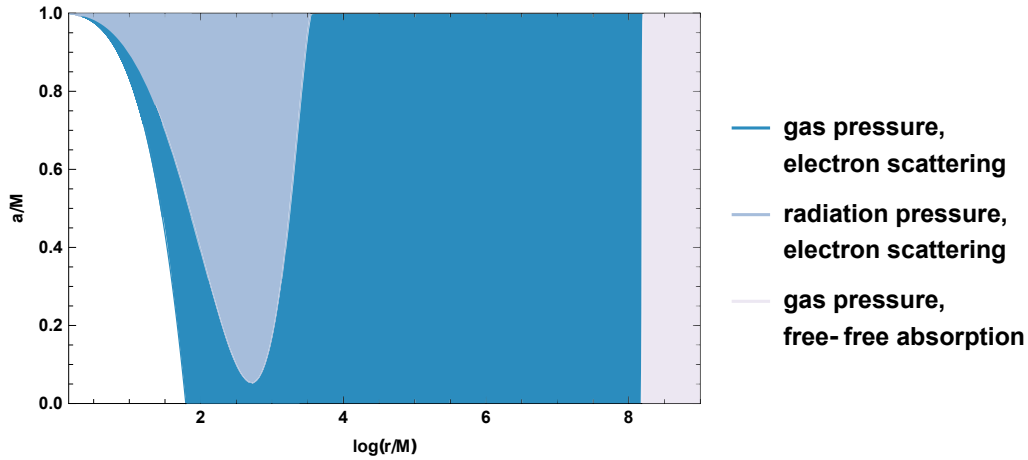

FIGURE 7.1: Disc regions for stellar-mass black holes with $(M_\star, \dot{M}_\star) = (1,1)$ and $\alpha = 0.2$ in the spin range $0 \leq a \leq 0.999M$.

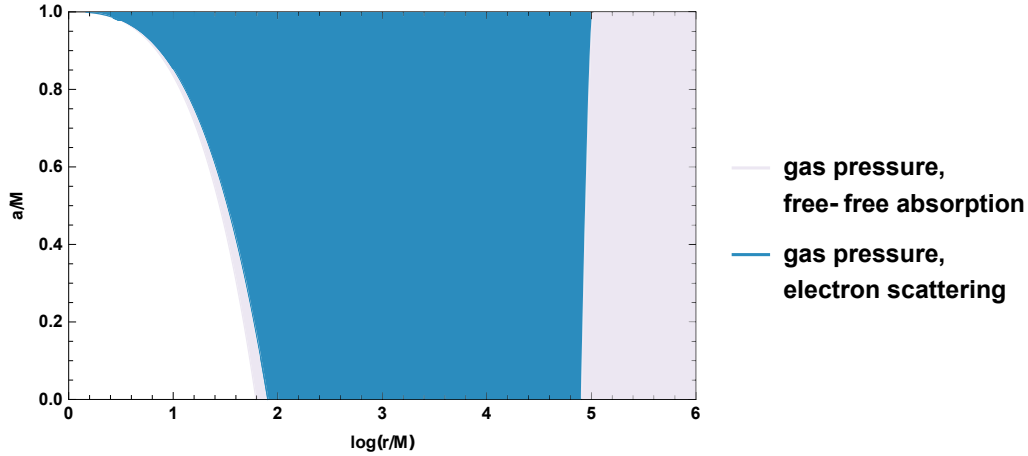

FIGURE 7.2: Disc regions for supermassive black holes with $(M_\star, \dot{M}_\star) = (10^7, 10^5)$ and $\alpha = 0.2$ in the spin range $0 \leq a \leq 0.999M$.

occurs when the gas pressure becomes dominant again over radiation pressure and the resulting region is called the *middle region*. For very low spins, the inner region is absent and the edge and middle regions merge. The *outer region* is still gas-pressure-dominated, but the main mechanism responsible for the opacity is the free-free absorption. We checked that the height satisfies $h \ll \alpha = 0.2$ for $r \ll 10^{13}M$ where the model breaks down for other reasons (because self-gravitation is not negligible). The temperature of the accretion disc is hotter in the region near the ISCO, and in general the temperature is higher for faster spin. By evaluating the temperature at the ISCO for $a = 0.999M$, we found $T \sim 10^7$K. This implies that the assumption of conservation of mass is valid. We also checked that the sound speed is negligible with respect to light speed, $c_s = \sqrt{p/\rho} \ll c$, in the entire disc.

The original Novikov-Thorne model did not contain the edge region, but it should contain it by consistency: for standard spins, the radiation pressure in the

inner region goes to zero at the ISCO and therefore the gas pressure needs to dominate at low enough radius. Yet, if one assumes the no-torque boundary condition, the Novikov-Thorne model is singular at the ISCO in the edge region. The reason is readily seen because in the [Gas-es] solution (3.55) the function $\mathscr{P}$ defined in Eq. (B.10) vanishes at the ISCO if $\mathscr{P}_0 = 0$, and the radial velocity is then divergent at the ISCO. The non-zero torque introduced by the sonic-ISCO boundary condition allows us to regulate the model as claimed earlier.

In Fig. 7.2, the disc is always dominated by gas pressure, but the dominant contribution to opacity varies with radius. In the *edge region*, where the ISCO lies, the free-free absorptions are dominant. The disc height is therefore given by Eq. (7.13). The *middle region* is dominated by electron scattering. The *outer region* is again dominated by free-free absorption. The assumption $h \ll \alpha = 0.2$ is obeyed for $r \ll 10^{21} M$ where the model breaks down. The accretion disc for supermassive black holes is colder with respect to the stellar-mass black holes; it never exceeds $T \sim 10^4$K and the conservation of mass is obeyed. We also checked that the sound speed is negligible with respect to light speed, $c_s \ll c$, in the entire disc.

7.3.2 Radiation-pressure-dominated ISCO

Let us now discuss the configurations where the ISCO lies in the region dominated by radiation pressure and electron scattering (Region [Rad-es] of section 3.5). This scenario happens for very high spins as we will discuss below. A new feature arises as a result of the sonic-ISCO boundary condition: a constraint relates the accretion rate $\dot{M}$, the mass, spin and α parameter, while the opening angle at the ISCO is unconstrained.

Indeed, the disc height (3.57d) in geometric units is given by

$$h = \frac{\bar{\kappa}_{es}}{2\pi} \frac{\dot{M}}{M} x^{-3} \mathscr{C}^{-1} \mathscr{R}^{-1} \mathscr{P}. \tag{7.14}$$

At the ISCO, $\mathscr{P}$ is given by $\mathscr{P}_0$ (see Eq. (B.10)) that can be evaluated using the expression for the sonic-ISCO boundary condition in Eq. (7.6). Therefore, h_0 appears linearly in both sides and we are left with a constraint among the parameters of the model given by

$$\frac{\alpha \bar{\kappa}_{es}}{4\pi} \frac{\dot{M}}{M} = \frac{1}{\sqrt{2}} x_0^2 \mathscr{C}_0 \mathscr{D}_0^{-1/2} \mathscr{R}_0^{1/2} \equiv f\left(\frac{a}{M}\right). \tag{7.15}$$

The function $f\left(\frac{a}{M}\right)$ monotonically decreases and vanishes at extremality.

It is instructive to compare the accretion rate in Eq. (7.15) with the Eddington accretion rate $\dot{M}_{Edd} = 4\pi M/(\bar{\kappa}_{es}\eta)$, where η is the radiative efficiency defined in

Eq. (7.9). We find the reduced accretion rate

$$\dot{m} \equiv \frac{\dot{M}}{\dot{M}_{Edd}} = \frac{\eta}{\alpha} f\left(\frac{a}{M}\right). \tag{7.16}$$

Since the α parameter is usually hard to estimate, it is useful to solve the relation (7.16) for α in terms of $\dot{m}$ using Eq. (7.9). The accretion rate is then determined from Eq. (7.15) and we obtain

$$\alpha = \frac{\eta_0 f}{\dot{m} - h_0 f g}, \qquad \dot{M} = \frac{4\pi M}{\eta_0 \bar{\kappa}_{es}} (\dot{m} - h_0 f g). \tag{7.17}$$

The free parameters of the model where the ISCO lies in a radiation-dominated region can be finally taken to be $(M, a, \dot{m}, h_0)$.

In the phase diagrams of both typical stellar-mass and supermassive black holes displayed in Figs 7.1 and 7.2, the gas pressure dominates at the ISCO for all standard spins. However, for sufficiently high spins, radiation pressure dominates as we will now show. Let us first discuss configurations where the ISCO lies in the Region [Gas-es] for standard spins such as the case studied in Fig. 7.1.

If one (wrongly) assumes that the ISCO lies in Region [Gas-es] for very high spins, one deduces from Eqs. (3.56a) and (7.12) that the ratio of pressures at the ISCO is

$$\left.\frac{p_{rad}}{p_{gas}}\right|_0 = \frac{\alpha \kappa_{es}}{2\sqrt{2}\pi} \frac{\dot{M}}{M} \frac{\sqrt{\mathscr{D}_0}}{\mathscr{C}_0 \sqrt{\mathscr{R}_0} x_0^2} = 0.27 \frac{\alpha \dot{M}_\star}{M_\star} \sigma^{-2/3} + \mathscr{O}(\sigma), \tag{7.18}$$

where in the last step we took the near-extreme scaling $a/M = \sqrt{1-\sigma^2}$. For $\sigma \ll 1$, one obtains that radiation pressure will instead dominate. In the example of $M_\star = \dot{M}_\star = 1$ and $\alpha = 0.2$, the transition occurs (in the sense that $p_{rad} = p_{gas}$) at $a/M = 0.99996$ which is much above the Thorne's bound of 0.998 (Thorne, 1974) and therefore much probably unrealistic.

If instead the ISCO lies in the Region [Gas-ff] for standard spins such as the case studied in Fig. 7.2, one deduces from Eqs. (3.60a) and (7.13) that the ratio of pressures at the ISCO is

$$\left.\frac{p_{rad}}{p_{gas}}\right|_0 = 0.02 \frac{\alpha^{8/17} \dot{M}_\star^{7/17}}{M_\star^{6/17}} \sigma^{-14/51} + \mathscr{O}\left(\sigma^{19/51}\right), \tag{7.19}$$

which is divergent for $\sigma \ll 1$. Again, radiation pressure dominates for sufficiently high spins and a new *near-ISCO region* opens up. However, for typical parameters $M_\star = 10^7$, $\dot{M}_\star = 10^5$ and $\alpha = 0.2$, the transition to the near region occurs at $a/M = 1 - 10^{-18}$ which is unreasonably high to be realistic.

However, there are more interesting parameters to consider. Let us take an accretion rate at 23% Eddington ($\dot{m} = 0.23$) as a model for the plateau state of GRS 1915+105 (Miller et al., 2013) with the spin estimate $J/M^2 = 0.98$ (Reid et al., 2014). Assuming a radiation-dominated ISCO, we can derive the α parameter using Eq. (7.17) after fixing an estimate for h_0. We checked that for any value $0 < h_0 < 0.01$, the resulting values of $\alpha = 0.43$ and $\dot{M}_\star = 16.5$ differ by 1% or less. The continuous transition between the gas-pressure- and radiation-dominated phases occurs at $a/M = 0.980 \pm 0.001$. For definiteness, we choose $h_0 = 0.002$, so that the transition exactly occurs at $a/M = 0.98$.

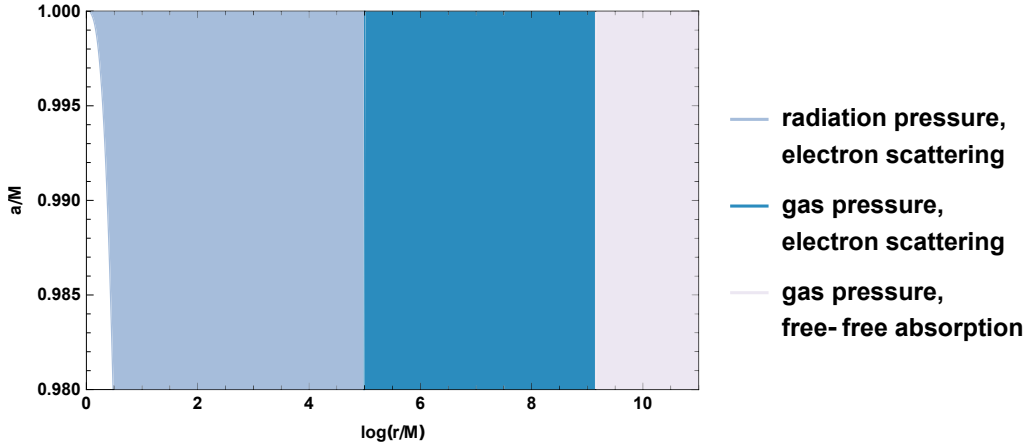

FIGURE 7.3: Disc regions for rapidly accreting highly spinning stellar-mass black hole with $M_\star = 4$, accretion rate at 23% of the Eddington limit and disc height at the ISCO $h_0 = 0.002$. The radiation-dominated region extends from the ISCO up to $r \sim 150M$.

We conclude that GRS 1915+105 could be modelled by a high spin $a/M > 0.98$ and rapidly accreting thin disc, which is radiation-dominated at the ISCO. As an example, we depict in Fig. 7.3 the phase diagram for the parameters $M_\star = 4$, $\dot{m} = 0.23$, $h_0 = 0.002$ and spins $0.98 < a/M < 1$. The *inner region* is radiation-dominated. At finite radius away from the ISCO, there is a transition to a *middle region*, which is gas pressure-dominated, but whose opacity is still dominated by electron scattering. There is also an *outer region* further away, where the main mechanism for opacity is free-free absorption.

7.4 Near-horizon near-extreme solution

In the near-extreme regime, a new space-time region, the NHEK region, opens up as explained in section 1.3, which is characterized by conformal symmetry. Since the radiation-dominated solution is the only one relevant in the limit of extremely

high spins, we will perform the near-extreme near-horizon limit of the solution (3.57) in order to exhibit its conformal properties.

We perform the scaling (1.13) with $a/M = \sqrt{1-\bar{\sigma}^2\lambda^3}$ and let $\lambda \to 0$. The ISCO is located at $R_0 = 2^{1/3}\bar{\sigma}^{2/3}$. The accretion rate $\dot{M}$ (in terms of asymptotic time) is constrained as in Eq. (7.15) which implies the scaling $\dot{M} \sim \lambda$. In terms of near-horizon time T, the accretion rate M' is finite,

$$M' = \frac{\partial t}{\partial T}\dot{M} = \frac{2M}{\lambda}\dot{M} = \pi\sqrt{6(7-\sqrt{3})}\frac{M^2}{\alpha\bar{\kappa}_{es}}R_0. \tag{7.20}$$

Therefore, contrary to the asymptotically flat observer, the NHEK observer measures a finite non-zero accretion rate M'. The ratio M'/R_0 is fixed by the parameters of the model.

The near-horizon behaviour of the solution (3.57) can be obtained by performing the near-extreme near-horizon scaling and trading $\dot{M}$ for M'. We get the following expressions at leading order, *i.e.*, $\mathcal{O}(\lambda^0)$:

$$F = \frac{7-\sqrt{3}}{4}\frac{h_0}{M\bar{\kappa}_{es}}\left(\frac{R_0}{R}\right)^2 = \left(2.0\times10^{26} erg/(cm^2 sec)\right)\left(h_0 M_\star^{-1}\right)\left(\frac{R_0}{R}\right)^2, \tag{7.21a}$$

$$\Sigma = \frac{3}{2}\frac{1}{\alpha h_0\bar{\kappa}_{es}}\left(\frac{R}{R_0}\right)^2 = \left(3.75 g/cm^2\right)\left(\alpha^{-1}h_0^{-1}\right)\left(\frac{R}{R_0}\right)^2, \tag{7.21b}$$

$$h = h_0\left(\frac{R_0}{R}\right)^2, \tag{7.21c}$$

$$u^R = -\sqrt{\frac{7-\sqrt{3}}{6}}\frac{h_0 R_0}{M}\left(\frac{R_0}{R}\right)^2 = \left(-6.3\times10^4/sec\right)\left(h_0 R_0 M_\star^{-1}\right)\left(\frac{R_0}{R}\right)^2, \tag{7.21d}$$

$$p = \frac{7-\sqrt{3}}{8}\frac{1}{\alpha M\bar{\kappa}_{es}} = \left(3.4\times10^{15} dyn/cm^2\right)\left(\alpha^{-1}M_\star^{-1}\right), \tag{7.21e}$$

$$\rho = \frac{3}{4}\frac{1}{M\alpha h_0^2\bar{\kappa}_{es}}\left(\frac{R}{R_0}\right)^4 = \left(4.21\times10^{-6} g/cm^3\right)\left(\alpha^{-1}h_0^{-2}M_\star^{-1}\right)\left(\frac{R}{R_0}\right)^4, \tag{7.21f}$$

$$T = \left(\frac{3(7-\sqrt{3})}{8\alpha b M\bar{\kappa}_{es}}\right)^{1/4} = \left(3.39\times10^7 K\right)\left(\alpha^{-1/4}M_\star^{-1/4}\right). \tag{7.21g}$$

All these quantities are defined for $R \geq R_0$. Note that all quantities, except p and T, depend on the ratio

$$\frac{R_0}{R} = \frac{\left[2\left(1-(a/M)^2\right)\right]^{1/3}}{x^2-1}, \tag{7.22}$$

which is independent of the choice of the constant $\bar{\sigma}$. The only exception is the radial component of the four-velocity, which has an additional power of R_0, and therefore depends on the position of the ISCO. Note one unusual property of the self-similar solution: starting from h_0 at the ISCO the disc height h *decreases* with the radius and it increases again outside of the range of validity of the self-similar

solution.

From Eqs. (7.21), and thanks to Eq. (1.21), we explicitly read off the critical exponents for thin accretion disc within the Novikov-Thorne model. In conclusion, one finds that the critical exponent h_O associated to the observable O is given by

$$h_F = h_h = h_{u^R} = 2, \qquad h_p = h_T = 0, \qquad h_\rho = -4. \tag{7.23}$$

As a final remark, we emphasise that the solution presented in Eqs. (7.21) is an analytic solution of thin accretion discs in NHEK space-time. It is the analogue of the analytic force-free solutions (5.102) and (5.103) in NHEK space-time presented in chapter 5. It worth mentioning that, while we do not know the exact solutions in Kerr space-time that originate (5.102) and (5.103), in this case we know that the Novikov-Thorne model with the sonic-ISCO condition in Kerr space-time gives rise to a well-behaved solution in NHEK space-time.

7.4.1 Approaching the self-similar solution

The self-similar solution is an approximate solution of the disc around the ISCO. It is worth discussing quantitatively its range of validity. The critical temperature does not depend upon the accretion rate $\dot{M}$ or the height of the disc h_0. Since α or M are overall factors of the temperature profile (3.57h), the relative error between the actual temperature profile and the constant critical temperature only depends upon the radius and the spin. We find that for near-extreme spins $0.96 \leq a/M \leq 1$, the actual temperature profile deviates from the critical temperature by less than 25% only in the range $r_0 \leq r \leq 2.1 - 2.2M$, where the upper bound is nearly independent of the spin. This very limited *near-ISCO region* is the region where the disc is approximately described by the self-similar solution. The region is biggest when the ISCO approaches M, which occurs closest to extremality. If a higher precision is required, the region of validity shrinks accordingly. We plot in Fig. 7.4 the range of validity of the temperature of the self-similar solution with 25%, 15% and 10% relative precision.

Other physical quantities can be analysed similarly. Unfortunately, the relative precision of the pressure requires a spin higher than the Thorne bound $a/M = 0.998$ and a narrower region around the ISCO, as plotted in Fig. 7.5.

Another important physical quantity is the radiation flux F. Fig. 7.6 shows that the range of validity of the self-similar solution is limited to a narrow region around the ISCO. The physical relevance of the self-similar solution (7.21) is therefore uncertain.

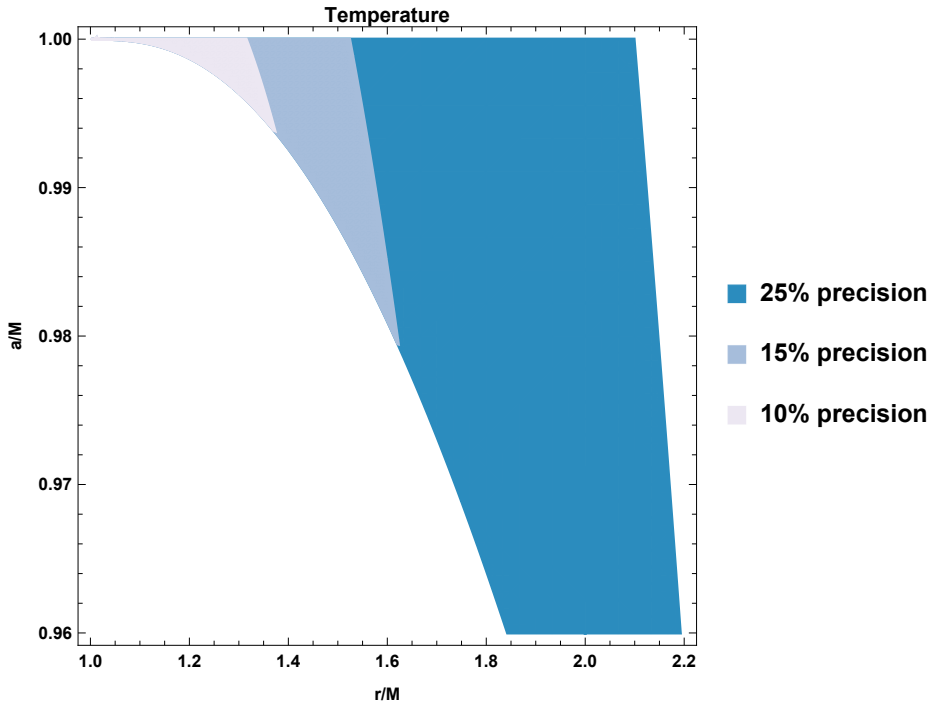

FIGURE 7.4: Relative precision of the self-similar critical temperature with respect to the actual temperature profile in the radiation-dominated region around the ISCO as a function of the spin. The relative precision is independent of other parameters of the model.

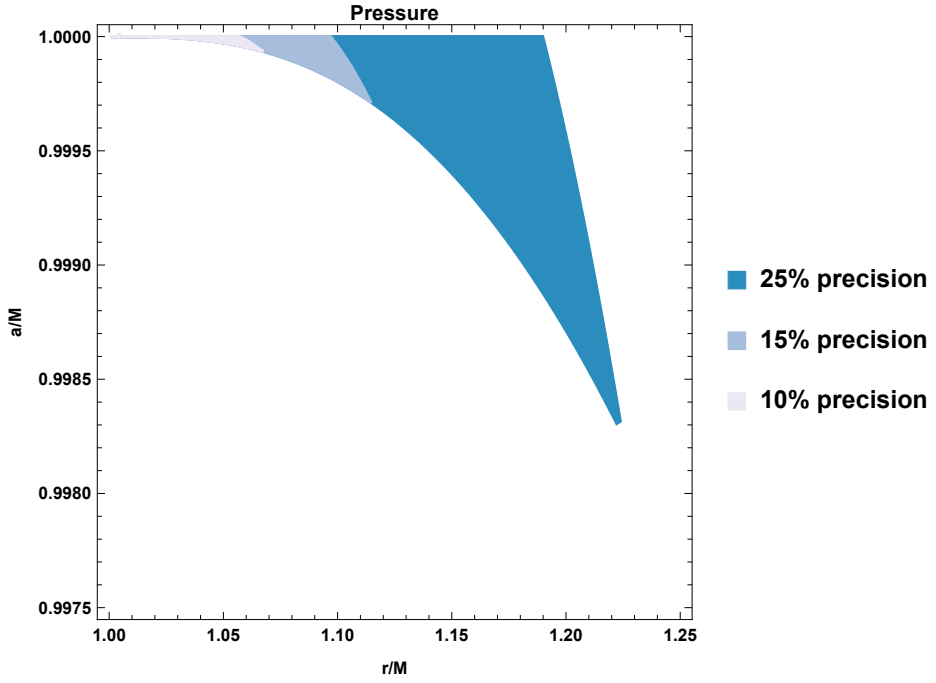

FIGURE 7.5: Relative precision of the self-similar critical pressure with respect to the actual pressure profile in the radiation-dominated region around the ISCO as a function of the spin. The relative precision is independent of other parameters of the model.

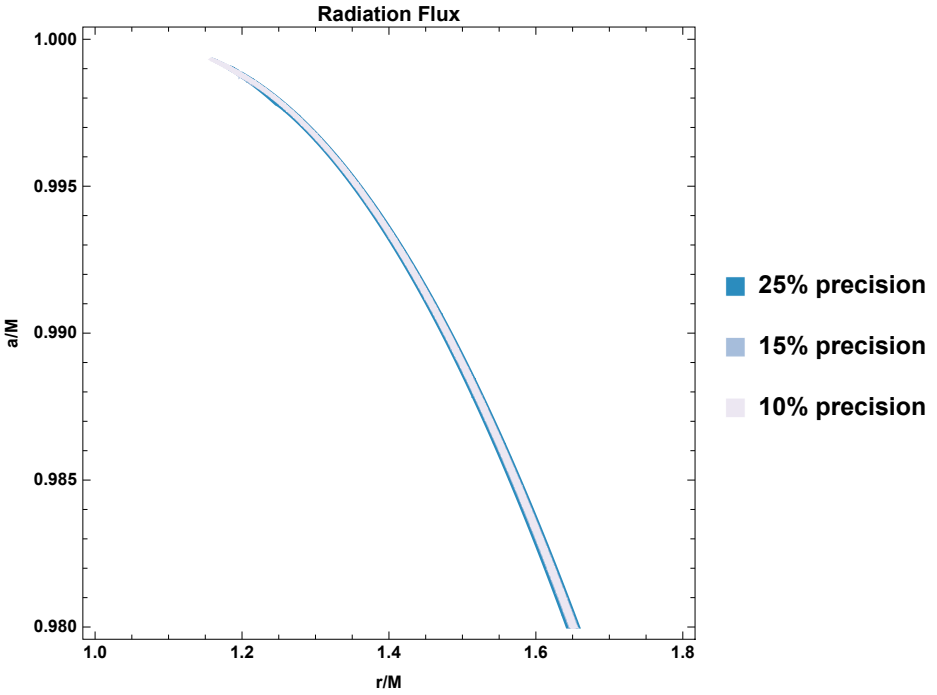

FIGURE 7.6: Relative precision of the self-similar critical radiation flux with respect to the actual radiation flux profile in the radiation-dominated region around the ISCO as a function of the spin for $h_0 = 0.002$, $\dot{m} = 0.23$. The auxiliary parameter α is fixed through Eq. (7.17). The relative precision is independent of the mass, because it factors out upon substituting the accretion rate (7.17) into Eq. (3.57a) and taking the ratio with Eq. (7.21a).

7.5 Discussion and conclusions

In this chapter, we considered the Novikov-Thorne thin accretion disc model around a rapidly rotating Kerr black hole.

First, we refined the self-consistent boundary condition at the innermost stable circular orbit (ISCO), originally proposed by Penna, Sadowski, and McKinney (2012). Such a boundary condition plays a crucial importance, because it regularises the Novikov-Thorne model at the ISCO, and it is a key ingredient for the results obtained in the chapter. We constructed piece-wisely the global solution from the local solutions to the Novikov-Thorne model and, for the first time in the literature, we explicitly showed the phase diagrams of thin accretion discs for stellar-mass and supermassive black holes. We observed a novel phase transition close to the ISCO in the high spin regime from the gas-dominated-pressure to the radiation-dominated-pressure phase[1]. As a consequence of the model in that regime, we found a new feature: the accretion rate is not a free parameter and it

[1] It is well-known that thin accretion discs with the α-viscosity prescription suffer from thermal and viscous instabilities in the radiation-dominated phase (Lightman and Eardley, 1974; Shibazaki

can be expressed in terms of the spin, the Shakura-Sunyaev viscosity parameter and the radiative efficiency.

Motivated by this result, we considered rapidly rotating black holes and investigated the effects of emergent conformal symmetries on the dynamics of matter discs orbiting around them. Then, by computing the near-horizon limit of the Novikov-Thorne model in the high spin regime, we showed how conformal symmetry constrains finite observables and we found a novel self-similar radiation-dominated solution. Finally, we discussed the critical-like behaviour of the accretion disc, dictated by the conformal symmetries of the background geometry in the near-horizon region, and we quantitatively studied its range of validity. This self-similar solution is a first example of critical accretion around a near-extreme black hole, which admits scale invariance in a region close to the ISCO.

More elaborated models are required to find more realistic solutions and make contact with observations. In the thin accretion disc, the inner edge is set at the ISCO. However, the inner edge of the accretion disc is placed within few Schwarzschild radii from the compact object (Bromley, Miller, and Pariev, 1998). In general, its location depends on the accretion rate, the viscosity, the presence of magnetic fields, the thickness of the disc and other physical effects. Several definitions of inner edge have been proposed in Krolik and Hawley (2002) and Abramowicz et al. (2010) to probe accretion physics in the strong gravity regime. This analysis has been carried out for Schwarzschild black hole in Abramowicz et al. (2010). It is important to generalise these results in the case of Kerr black holes (or other astrophysically motivated black hole solutions to modified gravity (see, *e.g.*, Johannsen, 2013, for an early attempt), as the inner edge sits closer to the compact object than ISCO, magnifying strong gravity effects in the electromagnetic spectrum. Moreover, a better theoretical knowledge of the inner edge will help our understanding of phenomena, like QPOs and iron Kα lines, occurring in the inner region of accretion discs, that serve as test of Einstein's gravity (see, *e.g.*, Bambi (2017) and references therein) or modified theories of gravity in the strong field regime (Maselli et al., 2015; Zhang et al., 2017).

and Hoshi, 1975; Shakura and Sunyaev, 1976). Such instabilities have also been observed in numerical simulations (see, *e.g*, Mishra et al., 2016). See also the recent review by Ciesielski et al. (2012) and references therein.

Chapter 8

Gravitational multipole moments from Noether charges

Contents

This chapter deals with the results published in Compère, Oliveri, and Seraj (2018), where a new way to compute gravitational multipole moments is presented. We introduce the results in section 8.1. In section 8.2, we define the canonical harmonic gauge independently of field equations and, after an overview of several concepts of symmetries, we find the multipole symmetries. In section 8.3, we compute the canonical charges associated to multipole symmetries for non-linear stationary configurations in Einstein gravity and relate them to the multipole moments of the source. In section 8.4, we discuss radiating geometries at the

linearised level. We express the multipole moments as Noether charges and we derive their conservation equation. We conclude with several avenues for further research in section 8.5.

8.1 Introduction

In this chapter, we provide a definition of *mass* and *current multipole moments* for an arbitrary generally covariant theory of gravity. Such a new definition agrees, in the case of Einstein gravity, with Thorne's definition of source multipole moments both for outgoing-wave linearised configurations and for stationary non-linear configurations introduced in chapter 4.

Our programme is achieved by defining multipole moments from the canonical Noether charges associated with specific residual symmetries of canonical harmonic gauge. First, we will characterize the infinitesimal form of three sets of *large coordinate transformations* that preserve the canonical harmonic gauge and that generalize the Poincaré algebra of Killing symmetries. The vector fields generating these transformations will be denoted *multipole symmetries*. Given an arbitrary generally covariant Lagrangian, one can define surface charges associated with an arbitrary vector field using either covariant phase space methods (Iyer and Wald, 1994) or cohomological methods (Barnich and Brandt, 2002; Barnich and Compère, 2008). The explicit expressions are summarized in appendix E.4 for General Relativity and in Iyer and Wald (1994); Compère, Murata, and Nishioka (2009); Azeyanagi et al. (2009) for a large class of higher curvature gravity theories coupled to bosonic matter. We will provide expressions for the gravitational multipole moments in terms of the canonical multipole charges, and find precise agreement with Thorne's definitions, up to a choice of normalisation. This will allow us to calibrate our definition, which then straightforwardly extends to a general theory.

The multipole symmetries are generically *outer symmetries*: they are not tangent to the phase space defined by the boundary conditions (*i.e.*, the Lie derivative of the metric with respect to these symmetries do not fall off sufficiently fast), except for the lowest harmonic modes which form the Poincaré algebra. Yet, these symmetries are associated with well-defined conserved Noether charges at spatial infinity, as we will show.

In the radiative case, the conservation equation will be used to relate the variation of source multipole moments, evaluated in the near-zone region, to the flux of multipole charges at null infinity, by means of the *generalized Noether theorem* for gauge theories (Wald, 1993; Barnich, Brandt, and Henneaux, 2000; Barnich and

Brandt, 2002). The flux of multipole charges is not the observable radiative multipole moments encoded in the Bondi news tensor. Instead, it is the time variation of the source multipole moments which is encoded in sub-leading components of the metric in radiation (Bondi) gauge.

Our construction extends to gravity theories the analysis of electromagnetic multipole charges in Maxwell theory, recently studied by Seraj (2016).

8.2 Harmonic gauge and residual transformations

8.2.1 Prelude on symmetries in gravity and gauge theories

It is by now a well know fact that gauge transformations exhibit novel features on manifolds with (asymptotic or finite) boundaries. This effect is sometimes interpreted as the spontaneous breaking of gauge invariance by the boundary conditions. More precisely, while the local gauge transformations are degeneracies of the pre-symplectic form of the theory and are hence quotiented out in the physical phase space (Lee and Wald, 1990), those with support at the boundary are not degeneracies and form vector fields acting on the phase space. These "asymptotic symmetries" are required to generate Hamiltonian vector fields on the phase space whose generators are finite and conserved quantities. In other words, the boundary conditions require that all canonical charges associated with asymptotic symmetries be finite, conserved and integrable in the sense of Regge and Teitelboim (1974) and Iyer and Wald (1994). When these conditions are met, one obtains, after quotienting by local gauge symmetries, the asymptotic symmetry group (ASG), *i.e.*

$$\text{ASG} = \frac{\text{Boundary conditions preserving gauge transformations}}{\text{Local gauge transformations}}.$$

For asymptotically flat space-times, the asymptotic symmetry group at spatial infinity is the BMS group, consisting of super-translations and Lorentz transformations, which contains the Poincaré group as a subgroup[1]:

- Asymptotic symmetries $\simeq$ BMS symmetries $\supset$ Poincaré symmetries.

Now, one may find Hamiltonian vector fields that are *not* tangent to the phase space, but still associated with finite, conserved and integrable canonical charges

[1] See, *e.g.*, (Arnowitt, Deser, and Misner, 1959; Bondi, van der Burg, and Metzner, 1962; Sachs, 1962; Regge and Teitelboim, 1974; Ashtekar and Hansen, 1978; Blanchet and Damour, 1992; Christodoulou and Klainerman, 1993; Barnich and Troessaert, 2010; Compere and Dehouck, 2011; Barnich and Troessaert, 2011; Virmani, 2012; Strominger, 2013; Troessaert, 2018) and references therein for a better account of the huge literature on the topic.

on the phase space. We call *phase space symmetries* the coordinate transformations that are associated with finite, conserved and integrable canonical charges on the phase space. The phase space symmetries contain the asymptotic symmetries and other symmetries that violate the boundary conditions, which we call *outer symmetries*:

$$\text{Phase space symmetries} = \text{Asymptotic symmetries} \cup \text{Outer symmetries}.$$

In geometrical terms, the boundary conditions impose a set of constraints which determine the phase space as a submanifold in the space of field configurations (further quotiented by local gauge transformations). The asymptotic symmetries then generate vector fields tangent to this constraint submanifold and their corresponding canonical charges are functions on the phase space. However, there is still the possibility of Hamiltonian vector fields that are not tangent to the phase space, but such that their canonical charges *are* functions on the phase space. This is another way to say that outer symmetries violate the boundary conditions, but are associated with finite and integrable charges.

We will not attempt at a rigorous analysis of the mathematical framework for describing outer symmetries. Instead, we will discuss how this concept is useful in gravity: we will show that the two sets of multipole moments of Einstein gravity are precisely associated with particular phase space symmetries. We call these *multipole symmetries* which form a natural extension of the Poincaré generators, distinct from the BMS symmetries:

- Phase space symmetries $\supset$ Multipole symmetries $\supset$ Poincaré symmetries.

Since the multipolar structure of a metric configuration defines a hierachical subleading structure at spatial infinity, the multipole symmetries form in compensation a fine-tuned overleading hierarchy, such that the resulting canonical charges are finite. The lowest multipolar modes are the Poincaré symmetries, while the higher modes are outer symmetries that violate the boundary conditions.

Several other examples of outer symmetries have recently appeared in electromagnetism (Campiglia and Laddha, 2016; Seraj, 2016) and in gravity (Compère and Long, 2016; Mirbabayi and Simonović, 2016; Conde and Mao, 2017b) (see also an alternative perspective in Conde and Mao (2017a); Mao and Wu (2017)).

8.2.2 Residual transformations of the harmonic gauge

We work in harmonic gauge, discussed previously in section 4.3. As we have fixed the harmonic gauge (4.2), the gauge transformations of the theory reduce to the

residual transformations of harmonic gauge. It can be shown that an infinitesimal diffeomorphism $x^\mu \to x^\mu + \xi^\mu$ respecting harmonic gauge (4.2) solves the equation

$$\Box_g \xi^\mu = 0. \tag{8.1}$$

We further restrict the phase space and, accordingly, the harmonic vector fields (8.1) to those preserving the following asymptotic behaviour of the lapse and shift at spatial infinity

$$g_{0\mu} = \eta_{0\mu} + \mathcal{O}(1/r). \tag{8.2}$$

However, since we are considering outer symmetries, we do *not* enforce the vector fields to preserve the boundary conditions $g_{ij} = \mathcal{O}(1/r)$ on the spatial components. At this step of our procedure, we break Lorentz covariance by explicitly choosing an asymptotic time foliation and therefore a notion of asymptotic observer at rest. Our reasoning herebelow will not depend upon the boundary conditions at future or past null infinity (see later on Eq. (8.27)).

Setting $\mu = 0$ in (8.2) implies that $\partial_0 \xi^0 = \mathcal{O}(1/r)$, hence

$$\xi^0 = \epsilon(\mathbf{x}) + \mathcal{O}(1/r). \tag{8.3}$$

Setting $\mu = i$ in (8.2), we find

$$\xi^\mu = \Big(\epsilon(\mathbf{x})\,,\, \chi^i(\mathbf{x}) + t\,\eta^{ij}\partial_j \epsilon(\mathbf{x})\Big) + \mathcal{O}(1/r). \tag{8.4}$$

The de Donder gauge condition (4.2) now amounts to

$$\nabla^2 \epsilon(\mathbf{x}) = 0, \qquad \nabla^2 \chi_i(\mathbf{x}) = 0, \tag{8.5}$$

where $\nabla^2 = \eta^{ij}\partial_i\partial_j$ is the spatial Laplacian operator. The harmonic function ϵ admits two branches of solutions: either of the form $r^{-(l+1)}Y^{lm}(\theta,\phi)$ or $r^l Y^{lm}(\theta,\phi)$ in terms of spherical harmonics. The first set are gauge transformations that we discard. We, instead, consider the sum of *regular solid scalar harmonics* $r^l Y^{lm}(\theta,\phi)$

$$\epsilon(r,\theta,\phi) = \sum_{l=0}^{\infty} \sum_{m=-l}^{l} \epsilon_{lm} r^l Y_{lm}(\theta,\phi), \tag{8.6}$$

where ϵ_{lm} are arbitrary coefficients. The function can also be expanded in Cartesian harmonics

$$\epsilon = \sum_{l=0}^{\infty} \epsilon_{A_l} \mathcal{X}_{A_l} = \epsilon_0 + (\epsilon_x x + \epsilon_y y + \epsilon_z z) + \epsilon_{ij}\left(x^i x^j - \frac{x^2}{3}\delta^{ij}\right) + \cdots \tag{8.7}$$

This expression defines the monopole term ($l = 0$), dipole term ($l = 1$), quadrupole term ($l = 2$) and so on. Our notation and conventions are relegated to appendix E.1 and properties of spherical harmonics are summarized in appendix E.2.

The intuitive idea for defining multipole symmetries is that a vector of components of order r^l will be able to probe terms of order r^{-l} in the metric, and therefore, allow to define the l-multipole. The harmonic equation ensures that there is a correlation between the radial behaviour r^l of the components of the vector field and the spherical harmonic Y^{lm}. Thanks to the orthogonality of spherical harmonics, it will allow to single out the corresponding multipole; see also the discussion around Eq. (8.16).

In the vector case, a general harmonic is a linear combination of three pure gauge transformations, which we discard, and three large gauge transformations of the form (see appendix E.3.2 for details)

$$\boldsymbol{\chi} = \chi^i \partial_i = \boldsymbol{r} \times \nabla \epsilon_1(\mathbf{x}) + \nabla \epsilon_2(\mathbf{x}) + \boldsymbol{V}(\mathbf{x}), \tag{8.8}$$

where $\nabla\epsilon = \eta^{ij}\,\partial_i\epsilon\,\partial_j$ and $\times$ denotes the cross product defined in three-dimensional flat space. The functions ϵ_1, ϵ_2 are combinations of regular solid scalar harmonics and $\boldsymbol{V}$ defined in (E.44), is a combination of irreducible vector harmonics which cannot be expressed in terms of one harmonic scalar. However, we discard this vector since the associated charge does not contain any non-trivial information in Einstein theory, as discussed below equation (E.50). However, it might be relevant for a general theory of gravity, as discussed in section 8.5.

In summary, we define the *multipole symmetries* as the three sets of residual transformations:

$$K_\epsilon = \epsilon\,\partial_t + t\,\nabla\epsilon\,, \tag{8.9a}$$

$$L_\epsilon = -\boldsymbol{r} \times \nabla\epsilon\,, \tag{8.9b}$$

$$P_\epsilon = \nabla\epsilon\,. \tag{8.9c}$$

These symmetries can be expanded in terms of scalar and vector spherical harmonics (introduced in E.2.2) as

$$K_\epsilon = \sum_{l=0}^{\infty}\sum_{m=-l}^{l} \epsilon_{lm}\left[r^l Y_{lm}\partial_t + t\, r^{l-1}\left(\sqrt{l(l+1)}\,{}^E Y^i_{lm} + l\,{}^R Y^i_{lm}\right)\partial_i\right], \tag{8.10a}$$

$$L_\epsilon = -\sum_{l=1}^{\infty}\sum_{m=-l}^{l} \epsilon_{lm}\sqrt{l(l+1)}\, r^l\,{}^B Y^i_{lm}\partial_i, \tag{8.10b}$$

$$P_\epsilon = \sum_{l=1}^{\infty}\sum_{m=-l}^{l} \epsilon_{lm}\, r^{l-1}\left(\sqrt{l(l+1)}\,{}^E Y^i_{lm} + l\,{}^R Y^i_{lm}\right)\partial_i. \tag{8.10c}$$

Upon expanding in Cartesian harmonics (8.7) or, equivalently, in *real* spherical harmonics Y_l^m defined in (E.11), we find the Poincaré algebra as the $l = 0, 1$ subset of harmonics of the three vectors K_ϵ, L_ϵ, P_ϵ. To show this, let us expand the harmonic function ϵ in terms of the real spherical harmonics and define ${L_l}^m = L_{\epsilon = r^l Y_l^m}$ and similarly ${K_l}^m$, ${P_l}^m$. Then, it can be checked that

Rotations The $SO(3)$ rotations are generated by the $(l = 1, m)$ modes of L_ϵ

$${L_1}^1 = y\partial_z - z\partial_y = L_x, \tag{8.11a}$$

$${L_1}^{-1} = z\partial_x - x\partial_z = L_y, \tag{8.11b}$$

$${L_1}^0 = x\partial_y - y\partial_x = L_z, \tag{8.11c}$$

where the last equality in each line refers to the Cartesian expansion (8.7) (*i.e.*, $L_x = L_{\epsilon = x}$), which also coincides with the standard notation for generators of rotation. We fixed the sign convention in (8.9b) so that $L_z = +\partial_\phi$ with $\epsilon_{r\theta\phi} = +1$, which is the opposite convention than Iyer and Wald (1994).

Boosts The $(l = 1, m)$ modes of K_ϵ give the Poincaré boosts

$${K_1}^1 = x\partial_t + t\partial_x = K_x, \tag{8.12a}$$

$${K_1}^{-1} = y\partial_t + t\partial_y = K_y, \tag{8.12b}$$

$${K_1}^0 = z\partial_t + t\partial_z = K_z. \tag{8.12c}$$

Translations The $l = 0$ mode of K_ϵ gives the translation in time

$${K_0}^0 = \partial_t, \tag{8.13}$$

while the $(l=1,m)$ modes of P_ϵ give spatial translations

$$P_1^{\ 1} = \partial_x = P_x, \tag{8.14a}$$

$$P_1^{-1} = \partial_y = P_y, \tag{8.14b}$$

$$P_1^{\ 0} = \partial_z = P_z. \tag{8.14c}$$

All vectors that are distinct from the standard Poincaré vectors are outer symmetries. Note that, contrary to the $l=0,1$ vectors, they do not generate a closed algebra under the Lie bracket. We leave as an open problem to determine whether an algebra of multipole symmetries exists using a modified bracket, along the lines of Seraj and Bleeken, 2017. The various vectors and their physical interpretation are summarized in Table 8.1.

The terminology of mass and current multipole symmetries is standard and will be clear once we compute the conserved charges associated with these transformations in the next sections. We will name the multipoles associated with P_{lm} as the momentum multipoles. We will interpret these multipoles in sections 8.3 and 8.4.

	$l=0$	$l=1$	$l\geq 2$
K_{lm}	Time translation	Boosts	Mass multipole symmetries
L_{lm}	$\varnothing$	Rotations	Current multipole symmetries
P_{lm}	$\varnothing$	Spatial translations	Momentum multipole symmetries

TABLE 8.1: Multipole symmetries and the Poincaré algebra

8.2.3 Canonical harmonic gauge: revisited and extended

As shown by many authors and briefly discussed in chapter 4, the definition of multipole moments is ambiguous in harmonic gauge. Here, we will further fix the gauge in order to uniquely fix the multipole moments. Since our aim is to derive a definition of multipole moments for *any* theory of gravity, we cannot rely on properties of Einstein solutions in order to determine the gauge fixing conditions (see Thorne, 1980, and section 4.3.1 in the case of linearised General Relativity). Instead, we will only rely on the harmonic decomposition of tensor representations of $SO(3)$.

For that purpose, we decompose the field $\mathfrak{g}^{\mu\nu}$ in $SO(3)$ scalar, vector and tensor, respectively, $\mathfrak{g}^{00}$, $\mathfrak{g}^{0i}$, $\mathfrak{g}^{ij}$. We only consider non-linear metrics which can be obtained from a perturbative construction starting from a linearised metric

$g_{\mu\nu} = \eta_{\mu\nu} + h_{\mu\nu}$. At the linearised level, the field $\mathfrak{g}^{\mu\nu} = \gamma^{\mu\nu} + \mathcal{O}(h^2)$ is the trace-reversed metric perturbation, $\gamma^{\mu\nu} = \eta^{\mu\alpha}\eta^{\nu\beta}h_{\alpha\beta} - \frac{1}{2}\eta^{\mu\nu}\eta^{\alpha\beta}h_{\alpha\beta}$.

A gauge transformation acts as $h_{\mu\nu} \mapsto h_{\mu\nu} + \partial_\mu\xi_\nu + \partial_\nu\xi_\mu$ and therefore as

$$\gamma_{\mu\nu} \mapsto \gamma_{\mu\nu} + \partial_\mu\xi_\nu + \partial_\nu\xi_\mu - \eta_{\mu\nu}\partial_\alpha\xi^\alpha, \tag{8.15}$$

where all indices are lowered with the flat metric.

As explained by Thorne (1980), the symmetric trace-free (STF) harmonic tensor decomposition is the most adapted to describe the multipolar structure of the gravitational field. Indeed, remember that the very definition of multipole moments originates from a STF decomposition or, equivalently, a spherical harmonic decomposition in canonical harmonic gauge. Conceptually, we aim to deduce the definition of some lm-multipole moment M^{lm} from a projection of the metric using a vector $\xi[\epsilon]$ depending on a scalar harmonic $\epsilon = \epsilon_{lm}$. Schematically,

$$M^{lm} \sim \langle \xi[\epsilon], g_{\mu\nu} \rangle. \tag{8.16}$$

The projection operator $\langle\cdot\rangle$ will be soon defined in Eq. (8.20) and in Eqs. (8.25)-(8.33) as particular integrals over the sphere. Here, we simply note that the multipole moments will be extracted from the metric thanks to the property of orthogonality of spherical harmonics or, equivalently, of the STF tensors. Therefore, it is computationally simpler to consider the STF decomposition of the metric.[2]

In Thorne's analysis, however, the linearised Einstein's equations were used. Here, we simply generalize his considerations to a general STF decomposition without resorting to field equations. The general linearised metric can be decomposed in STF tensors as (see appendix E.1 for notations)

$$\begin{aligned}
\gamma_{00} &= \partial_{A_l}\mathcal{A}_{A_l}(u,r) \\
\gamma_{0i} &= \partial_{A_{l-1}}\mathcal{B}_{iA_{l-1}}(u,r) + \partial_{pA_{l-1}}\left(\epsilon_{ipq}\mathcal{C}_{qA_{l-1}}(u,r)\right) + \partial_{iA_l}\mathcal{D}_{A_l}(u,r) \\
\gamma_{ij} &= \delta_{ij}\partial_{A_l}\mathcal{E}_{A_l}(u,r) + \partial_{A_{l-2}}\mathcal{F}_{ijA_{l-2}}(u,r) + \partial_{pA_{l-2}}\left(\epsilon_{pq(i}\mathcal{G}_{j)qA_{l-2}}(u,r)\right) + \\
&+ \left[\partial_{jA_{l-1}}\mathcal{H}_{iA_{l-1}}(u,r) + \partial_{jpA_{l-1}}\left(\epsilon_{ipq}\mathcal{N}_{qA_{l-1}}(u,r)\right)\right]^S + \partial_{ijA_l}\mathcal{K}_{A_l}(u,r),
\end{aligned} \tag{8.17}$$

[2] Yet, one might think to perform the same projection operation by using another decompositions such as the SVT (scalar-vector-tensor) decomposition used in cosmological perturbation theory.

where all coefficients are functions of r and $u = t - r$. The de Donder gauge fixes the constraints

$$\mathcal{B}_{A_l} = \dot{\mathcal{A}}_{A_l} - \nabla^2 \mathcal{D}_{A_l}, \tag{8.18a}$$

$$\mathcal{E}_{A_l} = \dot{\mathcal{D}}_{A_l} - \frac{1}{2}\mathcal{H}_{A_l} - \nabla^2 \mathcal{K}_{A_l}, \tag{8.18b}$$

$$\mathcal{F}_{A_l} = \ddot{\mathcal{A}}_{A_l} - \nabla^2 \dot{\mathcal{D}}_{A_l} - \frac{1}{2}\nabla^2 \mathcal{H}_{A_l}, \tag{8.18c}$$

$$\mathcal{G}_{A_l} = 2\dot{\mathcal{C}}_{A_l} - \ddot{\mathcal{N}}_{A_l}, \tag{8.18d}$$

where dots denote time derivatives. For retarded harmonic fields, which therefore obey linearised Einstein's equations, all functions $\mathcal{A}_{A_l}(u,r), \mathcal{B}_{A_l}(u,r), \ldots$ take the form $\frac{1}{r}\mathcal{A}_{A_l}(u)$, $\frac{1}{r}\mathcal{B}_{A_l}(u)$, etc. We assume that all such functions are $\mathcal{O}(1/r)$ in general as a result of asymptotically flat boundary conditions.

A generic retarded harmonic vector field, which preserves the asymptotically flat boundary conditions, can be used to further gauge fix the de Donder gauge to the canonical harmonic gauge (see Eq. (8.9b) of Thorne, 1980, and Eq. (E.52) for its explicit expression in spherical harmonics). One can use this vector field to remove the $1/r$ components of $\mathcal{D}_{A_l}(u,r), \mathcal{H}_{A_l}(u,r), \mathcal{N}_{A_l}(u,r), \mathcal{K}_{A_l}(u,r)$, which leads to

$$\{\mathcal{D}_{A_l}(u,r), \mathcal{H}_{A_l}(u,r), \mathcal{N}_{A_l}(u,r), \mathcal{K}_{A_l}(u,r)\} = \mathcal{O}\left(\frac{1}{r^2}\right). \tag{8.19}$$

In Einstein gravity, these functions are then exactly zero (see the discussion at the end of section 4.3.1), but they may be non-zero in alternative theories of gravity. We further apply a Lorentz boost and a spatial translation to put the system in the centre of mass frame, leading to $\mathcal{A}_i = \mathcal{O}(r^{-2})$. This defines the canonical harmonic gauge in the linearised theory.

In the non-linear theory, one computes at each perturbative order the next metric perturbation up to a linearised diffeomorphism. We fix the linearised diffeomorphism ambiguity in this expansion (of the form $\partial_\mu \xi_\nu + \partial_\nu \xi_\mu - \eta_{\mu\nu}\partial_\alpha \xi^\alpha$) by cancelling again the same coefficients in the radial harmonic decomposition of $\mathfrak{g}^{\mu\nu}$. Non-linearities will introduce additional radial subleading terms for each STF tensor harmonic which will not be gauged fixed. Only the leading $1/r$ terms in the radial expansion of each STF tensor harmonic will be gauge fixed. This defines the canonical harmonic gauge for the non-linear theory.

The resulting asymptotic expansion of the non-linear field in STF tensor harmonics has been presented explicitly for Einstein gravity in Thorne (1980) and Blanchet and Damour (1986).

8.3 Multipole charges for stationary solutions

In the following, we will present our definition of mass and current multipole moments in terms of Noether charges, which are defined with respect to the vectors fields (8.9) and the Lagrangian. We will explicit our definition only for vacuum Einstein solutions which will allow us to verify the complete equivalence to Thorne's definition. This allows us to calibrate our definition. Now, given an arbitrary generally covariant Lagrangian, we propose to define the multipole moments as the Noether charges associated with the very same vector fields (8.9). This provides a precise canonical definition of gravitational multipole moments for any generally covariant theory.

The canonical charge of a solution $g_{\mu\nu}$ associated with the vector field ξ^μ is defined as a surface integral over a sphere and as an integral in phase space from the reference solution (here Minkowski $\eta_{\mu\nu}$) to the solution $g_{\mu\nu}$ (Regge and Teitelboim, 1974; Iyer and Wald, 1994; Barnich and Brandt, 2002; Barnich and Compère, 2008)

$$Q_\xi[g] = \frac{1}{8\pi G}\int_\eta^g \int_S \mathbf{k}_\xi[dg'; g']. \tag{8.20}$$

The 2-form $\mathbf{k}_\xi$ is linear in its first argument and non-linear in its second argument. It can be constructed from the Lagrangian, up to an ambiguous term proportional to $\mathscr{L}_\xi g_{\mu\nu} = \nabla_\mu \xi_\nu + \nabla_\nu \xi_\mu$. There are two covariant prescriptions that exist in the literature to fix this ambiguity. We find convenient to label the surface charge by the parameter α multiplying the covariant ambiguous term. For $\alpha = 0$, one has the Iyer-Wald charge (Iyer and Wald, 1994). For $\alpha = 1$, one has the Abbott-Deser (Abbott and Deser, 1982) or, equivalently, the Barnich-Brandt charge (Barnich and Brandt, 2002). Such an ambiguity enters the normalisation factor and might me eliminated by a careful rescaling of the vector field ξ. We keep α in the future computation and we emphasise that the choice with $\alpha = 1$ only depends on the equations of motion of the Lagrangian. The explicit expression for the surface charge in Einstein gravity is given in appendix E.4.

Let us now evaluate the surface charge at spatial infinity for each of the three families of vector fields defined in (8.9). We first compute the spherical harmonic decomposition of each vector field. Let us discuss the (l)pole symmetries. We note that all subleading $(l+k)$pole moments in (4.14) $(k \geq 1)$ do not contribute to the charges. This non-trivial property originates from the orthogonality of spherical harmonics, and the fact that the subleading $(l+k)$pole moments are suppressed by negative powers of r with respect to the leading (l)pole moment of order $r^{-(l+1)}$. It can be checked by explicitly evaluating the charge. Since all non-linearities belong to such terms, only linear terms matter. The surface charge at spatial infinity can

be equivalently defined using the linearised theory as

$$Q_\xi[h] = \lim_{r\to\infty}\left(\frac{1}{8\pi G}\int_S \mathbf{k}_\xi[h;\eta]\right), \tag{8.21}$$

where $h_{\mu\nu}$ is the linear perturbation around $\eta_{\mu\nu}$ in the post-Minkowskian expansion of $g_{\mu\nu}$. The proof that all subleading monopole terms do not contribute to the definition of multipole moments was essentially performed in Thorne (1980). It also shows that any change of coordinates which preserves the canonical harmonic gauge does not change the definition of multipole moments.

8.3.1 Mass multipole charges

The mass multipole charges are associated to the multipole symmetries K_ϵ. They read as

$$Q_K^{lm} = \frac{2(2l+1)!!}{l!} I^{lm}. \tag{8.22}$$

Note that the result is independent of the α prescription. Here I^{lm} is the harmonic coefficient of the multipole moment $\mathcal{I}_{A_l}$ in Eq. (4.14).

8.3.2 Current multipole charges

The current multipole charges are associated to the multipole symmetries L_ϵ. They read as

$$Q_L^{lm} = -\sqrt{\frac{l}{l+1}}\frac{(2l-1)!!}{(l-1)!}\left(2(l+2)+\alpha(l-1)\right) S^{lm}. \tag{8.23}$$

The normalization constant depends upon the definition of the canonical charges through the α prescription. Here S^{lm} is the harmonic coefficient of the multipole moment $\mathcal{S}_{A_l}$ in Eq. (4.14).

8.3.3 Momentum multipole charges

The momentum multipole charges are identically zero for stationary configurations,

$$Q_P^{lm} = 0. \tag{8.24}$$

There is no role to the momentum multipole charges in stationary Einstein gravity, but we expect that they might play a role in stationary configurations in other theories of gravity.

Equations (8.22)-(8.23)-(8.24) are the main result of this section. Thorne's definition and the Noether charge definition agree up to a unique and well-defined normalization constant.

Let us make some additional comments. In the linear case, it turns out that the surface charge can be evaluated at any radius and yet gives the identical answers (8.22)-(8.23)-(8.24). This is due again to the orthogonality of spherical harmonics and the fact that, in the linear theory, each harmonic mode is associated with a particular radial falloff. The multipole symmetries generating such charges are therefore *symplectic symmetries* in the linear theory in the terminology of Compère et al. (2015); Compère et al. (2016).

A natural question is whether the charges associated with the multipole symmetries are affected by a change of gauge. In this thesis, we did not investigate a generic change of gauge. Instead, we investigated the change of gauge from canonical harmonic gauge to generic mass-centred de Donder gauge in the linearised theory. The details are relegated to appendix E.4.2. The result is that for linear stationary configurations, the current and momentum multipole charges $Q^{lm}_{L_\epsilon}$, $Q^{lm}_{P_\epsilon}$ are *unaffected* by a change of gauge which preserves stationarity within de Donder gauge, while the mass multipole charges $Q^{lm}_{K_\epsilon}$ are affected, but only by gauge transformations of the form $\mathbf{x} \to \mathbf{x} + \nabla\epsilon$ with $\nabla^2\epsilon = 0$, $\epsilon = O(r^{-1})$.

The conclusion is that the current multipole moments can be computed in *any* mass-centred de Donder gauge coordinate system. This is very useful in practice since work is only needed to reach de Donder gauge, but it is not necessary to further restrict to canonical harmonic gauge. However, the mass multipole moments need to be defined in the canonical harmonic gauge, or at least in mass-centred de Donder gauge where the gauge transformations $\mathbf{x} \to \mathbf{x} + \nabla\epsilon$ have been fixed according to the canonical prescription. This illustrates the gauge dependence in the definition of mass multipole moments.

8.4 Multipole charges for linearised radiating solutions

In this section, we turn our attention to dynamical radiating solutions in the linearised regime. We introduce the multipole charges at spatial infinity as conserved surface charges, while the source multipole moments are expressed in terms of surface charges in the near zone region. We will discuss the relation between these two and the implications of conservation laws for the time variation of the source multipole moments. We expect that the results for the linear theory can be extended to the non-linear theory essentially in the same way as discussed in the last section, but this problem is beyond the scope of this thesis.

The covariant phase space charges are defined in the linear theory as (Regge and Teitelboim, 1974; Iyer and Wald, 1994; Barnich and Brandt, 2002; Barnich and Compère, 2008)

$$Q_\xi[h] = \frac{1}{8\pi G}\int_S \mathbf{k}_\xi[h;\eta], \tag{8.25}$$

where $\eta_{\mu\nu}$ is the Minkowski background and $h_{\mu\nu}$ the perturbation. The precise definition of the 2-form $\mathbf{k}_\xi$ is given in appendix E.4.

We now compute the Noether charges associated with the three sets of residual symmetries L_ϵ, K_ϵ and P_ϵ presented in (8.9). The explicit values of the charges evaluated on a sphere at arbitrary retarded time u and radius r are given by the following expressions

$$8\pi G\, Q_L^{lm} = \sum_{p=0}^{l+1} C_L(p,l)\; r^{p\;(p)}S^{lm}(u), \tag{8.26a}$$

$$8\pi G\, Q_K^{lm} = \sum_{p=0}^{l+1} C_K(p,l)\; r^{p\;(p)}I^{lm}(u) + 8\pi G\, t\, Q_P^{lm}, \tag{8.26b}$$

$$8\pi G\, Q_P^{lm} = \sum_{p=0}^{l} C_P(p,l)\; r^{p\;(p+1)}I^{lm}(u). \tag{8.26c}$$

The coefficients $C_L(p,l)$, $C_K(p,l)$, $C_P(p,l)$ are given in appendix E.4.1. These charges are not well defined as such and require further insight in order to extract their physical content. We will discuss these charges in detail in the following.

We will first define the *conserved multipole charges* at spatial infinity. We then define the *source multipole moments*. We finally define the *radiation multipole moments* at null infinity as derived quantities.

8.4.1 Conserved multipole charges at spatial infinity

Let us first assume stationarity at past of null infinity, in the sense that

$$I^{lm}(u) = I^{lm} + \mathcal{O}\left(\frac{1}{u}\right), \qquad u\to-\infty, \tag{8.27a}$$

$$S^{lm}(u) = S^{lm} + \mathcal{O}\left(\frac{1}{u}\right), \qquad u\to-\infty. \tag{8.27b}$$

We expect that we can relate these asymptotic conditions to the behaviour of the Bondi news and Bondi mass (Christodoulou and Klainerman, 1993). These conditions imply that at spatial infinity (*i.e.*, in the limit $r\to\infty$ at fixed $t = r+u$),

$$\lim_{\substack{t\ \text{fixed}\\ u\to-\infty}} r^{p\,(p)}I^{lm}(u) = 0 = \lim_{\substack{t\ \text{fixed}\\ u\to-\infty}} r^{p\,(p)}S^{lm}(u), \qquad \forall\, p\geq 1. \tag{8.28}$$

This follows from $r^{p\,(p)}I^{lm}(u) \sim u^{p\,(p)}I^{lm}(u) \sim \mathscr{O}(1/u)$ for $p \geq 1$.

Under this asymptotic stationarity hypothesis, the finite stationary multipole charges (8.22)-(8.23)-(8.24) are recovered at spatial infinity. These are the conserved multipole charges.

8.4.2 Source multipole moments in the near-zone

As we can see explicitly, the surface charges (8.26) are finite in the $r \to 0$ limit. This limit has a clear physical interpretation and gives the value of the surface charges in the near zone of the radiation zone. Indeed, one has in general that (see, *e.g.*, section IX.D of Thorne, 1980)

$$\left|\frac{r^{p\,(p)}S^{lm}}{S^{lm}}\right| \sim \left|\frac{r^{p\,(p)}I^{lm}}{I^{lm}}\right| \sim \left(\frac{r}{\lambda}\right)^p, \tag{8.29}$$

where λ is the typical wavelength of the radiation generated by the sources. Accordingly, in the near zone where $r \ll \lambda$, we have

$$Q = Q\Big|_{r=0} + \mathscr{O}\left(\frac{r}{\lambda}\right), \tag{8.30}$$

and all charges are finite. Moreover, all multipole moments are then functions of time t since $u = t$ at $r = 0$. In the post-Newtonian/post-Minkowskian matched asymptotic expansion scheme to solve Einstein's equations for a radiating nonlinear system, there exist surface integrals defined in terms of the sources in the outer near-zone (Blanchet, Damour, and Iyer, 2005). Here, we will obtain the corresponding matching surface charges in the near-zone of the radiation region, in the linear approximation. We will now explicitly describe which Noether charges give the source mass multipole moments $I^{lm}(t)$ and current multipole moments $S^{lm}(t)$.

Current multipole moments The current multipole moments are simply defined as the Noether charges associated with L_ϵ (8.9) in the near zone. Their values are

$$Q_L^{lm}\Big|_{r=0} = -\sqrt{\frac{l}{l+1}}\frac{(2l-1)!!}{(l-1)!}\left(2(l+2)+\alpha(l-1)\right)S^{lm}(t). \tag{8.31}$$

The numerical proportionality coefficient depends upon the detailed definition of the canonical charge through the α prescription.

Momentum multipole moments The momentum multipole moments are defined as the Noether charges associated with P_ϵ (8.9) in the near zone. Their values

are

$$Q_P^{lm}\Big|_{r=0} = -\frac{2(2l-3)!!}{l!}\left((2l-1)l+(1-\delta_{1l})\sqrt{\frac{l}{l+1}}\left[1+(3-2l)l+\alpha(l-1)(2l+1)\right]\right)\,{}^{(1)}I^{lm}(t). \tag{8.32}$$

Contrary to the stationary case, they are non-zero for radiating configurations. They are derived quantities in terms of the mass multipole moments I^{lm} and are therefore not fundamental, at least in Einstein gravity. They will however play a role in the definition of mass multipole moments as we describe next.

Mass multipole moments Finally, the mass multipole moments are defined as the following combination of Noether charges in the near zone,

$$Q_K^{lm}\Big|_{r=0} - t\,Q_P^{lm}\Big|_{r=0}. \tag{8.33}$$

After evaluation we find

$$Q_K^{lm}\Big|_{r=0} - t\,Q_P^{lm}\Big|_{r=0} = \frac{2(2l+1)!!}{l!}I^{lm}(t), \tag{8.34}$$

which exactly reproduce Thorne's definition $I^{lm}(t)$, upon adjusting the normalization constant. Remark that both the Iyer-Wald and the Abbott-Deser-Barnich-Brandt definitions agree in this case since there is no α dependence in the numerical coefficient.

The linear combination in the definition (8.33) can be explained very naturally in two different ways. First, the definition (8.33) is covariant under a time shift. The time dependence of the generator K_ϵ (8.9) is exactly compensated by the subtracting term in (8.33) and a time shift only shifts the source. More fundamentally, the definition (8.33) generalizes to gravitating configurations and to generic mass multipole moments the definition of boost charge defined in standard field theories around Minkowski space-time. For example, the Noether current of a scalar field of Lagrangian $\mathscr{L} = -\frac{1}{2}\partial_\mu\phi\partial^\mu\phi - V(\phi)$ associated with $x^\mu \to x^\mu - \xi^\mu$ is

$$J^\mu_\xi = \frac{\partial\mathscr{L}}{\partial(\partial_\mu\phi)}\delta_\xi\phi - \mathscr{L}\xi^\mu. \tag{8.35}$$

The boost charge along x is given by

$$K_x = \int d^3x\, x\left(\frac{\dot\phi^2+|\nabla\phi|^2}{2}+V(\phi)\right) + t\int\dot\phi\nabla_x\phi = \int d^3x\, x\,\mathscr{H} + t\,P_x\,, \tag{8.36}$$

where $\mathscr{H}$ is the Hamiltonian density and P_x is the total momentum along x. The $l=1$ mass multipole $\int d^3x\, x\, \mathscr{H}$ therefore equates the boost charge minus t times the momentum charge. Our definition of mass multipole moments (8.33) is therefore totally natural in that respect.

8.4.3 Multipole charges at future null infinity

Let us now describe how to define the multipole moments from Noether charges at future null infinity. We again assume the asymptotic stationarity hypothesis (8.27) at both future and past of null infinity.

For an arbitrary retarded time u, the charges (8.26) are formally infinite. However, they can be regularized by the finite part prescription of Blanchet and Damour (1986). After taking the finite part, we obtain in linearized Einstein gravity,

$$\underset{\substack{u \text{ fixed}\\ r\to\infty}}{\mathrm{FP}} \left(Q_K^{lm} - uQ_P^{lm}\right) = \frac{2(2l+1)!!}{l!} I^{lm}(u), \tag{8.37}$$

$$\underset{\substack{u \text{ fixed}\\ r\to\infty}}{\mathrm{FP}} Q_L^{lm} = -\sqrt{\frac{l}{l+1}}\frac{(2l-1)!!}{(l-1)!}\left(2(l+2)+\alpha(l-1)\right) S^{lm}(u). \tag{8.38}$$

In other words, all terms proportional to r are dropped and only the r^0 term is kept. This definition readily generalizes to an arbitrary theory of gravity.

Let us now contrast these definitions with the standard *radiative multipole moments*. At linear order, one can switch to radiative (Bondi) coordinates (U,R,θ,ϕ) by a simple change of coordinates, $U = u - \frac{2GM}{c^3}\log(r/r_0)$, $R=r$. The radiative mass and current multipole moments $U_{A_l}(U)$ and $V_{A_l}(U)$ are defined from the $1/R$ fall-off of the metric in radiative coordinates. It turns out that they match with the l-derivatives of the mass and current multipole moments, up to important non-linear corrections of $\mathscr{O}(G)$ that encode tails, non-linear memory and further non-linear terms (see the review of Blanchet (2014) and the latest update in Marchand, Blanchet, and Faye (2016))

$$U_{A_l}(U) = {}^{(l)}\mathcal{I}_{A_l}(U) + \mathscr{O}\left(\frac{G}{c^3}\right), \tag{8.39}$$

$$V_{A_l}(U) = {}^{(l)}\mathcal{S}_{A_l}(U) + \mathscr{O}\left(\frac{G}{c^3}\right). \tag{8.40}$$

While the radiative multipole moments are proportional to the l-th derivative of the source multipole moments (8.39), we notice from Eq. (8.37) that the Noether

charges instead allow one to directly extract the source multipole moments without any derivatives close to null infinity. This is mainly because the multipole symmetries are proportional to r^l and therefore extract information about the subleading r^{-l} part of the metric. The multipole charges at null infinity are therefore more elementary than the radiative multipole moments.

8.4.4 Conservation equation

The multipole moments in linearised Einstein gravity can be simply read off from the components of the metric in canonical harmonic gauge. Now, it is advantageous already in Einstein gravity to reformulate these multipole moments in terms of Noether charges for the following reason. Canonical Noether charges obey a conservation law which allows us to relate the multipole charges of the system sourcing the linear solution at different times to the flux of multipole charges at null infinity.

Let us derive this multipole moment conservation law. The generalized Noether theorem for gauge or diffeomorphism invariant theories (Wald, 1993; Barnich, Brandt, and Henneaux, 2000; Barnich and Brandt, 2002) implies that the surface charges obey the conservation equation

$$\int_{S_t^\infty} \boldsymbol{k}_\xi[h;\eta] - \int_{S_t^0} \boldsymbol{k}_\xi[h;\eta] = \int_{\Sigma_t} \boldsymbol{\omega}[h, \mathscr{L}_\xi \eta; \eta], \tag{8.41}$$

where Σ_t is a constant time hypersurface, whose boundary are two 2-spheres S_t^∞ and S_t^0. We choose S_t^∞ to be the 2-sphere at spatial infinity and S_t^0 to be close to $r = 0$, which is the near zone limit of the radiation zone. Let us choose two such hypersurfaces Σ_+ and Σ_-, respectively, at constant times t^+ and t^-, as shown in the left-hand-side of Figure 8.1. Such constant time hypersurfaces are not boosted with respect to each other at spatial infinity and, in that sense, approach the same boundary sphere S^∞. After fixing the ambiguity parameter α in the definition of the covariant charges, $\boldsymbol{\omega}$ is the Lee-Wald symplectic structure (Lee and Wald, 1990; Wald and Zoupas, 2000) for $\alpha = 0$, while $\boldsymbol{\omega}$ is the invariant symplectic structure (Barnich and Compère, 2008; Compère, 2007a) for $\alpha = 1$.

By rearranging terms, one can write the above equation as

$$Q^{\text{source}} + Q^{\text{rad}} = Q^{\text{total}}, \tag{8.42}$$

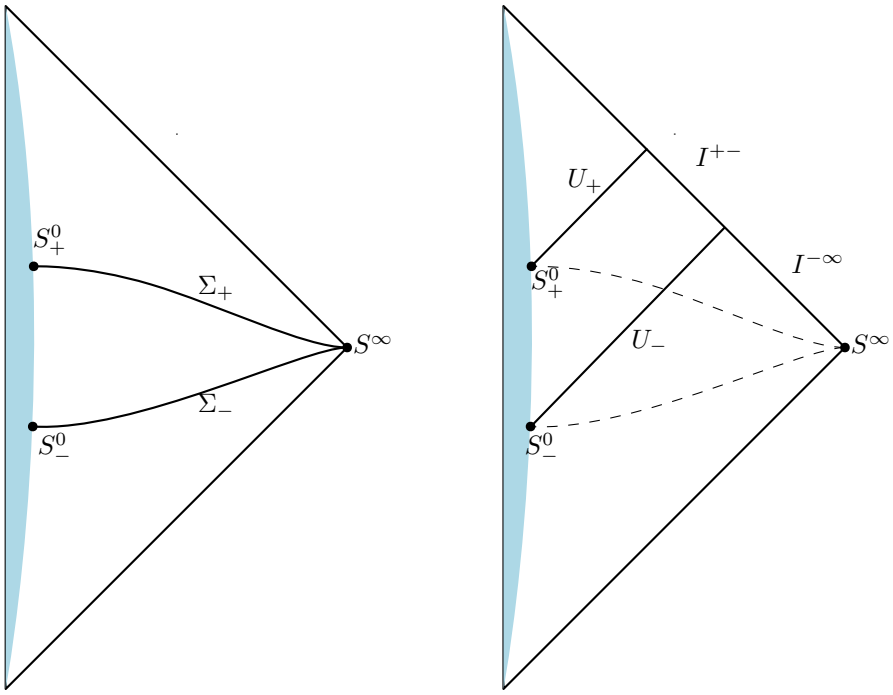

FIGURE 8.1: (Left) Two constant time slices $\Sigma_\pm$ both asymptote to the sphere S^∞ at spatial infinity. The coloured region $r \leq a$, where a is the size of the source, is not described by the linear solution and contains the source. The inner boundaries are denoted as $S^0_\pm$. (Right) One can smoothly deform $\Sigma_\pm$ such that the difference of $Q^{\text{rad}}_{\mathscr{I}^{+-}}$ between the two advanced times u_+ and u_- represents the multipole moment flux through null infinity.

where

$$Q^{\text{source}} = \int_{S^0_t} \boldsymbol{k}_\xi[h,\eta]\,, \qquad Q^{\text{total}} = \int_{S^\infty_t} \boldsymbol{k}_\xi[h,\eta], \qquad Q^{\text{rad}} = \int_{\Sigma_t} \boldsymbol{\omega}[h,\mathscr{L}_\xi\eta;\eta]\,. \tag{8.43}$$

The source charge is the actual multipole charge of the source, as the near zone limit of the radiation zone matches with the far zone of the source zone (see, *e.g.*, Blanchet, 2014). Under the hypothesis of asymptotic stationarity at initial retarded times, the multipole charges are time-independent at spatial infinity,

$$\frac{d}{dt}Q^{\text{total}} = 0. \tag{8.44}$$

The flux term is simply interpreted as the radiated multipole charge to future null infinity. More precisely, one can smoothly deform the hypersurfaces $\Sigma_\pm$ as shown in the right-hand-side of Figure 8.1, where we define $\Sigma_+ = U_+ \cup I^{+-} \cup I^{-\infty}$ and $\Sigma_- = U_- \cup I^{-\infty}$. Here $U_\pm$ are null hypersurfaces at constant retarded time $u_\pm$ and

I^{+-} is a surface at constant large r close to null infinity. We have the equality

$$Q^{\text{source}}_{t^+} - Q^{\text{source}}_{t^-} = Q^{\text{rad}}_{I^{+-}} + Q^{\text{rad}}_{U_+} - Q^{\text{rad}}_{U_-}. \tag{8.45}$$

The left-hand-side is the *finite* difference between the source multipole charge at time t^+ and at time t^-. The individual terms on the right-hand-side are diverging but the difference is finite. It is useful to again define the finite part FP of a diverging expression in r as the r^0 term of the expression with u fixed. In fact, we have

$$\underset{\substack{u \text{ fixed} \\ r\to\infty}}{\text{FP}} Q^{\text{rad}}_{U_\pm} = 0. \tag{8.46}$$

The reason is that from the generalized Noether theorem, this expression is the difference of charge between $r \to \infty$ and $r = 0$. From the explicit expression for the charges (in the case of the mass multipole, a subtraction of two Noether charges is necessary, as (8.33)), the only finite part is precisely the part at $r = 0$ which therefore cancels out. The remaining finite part of the right-hand side of (8.45) is the finite radiation flux in between u^+ and u^-,

$$F^{+-} \equiv \underset{\substack{u \text{ fixed} \\ r\to\infty}}{\text{FP}} Q^{\text{rad}}_{I^{+-}}. \tag{8.47}$$

The multipole charge conservation law can be finally written as

$$Q^{\text{source}}_{t^+} - Q^{\text{source}}_{t^-} = F^{+-}. \tag{8.48}$$

It follows from the generalized Noether theorem.

8.5 Discussion and conclusions

We reformulated Thorne's definition of mass and current multipole moments in Einstein gravity in terms of Noether charges associated with multipole symmetries, which are residual transformations of the harmonic gauge; see Eqs. (8.9). Since Noether charges are defined for any theory of gravity, it allows to define in principle all mass and current multipole moments for such an arbitrary theory. As an example, after overtaking the cumbersome task to reach the canonical harmonic gauge, it is possible to determine the multipole structure of the recently constructed black hole with scalar hair in Herdeiro and Radu (2014) from the Noether charge formula of Einstein gravity coupled to a scalar field (Barnich, 2002); see also appendix E.4.

We expressed the multipole moments of General Relativity as conserved Noether charges at spatial infinity. We also derived the conservation laws of multipole charges under the hypothesis of no incoming radiation. With suitable junction conditions between the past of future null infinity and the future of past null infinity (which would generalize Strominger, 2013; Hawking, Perry, and Strominger, 2017), one would relate the total change of source multipole moments between future and past timelike infinity to the corresponding fluxes at past and future null infinity. We expect that these conservation laws of canonical moments together with the conservation of canonical BMS super-translation charges at spatial infinity (Troessaert, 2018; Henneaux and Troessaert, 2018a; Henneaux and Troessaert, 2018b) (see also (Compere and Dehouck, 2011; Virmani, 2012; Compère and Fiorucci, 2017)) underly the conservation laws of the Bondi mass and angular momentum aspects obtained in Hawking, Perry, and Strominger (2017).

We mainly discussed in this chapter mass and current multipole moments. In a generic diffeomorphism invariant theory of gravity coupled to matter, there will be generically six independent STF tensors appearing in the linearised metric after gauge fixing; see Eq. (8.17).[3] Therefore, we would need to define six independent sets of gravitational source multipole moments. In our approach, these would be built from six multipole Noether charges associated with multipole symmetries.

Starting from our ansatz (8.2), we identified four sets of multipole symmetries, which include the mass, current, and momentum multipole symmetries, but discarded the irreducible harmonic vector $\boldsymbol{V}$, since it does not play a role in Einstein gravity. We expect that it might play a role in more general theories. Note that $l=0$ and $l=1$ harmonics of $\boldsymbol{V}$ are respectively the spatial scaling $x^i\partial_i$ and the vector $\xi^{(j)} = \left(x^i x^j - \frac{1}{3}x^2\delta^{ij}\right)\partial_i$ which is not a standard symmetry. It is also straightforward to relax the ansatz (8.2), and consider as candidate multipole charges the set of eight charges

$$Q_{\epsilon\partial_t + t\nabla\epsilon} - t\,Q_{\nabla\epsilon}, \quad Q_{\boldsymbol{r}\times\nabla\epsilon}, \quad Q_{\nabla\epsilon}, \quad Q_{V^i\partial_i}, \tag{8.49}$$

$$Q_{t\epsilon\partial_t} - t\,Q_{\epsilon\partial_t}, \quad Q_{t\boldsymbol{r}\times\nabla\epsilon} - t\,Q_{\boldsymbol{r}\times\nabla\epsilon}, \quad Q_{t\nabla\epsilon} - t\,Q_{\nabla\epsilon}, \quad Q_{tV^i\partial_i} - t\,Q_{V^i\partial_i}, \tag{8.50}$$

where Q_ξ denotes the Noether charge associated with ξ. These linear combinations ensure covariance under explicit time shifts, as for the mass multipole moments (8.33). It is not clear to us, however, whether the six independent multipole

[3] Also, in a generic diffeomorphism invariant theory of gravity with lightcone propagating planar waves, there are six distinct polarization modes for the linearised perturbations (Eardley et al., 1973), simply because the $1/r$ behaviour of the electric part of the Riemann tensor close to null infinity admits a decomposition into six distinct STF tensors. This leads to six distinct radiative multipole moments.

moments can be identified from this set of eight combinations of Noether charges.

Let us now discuss the connection of our results with gravitational electric-magnetic duality. In gauge theories, not every multipole moment might be associated with a Noether charge. Indeed, in the case of electromagnetism, electric multipole moments are Noether charges, but magnetic multipole moments cannot be expressed as Noether charges associated with the original gauge symmetry of Maxwell theory. In vacuo, it exists a dual formulation in terms of a dual gauge field A_D defined as $\star F = dA_D$. The emergent gauge symmetry of the dual formulation allows to define the magnetic multipole moments of the original formulation in terms of Noether charges as a simple consequence of electric-magnetic duality. Contrary to electromagnetism, it turns out that in Einstein gravity all multipole charges *are* Noether charges, as we have now demonstrated. In many instances the structure of dualities in Maxwell and in Einstein theories is similar, but not here. The reason of this asymmetry is that in Einstein gravity, the gauge parameter is a space-time vector which itself admits duality transformations. It has been shown that, in the formulation of spatial infinity foliated by de Sitter slices of unit normal n^μ, rotations and boosts are dual to each other, and the second sub-leading component of the electric part of the Weyl tensor is dual to its magnetic part (Mann et al., 2008; Compere, Dehouck, and Virmani, 2011). This is the reason why the Lorentz charges can be expressed in two distinct but equivalent ways (Ashtekar and Hansen, 1978; Mann, Marolf, and Virmani, 2006). In fact, it is a matter of simple algebra to show that such a duality persists between the mass multipole symmetries and the current multipole symmetries:

$$L_\epsilon = \frac{1}{2}\epsilon^{\mu\nu\rho\sigma} n_\mu \partial_\nu K_{\epsilon,\rho} \partial_\sigma \,. \tag{8.51}$$

We therefore are led to conjecture that the Noether l-multipole charges can be expressed from the $(l+1)$–subleading component of either the electric or the magnetic part of Weyl tensor, as its $l = 1$ Lorentz counterpart (Compere, Dehouck, and Virmani, 2011).

To conclude, the mass and current multipole symmetries are associated with an infinite number of conserved Noether charges. These outer symmetries provide a new concept to comprehend the asymptotic structure of gravity, or, after a suitable generalisation, of general gauge theories.

Conclusions and outlook

This thesis investigated applications of space-time symmetries to black holes and gravitational radiation. We mainly focused on two classes of symmetries:

a) symmetries in the near-horizon region of rapidly rotating Kerr black holes;

b) residual gauge symmetries.

In the first case, we aimed to address questions in the context of force-free electrodynamics and thin accretion discs. We exploited the presence of the isometry group $SO(2,1) \times U(1)$ to investigate its consequences on the dynamics of electromagnetic fields and accreting matter in the region close to the event horizon of Kerr black holes in the high-spin regime.

In the second case, we provided a new definition of multipole moments of the gravitational field. We showed that gravitational multipole moments are associated to a certain class of residual symmetries of the harmonic gauge and they are expressed in terms of the Noether charges. Our definition of gravitational multipole moments reproduces the results in General Relativity with the advantage that it can be applied to an arbitrary metric theory of gravity.

Moreover, the thesis contains applications of the covariant phase space formalism. Such a formalism has been adopted to address the problem to compute the total conserved mass of the Melvin-Kerr-Newman black hole and to write the gravitational multipole moments as Noether charges associated to certain residual gauge symmetries.

Several interesting avenues are to take for future work.

First, it would be interesting to predict the existence of observational "smoking guns" of the $SO(2,1) \times U(1)$ symmetry enhancement in the near-horizon geometry of high-spin Kerr black holes. This research line is still under intensive work for electromagnetic emission from accretion discs and gravitational radiation from extreme mass ratio inspirals. Along the same line, work should be done to better understand whether and how the symmetry enhancement can constrain the physics of jets emission from AGNs. Another interesting avenue is to investigate how the plasma and magnetic fields surrounding rapidly rotating black holes interact with each other. Relativistic magnetic reconnection is a viable astrophysical

phenomenon, beyond the force-free approximation, that might explain particle acceleration and non-thermal emission observed around compact objects.

Second, force-free electrodynamics around black hole space-times lacks of exact analytical solutions, with the exception of a few known results around both Schwarzschild and Kerr black holes. The main reason lies in the non-linearity of the equations of motion. It can be relevant for astrophysical purposes to study the mathematical properties of the differential equations governing force-free electrodynamics in order to develop new analytical methods to find exact solutions and to study their physical properties.

Third, another interesting future work is to study the behaviour of accretion discs in the near-horizon region. To this aim, one need more elaborated models than thin accretion discs to make contact with observations. In particular, one might point to investigate the physics near the physical edge of the accretion disc, which is usually closer to the black hole than the ISCO location, where gravitational effects in the strong gravity regime are present.

Finally, concerning the multipolar structure of the gravitational field, it is intriguing to apply our definition of gravitational multipole moments to other theories of gravity. Moreover, because the novel definition of moments in terms of Noether charges highlights the importance of a certain class of vector fields, it may be of interest to apply this approach in the context of tidal deformations of neutron stars with the hope to give an explanation for some “universal” relations among certain multipole moments.

Part III

Appendices

Appendix A

Differential forms

The Levi-Civita symbol and tensor are, respectively, defined by

$$\epsilon_{\mu_1\mu_2\ldots\mu_n} = \begin{cases} +1, & (\mu_1,\mu_2,\ldots,\mu_n) \text{ is an even permutation of } (1,\ldots,\mathrm{n}), \\ -1 & (\mu_1,\mu_2,\ldots,\mu_n) \text{ is an odd permutation } (1,\ldots,\mathrm{n}), \\ 0 & \text{otherwise.} \end{cases} \tag{A.1a}$$

$$\varepsilon_{\mu_1\mu_2\ldots\mu_n} = \sqrt{-g}\,\epsilon_{\mu_1\mu_2\ldots\mu_n}, \tag{A.1b}$$

where g is the determinant of the metric tensor $g_{\mu\nu}$.
It is useful to recall the following formula

$$\varepsilon^{\mu_1\mu_2\ldots\mu_p\alpha_1\ldots\alpha_{n-p}}\varepsilon_{\mu_1\mu_2\ldots\mu_p\beta_1\ldots\beta_{n-p}} = (-1)^s p!(n-p)!\delta^{[\alpha_1}_{\beta_1}\cdots\delta^{\alpha_{n-p}]}_{\beta_{n-p}}. \tag{A.2}$$

Here s is the number of negative eigenvalues of the metric tensor.

In a given coordinate system, a p-form can be written as

$$A = \frac{1}{p!}A_{\mu_1\mu_2\ldots\mu_p}dx^{\mu_1}\wedge dx^{\mu_2}\wedge\cdots\wedge dx^{\mu_p}. \tag{A.3}$$

Let A be a p-form and B be a q-form.
The wedge product is defined as

$$(A\wedge B)_{\mu_1\mu_2\ldots\mu_{p+q}} = \frac{(p+q)!}{p!q!}A_{[\mu_1\ldots\mu_p}B_{\mu_{p+1}\ldots\mu_{p+q}]}, \tag{A.4}$$

where the square brackets denote antisymmetrization with respect all indices.
The exterior derivative is given by

$$(dA)_{\mu_1\mu_2\ldots\mu_{p+1}} = (p+1)\partial_{[\mu_1}A_{\mu_2\ldots\mu_{p+1}]}. \tag{A.5}$$

It obeys the generalised Leibniz rule $d(A \wedge B) = dA \wedge B + (-1)^p A \wedge dB$.
A contraction of a $p+1$-form with a vector reads as

$$(i_v A)_{\mu_1 \ldots \mu_p} = (v \cdot A)_{\mu_1 \ldots \mu_p} = v^\mu A_{\mu\mu_1 \ldots \mu_p}. \tag{A.6}$$

The Hodge operator maps a p-form to a $(n-p)$-form, where n is the dimension of the space-time. It is defined as

$$\star A = \frac{1}{(n-p)!} (\star A)_{\mu_1 \ldots \mu_{n-p}} dx^{\mu_1} \wedge \cdots \wedge dx^{\mu_{n-p}}, \tag{A.7a}$$

$$(\star A)_{\mu_1 \ldots \mu_{n-p}} = \frac{1}{p!} \varepsilon^{\nu_1 \ldots \nu_p}{}_{\mu_1 \ldots \mu_{n-p}} A_{\nu_1 \ldots \nu_p}. \tag{A.7b}$$

The Hodge operator obeys the relation $\star(\star A) = (-1)^{s+p(n-p)} A$.

Appendix B

Kerr black hole

B.1 Line element

The Kerr line element in Boyer-Lindquist (BL) coordinates (t, r, θ, ϕ) is given by (Bardeen, Press, and Teukolsky, 1972)

$$ds^2 = -\frac{\Sigma\Delta}{A}dt^2 + \sin^2(\theta)\frac{A}{\Sigma}(d\phi - \omega dt)^2 + \frac{\Sigma}{\Delta}dr^2 + \Sigma d\theta^2, \tag{B.1}$$

where the metric functions read

$$\Delta(r) = r^2 - 2Mr + a^2, \tag{B.2a}$$
$$\Sigma(r,\theta) = r^2 + a^2\cos^2(\theta), \tag{B.2b}$$
$$A(r,\theta) = (r^2 + a^2)^2 - a^2\Delta\sin^2(\theta), \tag{B.2c}$$
$$\omega(r,\theta) = \frac{2Mar}{A}. \tag{B.2d}$$

Here, M is the mass and $a = J/M$ is the specific angular momentum of the Kerr black hole, which we assume to be non-negative. The event horizon is located at $r_+ = M + \left(M^2 - a^2\right)^{1/2}$. The Kerr black hole space-time is stationary and axisymmetric. The Killing vectors corresponding to time and axial symmetry are, respectively, $\eta = \delta^\mu_t\partial_\mu$ and $\xi = \delta^\mu_\phi\partial_\mu$.

B.1.1 Line element near and at the equatorial plane

In order to describe the region near the equatorial plane $\theta = \pi/2$, we introduce the cylindrical coordinate $z = r\cos(\theta)$ and neglect corrections of order $(z/r)^2$. The resulting line element in the near-equatorial region of coordinates (t, r, z, ϕ) is given by

$$ds^2 = -\frac{r^2\Delta}{A}dt^2 + \frac{A}{r^2}(d\phi - \omega dt)^2 + \frac{r^2}{\Delta}dr^2 + dz^2 + \mathcal{O}\left(\frac{z}{r}\right)^2. \tag{B.3}$$

Following Novikov and Thorne (1973), we define the dimensionless radial coordinate x and the spin parameter a_s, respectively, by

$$x \equiv \left(\frac{r}{M}\right)^{\frac{1}{2}}, \qquad a_s \equiv \frac{a}{M} \tag{B.4}$$

Thus, at fixed spin parameter in the range $a_s \in [0,1]$, $x \geq x_+ = \left[1+(1-a_s^2)^{1/2}\right]^{1/2}$ describes the Kerr space-time outside the event horizon. The ISCO is located at

$$x_0 = \left\{3 + Z_2 - [(3-Z_1)(3+Z_1+2Z_2)]^{1/2}\right\}^{1/2}, \tag{B.5a}$$

$$Z_1 = 1 + \left(1-a_s^2\right)^{1/3}\left[(1+a_s)^{1/3} + (1-a_s)^{1/3}\right], \tag{B.5b}$$

$$Z_2 = \left(3a_s^2 + Z_1^2\right)^{1/2}. \tag{B.5c}$$

Following the tradition, we define the dimensionless functions:[1]

$$\mathscr{A} = 1 + \frac{a_s^2}{x^4} + \frac{2a_s^2}{x^6}, \tag{B.6a}$$

$$\mathscr{B} = 1 + \frac{a_s}{x^3}, \tag{B.6b}$$

$$\mathscr{C} = 1 - \frac{3}{x^2} + \frac{2a_s}{x^3}, \tag{B.6c}$$

$$\mathscr{D} = 1 - \frac{2}{x^2} + \frac{a_s^2}{x^4}, \tag{B.6d}$$

$$\mathscr{F} = 1 - \frac{2a_s}{x^3} + \frac{a_s^2}{x^4}, \tag{B.6e}$$

$$\mathscr{G} = 1 - \frac{2}{x^2} + \frac{a_s}{x^3}, \tag{B.6f}$$

$$\mathscr{R} = \mathscr{C}^{-1}\mathscr{F}^2 - a_s^2 x^{-2}\left(\mathscr{C}^{-1/2}\mathscr{G} - 1\right). \tag{B.6g}$$

All functions in Eqs. (B.6) go to unity far from the black hole $x \gg 1$. The functions $\mathscr{A}$, $\mathscr{B}$ and $\mathscr{R}$ are monotonically decreasing, while the functions $\mathscr{C}$, $\mathscr{D}$, $\mathscr{F}$ and $\mathscr{G}$ are monotonically increasing in their domains of definition. The radial coordinates where $\mathscr{C} = 0$ are given by

$$x_1 = 2\cos\left[\frac{1}{3}\arccos(a_s) - \frac{\pi}{3}\right], \tag{B.7a}$$

$$x_2 = 2\cos\left[\frac{1}{3}\arccos(a_s) + \frac{\pi}{3}\right], \tag{B.7b}$$

$$x_3 = -2\cos\left[\frac{1}{3}\arccos(a_s)\right], \tag{B.7c}$$

[1] Note the typo in the exponent of a_s in Eq. (A4c) of Penna, Sadowski, and McKinney (2012).

with $x_1 \geq x_2 \geq x_3$. The last photon orbit is given by $x = x_1$ and is placed between the ISCO and the event horizon, $x_0 \geq x_1 \geq x_+$. The function $\mathscr{D}$ is positive outside the event horizon.

B.2 Circular equatorial geodesics

Circular equatorial geodesics have a four-velocity of the form

$$u = u^t \partial_t + u^\phi \partial_\phi = u^t (\eta + \Omega \xi). \tag{B.8a}$$

Here, we list the kinematic quantities characterizing the geodesic motion:

$$u^t = \mathscr{B}\mathscr{C}^{-1/2}, \tag{B.9a}$$
$$u^\phi = M^{-1} x^{-3} \mathscr{C}^{-1/2}, \tag{B.9b}$$
$$E = \eta^\mu u_\mu = \mathscr{C}^{-1/2}\mathscr{G}, \tag{B.9c}$$
$$L = \xi^\mu u_\mu = M x \mathscr{C}^{-1/2}\mathscr{F}, \tag{B.9d}$$
$$\Omega = u^\phi / u^t = M^{-1} x^{-3} \mathscr{B}^{-1}, \tag{B.9e}$$
$$\mathscr{L}_\star^2 = L^2 - a^2(E-1) = M^2 x^2 \mathscr{R}, \tag{B.9f}$$

respectively, the time component u^t, the azimuthal component u^ϕ, the conserved specific energy E, the conserved specific angular momentum L, the co-rotating Keplerian angular velocity Ω with respect to a stationary observer and a conserved quantity along the geodesic motion $\mathscr{L}_\star^2$, which appears in the thin disc vertical equation.

It is useful to introduce the function $\mathscr{P}$ defined by

$$\begin{aligned}\mathscr{P} &\equiv \mathscr{P}_0 + \frac{1}{M}\int_{x_0}^{x} (E - \Omega L) L_{,x'} \, dx' \\ &= \mathscr{P}_0 + x - x_0 - \frac{3}{2} a_s \ln\left(\frac{x}{x_0}\right) \\ &\quad - \sum_{i=1}^{3} \frac{3(x_i - a_s)^2}{x_i (x_i - x_{i+1})(x_i - x_{i+2})} \ln\left(\frac{x - x_i}{x_0 - x_i}\right).\end{aligned} \tag{B.10}$$

Here, $\mathscr{P}_0$ is a real constant to be fixed by imposing a boundary condition, as explained in section 7.2. In the above sum, we identify $x_i = x_{i+3}$. The function $\mathscr{Q}$ of Page and Thorne (1974) can be expressed as $\mathscr{Q} = x^{-1}\mathscr{B}\mathscr{C}^{-1/2}\mathscr{P}$ but we find more economical and natural to use $\mathscr{P}$.

B.3 Observer frames for circular equatorial geodesics

We define three privileged observers.

1. The stationary observer frame with four-velocity

$$u_{stat} = (-\eta^{\nu}\eta_{\nu})^{-1/2}\eta, \tag{B.11}$$

which is locally rotating in the sense that $L_{stat} = \xi_{\mu}u^{\mu}_{stat} \neq 0$.

2. The locally non-rotating frame (LNRF), sometimes also called local inertial frame or zero angular momentum observer (ZAMO), has four-velocity

$$u_{LNRF} = (\omega^2\xi^{\mu}\xi_{\mu} - \eta^{\mu}\eta_{\mu})^{-1/2}(\eta + \omega\xi), \tag{B.12}$$

with $\omega^2\xi^{\mu}\xi_{\mu} - \eta^{\mu}\eta_{\mu} = \mathscr{A}^{-1}\mathscr{D}$. It has $L_{LNRF} = \xi_{\mu}u^{\mu}_{LNRF} = 0$. With respect to the LNRF observer, circular equatorial geodesics have four-velocity components $u^{(a)} = u^{\mu}e^{(a)}_{\mu}$, where $e^{(a)}_{\mu}$ is the orthonormal tetrad attached to the LNRF, whose expression can be found in appendix (B.4) or in Eq. (3.2) of Bardeen, Press, and Teukolsky (1972). The only two non-vanishing components are

$$u^{(t)} = \frac{r\Delta^{1/2}}{A^{1/2}}u^t = \mathscr{A}^{-1/2}\mathscr{B}\mathscr{C}^{-1/2}\mathscr{D}^{1/2}, \tag{B.13}$$

$$\begin{aligned} u^{(\phi)} &= \frac{A^{1/2}}{r}(\Omega - \omega)u^t \\ &= x^{-1}\mathscr{A}^{1/2}\mathscr{C}^{-1/2} - 2a_s x^{-4}\mathscr{A}^{-1/2}\mathscr{B}\mathscr{C}^{-1/2}. \end{aligned} \tag{B.14}$$

Therefore, the only non-vanishing component of the three-velocity relative to the LNRF is

$$\mathscr{V}^{(\phi)} = \frac{u^{(\phi)}}{u^{(t)}} = \frac{A}{r^2\Delta^{1/2}}(\Omega - \omega) = x^{-1}\mathscr{B}^{-1}\mathscr{D}^{-1/2}\mathscr{F}. \tag{B.15}$$

We call $\mathscr{V}^{(\phi)} = \tilde{R}\tilde{\Omega}$ the linear velocity with respect to the LNRF , with $\tilde{R} = A/(r^2\Delta^{1/2})$ being the gyration radius, $\tilde{\Omega} = \Omega - \omega$ the angular velocity with respect to the local inertial frame and $\gamma = u^{(t)}$ the Lorentz gamma factor corresponding to this linear velocity. In other words, the four-velocity of circular equatorial geodesics as measured by an LNRF observer is $u^{\mu} = \gamma(u^{\mu}_{LNRF} + \mathscr{V}^{(\phi)}e^{\mu}_{(\phi)})$.

3. The local rest frame (LRF) of the particle in the circular equatorial orbit, whose orthonormal tetrad is defined in Eq. (5.4.5a) of Novikov and Thorne

(1973). In this frame, the shear tensor $\sigma_{\hat{\mu}\hat{\nu}}$ of circular equatorial geodesics has only one non-vanishing component

$$\sigma_{\hat{r}\hat{\phi}} = \sigma_{\hat{\phi}\hat{r}} = \frac{1}{2}\frac{A}{r^3}\gamma^2\Omega_{,r} = -\frac{3}{4}M^{-1}x^{-3}\mathscr{C}^{-1}\mathscr{D}. \tag{B.16}$$

B.4 LNRF tetrad

The orthonormal tetrad carried by a locally non-rotating frame (LNRF) is given by

$$\mathbf{e}_{(t)} = e^{\mu}_{(t)}\partial_\mu = \left(\frac{A}{\Sigma\Delta}\right)^{1/2}\left(\partial_t + \omega\partial_\phi\right) \approx \sqrt{\frac{\mathscr{A}}{\mathscr{D}}}\left(\partial_t + \omega\partial_\phi\right), \tag{B.17a}$$

$$\mathbf{e}_{(r)} = e^{\mu}_{(r)}\partial_\mu = \left(\frac{\Delta}{\Sigma}\right)^{1/2}\partial_r \approx \mathscr{D}^{1/2}\partial_r, \tag{B.17b}$$

$$\mathbf{e}_{(\theta)} = e^{\mu}_{(\theta)}\partial_\mu = \left(\frac{1}{\Sigma}\right)^{1/2}\partial_\theta \approx \partial_z, \tag{B.17c}$$

$$\mathbf{e}_{(\phi)} = e^{\mu}_{(\phi)}\partial_\mu = \left(\frac{\Sigma}{A}\right)^{1/2}\frac{1}{\sin\theta}\partial_\phi \approx \frac{1}{Mx^2\mathscr{A}^{1/2}}\partial_\phi \tag{B.17d}$$

and the corresponding one-forms are

$$\mathbf{e}^{(t)} = e^{(t)}_{\mu}dx^\mu = \left(\frac{\Sigma\Delta}{A}\right)^{1/2}dt \approx \sqrt{\frac{\mathscr{D}}{\mathscr{A}}}dt, \tag{B.18a}$$

$$\mathbf{e}^{(r)} = e^{(r)}_{\mu}dx^\mu = \left(\frac{\Sigma}{\Delta}\right)^{1/2}dr \approx \mathscr{D}^{-1/2}dr, \tag{B.18b}$$

$$\mathbf{e}^{(\theta)} = e^{(\theta)}_{\mu}dx^\mu = \Sigma^{1/2}d\theta \approx dz, \tag{B.18c}$$

$$\mathbf{e}^{(\phi)} = e^{(\phi)}_{\mu}dx^\mu = \left(\frac{A}{\Sigma}\right)^{1/2}\sin\theta(d\phi - \omega dt) \approx Mx^2\mathscr{A}^{1/2}(d\phi - \omega dt) \tag{B.18d}$$

where $\approx$ means in the near-equatorial region.

B.5 General near-equatorial orbits

Let us consider a more general four-velocity vector field than that of circular equatorial orbits. In order to match our notation with the traditional literature, we start by considering the most general four-velocity vector as measured by a LNRF, whose form is given by

$$u^\mu = \gamma\left(u^\mu_{LNRF} + \mathcal{V}^{(r)}e^\mu_{(r)} + \mathcal{V}^{(\theta)}e^\mu_{(\theta)} + \mathcal{V}^{(\phi)}e^\mu_{(\phi)}\right), \tag{B.19}$$

where $u^{\mu}_{LNRF} = e^{\mu}_{(t)}$ and $e^{\mu}_{(i)}$ are defined in (B.17), while $\mathcal{V}^{(i)}$ are the components of the three-velocity as measured by the LNRF and γ is the Lorentz gamma factor and it can be expressed as $\gamma^{-2} = 1 - \left(\mathcal{V}^{(r)}\right)^2 - \left(\mathcal{V}^{(\theta)}\right)^2 - \left(\mathcal{V}^{(\phi)}\right)^2$. Thus, the components of the four-velocity in the Boyer-Lindquist frame read

$$(u^t, u^r, u^\theta, u^\phi) = \gamma\left(\sqrt{\frac{\mathscr{A}}{\mathscr{D}}}, \mathscr{D}^{1/2}\mathcal{V}^{(r)}, \frac{\mathcal{V}^{(\theta)}}{r}, \omega\sqrt{\frac{\mathscr{A}}{\mathscr{D}}} + \frac{\mathcal{V}^{(\phi)}}{r\mathscr{A}^{1/2}}\right). \tag{B.20}$$

The angular velocity with respect to the stationary observer is, as usual, defined by $\Omega = u^\phi/u^t$. From this definition, we obtain that the azimuthal linear velocity $\mathcal{V}^{(\phi)} = \tilde{R}\tilde{\Omega}$ is the product of the gyration radius $\tilde{R} = A/(r^2\Delta^{1/2})$ and the angular velocity measured by the LNRF $\tilde{\Omega} = \Omega - \omega$. We call this the kinematic expression of $\mathcal{V}^{(\phi)}$. An alternative useful expression can be derived from the specific angular momentum $L = u_\phi$ and one gets $\mathcal{V}^{(\phi)} = L/(\gamma r\mathscr{A}^{1/2})$.

In order to describe the orbit, we need three variables. Following the traditional literature (see, *e.g.*, Abramowicz et al., 1996; Gammie and Popham, 1998), we choose (a) the rescaled radial velocity V, defined by

$$\frac{V}{\sqrt{1-V^2}} = \gamma\mathcal{V}^{(r)} = \mathscr{D}^{-1/2}u^r, \tag{B.21}$$

(b) the vertical velocity $\mathcal{V}^{(\theta)} = U\cos\theta$ (Abramowicz, Lanza, and Percival, 1997), and (c) the specific angular momentum $L = u_\phi$. The four-velocity (B.20), in terms of the variables V, U and L, is

$$(u^t, u^r, u^\theta, u^\phi) = \left(\gamma\sqrt{\frac{\mathscr{A}}{\mathscr{D}}}, \frac{V\mathscr{D}^{1/2}}{\sqrt{1-V^2}}, \gamma\frac{U}{r}\cos\theta, \gamma\omega\sqrt{\frac{\mathscr{A}}{\mathscr{D}}} + \frac{L}{r^2\mathscr{A}}\right), \tag{B.22}$$

and the covariant components are given by

$$(u_t, u_r, u_\theta, u_\phi) = \left(-\gamma\sqrt{\frac{\mathscr{D}}{\mathscr{A}}} - L\omega, \frac{V\mathscr{D}^{-1/2}}{\sqrt{1-V^2}}, \gamma r U\cos\theta, L\right). \tag{B.23}$$

Because the vertical velocity $\mathcal{V}^{(\theta)}$ is proportional to $\cos\theta = z/r$, we may write the Lorentz gamma factor, at first order in z/r, as

$$\gamma^2 = \frac{1}{1-(\mathcal{V}^{(r)})^2 - (\mathcal{V}^{(\phi)})^2} = \frac{1}{1-V^2} + \frac{L^2}{r^2\mathscr{A}}, \tag{B.24}$$

where we used the expressions of $\mathcal{V}^{(r)}$ in (B.21) and $\mathcal{V}^{(\phi)} = L/(\gamma r \mathscr{A}^{1/2})$. An equivalent expression of the Lorenz gamma factor can be obtained by using the kinematic expression of $\mathcal{V}^{(\phi)}$. From the very definition of γ, one finds that

$$\gamma^2 = \frac{1}{1-(\tilde{R}\tilde{\Omega})^2}\frac{1}{1-V^2} \equiv \gamma_\phi^2 \gamma_r^2, \tag{B.25}$$

is the product of the Lorentz gamma factors relative to $\mathcal{V}^{(\phi)}$ and V. As pointed in Abramowicz et al., 1996; Gammie and Popham, 1998, V is the radial velocity measured by a frame co-rotating with the fluid at a fixed radial position.

As a remark, we notice that for the particular choice $V = 0 = U$, we get the four-velocity of circular equatorial geodesics with $L = Mx\mathscr{C}^{-1/2}\mathscr{F}$ and $\gamma = \mathscr{A}^{-1/2}\mathscr{B}\mathscr{C}^{-1/2}\mathscr{D}^{1/2}$.

B.5.1 Properties of the four-velocity profile in Eq. (B.22)

Since $S_{\mu\nu} \propto \sigma_{\mu\nu}$ by the second law of thermodynamics, it is useful to know the components of the shear tensor for the velocity profile (B.22). Here we list the nonvanishing covariant derivatives evaluated in the equatorial plane[2]

$$u_{t;t} = -\frac{M}{r^2}\frac{V\mathscr{D}^{1/2}}{\sqrt{1-V^2}}, \qquad u_{t;r} = \frac{dE}{dr} + u_{r;t}, \qquad u_{t;\phi} = \frac{aM}{r^2}\frac{V\mathscr{D}^{1/2}}{\sqrt{1-V^2}} = u_{\phi;t}, \tag{B.26a}$$

$$u_{r;t} = \frac{M\gamma}{r^2}\sqrt{\frac{\mathscr{A}}{\mathscr{D}}}(1-a\Omega), \quad u_{r;r} = \frac{dV/dr}{\mathscr{D}^{1/2}(1-V^2)^{3/2}}, \quad u_{r;\phi} = -\frac{\gamma}{r^2}\sqrt{\frac{\mathscr{A}}{\mathscr{D}}}(aM - a^2M\Omega + r^3\Omega), \tag{B.26b}$$

$$u_{\theta;\theta} = r\frac{V\mathscr{D}^{1/2}}{\sqrt{1-V^2}}, \qquad u_{\phi;r} = \frac{dL}{dr} + u_{r;\phi}, \qquad u_{\phi;\phi} = r\left(1-\frac{Ma^2}{r^3}\right)\frac{V\mathscr{D}^{1/2}}{\sqrt{1-V^2}}, \tag{B.26c}$$

where $E = u_t$ and its radial derivative is given by

$$-\frac{dE}{dr} = \frac{1}{\gamma}\sqrt{\frac{\mathscr{D}}{\mathscr{A}}}\left[\frac{V}{(1-V^2)^2}\frac{dV}{dr} - \frac{L^2}{r^3\mathscr{A}^2}\left(1-\frac{a^2M}{r^3}\right)\right] + \Omega\frac{dL}{dr} - \frac{\omega L}{r\mathscr{A}}\left(3+\frac{a^2}{r^2}\right) + \\ + \frac{\gamma}{r^2\sqrt{\mathscr{A}\mathscr{D}}}\left[\frac{a^2\mathscr{D}}{r\mathscr{A}}\left(1+\frac{3M}{r}\right) + M\left(1-\frac{a^2}{Mr}\right)\right]. \tag{B.27}$$

The expansion scalar is

$$\theta = u^r\left(\frac{2}{r} + \frac{1}{u^r}\frac{du^r}{dr}\right) = \frac{V\mathscr{D}^{1/2}}{\sqrt{1-V^2}}\left[\frac{2}{r} + \frac{M}{r^2\mathscr{D}}\left(1-\frac{a^2}{Mr}\right) + \frac{1}{1-V^2}\frac{1}{V}\frac{dV}{dr}\right]. \tag{B.28}$$

[2] We agree with the expressions of the covariant derivatives listed in appendix A of Gammie and Popham (1998), except for $u_{r;r}$ and $u_{\theta;\theta}$.

Notice that for $V \to 0$, the only nonvanishing components are $u_{t;r}$, $u_{r;t}$, $u_{r;\phi}$ and $u_{\phi;r}$ and the velocity profile becomes divergence free.

From covariant derivatives, we might compute the components of the shear tensor $\sigma_{\mu\nu}$. In particular, we need the following components:

$$\begin{aligned}
\sigma_{rr} &= u_{r;r} + u_r a_r - \frac{1}{3}\left((u_r)^2 + \frac{1}{\mathscr{D}}\right) u^r \left(\frac{2}{r} + \frac{1}{u^r}\frac{du^r}{dr}\right), \\
&= \frac{\mathscr{D}^{-1/2}}{(1-V^2)^{3/2}}\left[\frac{2+V^2}{3(1-V^2)}\frac{dV}{dr} - \frac{V}{3}\left(\frac{2}{r} + \frac{M}{r^2\mathscr{D}}\left(1 - \frac{a^2}{Mr}\right) + 3f_r\right)\right]; \qquad \text{(B.29a)} \\
\sigma_{r\phi} &= \frac{1}{2}\left(2u_{r;\phi} + u_r a_\phi + a_r L + \frac{dL}{dr}\right) - \frac{1}{3}L u_r u^r \left(\frac{2}{r} + \frac{1}{u^r}\frac{du^r}{dr}\right), \\
&= -\frac{\gamma}{r^2}\sqrt{\frac{\mathscr{A}}{\mathscr{D}}}\left[aM + r^3\left(1 - \frac{a^2 M}{r^3}\right)\Omega\right] + \qquad \text{(B.29b)} \\
&\quad + \frac{1}{2}\frac{L}{1-V^2}\left\{\frac{1}{L}\frac{dL}{dr} + \frac{1}{3}\frac{V}{1-V^2}\frac{dV}{dr} - \frac{2V^2}{3}\left[\frac{2}{r} + \frac{M}{r^2\mathscr{D}}\left(1 - \frac{a^2}{Mr}\right)\right] - f_r\right\};
\end{aligned}$$

The expression (B.29b) is the exact expression derived by the expression of the four velocity (B.22) and by the definition of shear tensor, without any assumption or further simplifications. The common approach in the literature (Lasota, 1994; Abramowicz et al., 1996) is the following: from the Keplerian (exact) expression

$$\sigma^k_{r\phi} = \frac{1}{2}\frac{\gamma_k^3}{r^3}\frac{A^{3/2}}{\Delta^{1/2}}\frac{d\Omega_k}{dr}, \qquad \text{(B.30)}$$

one replaces the Keplerian gamma factor by the full gamma factor $\gamma_k \to \gamma$ and the Keplerian angular velocity by the general angular velocity $\Omega_k \to \Omega$. Thus, the expression of the $(r\phi)$ component of the shear tensor for non-Keplerian flows is assumed to have the same functional form, as noted for the first time in Peitz and Appl (1997).

Appendix C

Near-Horizon Extreme Kerr

C.1 Line element

The four-dimensional NHEK line element can be written in a manifestly $SL(2,\mathbb{R}) \times U(1)$ invariant form

$$ds^2_{NHEK} = 2M^2\Gamma(\theta)\left[ds^2_{AdS_2} + d\theta^2 + \gamma^2(\theta)\,(d\Psi + \Theta)^2\right], \tag{C.1}$$

where $ds^2_{AdS_2}$ is the AdS_2 line element, Θ is a left-invariant 1-form on AdS_2 with norm -1, $\Psi \in [0, 2\pi]$ is the azimuthal coordinate and $\theta \in [0,\pi]$ is the polar coordinate. The two functions Γ and γ are, respectively,

$$\Gamma(\theta) = \frac{1+\cos^2(\theta)}{2}, \quad \gamma(\theta) = \frac{\sin(\theta)}{\Gamma(\theta)}. \tag{C.2}$$

The NHEK line element has four Killing vector fields. The generators of its isometry group obey the $SL(2,\mathbb{R}) \times U(1)$ commutation relations

$$[H_0, H_\pm] = \mp H_\pm, \quad [H_+, H_-] = 2H_0, \quad [Q_0, H_\pm] = 0 = [Q_0, H_0]. \tag{C.3}$$

We define the highest weight scalar $\Phi_{(h,q)}$ of weight h and charge q as

$$H_+\Phi_{(h,q)} = 0, \quad H_0\Phi_{(h,q)} = h\Phi_{(h,q)}, \quad Q_0\Phi_{(h,q)} = iq\Phi_{(h,q)}, \quad \partial_\theta\Phi_{(h,q)} = 0, \tag{C.4}$$

and we denote $\Phi = \Phi_{(1,0)}$ and $\lambda = \Phi_{(0,1)}$ so that $\Phi_{(h,q)} = \Phi^h\lambda^q$.

C.2 Coordinate systems

C.2.1 Poincaré coordinates

Let (T, R, θ, Φ) be the Poincaré coordinates. The NHEK line element is

$$ds^2_{NHEK} = 2M^2\,\Gamma(\theta)\left[-R^2 dT^2 + \frac{dR^2}{R^2} + d\theta^2 + \gamma^2(\theta)\,(d\Phi + R dT)^2\right], \tag{C.5}$$

and the generators of its isometry group are

$$H_+ = \sqrt{2}\partial_T, \tag{C.6a}$$
$$H_0 = T\partial_T - R\partial_R, \tag{C.6b}$$
$$H_- = \sqrt{2}\left[\frac{1}{2}\left(T^2 + \frac{1}{R^2}\right)\partial_T - TR\partial_R - \frac{1}{R}\partial_\Phi\right], \tag{C.6c}$$
$$Q_0 = \partial_\Phi. \tag{C.6d}$$

Moreover, $\Phi = 1/R$ and $\lambda = e^{i\Phi}$.

C.2.2 Global coordinates

Let $(\tau, y, \theta, \varphi)$ be the global coordinates. The NHEK line element is

$$ds^2_{NHEK} = 2M^2\,\Gamma(\theta)\left[-(1+y^2)d\tau^2 + \frac{dy^2}{1+y^2} + d\theta^2 + \gamma^2(\theta)\left(d\varphi + y d\tau\right)^2\right], \tag{C.7}$$

and the generators of its isometry group are

$$H_+ = i\frac{e^{i\tau}}{\sqrt{1+y^2}}\left(-y\partial_\tau + i(1+y^2)\partial_y - \partial_\varphi\right), \tag{C.8a}$$
$$H_0 = i\partial_\tau, \tag{C.8b}$$
$$H_- = -i\frac{e^{i\tau}}{\sqrt{1+y^2}}\left(y\partial_\tau + i(1+y^2)\partial_y + \partial_\varphi\right), \tag{C.8c}$$
$$Q_0 = \partial_\varphi. \tag{C.8d}$$

Moreover, $\Phi = i\sqrt{2}e^{-i\tau}/\sqrt{1+y^2}$ and $\lambda = e^{i\varphi + \arctan(y)}$.

C.2.3 Black hole coordinates

Let (T, Y, θ, ψ) be the global coordinates. The NHEK line element is

$$ds^2_{NHEK} = 2M^2\,\Gamma(\theta)\left[-(-1+Y^2)dT^2 + \frac{dY^2}{-1+Y^2} + d\theta^2 + \gamma^2(\theta)\left(d\psi + Y dT\right)^2\right], \tag{C.9}$$

and the generators of its isometry group are

$$H_+ = \frac{e^{-T}}{\sqrt{-1+Y^2}}\left(Y\partial_T + (-1+Y^2)\partial_Y - \partial_\psi\right), \tag{C.10a}$$

$$H_0 = \partial_T, \tag{C.10b}$$

$$H_- = \frac{e^{T}}{\sqrt{-1+Y^2}}\left(Y\partial_T - (-1+Y^2)\partial_Y - \partial_\psi\right), \tag{C.10c}$$

$$Q_0 = \partial_\psi. \tag{C.10d}$$

Moreover, $\Phi = \sqrt{2}e^T/\sqrt{-1+Y^2}$ and $\lambda = e^{i\psi - i\,\mathrm{arctanh}(Y)}$.

C.3 $SL(2,\mathbb{R})$ covariant basis

C.3.1 Basis for 1-forms

We define a basis for 1-forms by demanding $\mathscr{L}_{H_+}\mu = 0 = \mathscr{L}_{H_0}\mu$. One has that

$$\mu^1 = \gamma^2(\theta)\hat{Q}_0 - \frac{1}{\sqrt{2}}\frac{1}{\Gamma(\theta)}\Phi H_+, \tag{C.11a}$$

$$\mu^2 = \left(1-\gamma^2(\theta)\right)\hat{Q}_0 + \frac{1}{\sqrt{2}}\frac{1}{\Gamma(\theta)}\Phi H_+, \tag{C.11b}$$

$$\mu^3 = \frac{d\theta}{\gamma(\theta)}, \tag{C.11c}$$

$$\mu^4 = \frac{d\Phi}{\Phi}. \tag{C.11d}$$

C.3.2 Basis for 2-forms

We define a basis for 2-forms by demanding $\mathscr{L}_{H_+} w = 0$ and $\mathscr{L}_{H_0} w = w$. One has that

$$w^1 = \Phi\, \mu^4 \wedge \mu^3, \tag{C.12a}$$
$$w^2 = \Phi\, \mu^1 \wedge \mu^3, \tag{C.12b}$$
$$w^3 = \Phi\, \gamma^2(\theta) \hat{Q}_0 \wedge \mu^3, \tag{C.12c}$$
$$w^4 = \Phi\, d\hat{Q}_0, \tag{C.12d}$$
$$w^5 = \Phi\, \hat{Q}_0 \wedge \mu^4, \tag{C.12e}$$
$$w^6 = \Phi\, \mu^2 \wedge \mu^1. \tag{C.12f}$$

Moreover, they obey the following properties

$$dw^i = 0 \quad \forall i \neq 3, \quad \star dw^3 = \frac{1}{\sqrt{2}} \frac{\Phi^2}{\Gamma^2(\theta)} \Phi H_+, \tag{C.13a}$$
$$\star w^1 = -w^6, \quad \star w^2 = -w^5, \quad \star w^3 = -w^4. \tag{C.13b}$$

C.3.3 Automorphism of the $SL(2,\mathbb{R}) \times U(1)$ algebra

There is a large automorphism group of the $SL(2,\mathbb{R}) \times U(1)$ algebra which allows us to change basis while preserving the commutation relations (C.3). Continuous automorphisms are parametrized by complex $(\alpha, \beta, \gamma, \delta)$ and given by

$$H_+ \to e^{-\gamma} \left[(1+\alpha\beta)^2 H_+ + 2\beta(1+\alpha\beta) H_0 + \beta^2 H_- \right], \tag{C.14a}$$
$$H_0 \to \alpha(1+\alpha\beta) H_+ + (1+2\alpha\beta) H_0 + \beta H_-, \tag{C.14b}$$
$$H_- \to e^{\gamma} \left[\alpha^2 H_+ + 2\alpha H_0 + H_- \right], \tag{C.14c}$$
$$Q_0 \to \delta\, Q_0. \tag{C.14d}$$

The rescaling of Q_0 parametrized by δ can be absorbed into a rescaling of the angle ϕ and we do not consider it any further. Note that when $\alpha = -\beta^{-1}$, $e^{\gamma} = \beta^2$, $\delta = 1$ and in the limit $\beta \to 0$ one finds the discrete automorphism given by

$$H_\pm \to H_\mp, \qquad H_0 \to -H_0, \qquad Q_0 \to Q_0. \tag{C.15}$$

Appendix D

Solutions to force-free electrodynamics in NHEK space-time

D.1 Relevant ordinary differential equations

In this section we list the five ordinary differential equations whose solutions are present in section 5.5.4.

During the resolution of the three coupled nonlinear ODEs in θ as described in section 5.5, we encountered the following nonlinear ODE for $X(\theta;h,c_1,c_2)$:

$$\begin{aligned} h^2X^2\Big[X(\gamma'X'-\gamma X'')-\gamma(h-1)(c_2^2+X^2+X'^2)\Big]+\gamma^2\gamma' XX'\Big[(h-1)c_1+hkX\Big]^2 \\ +\gamma^3\Big[(h-1)c_1+hkX\Big]\Big\{(h-1)\Big[hX^2(c_1+kX)+\big[(h-2)c_1+hkX\big]X'^2\Big] \\ +X\Big[(h-1)c_1+hkX\Big]X''\Big\}=0. \end{aligned} \tag{D.1}$$

In the case $c_1\neq 0$, one might substitute $X=c_1X_3$ and define $\xi\equiv\frac{c_2^2}{c_1^2}$. Then all the dependence in c_1 factors out. We then obtain the differential equation for $X_3(\theta;h,\xi)$ which is listed below. This ODE was also found in Zhang, Yang, and Lehner (2014). Upon setting $c_1=0$ one gets another non-linear ODE. When $c_2\neq 0$, $h\neq 0$, c_2 can be factored out of the equation upon a rescaling of X. We denote the resulting function as $X=c_2X_4^{1/h}(\theta;\Delta(h))$. The ODE for X_4 is listed below. When both $c_1=c_2=0$ and $h\neq 0$ we find a linear ODE that we denote as $X=X_1^{1/h}(\theta;\Delta(h))$.

Recall that the unphysical region beyond the velocity of light surface lies in the range $\theta_*\leq\theta\leq\pi-\theta_*$. In the following, we will assume that all functions $X(\theta)$ together with their first derivatives are finite in the physical region $0\leq\theta\leq\theta_*$ and $\pi-\theta_*\leq\theta\leq\pi$, *i.e.*, $X(\theta)<\infty$, $X'(\theta)<\infty$.

For the extreme Kerr black hole $k=1$ and γ,Γ are given in (C.2). In particular it is useful to note that $\gamma(\pi-\theta)=\gamma(\theta)$, $\gamma(0)=\gamma(\pi)=0$, $\gamma'(0)=1$, $\gamma'(\pi)=-1$ where $\theta=0$ is the north pole and $\theta=\pi$ is the south pole. Also, $\theta_*=\arcsin[\sqrt{3}-1]$ is the

lowest positive root of $\gamma(\theta)-1$. All numerical solutions will be plotted only for the extreme Kerr black hole.

1) $X_1(\theta;\Delta(h))$

$$\mathrm{ODE}_1[X_1;\Delta(h)] \equiv X_1'' + \frac{\gamma'}{\gamma}\frac{k^2\gamma^2+1}{k^2\gamma^2-1}X_1' + \Delta(h)X_1 = 0, \tag{D.2}$$

where $\Delta(h) = h(h-1)$. This ODE appears only in solution (5.65). From the physical requirement that there should not be any singular magnetic flux at the north and south poles (see Eq. (D.33)), we impose the boundary condition $X_1(0) = X_1(\pi) = 0$.

The equation is invariant under the transformations $h \to 1-h$ which leaves $\Delta(h)$ invariant: that is $X_1(\theta;h) = X_1(\theta;1-h)$. Moreover, the equation is invariant under the reflection $\theta \to \pi-\theta$ so that if $X_1(\theta)$ is a solution, so is $X_1(\pi-\theta)$.[1]

For the special case $\Delta = 0$, i.e. $h = 0$ or $h = 1$, the solution is

$$X_1(\theta;0) = C_1 + C_2\frac{5\sin\theta+\sin 3\theta}{19-16k^2+4(3+4k^2)\cos 2\theta+\cos 4\theta}. \tag{D.3}$$

However, regularity at the velocity of light surface implies $C_2 = 0$ and $X_1(\theta,0)$ is therefore constant which we fix to 0 by the boundary condition $X_1(0) = 0$. There is therefore no solution.

In general, the differential equations have regular singular points at the zeros of γ and $k^2\gamma^2-1$ which are located at $\theta_o = 0, \theta_*, \pi-\theta_*, \pi$. Indeed, for each root θ_o we have

$$\frac{\gamma'}{\gamma}\frac{\gamma^2+1}{\gamma^2-1} = \frac{1}{\theta-\theta_o} + \text{regular terms}. \tag{D.4}$$

Therefore, Frobenius' method is applicable. In the generic case, the solution reads close to the pole θ_o as a linear superposition of the power series solutions $(\theta-\theta_o)^{\lambda_\pm}\sum_{n=0} a_n(\theta-\theta_o)^n$ where $\lambda_\pm$ are the two roots of the indicial equation. In case of double roots, a logarithmic branch appears. Frobenius' series converges in the open complex disk that contains only one root.

In the range $0 \le \theta \le \theta_*$ we could start the series from the north pole or the velocity of light surface. Now, the indicial roots are 0 and 2 around the north pole while there is a double root 0 around the velocity of light surface which leads to a logarithmically divergent solution. One might however question whether such

[1] The function solution to this ODE was denoted as $S_h(\theta)$ or $S_{h,m=0}(\theta)$ in Lupsasca and Rodriguez (2015) but was not explicitly solved.

a logarithmic divergence is admissible. After all, the geometry around the velocity of light surface will be modified significantly when considering the asymptotically flat extension of the geometry. If the logarithmic divergence at the velocity of light is acceptable, one can simply write an expansion close to the north pole $X_1 \sim a_0\theta^0 + a_2\theta^2 + O(\theta^4)$ with the boundary condition $a_0 = 1$ and the choice of normalization $a_2 = 1$. The solution then exists for all (complex) values of h and is defined by a power series expansion.

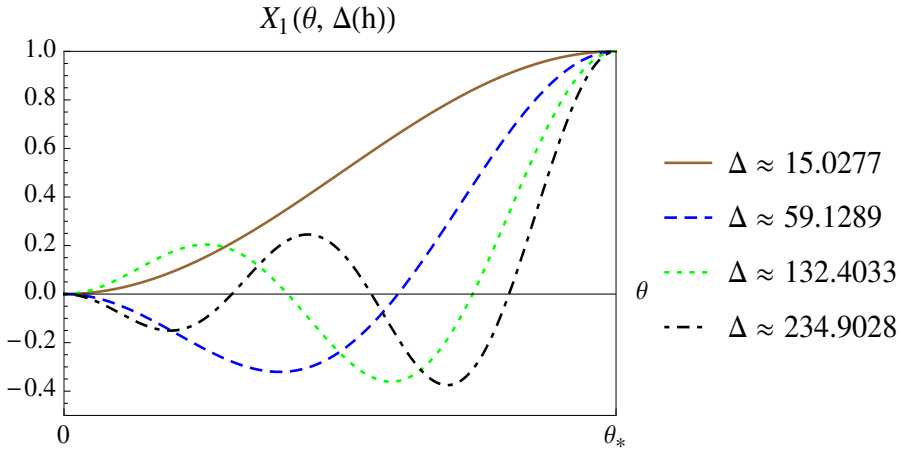

FIGURE D.1: Solutions to $\mathrm{ODE}_1[X_1;\Delta(h)]$ for the first discrete values of the parameter $\Delta(h)$ which obey the boundary conditions $X_1(0) = 0$, $X_1(\theta_*) = 1$.

If one removes the logarithmic branch, there is only one constant of integration which we fix by setting $X_1(\theta_*;\Delta(h)) = 1$. The solution then takes the form

$$X_1(\theta;\Delta(h)) = 1 + \sum_{n\geq 1} a_n(h)(\theta-\theta_*)^n, \tag{D.5}$$

where the coefficients $a_n(h)$ can easily be obtained. Now, the physical boundary condition $X_1(0) = 0$ will be obtained only for a discrete spectrum of $\Delta(h)$. The first real values of $\Delta(h)$ together with the plot of the solution $X_1(\theta;\Delta(h))$ in the physical domain are given in Fig. D.1.

2) $X_2(\theta;\Delta(h,q),c_1)$

$$\mathrm{ODE}_2[X_2;\Delta(h,q),c_1] \equiv X_2'' + \frac{\gamma'}{\gamma}X_2' + \left[\Delta(h,q) - \frac{c_1}{\gamma^2}\right]X_2 = 0, \tag{D.6}$$

where $\Delta(h,q) = h(h-1) + k^2q^2$. This equation appears in (5.89) with $c_1 = q^2$, in (5.66) with c_1 arbitrary and in (5.67) with $c_1 = 0$. The equation is invariant under all transformations of h,q that leave $\Delta(h,q)$ invariant. In the axisymmetric case

$q = 0$ and when $c_1 \neq 0$ we require from the analysis around (D.34) the boundary condition $X_2(0) = X_2(\pi) = 0$.

Let us first analyze the simplest case $c_1 = 0$. This ODE_2 generalizes the one written in Lupsasca and Rodriguez (2015) [see their Eq. (4.9)] for q arbitrary. We concentrate on solutions which are symmetrical around the equator and therefore we only consider the interval $\theta = [0, \frac{\pi}{2}]$. After performing the substitution $x = \sin^2(\theta)$, ODE_2 takes the form of the generalized Heun's equation

$$X_2'' + \frac{(\alpha+\beta+1)x^2 - (\alpha+\beta+1+a(\gamma+\delta)-\delta)x + a\gamma}{x(x-1)(x-a)} X_2' + \frac{\alpha\beta x - b}{x(x-1)(x-a)} X_2 = 0,$$

where

$$a = 2, \quad b = -\frac{\Delta}{2}, \quad \alpha\beta = -\frac{\Delta}{4}, \quad \alpha+\beta = -\frac{1}{2}, \quad \gamma = 1, \quad \delta = \frac{1}{2}. \tag{D.7}$$

Frobenius' method can be applied. There are poles at the north and south poles and at the fake pole $x = 2$. One could therefore expand in a power series at the north pole and it will converge over the region $x \in [0,1[$. It is important to note that the equator $x = 1$ ($\theta = \frac{\pi}{2}$) is not included in the radius of convergence so care should be taken. At the north pole we find 0 as a double root of the indicial equation. Removing the logarithmically divergent branch, we get the following regular convergent power series in the domain $\theta \in [0, \frac{\pi}{2}[$:

$$X_2(\theta; \Delta(h,q)) = \sum_{n=0}^{\infty} d_n(\Delta(h,q)) \sin^{2n}(\theta). \tag{D.8}$$

The solution (D.8) behaves close to the north pole as $X_2(0) = d_0$ where d_0 is arbitrary (which we fix to 1 by linearity of the equation) and $X_2'(0) = 0$. The coefficients obey the second-order recurrence relation $d_{n+1} = A_n d_n + B_n d_{n-1}$ with $d_1 = -\frac{\Delta}{4} d_0$ and

$$A_n = \frac{6n^2 - \Delta}{4(n+1)^2}, \quad B_n = -\frac{2(n-1)(2n-3) - \Delta}{8(n+1)^2}. \tag{D.9}$$

Now, a numerical convergence analysis reveals that the series expansion does not converge at the equator $x = 1$ unless $\Delta = 0$. We interpret this by the presence of a source at the equator for generic values of Δ. In Fig. D.2, we plot $X_2(\theta, \Delta(h,q))$ obtained from the series expansion truncated to order 20 for some real values of the parameter $\Delta(h,q)$ (the value of the function around $\frac{\pi}{2}$ for $\Delta \neq 0$ should be taken with a grain of salt since the series does not converge there).

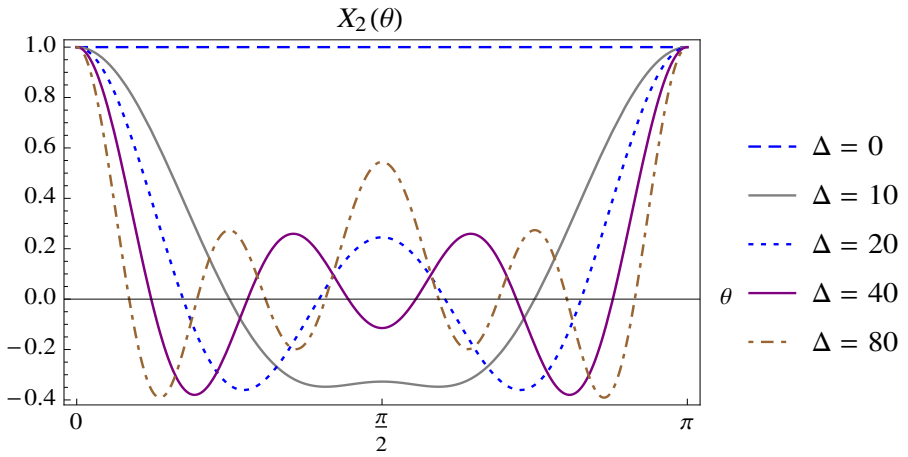

FIGURE D.2: Solutions to $\mathrm{ODE}_2[X_2;\Delta(h,q);0]$ for different values of the parameter $\Delta(h,q)$.

Let us now analyze the more general case $c_1 \neq 0$. [2] The ODE_2 is still only singular at the zeros of γ, *i.e.*, at points $\theta = 0,\pi$. After performing the substitution $z = \sin^2(\theta)$, the ODE_2 takes the following form

$$X_2''(z) + \frac{z^2-6z+4}{2z(z-1)(z-2)} X_2'(z) + \frac{(z-2)^2 c_1 - 4\Delta z}{16z(z-1)} X_2(z) = 0. \tag{D.10}$$

This makes it clear that $z = 0,1$ are regular singular points so that Frobenius's method applies. The two solutions of the indicial equation at the north pole are $\lambda_\pm = \pm\frac{\sqrt{c_1}}{2}$. In order to avoid oscillations at the poles we enforce $c_1 > 0$ from now on. Only the solution λ_+ is admissible since otherwise the solution will diverge at the north pole. In the special case where $\lambda_+ - \lambda_-$ is an integer q which incidentally occurs for $c_1 = q^2$, one independent solution contains a logarithmic branch which again diverges. Again in this case, only the solution which behaves as z^{λ_+} is admissible.

In all cases, the regular solution is given for $c_1 > 0$ by

$$X_2(z) = z^{\lambda_+} \sum_{n=0}^{\infty} a_n z^n, \tag{D.11}$$

where a_0 is an arbitrary constant and

$$a_1 = -\frac{\Delta}{4(1+\sqrt{c_1})} a_0, \tag{D.12}$$

$$a_2 = \frac{\Delta^2 - 4\Delta(1+\sqrt{c_1}) + 3c_1 + (2+c_1)\sqrt{c_1}}{32(2+c_1+3\sqrt{c_1})} a_0. \tag{D.13}$$

[2] In the case $c_1 = q^2$ this equation was considered in Lupsasca and Rodriguez (2015); see their Eq. (5.23).

For $n \geq 2$, we have $a_{m+1} = A_m a_m + B_m a_{m-1} + C_m a_{m-2}$ where

$$A_m = \frac{6m(m+\sqrt{c_1}) - \Delta}{4(m+1)(m+1+\sqrt{c_1})}, \tag{D.14}$$

$$B_m = \frac{2\Delta - 4(m-1)(2m-3) + c_1 + 2(9-4m)\sqrt{c_1}}{16(m+1)(m+1+\sqrt{c_1})}, \tag{D.15}$$

$$C_m = -\frac{c_1}{32(m+1)(m+1+\sqrt{c_1})}. \tag{D.16}$$

We fix $a_0 = 1$ without loss of generality. In the case $c_1 = 0$, we recover the recurrence relation (D.8). From (D.11) we directly see that for all $c_1 > 0$, the function X_2 obeys the boundary condition $X_2(0) = X_2(\pi) = 0$. We again observe numerically that the series (D.11) does not converge at the equator $\theta = \frac{\pi}{2}$ unless c_1 is fixed as a definite function of $\Delta(h)$,

$$c_1 = c_1(\Delta(h)), \tag{D.17}$$

which asymptotes to 0 for $\Delta = 0$ and to ∞ for $\Delta \to \infty$. For example, for $c_1(10) \approx 4.90$, $c_1(20) \approx 8.48$, $c_1(40) \approx 15.02$, $c_1(80) \approx 27.23$. In Fig. D.3, we plotted the power series solution truncated to order 20 to $\mathrm{ODE}_2[X_2; \Delta(h,q) = 15, c_1]$ for different values of the parameter c_1. Note that the boundary condition $X_2(0) = 0$ is true only for $c_1 > 0$.

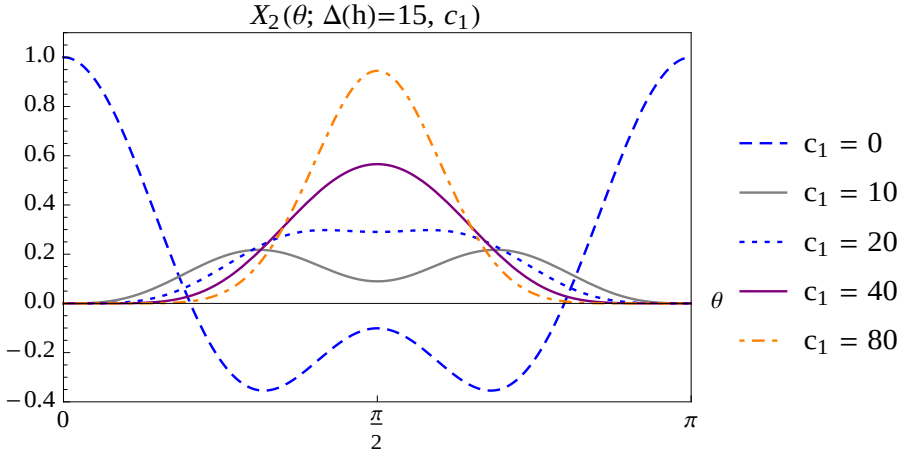

FIGURE D.3: Solutions to $\mathrm{ODE}_2[X_2; \Delta(h,q), c_1]$ for $\Delta(h,q) = 15$ and different values of c_1.

In Fig. D.4, we studied the behavior of solutions (except at $\theta = \frac{\pi}{2}$) to $\mathrm{ODE}_2[X_2; \Delta(h,q), c_1 = 3]$ by varying $\Delta(h,q)$ at constant $c_1 = 3$.

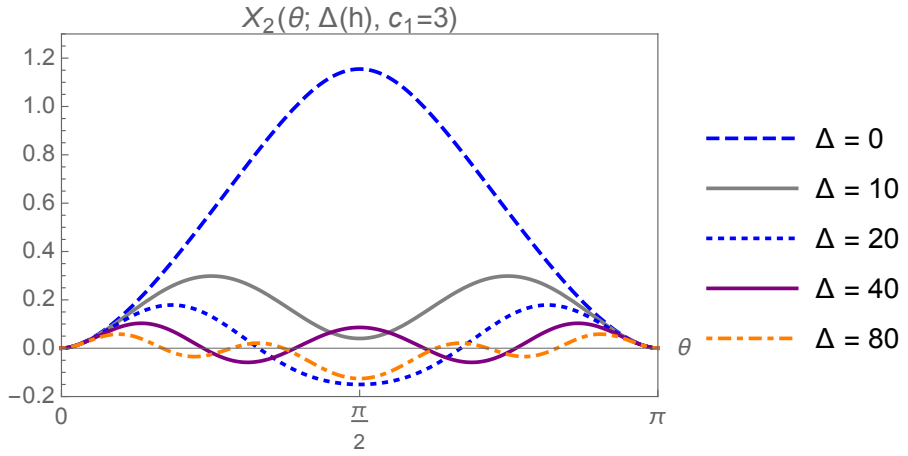

FIGURE D.4: Solutions to $\text{ODE}_2[X_2;\Delta(h,q);c_1]$ for $c_1 = 3$ and different values of $\Delta(h,q)$.

3) $X_3(\theta;h,\xi)$

$$\begin{aligned}\text{ODE}_3[X_3;h,\xi] \equiv\ & h^2X_3^2\Big[X_3(\gamma' X_3' - \gamma X_3'') - \gamma(h-1)(\xi + X_3^2 + X_3'^2)\Big] \\ & + \gamma^2\gamma' X_3 X_3'\Big[(h-1)+hkX_3\Big]^2 + \gamma^3\Big[(h-1)+hkX_3\Big]\Big\{(h-1)\Big[hX_3^2(1+kX_3) \\ & + \big[(h-2)+hkX_3\big]X_3'^2\Big] + X_3\Big[(h-1)+hkX_3\Big]X_3''\Big\} = 0.\end{aligned}$$

This ODE appears in solution (5.63). According to the discussion around (D.30) we require the boundary condition $X_3(0) = X_3(\pi) = 0$.

When $h = 0$, the equation reduces to

$$\partial_\theta\left(\gamma\partial_\theta(X_3^{-1})\right) = 0. \tag{D.18}$$

When $h = 1$, the equation reduces to $\text{ODE}_1[X_3(\theta),\Delta = 0]$, therefore

$$X_3(\theta, h = 1, \xi) = X_1(\theta;\Delta = 0). \tag{D.19}$$

We will not solve this nonlinear ODE here. When $h \neq 0,1$, the equation was considered in Zhang, Yang, and Lehner (2014); Lupsasca and Rodriguez (2015) and solved in Zhang, Yang, and Lehner (2014) for the case $h = -1$.

4) $X_4(\theta;\Delta(h))$

$$\text{ODE}_4[X_4;\Delta(h)] \equiv X_4'' + \frac{\gamma'}{\gamma}\frac{k^2\gamma^2+1}{k^2\gamma^2-1}X_4' + \Delta(h)X_4 + \frac{\Delta(h)}{1-k^2\gamma^2}X_4^{\frac{h-2}{h}} = 0, \tag{D.20}$$

where $\Delta(h) = h(h-1)$ which we can rewrite as

$$\text{ODE}_1[X_4;\Delta(h)] + \frac{\Delta(h)}{1-k^2\gamma^2}X_4^{\frac{h-2}{h}} = 0. \tag{D.21}$$

This ODE appears in solution (5.64). According to the discussion around (D.32) we require the boundary condition $X_4(0) = X_4(\pi) = 0$.

We will not solve this nonlinear ODE here. Note that when $h = 2$ the equation becomes linear with a nonhomogenous term.

5) $X_5(\theta; h, q)$

$$X_5'' + \frac{\gamma'}{\gamma}\left[1 - \frac{2h(h-1)\gamma^2}{(1-k^2\gamma^2)(\Delta(h,q)\gamma^2 - q^2)}\right]X_5' + \left[\Delta(h,q) - \frac{q^2}{\gamma^2}\right]X_5 = 0, \tag{D.22}$$

where $\Delta(h,q) = h(h-1) + k^2q^2$. This linear ODE appears in solution (5.61).

It admits the symmetries

$$X_5(\theta; h, q) = X_5(\theta; 1-h, q) = X_5(\theta; h, -q) = X_5(\theta; 1-h, -q). \tag{D.23}$$

We note the special cases

$$X_5(\theta; h, q=0) = X_1(\theta, \Delta(h)), \tag{D.24}$$

$$X_5(\theta; h=0, q) = X_2(\theta; \Delta = k^2q^2, q^2), \tag{D.25}$$

$$X_5(\theta; h=1, q) = X_2(\theta; \Delta = k^2q^2, q^2). \tag{D.26}$$

Since the ODE for X_1 was analyzed previously we concentrate on $q \neq 0$ only. [3]

There are always two regular singular points in the range $0 \leq \theta \leq \frac{\pi}{2}$: first at $\theta = 0$ (north pole), and then at $\theta = \theta_* = \arcsin(\sqrt{3}-1)$ (velocity of light surface). When h is real and for $q \neq 0$, there is a regular singular point at the real root of $\Delta\gamma^2 = q^2$ which is always in the range $0 \leq \theta \leq \frac{\pi}{2}$. There is also an imaginary root which obeys $\sin\theta \geq \sqrt{\frac{1}{2}(7+\sqrt{33})} \approx 2.52$ (bound reached at $h = \frac{1}{2}$, $q = 1$) so it is irrelevant for discussing convergence in the interval $0 \leq \sin\theta \leq 1$.

The two independent solutions behave close to $\theta = 0$ as θ^q and θ^{-q}, while they behave close to $\theta = \theta_*$ as $\log(\theta - \theta_*)$ and $(\theta - \theta_*)^0$. If one only insists in having a solution smooth at the north (and south) poles, a solution always exists but it will be generically logarithmically divergent at the velocity of light surface. In order to avoid singularities, we need to interpolate between the solutions θ^q (we assume $q > 0$) at $\theta = 0$ and $(\theta - \theta_*)^0$ at $\theta = \arcsin(\sqrt{3}-1)$. This involves a shooting method which will discretize the possible values of h as a function of q. We then normalize the solution with $X_5(\theta_*) = 1$. There is therefore no more free continuous constant of integration. In the range $0 \leq h \leq 1$ and $q > 0$ the other singularities are not in the range between the north pole and the velocity of light surface. For $h \geq 1$ and

[3] This ODE was also found in Lupsasca and Rodriguez (2015); see their Eq. (3.29) where X_5 is denoted as $S_{h,m}$. Our analysis of the ODE however slightly differs.

$h \leq 0$, they are but we checked that the indicial equation around the real pole and imaginary pole has exponents 0 and 2 so an interpolating function between the velocity of light surface and the north pole will be smooth. The regular solutions for the first four real values of h are depicted on Fig. D.5 for $q = 1$.

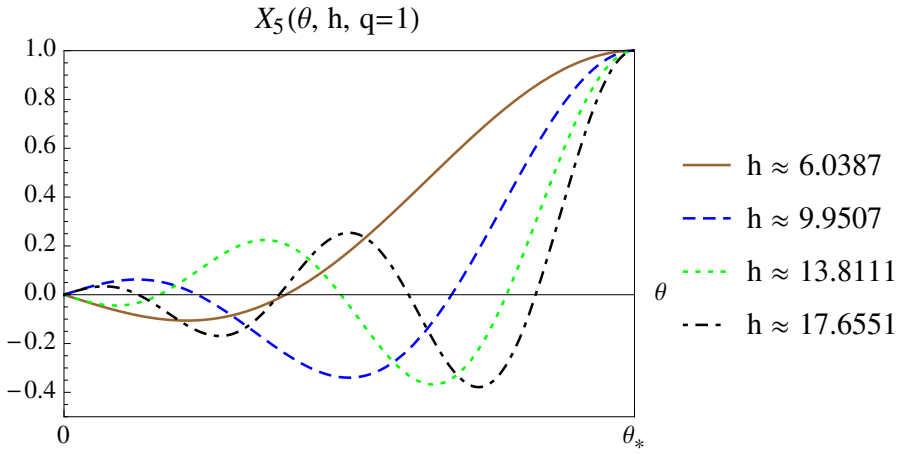

FIGURE D.5: Solutions to $\mathrm{ODE}_5[X_5; h; q = 1]$ for $q = 1$ and different values of h such that $X_5(0) = 0$.

D.2 Properties of all highest-weight solutions

In this section, we analyze the properties of all solutions listed in section 5.5.4. In particular, for each vector potential we compute and list its field strength and its current. These properties constitute the ID card of each solution. We also compute the canonical Euler potentials (for definitiveness in Poincaré coordinates) defined in section 5.3. We finally check for regularity of the solutions at the poles in order to derive the relevant boundary conditions for the ODEs that the solutions depend on.

We recall the definitions $\Delta(h) = h(h-1)$ and $\Delta(h,q) = h(h-1) + k^2 q^2$.

(h,q)-eigenstates

There are two classes of solutions with arbitrary nonvanishing highest-weight h and $U(1)$-charge q, describing stationary and nonaxisymmetric field configurations.

Poincaré magnetic

$$
\begin{aligned}
A_{(h,q)} &= \Phi^h \lambda^q \left[X_5 \mu^2 - \frac{i q \gamma (1-k^2\gamma^2)}{q^2 - \Delta(h,q)\gamma^2} X_5' \mu^3 \right] \\
F_{(h,q)} &= h \Phi^{h-1} \lambda^q \left[\frac{\gamma X_5'}{q^2 - \Delta(h,q)\gamma^2} \Big(- i q (1-k^2\gamma^2) w^1 + (1-h) k \gamma^2 w^2 - \frac{w^3}{k} \Big) \right. \\
&\qquad \left. + X_5 (w^4 - w^5) \right] \\
J_{(h,q)} &= -\Phi^h \lambda^q h k \left[X_5 + \frac{2(1-h)\gamma\gamma'}{(1-k^2\gamma^2)(q^2 - \Delta(h,q)\gamma^2)} X_5' \right] \frac{\Phi H_+}{\sqrt{2}\Gamma^2}
\end{aligned}
$$

where $X_5 = X_5(\theta; h, q)$. Since the current keeps its direction upon changing h, q, one might linearly superpose solutions with different h, q. The current $J_{(h,q)}$ and its complex conjugate $(J_{(h,q)})^*$ are proportional to each other. Then, we can obtain a real solution by adding up the vector potential $A_{(h,q)}$ and its complex conjugate.

We do not consider the trivial case $h = 0$, because it gives no field strength $F = 0$. For $h = 1$, $q \neq 0$ the solution exists and the function X_5 becomes $X_5(\theta; 1, q) = X_2(\theta, k^2 q^2, q^2)$. In the case $q = 0$, $h \neq 0, 1$, we recover the Poincaré magnetic solution (5.65) after using the identity $X_5(\theta; h, 0) = X_1(\theta; h)$.

In order to get physical insight, it is useful to derive the functional expression of Euler potentials. We only consider Poincaré coordinates and $q \neq 0$. The field strength describes a stationary and Q_0-eigenstate configuration with $i_{\partial_T} F = 0$ and $df = 0$ according to the analysis of section 5.3. Therefore it takes the form (5.34) with

$$
\psi(R,\theta) = \frac{X_5}{R^h}, \qquad \partial_\theta \psi_2(R,\theta) = -iq \left(\frac{1-k^2\gamma^2}{q^2 - \Delta(h,q)\gamma^2} \right) \frac{X_5'}{X_5} \tag{D.27}
$$

The Euler potential ψ is singular at the Poincaré horizon $R = 0$, unless h is negative. In the special case $h = 1$ and $q \neq 0$, we can easily integrate ψ_2 and obtain $\psi_2(\theta) = -\frac{i}{q} \ln(X_5) + \text{const}$.

Poincaré generic

$$
\begin{aligned}
A_{(h,q)} &= \Phi^h \lambda^q \left[h(h-1) X_2 \mu^1 - k q^2 X_2 \mu^2 + i k q \gamma X_2' \mu^3 \right] \\
F_{(h,q)} &= \Phi^{h-1} \lambda^q h \left[\gamma X_2' (i k q w^1 - (h-1) w^2) + \right. \\
&\qquad \left. + X_2 \Big(- \frac{k^2 q^2 + (h-1)^2}{k} w^4 + k q^2 w^5 + i (h-1) q w^6 \Big) \right] \\
J_{(h,q)} &= \Phi^h \lambda^q \frac{hk}{\Gamma} X_2 \left[(h-1)^2 \gamma^2 \hat{Q}_0 + k q^2 \frac{\Phi H_+}{\sqrt{2}\Gamma} - i q (h-1) \mu^4 \right]
\end{aligned}
$$

where $X_2 = X_2(\theta;\Delta(h,q),c_1 = q^2)$.

The case $h = 0$ is trivial since $F = 0$. The current is not proportional to its complex conjugate, unless for the special cases $q = 0$ or $h = 1$ or $h = 1 + i\mu$ for any real μ. The case $q = 0$ coincides with the solution (5.67) and it will be analyzed below. The case $h = 1$ actually coincides with the solution (5.61) for $h = 1$. It was just analyzed in the previous subsection. The third class is an independent real solution.

In the generic case $q \neq 0$, $h \neq 0,1$, the field strength describes a stationary and Q_0-eigenstate configuration with $i_{\partial_T} F \neq 0$. The canonical Euler potentials in Poincaré coordinates can therefore be written as (5.22) where

$$\boxed{\chi_1(R,\theta) = h(h-1)\frac{X_2}{R^{h-1}}, \qquad \chi_2(R) = -\frac{ikq}{h-1}\frac{1}{R}, \qquad \kappa(e^{iq\Phi}\chi_1) = 0.} \tag{D.28}$$

$(h \neq 0, q = 0)$-eigenstates

Poincaré generic

$$\boxed{\begin{aligned}
A_{(h,0)} &= c_1^h \Phi^h \left[-X_3^{h-1}\mu^1 + X_3^h \mu^2 \pm \sqrt{\xi} X_3^{h-1}\mu^3\right], \qquad c_1 \neq 0 \\
F_{(h,0)} &= c_1^h \Phi^{h-1} X_3^{h-2}\left[\pm h\sqrt{\xi} X_3 w^1 + \gamma((h-1)+hkX_3)X_3' w^2 - \frac{h}{k\gamma}X_3' X_3 w^3 + \right. \\
&\quad \left. + \left(hX_3 + \frac{(h-1)}{k}\right)X_3 w^4 - hX_3^2 w^5\right] \\
J_{(h,0)} &= c_1^h \Phi^h X_3^{h-2}\left[(h-1)A(\theta;h,\xi)\hat{Q}_0 - hX_3\frac{h\xi/\Gamma - A(\theta;h,\xi)}{\gamma^2}\frac{\Phi H_+}{\sqrt{2}\Gamma}\right. \\
&\quad \left. \mp \frac{h(h-1)\sqrt{\xi}}{\Gamma}X_3\mu^3 \pm \frac{h(h-1)\sqrt{\xi}}{\gamma\Gamma}X_3'\mu^4\right]
\end{aligned}}$$

where $A(\theta;h,\xi)$ is given by

$$\begin{aligned}
&(\Gamma[\gamma^2(h-1+hkX_3)^2 - h^2X_3^2])A(\theta;h,\xi) = \\
&\quad X_3[h^2\xi - \gamma^2(h-1+hkX_3)][-hX_3 + k\gamma^2(h-1+hkX_3)] \\
&\quad + 2h\gamma X_3(h-1+hkX_3)\gamma' X_3' - h(h-1)\gamma^2 X_3'^2,
\end{aligned} \tag{D.29}$$

where $X_3 = X_3(\theta;h,\xi)$. In the case $h, c_1 \in \mathbb{R}$ and $\xi \geq 0$, the expression of the vector potential $A_{(h,0)}$ is real. For $h = 1$, we get the Poincaré generic solution (5.74) [because $X_3(\theta,1,\xi) = X_1(\theta;0) = \text{constant}$].

The Euler potentials for this stationary and axisymmetric configuration fall in the category (5.4) where in Poincaré coordinates

$$\boxed{\psi(R,\theta)=\left(\frac{c_1X_3}{R}\right)^h,\qquad I(\psi)=\mp hc_1\sqrt{\xi}\psi^{\frac{h-1}{h}},\qquad \Omega(\psi)=c_1\frac{h-1}{h}\psi^{-\frac{1}{h}}} \tag{D.30}$$

Since $2\pi\psi(R,\theta)$ is the magnetic flux through the loop of revolution defined by (r,θ), the requirement of having no singular magnetic flux at the north and south poles is equivalent to the boundary conditions $X_3(0)=X_3(\pi)=0$.

These potentials allow us to recognize the solution as the one described in Zhang, Yang, and Lehner (2014) upon identifying their quantities in terms of ours as

$$\alpha=-h,\quad f(\theta)=(c_1X_3)^h,\quad g(\theta)=\frac{h-1}{h}\frac{1}{X_3},\quad C=c_1\frac{h-1}{h},\quad D=\pm\frac{c_1}{2\pi}\sqrt{\xi}.$$

Poincaré magnetic

$$\boxed{\begin{aligned}
A_{(h,0)}&=c_2^h\Phi^h\left[X_4\mu^2\pm X_4^{\frac{h-1}{h}}\mu^3\right]\\
F_{(h,0)}&=c_2^h\Phi^{h-1}\left[\pm hX_4^{\frac{h-1}{h}}w^1+k\gamma X_4'w^2-\frac{1}{k\gamma}X_4'w^3+hX_4(w^4-w^5)\right]\\
J_{(h,0)}&=c_2^h\frac{\Phi^h}{\Gamma}\left[h(h-1)X_4^{\frac{h-2}{h}}\hat{Q}_0-kX_4\frac{C(\theta;h)}{\gamma(k^2\gamma^2-1)}\frac{\Phi H_+}{\sqrt{2\Gamma}}\mp h(h-1)X_4^{\frac{h-1}{h}}\mu^3\right.\\
&\qquad\left.\pm\frac{h(h-1)}{\gamma}X_4^{-\frac{1}{h}}X_4'\mu^4\right]
\end{aligned}}$$

where $C(\theta;h)$ is given by

$$C(\theta;h)=h\gamma\left((h-1)X_4^{-2/h}-1\right)-\frac{2\gamma'X_4'}{X_4}+hk^2\gamma^3. \tag{D.31}$$

Since $\partial_T F=0$, the Euler potentials for this stationary and axisymmetric configuration are given by (5.4) where in Poincaré coordinates

$$\boxed{\psi(R,\theta)=\left(\frac{c_2}{R}\right)^h X_4,\qquad I(\psi)=\mp hc_2\psi^{\frac{h-1}{h}},\qquad \Omega(\psi)=0} \tag{D.32}$$

Since $2\pi\psi(R,\theta)$ is the magnetic flux through the loop of revolution defined by (R,θ), the requirement of having no singular magnetic flux at the north and south poles is equivalent to the boundary conditions $X_4(0)=X_4(\pi)=0$. In turn, regularity of the current at the poles then requires $h\geq 2$.

Poincaré magnetic

$$\boxed{\begin{aligned} A_{(h,0)} &= \Phi^h X_1 \mu^2 \\ F_{(h,0)} &= \Phi^{h-1}\left[k\gamma X_1^{'} w^2 - \frac{1}{k\gamma} X_1^{'} w^3 + h X_1 (w^4 - w^5)\right] \\ J_{(h,0)} &= \Phi^{h-1} \frac{2k\gamma' X_1' + hk\gamma X_1 (1-k^2\gamma^2)}{(-1+k^2\gamma^2)\gamma\Gamma} \frac{\Phi H_+}{\sqrt{2}\Gamma} \end{aligned}}$$

where $X_1 = X_1(\theta;\Delta(h))$. Currents with different values of h are collinear so one might linearly superpose such solutions.

The Euler potentials for this stationary and axisymmetric configuration are

$$\boxed{\psi(R,\theta) = \frac{X_1}{R^h}, \qquad I(\psi) = 0, \qquad \Omega(\psi) = 0} \tag{D.33}$$

Since $2\pi\psi(R,\theta)$ is the magnetic flux through the loop of revolution defined by (R,θ), the requirement of having no singular magnetic flux at the north and south poles is equivalent to the boundary conditions $X_1(0) = X_1(\pi) = 0$.

Poincaré nontoroidal

$$\boxed{\begin{aligned} A_{(h,0)} &= \Phi^h X_2 \left[h\mu^1 \pm \sqrt{c_1}\mu^3\right] \\ F_{(h,0)} &= h\Phi^{h-1} X_2 \left(\pm\sqrt{c_1} w^1 - \gamma \frac{X_2'}{X_2} w^2 - \frac{(h-1)}{k} w^4\right) \\ J_{(h,0)} &= \Phi^h \frac{hX_2}{\gamma^2\Gamma}\left[k\gamma^2[(h-1)\gamma^2 - c_1]\hat{Q}_0 + c_1 \frac{\Phi H_+}{\sqrt{2}\Gamma} \mp (h-1)\gamma^2\sqrt{c_1}\mu^3 \right. \\ &\qquad \left. \pm \gamma\sqrt{c_1}\frac{X_2'}{X_2}\mu^4\right] \end{aligned}}$$

where $X_2 = X_2(\theta;h,c_1)$.

For $h = 0$ this solution has vanishing field strength so is pure gauge. For $c_1 = 0$ we get a Poincaré electric and nontoroidal solution, which has the special property to admit descendants solutions. The solution is real in Poincaré coordinates for $c_1 \geq 0$, $h \in \mathbb{R}$.

Since $i_\Phi F = 0$, the electromagnetic field in terms of Euler potentials takes the special form (5.8) where in Poincaré coordinates,

$$\boxed{\chi(R,\theta) = h\frac{X_2}{R^{h-1}}, \qquad I(\chi) = \mp\sqrt{c_1}\chi} \tag{D.34}$$

We observe that in order to prevent singular line currents we need to enforce a vanishing polar current I at north and south poles, which requires the existence of

the boundary conditions $X_2(0) = X_2(\pi) = 0$ for $c_1 \neq 0$. For $c_1 = 0$ the polar current vanishes but the electrostatic potential χ is constant on the north and south poles.

$(h = 0, q \neq 0)$-eigenstates

Poincaré electric

$$\boxed{\begin{aligned} A_{(0,q)} &= \lambda^q e^{\pm\int \frac{q}{\gamma} d\theta} \mu^1, \\ F_{(0,q)} &= \lambda^q e^{\pm\int \frac{q}{\gamma} d\theta} \left(\mp q w^1 + \frac{1}{k} w^4 + i q w^6 \right) \\ J_{(0,q)} &= \lambda^q \frac{k}{\Gamma} e^{\pm\int \frac{q}{\gamma} d\theta} \left[-(q^2+\gamma^2)\hat{Q}_0 + iq(\pm q\mu^3 - \mu^4) \right] \end{aligned}}$$

The field strength is singular at either the north or south pole depending upon the sign. The solution might however be interesting if it is split at the equator with regular north and south branches.

In terms of Euler potentials and in Poincaré coordinates, we are in the case (5.22) where

$$\boxed{\chi_1(R,\theta) = R e^{\pm\int \frac{q}{\gamma} d\theta}, \qquad \chi_2(R,\theta) = 0, \qquad \kappa(\phi_1) = 0} \tag{D.35}$$

The vanishing of χ_2 is related to the absence of magnetic field.

$(h = 1, q \neq 0)$-eigenstates

Poincaré electric - admitting descendants

$$\boxed{\begin{aligned} A_{(1,q)} &= \Phi \lambda^q e^{\pm\int \frac{q}{\gamma} d\theta} \mu^1 \\ F_{(1,q)} &= q \lambda^q e^{\pm\int \frac{q}{\gamma} d\theta} (\mp w^2 + i w^6) \\ J_{(1,q)} &= \Phi \lambda^q e^{\pm\int \frac{q}{\gamma} d\theta} \frac{k q^2}{\Gamma} (-Q_0 \pm i\mu^3) \end{aligned}}$$

The field strength is again singular at either the north or south pole depending upon the sign. The solution might however be interesting if it is split at the equator with regular north and south branches. The direction of the current does not depend upon q and therefore one can linearly superpose solutions with different q's. The solution admits descendants.

In terms of Euler potentials and in Poincaré coordinates, we are again in the case (5.22) where

$$\boxed{\chi_1(\theta) = e^{\pm\int \frac{q}{\gamma} d\theta}, \qquad \chi_2(R,\theta) = 0, \qquad \kappa(\phi_1) = 0} \tag{D.36}$$

$(h(q) = \pm ikq, q \neq 0)$-eigenstates

The two following classes of solutions feature a charge-dependent weight h.

Poincaré generic

$$\boxed{\begin{aligned}
A_{(h(q),q)} &= \Phi^h \lambda^q e^{s_2 \int \frac{d\theta}{\gamma}} \Big(ikq\mu^1 + iq\mu^2 + s_2\mu^3 \Big), \qquad s_2 = -1 \text{ or } 1 \\
F_{(h(q),q)} &= ikq\Phi^{h-1}\lambda^q e^{s_2 \int \frac{d\theta}{\gamma}} \Big(\pm s_2 w^1 - s_2 w^2 + \frac{1}{k} w^4 \mp iq w^5 + iq w^6 \Big) \\
J_{(h(q),q)} &= \Phi^h \lambda^q \frac{kq}{\Gamma} e^{s_2 \int \frac{d\theta}{\gamma}} \Big([\mp q + ik(q^2-1) - k(i \pm kq)\gamma^2]\hat{Q}_0 \\
&\quad + [\pm kq - \frac{i(q^2-1)}{\gamma^2}] \Big(\frac{\Phi H_+}{\sqrt{2}\Gamma} \pm \mu^4 \Big) \pm is_2\mu^3 \Big)
\end{aligned}}$$

The solution is pure gauge when $q = 0$. In terms of Euler potentials and in Poincaré coordinates, we are in the case (5.22) where

$$\boxed{\chi_1(R,\theta) = \frac{ikq}{R^{h-1}} e^{s_2 \int \frac{d\theta}{\gamma}}, \qquad \chi_2(R) = \mp \frac{1}{R}, \qquad \kappa(\phi_1) = 0} \tag{D.37}$$

Poincaré generic

$$\boxed{\begin{aligned}
A_{(h(q),q)} &= \Phi^h \lambda^q \Big[k\mu^1 + \mu^2 \Big] \\
F_{(h(q),q)} &= \Phi^{h-1}\lambda^q \Big(w^4 + ikq(\mp w^5 + w^6) \Big) \\
J_{(h(q),q)} &= \Phi^h \lambda^q \frac{k}{\Gamma} (\pm q + ik\gamma^2) \Big((i \pm kq) Q_0 + \frac{q}{\gamma^2} \Big(\mp \frac{\Phi H_+}{\sqrt{2}\Gamma} - \mu^4 \Big) \Big)
\end{aligned}}$$

In terms of Euler potentials and in Poincaré coordinates, we are in the case (5.22) where

$$\boxed{\chi_1(R) = \frac{k}{R^{h-1}}, \qquad \chi_2(R) = \pm \frac{1}{R}, \qquad \kappa(\phi_1) = 0} \tag{D.38}$$

$(h(q) = 1 \pm ikq, q \neq 0)$-eigenstates

Poincaré generic - null

$$\boxed{\begin{aligned}
A_{(h(q),q)} &= \Phi^h \lambda^q \Big[ha_1(\theta)\mu^1 \pm iqa_1(\theta)\mu^2 \pm \gamma a_1'(\theta)\mu^3 \Big] \\
F_{(h(q),q)} &= h\Phi^{h-1}\lambda^q \Big[\gamma a_1'(\theta)(\pm w^1 - w^2) + iqa_1(\theta)(\mp w^5 + w^6) \Big] \\
J_{(h(q),q)} &= \Phi^h \lambda^q \frac{(1 \pm ikq)[q^2 a_1 - \gamma \partial_\theta(\gamma a_1')]}{\gamma^2 \Gamma} \Big(k\gamma^2 \hat{Q}_0 - \frac{\Phi H_+}{\sqrt{2}\Gamma} \mp \mu^4 \Big)
\end{aligned}}$$

where $a_1(\theta)$ is an arbitrary function. It is a null solution ($F_{\mu\nu}F^{\mu\nu} = 0$). The current is nonvanishing for $q \neq 0$. Indeed, the current vanishes when $a_1(\theta)$ obeys $a_1'' + \frac{\gamma'}{\gamma} a_1' - \frac{q^2}{\gamma^2} a_1 = 0$. After a closer look at this differential equation, we conclude that

a solution is given by $X_2(\theta;\Delta(h(q),q)=0,c_1=q^2)$. The constraint $\Delta(h(q),q)=0$ however implies $q=0$ in contradiction to our assumption $q\neq 0$.

In terms of Euler potentials and in Poincaré coordinates, we are in the case (5.22) where

$$\boxed{\chi_1(R,\theta)=\frac{ha(\theta)}{R^{h-1}},\qquad \chi_2(R)=\pm\frac{1}{R},\qquad \kappa(\phi_1)=0} \tag{D.39}$$

$(h=1,q=0)$-eigenstates

Poincaré nontoroidal - null

$$\boxed{\begin{aligned}A_{(1,0)}&=\Phi\Big[a_1(\theta)\mu^1\pm\sqrt{c_3+[\gamma a_1'(\theta)]^2}\mu^3\Big]\\ F_{(1,0)}&=\pm\sqrt{c_3+[\gamma a_1'(\theta)]^2}\,w^1-\gamma a_1'(\theta)\,w^2\\ J_{(1,0)}&=\Phi\frac{\partial_\theta(\gamma a_1')}{\Gamma}\left[-k\gamma\hat{Q}_0+\frac{\Phi H_+}{\sqrt{2}\Gamma}\pm\frac{a_1'}{\sqrt{c_3+[\gamma a_1'(\theta)]^2}}\mu^4\right]\end{aligned}}$$

It is a null solution ($F_{\mu\nu}F^{\mu\nu}=0$). This class of solutions does not overlap with the class above. The current is vanishing when $\partial_\theta(\gamma a_1')=0$, i.e., when $a_1=c_2+\int\frac{c_1}{\gamma}d\theta$, where c_1 and c_2 are two real constants. Regularity fixes $c_1=0$ so only constant a_1 solutions obey Maxwell's equations.

In terms of Euler potentials, the field strength reads as (5.8) where

$$\boxed{\chi(R,\theta)=a_1(\theta),\qquad I(\chi)=\mp\sqrt{c_3+[\gamma\chi']^2}} \tag{D.40}$$

We see that we need $c_3=0$ in order to have a regular configuration (no polar current on the $\theta=0$ axis). We also impose that $a_1(\theta)$ must be regular at the poles.

$(h=0,q=0)$-eigenstates

Poincaré generic - admitting descendants

$$\boxed{\begin{aligned}A_{(0,0)}&=\Big(c_1+c_3\int\frac{d\theta}{\gamma}\Big)\mu^1\\ F_{(0,0)}&=\Phi^{-1}\Big(-c_3w^2+\frac{c_1+c_3\int\frac{d\theta}{\gamma}}{k}w^4\Big)\\ J_{(0,0)}&=-\frac{k\gamma^2}{\Gamma}\Big(c_1+c_3\int\frac{d\theta}{\gamma}\Big)Q_0\end{aligned}}$$

The solution with $c_3\neq 0$ is singular at the poles. Indeed,

$$\int\frac{d\theta}{\gamma}=\frac{\cos(\theta)}{2}+\ln\Big[\tan\Big(\frac{\theta}{2}\Big)\Big]. \tag{D.41}$$

Therefore we fix $c_3 = 0$. The solution then becomes electric without toroidal fields. In fact, it is just the maximally symmetric solution. It is related to (5.75) by a gauge transformation.

Appendix E

Spherical harmonics, multipole moments and surface charges

E.1 Notation and conventions

Throughout this appendix, we use the conventions in Thorne (1980). We adopt geometric units, $G = 1$, $c = 1$, and Minkowski metric with mostly plus signature, $\eta = \text{diag}(-1,+1,+1,+1)$, to raise and lower space-time indices. Space-time indices are denoted by Greek letters, while spatial indices are denoted by Latin letters. Multi-index tensors are abbreviated as

$$T_{A_l} \equiv T_{a_1 a_2 \ldots a_l}. \tag{E.1}$$

Round brackets stand for symmetrization $T_{(ab)} = \frac{1}{2}(T_{ab}+T_{ba})$, while squared brackets stand for antisymmetrization $T_{[ab]} = \frac{1}{2}(T_{ab} - T_{ba})$. The unit radial vector in the x_i direction is denoted as $n_i = x_i/r$, where $r = |\mathbf{x}| = \sqrt{x^2+y^2+z^2}$, and $N_{A_l} = n_{a_1} \ldots n_{a_l}$. The transverse projection tensor $P_{ij} = \delta_{ij} - n_i n_j$ is used to construct the *transverse* (T) part of a tensor field

$$[T_{a_1 a_2 \ldots a_l}]^T = P_{a_1 a_1'} P_{a_2 a_2'} \ldots P_{a_l a_l'} T_{a_1' a_2' \ldots a_l'}. \tag{E.2}$$

The *transverse-traceless* (TT) part of a rank-two tensor field is defined as

$$[T_{ij}]^{TT} = P_{ia} P_{jb} T_{ab} - \frac{1}{2} P_{ij} \left(P_{ab} T_{ba}\right). \tag{E.3}$$

The *symmetric-transverse-traceless* (STT) part of a tensor field of rank-two $[T_{ij}]^{STT}$ is the symmetric part of $[T_{ij}]^{TT}$. Finally, we denote by capital script letters those

tensor fields that are fully *symmetric and trace-free* (STF):

$$\begin{aligned} \mathcal{T}_{A_l} \equiv [T_{A_l}]^{STF} &= \sum_{n=0}^{[l/2]} a_n \delta_{(a_1 a_2} \dots \delta_{a_{2n-1} a_{2n}} S_{a_{2n+1} \dots a_l) j_1 j_1 \dots j_n j_n}, \\ a_n &= (-1)^n \frac{l!(2l-2n-1)!!}{(l-2n)!(2l-1)!!(2n)!!}, \end{aligned} \tag{E.4}$$

where $S_{A_l} = [T_{A_l}]^S$ is the fully symmetric tensor field constructed from T_{A_l}. As an explicit example of a tensor of rank-2, one has $\mathcal{T}_{ij} = [T_{ij}]^S - \frac{1}{3}\delta_{ij} T_{kk}$.

E.2 Spherical harmonics

In this Appendix, we recall the definitions and the main properties of spherical harmonics used throughout this thesis and strictly necessary for our computation. We refer the reader to Thorne (1980) for further properties.

E.2.1 Scalar spherical harmonics

The *pure-orbital scalar spherical harmonics* $Y^{lm}(\theta,\phi)$ are eigenfunctions of the squared *orbital angular momentum* operator $\mathbf{L}^2$, which is defined as the angular part of the Laplacian operator ∇^2 in spherical coordinates (r,θ,ϕ):

$$\nabla^2 = \frac{1}{r^2}\frac{\partial}{\partial r}\left(r^2 \frac{\partial}{\partial r}\right) - \frac{\mathbf{L}^2}{r^2}, \qquad \mathbf{L}^2 = -\left[\frac{1}{\sin\theta}\frac{\partial}{\partial\theta}\left(\sin\theta\frac{\partial}{\partial\theta}\right) + \frac{1}{\sin^2\theta}\frac{\partial^2}{\partial\phi^2}\right]. \tag{E.5}$$

The minus sign in the definition of $\mathbf{L}^2$ is taken in order to have positive eigenvalues $l(l+1)$. Explicitly, the pure-orbital scalar spherical harmonics are given by

$$Y^{lm}(\theta,\phi) = C^{lm} e^{im\phi} P^{lm}(\cos(\theta)), \tag{E.6}$$

where $P^{lm}(x)$ are the associated Legendre polynomials

$$P^{lm}(x) = (-1)^m \left(1-x^2\right)^{m/2} \frac{d^m P^l(x)}{dx^m}, \tag{E.7}$$

and C^{lm} are the normalization factors

$$C^{lm} = (-1)^m \sqrt{\frac{2l+1}{4\pi}\frac{(l-m)!}{(l+m)!}}. \tag{E.8}$$

Scalar spherical harmonics are orthonormal on the two-sphere S^2

$$\int Y^{lm} \bar{Y}^{l'm'} d\Omega = \delta_{ll'}\delta_{mm'}, \tag{E.9}$$

where $\bar{Y}^{lm} = (-1)^m Y^{l-m}$ is the complex conjugate of Y^{lm} and $d\Omega = \sin\theta d\theta d\phi$.

Any smooth scalar function $f(\theta,\phi)$ can be expanded either in pure-orbital scalar spherical harmonics with complex coefficients or in terms of tensor product of l unit radial vectors with STF-l tensor coefficients:

$$f(\theta,\phi) = \sum_{l=0}^{\infty}\sum_{m=-l}^{m=l} F^{lm} Y^{lm} = \sum_{l=0}^{\infty} \mathcal{F}_{A_l} N_{A_l}. \tag{E.10}$$

In the main text we sometimes switch between Y^{lm} and Y_{lm} for the ease of notation.

For practical applications, it is convenient to expand functions in terms of the *real* spherical harmonics Y_l^m which we define in terms of standard complex spherical harmonics Y_{lm} as

$$C^{lm} Y_l^m \equiv \begin{cases} \frac{i}{\sqrt{2}}(Y_{l,m} - (-1)^m Y_{l,-m}) & m<0, \\ Y_{l,0} & m=0, \\ \frac{1}{\sqrt{2}}(Y_{l,-m} + (-1)^m Y_{l,m}) & m>0. \end{cases} \tag{E.11}$$

Note that we have removed the normalization factor for the real harmonics. For example, the first few real harmonics will be

$$Y_0^0 = 1, \qquad Y_1^1 = \frac{x}{r}, \qquad Y_1^{-1} = \frac{y}{r}, \qquad Y_1^0 = \frac{z}{r}. \tag{E.12}$$

E.2.2 Vector spherical harmonics

The *pure-spin vector spherical harmonics* of magnetic ($B-$), electric ($E-$) and radial ($R-$) type are defined as (Thorne, 1980)

$$^B\mathbf{Y}^{lm} = \frac{1}{\sqrt{l(l+1)}} i\mathbf{L} Y^{lm} = \mathbf{n} \times {}^E\mathbf{Y}^{lm}, \tag{E.13a}$$

$$^E\mathbf{Y}^{lm} = \frac{1}{\sqrt{l(l+1)}} r\nabla Y^{lm} = -\mathbf{n} \times {}^B\mathbf{Y}^{lm}, \tag{E.13b}$$

$$^R\mathbf{Y}^{lm} = \mathbf{n}\, Y^{lm}. \tag{E.13c}$$

Here, ∇ is the Euclidean gradient operator, $\mathbf{L} = -i\mathbf{r}\times\nabla$ is the orbital angular momentum operator, and $\mathbf{n}$ is the unit radial vector. The B- and E-type vector spherical harmonics are defined for $l \geq 1$ and are identically zero for $l = 0$. All of them are orthonormal, *i.e.*,

$$\int {}^J\mathbf{Y}^{lm} \cdot {}^{J'}\bar{\mathbf{Y}}^{l'm'} d\Omega = \delta_{JJ'}\delta_{ll'}\delta_{mm'}, \qquad \forall J = B, E, R \tag{E.14}$$

where ${}^{J}\bar{\mathbf{Y}}^{lm} = (-1)^m\, {}^{J}\mathbf{Y}^{l\,-m}$ is the complex conjugated.
The B- and E-type are transverse, while the R-type is radial:

$$\mathbf{n}\cdot\, {}^{B}\mathbf{Y}^{lm} = 0, \quad \mathbf{n}\cdot\, {}^{E}\mathbf{Y}^{lm} = 0, \quad \mathbf{n}\cdot\, {}^{R}\mathbf{Y}^{lm} = Y^{lm}. \tag{E.15}$$

A useful property of the pure-spin vector spherical harmonics is their divergence

$$\nabla\cdot\, {}^{B}\mathbf{Y}^{lm} = 0, \quad \nabla\cdot\, {}^{E}\mathbf{Y}^{lm} = -\sqrt{l(l+1)}\frac{Y^{lm}}{r}, \quad \nabla\cdot\, {}^{R}\mathbf{Y}^{lm} = 2\frac{Y^{lm}}{r}. \tag{E.16}$$

The magnetic type pure-spin vector spherical harmonics are eigenvectors of $\mathbf{L}^2$, while the electric and radial type are not. Explicit computations give

$$\mathbf{L}^2\, {}^{B}\mathbf{Y}^{lm} = l(l+1)\, {}^{B}\mathbf{Y}^{lm}, \tag{E.17a}$$

$$\mathbf{L}^2\, {}^{E}\mathbf{Y}^{lm} = l(l+1)\, {}^{E}\mathbf{Y}^{lm} - 2\sqrt{l(l+1)}\, {}^{R}\mathbf{Y}^{lm}, \tag{E.17b}$$

$$\mathbf{L}^2\, {}^{R}\mathbf{Y}^{lm} = (l(l+1)+2)\, {}^{R}\mathbf{Y}^{lm} - 2\sqrt{l(l+1)}\, {}^{E}\mathbf{Y}^{lm}. \tag{E.17c}$$

The STF version of the pure-spin vector spherical harmonics are obtained by inserting the decomposition of the scalar spherical harmonics Y^{lm} in terms of STF-l tensors $\mathcal{Y}^{lm}_{A_l}$ (defined in Eq. (2.12) of Thorne, 1980), $Y^{lm} = \mathcal{Y}^{lm}_{A_l} N_{A_l}$, in the defining equations (E.13). The result is given by Thorne (1980)

$${}^{B}Y^{lm}_{i} = \sqrt{\frac{l}{l+1}}\epsilon_{ipq} n_p \mathcal{Y}^{lm}_{qA_{l-1}} N_{A_{l-1}}, \tag{E.18a}$$

$${}^{E}Y^{lm}_{i} = \sqrt{\frac{l}{l+1}}\left[\mathcal{Y}^{lm}_{iA_{l-1}} N_{A_{l-1}}\right]^{T}, \tag{E.18b}$$

$${}^{R}Y^{lm}_{i} = n_i \mathcal{Y}^{lm}_{A_l} N_{A_l}. \tag{E.18c}$$

For completeness, we also write the STF version of the *pure-orbital vector spherical harmonics* that are eigenvectors of $\mathbf{L}^2$ with eigenvalues $l'(l'+1)$ and $l' = (l-1, l, l+1)$:

$$Y^{l-1,lm}_{i} = \sqrt{\frac{l}{2l+1}}\mathcal{Y}^{lm}_{iA_{l-1}} N_{A_{l-1}}, \tag{E.19a}$$

$$Y^{l,lm}_{i} = -i\sqrt{\frac{l}{l+1}}\epsilon_{ipq} n_p \mathcal{Y}^{lm}_{qA_{l-1}} N_{A_{l-1}}, \tag{E.19b}$$

$$Y^{l+1,lm}_{i} = -\sqrt{\frac{2l+1}{l+1}}\left[n_i \mathcal{Y}^{lm}_{A_l} N_{A_l} - \left(\frac{l}{2l+1}\right)\mathcal{Y}^{lm}_{iA_{l-1}} N_{A_{l-1}}\right]. \tag{E.19c}$$

Any spatial vector field v_i can be expanded either in pure-spin vector harmonics or in pure-orbital vector harmonics:

$$v_i = \sum_{l=0}^{\infty}\sum_{m=-l}^{l} R^{lm\,R}Y_i^{lm} + \sum_{l=1}^{\infty}\sum_{m=-l}^{l}\left(B^{lm\,B}Y_i^{lm} + E^{lm\,E}Y_i^{lm}\right), \tag{E.20a}$$

$$= \sum_{l=0}^{\infty} n_i \mathcal{R}_{A_l} N_{A_l} + \sum_{l=1}^{\infty}\left(\epsilon_{ipq} n_p \mathcal{B}_{qA_{l-1}} N_{A_{l-1}} + \left[\mathcal{E}_{iA_{l-1}} N_{A_{l-1}}\right]^{T}\right), \tag{E.20b}$$

from which one deduces, by using the STF decomposition of the pure-spin vector harmonics in Eqs. (E.18), the relations between the STF coefficients and the vector harmonic coefficients (Thorne, 1980)

$$\mathcal{B}_{A_l} = \sqrt{\frac{l}{l+1}}\sum_{m=-l}^{l} B^{lm}\mathcal{Y}_{A_l}^{lm}, \tag{E.21a}$$

$$\mathcal{E}_{A_l} = \sqrt{\frac{l}{l+1}}\sum_{m=-l}^{l} E^{lm}\mathcal{Y}_{A_l}^{lm}, \tag{E.21b}$$

$$\mathcal{R}_{A_l} = \sum_{m=-l}^{l} R^{lm}\mathcal{Y}_{A_l}^{lm}. \tag{E.21c}$$

E.2.3 Tensor spherical harmonics

The *pure-spin tensor spherical harmonics* are defined as (Thorne, 1980)

$${}^{L0}\mathbf{T}^{lm} = \mathbf{n}\otimes\mathbf{n}Y^{lm}, \tag{E.22a}$$

$${}^{T0}\mathbf{T}^{lm} = \frac{1}{\sqrt{2}}\mathbf{P}Y^{lm}, \tag{E.22b}$$

$${}^{E1}\mathbf{T}^{lm} = \sqrt{\frac{2}{l(l+1)}}r\left[\mathbf{n}\otimes\nabla Y^{lm}\right]^{S}, \tag{E.22c}$$

$${}^{B1}\mathbf{T}^{lm} = \sqrt{\frac{2}{l(l+1)}}\left[\mathbf{n}\otimes i\mathbf{L}Y^{lm}\right]^{S}, \tag{E.22d}$$

$${}^{E2}\mathbf{T}^{lm} = \sqrt{2\frac{(l-2)!}{(l+2)!}}r^2\left[\nabla\nabla Y^{lm}\right]^{STT}, \tag{E.22e}$$

$${}^{B2}\mathbf{T}^{lm} = \sqrt{2\frac{(l-2)!}{(l+2)!}}ir\left[\nabla\mathbf{L}Y^{lm}\right]^{STT}. \tag{E.22f}$$

The longitudinal (L0) and transverse (T0) spin-0 tensor harmonics are defined for $l \geq 0$, the E1- and B1-type spin-1 tensor harmonics for $l \geq 1$, and the transverse

and traceless (E2 and B2) spin-2 tensor harmonics for $l \geq 2$. All of them are orthonormal, in the sense that

$$\int \mathrm{Tr}\left({}^{JS}\mathbf{T}^{lm\ J'S'}\bar{\mathbf{T}}^{l'm'} \right) d\Omega = \delta_{JJ'}\delta_{SS'}\delta_{ll'}\delta_{mm'}, \tag{E.23}$$

where ${}^{JK}\bar{\mathbf{T}}^{lm} = (-1)^m\ {}^{JK}\mathbf{T}^{l-m}$ is the complex conjugated. Pure-spin tensor harmonics obey the following directional properties

$$\mathbf{n}\cdot\ {}^{L0}\mathbf{T}^{lm} = {}^{R}\mathbf{Y}^{lm}, \qquad \mathbf{n}\cdot\ {}^{T0}\mathbf{T}^{lm} = 0, \qquad \mathbf{n}\cdot\ {}^{E1}\mathbf{T}^{lm} = \frac{1}{\sqrt{2}}\ {}^{E}\mathbf{Y}^{lm}, \tag{E.24a}$$

$$\mathbf{n}\cdot\ {}^{B1}\mathbf{T}^{lm} = \frac{1}{\sqrt{2}}\ {}^{B}\mathbf{Y}^{lm}, \qquad \mathbf{n}\cdot\ {}^{E2}\mathbf{T}^{lm} = 0, \qquad \mathbf{n}\cdot\ {}^{B2}\mathbf{T}^{lm} = 0. \tag{E.24b}$$

The trace of the pure-spin tensor harmonics read as

$$\mathrm{Tr}\left({}^{L0}\mathbf{T}^{lm}\right) = Y^{lm}, \tag{E.25a}$$

$$\mathrm{Tr}\left({}^{T0}\mathbf{T}^{lm}\right) = \sqrt{2}Y^{lm}, \tag{E.25b}$$

$$\mathrm{Tr}\left({}^{JS}\mathbf{T}^{lm}\right) = 0, \qquad JS = (E1, E2, B1, B2) \tag{E.25c}$$

and their divergence is given by

$$\nabla\cdot\ {}^{L0}\mathbf{T}^{lm} = 2\frac{{}^{R}\mathbf{Y}^{lm}}{r}, \tag{E.26a}$$

$$\nabla\cdot\ {}^{T0}\mathbf{T}^{lm} = \frac{1}{\sqrt{2}}\left[\sqrt{l(l+1)}\frac{{}^{E}\mathbf{Y}^{lm}}{r} - 2\frac{{}^{R}\mathbf{Y}^{lm}}{r}\right], \tag{E.26b}$$

$$\nabla\cdot\ {}^{E1}\mathbf{T}^{lm} = \frac{1}{\sqrt{2}}\left[3\frac{{}^{E}\mathbf{Y}^{lm}}{r} - \sqrt{l(l+1)}\frac{{}^{R}\mathbf{Y}^{lm}}{r}\right], \tag{E.26c}$$

$$\nabla\cdot\ {}^{B1}\mathbf{T}^{lm} = \frac{3}{\sqrt{2}}\frac{{}^{B}\mathbf{Y}^{lm}}{r}, \tag{E.26d}$$

$$\nabla\cdot\ {}^{E2}\mathbf{T}^{lm} = -\sqrt{\frac{(l+2)!}{2(l-2)!}\frac{1}{l(l+1)}}\frac{{}^{E}\mathbf{Y}^{lm}}{r}, \tag{E.26e}$$

$$\nabla\cdot\ {}^{B2}\mathbf{T}^{lm} = -\sqrt{\frac{(l+2)!}{2(l-2)!}\frac{1}{l(l+1)}}\frac{{}^{B}\mathbf{Y}^{lm}}{r}. \tag{E.26f}$$

The STF version of the pure-spin tensor spherical harmonics are derived in Eqs. (2.39) of Thorne (1980)

$$ {}^{L0}T^{lm}_{ij} = n_i n_j \mathcal{Y}^{lm}_{A_l} N_{A_l}, \tag{E.27a} $$

$$ {}^{T0}T^{lm}_{ij} = \frac{1}{\sqrt{2}} P_{ij} \mathcal{Y}^{lm}_{A_l} N_{A_l}, \tag{E.27b} $$

$$ {}^{E1}T^{lm}_{ij} = \sqrt{\frac{2l}{l+1}} \left(n_{(i} \mathcal{Y}^{lm}_{j)A_{l-1}} N_{A_{l-1}} - n_i n_j \mathcal{Y}^{lm}_{A_l} N_{A_l} \right), \tag{E.27c} $$

$$ {}^{B1}T^{lm}_{ij} = \sqrt{\frac{2l}{l+1}} n_{(i} \epsilon_{j)pq} n_p \mathcal{Y}^{lm}_{qA_{l-1}} N_{A_{l-1}}, \tag{E.27d} $$

$$ {}^{E2}T^{lm}_{ij} = \sqrt{\frac{2(l-1)l}{(l+1)(l+2)}} \left[\mathcal{Y}^{lm}_{ijA_{l-2}} N_{A_{l-2}} \right]^{TT}, \tag{E.27e} $$

$$ {}^{B2}T^{lm}_{ij} = \sqrt{\frac{2(l-1)l}{(l+1)(l+2)}} \left[n_p \epsilon_{pq(i} \mathcal{Y}^{lm}_{j)qA_{l-2}} N_{A_{l-2}} \right]^{TT}. \tag{E.27f} $$

It is useful to notice that the pure-spin tensor spherical harmonics of type E2 and B2 are proportional to the TT part of the following pure-orbital tensor spherical harmonics (Thorne, 1980)

$$ T^{2\,l-2,lm}_{ij} = \sqrt{\frac{(l-1)l}{(2l-1)(2l+1)}} \mathcal{Y}^{lm}_{ijA_{l-2}} N_{A_{l-2}}, \tag{E.28a} $$

$$ T^{2\,l-1,lm}_{ij} = i \sqrt{\frac{2(l-1)l}{(l+1)(2l+1)}} n_p \epsilon_{pq(i} \mathcal{Y}^{lm}_{j)qA_{l-2}} N_{A_{l-2}}, \tag{E.28b} $$

that are eigenfunctions of the squared angular momentum operator $\mathbf{L}^2$ with eigenvalues $l'(l'+1)$ with $l' = l-2$ for $T^{2\,l-2,lm}_{ij}$ and $l' = l-1$ for $T^{2\,l-1,lm}_{ij}$. These pure-orbital tensor harmonics can be rewritten as linear combination of pure-spin tensor harmonics as follows (Thorne, 1980):

$$ \begin{aligned} T^{2\,l-2,lm}_{ij} = {} & \sqrt{\frac{(l-1)l}{(2l-1)(2l+1)}} \, {}^{L0}T^{lm}_{ij} - \sqrt{\frac{(l-1)l}{2(2l-1)(2l+1)}} \, {}^{T0}T^{lm}_{ij} \\ & + \sqrt{\frac{2(l-1)(l+1)}{(2l-1)(2l+1)}} \, {}^{E1}T^{lm}_{ij} + \sqrt{\frac{(l+1)(l+2)}{2(2l-1)(2l+1)}} \, {}^{E2}T^{lm}_{ij}, \end{aligned} \tag{E.29a} $$

$$ T^{2\,l-1,lm}_{ij} = i \sqrt{\frac{l-1}{2l+1}} \, {}^{B1}T^{lm}_{ij} + i \sqrt{\frac{l+2}{2l+1}} \, {}^{B2}T^{lm}_{ij}. \tag{E.29b} $$

E.3 Proofs

E.3.1 The linearised radiating configuration (4.13) in terms of spherical harmonics

The linearised perturbation $h_{\mu\nu}$ in Eqs. (4.13) can alternatively be expanded in terms of scalar, vector and tensor harmonics as follows

$$h_{00} = \sum_{l=0}^{\infty}\sum_{m=-l}^{l}\frac{2}{l!}\sum_{k=0}^{l}\frac{1}{2^k k!}\frac{(l+k)!}{(l-k)!}\frac{{}^{(l-k)}I^{lm}(u)\,Y^{lm}}{r^{k+1}}, \qquad \text{with } I^{1m}\equiv 0, \tag{E.30a}$$

$$h_{0j} = \sum_{l=1}^{\infty}\sum_{m=-l}^{l}\frac{4l}{(l+1)!}\sum_{k=0}^{l}\frac{1}{2^k k!}\frac{(l+k)!}{(l-k)!}\frac{{}^{(l-k)}S^{lm}(u)\,{}^{B}Y_j^{lm}}{r^{k+1}}+ \tag{E.30b}$$
$$-\sum_{l=2}^{\infty}\sum_{m=-l}^{l}\frac{4}{l!}\sum_{k=0}^{l-1}\frac{1}{2^k k!}\frac{(l-1+k)!}{(l-1-k)!}\frac{{}^{(l-k)}I^{lm}(u)}{r^{k+1}}\left({}^{E}Y_j^{lm}+\sqrt{\frac{l}{l+1}}\,{}^{R}Y_j^{lm}\right),$$

$$h_{ij} = h_{00}\delta_{ij}+ \tag{E.30c}$$
$$-\sum_{l=2}^{\infty}\sum_{m=-l}^{l}\frac{8l}{(l+1)!}\sum_{k=0}^{l-1}\frac{1}{2^k k!}\frac{(l-1+k)!}{(l-1-k)!}\frac{{}^{(l-k)}S^{lm}(u)}{r^{k+1}}\left(\sqrt{\frac{l-1}{l+2}}\,{}^{B1}T_{ij}^{lm}+{}^{B2}T_{ij}^{lm}\right)+$$
$$+\sum_{l=2}^{\infty}\sum_{m=-l}^{l}\frac{4}{l!}\sum_{k=0}^{l-2}\frac{1}{2^k k!}\frac{(l-2+k)!}{(l-2-k)!}\frac{{}^{(l-k)}I^{lm}(u)}{r^{k+1}}\times$$
$$\times\left(\sqrt{\frac{2(l-1)l}{(l+1)(l+2)}}\,{}^{L0}T_{ij}^{lm}-\sqrt{\frac{(l-1)l}{(l+1)(l+2)}}\,{}^{T0}T_{ij}^{lm}+2\sqrt{\frac{l-1}{l+2}}\,{}^{E1}T_{ij}^{lm}+{}^{E2}T_{ij}^{lm}\right).$$

The main elements of proof of the equivalence of STF tensor decomposition (4.13) and the spherical harmonic decomposition (E.30) are presented below. The expression (E.30) has been useful in chapter 8.

The multi-index derivative of a STF-l tensor, which is function of the retarded time $u=t-r$, can be expanded in terms of its derivatives as (Thorne, 1980)

$$\partial_{A_l}\left(\frac{\mathcal{A}_{A_l}(u)}{r}\right)=(-1)^l\sum_{k=0}^{l}c_{kl}\frac{{}^{(l-k)}\mathcal{A}_{A_l}(u)N_{A_l}}{r^{k+1}}, \qquad c_{kl}=\frac{1}{2^k k!}\frac{(l+k)!}{(l-k)!} \tag{E.31}$$

where ${}^{(l-k)}\mathcal{A}_{A_l}(u)$ is the $(l-k)$-th derivative of $\mathcal{A}_{A_l}(u)$ with respect to the retarded time coordinate u. In particular, we have

$$\partial_{A_l}\left(\frac{1}{r}\right)=\frac{(-1)^l(2l-1)!!}{r^{l+1}}N_{A_l}. \tag{E.32}$$

The relations between the STF-l coefficients (and their derivatives) and the harmonic coefficients can be read from the STF-l version of the scalar, vector and

tensor harmonics in Eqs. (E.10)-(E.18)-(E.27):

$$ {}^{(l-k)}\mathcal{I}_{A_l} = \sum_{m=-l}^{l} {}^{(l-k)}I^{lm}\mathcal{Y}^{lm}_{A_l}, \tag{E.33a} $$

$$ {}^{(l-k)}\mathcal{I}_{jA_{l-1}} = \sqrt{\frac{l}{l+1}} \sum_{m=-l}^{l} {}^{(l-k)}I^{lm}\mathcal{Y}^{lm}_{jA_{l-1}}, \tag{E.33b} $$

$$ {}^{(l-k)}\mathcal{S}_{jA_{l-1}} = \sqrt{\frac{l}{l+1}} \sum_{m=-l}^{l} {}^{(l-k)}S^{lm}\mathcal{Y}^{lm}_{jA_{l-1}}, \tag{E.33c} $$

$$ {}^{(l-k)}\mathcal{I}_{ijA_{l-2}} = \sqrt{\frac{2(l-1)l}{(l+1)(l+2)}} \sum_{m=-l}^{l} {}^{(l-k)}I^{lm}\mathcal{Y}^{lm}_{ijA_{l-2}}, \tag{E.33d} $$

$$ {}^{(l-k)}\mathcal{S}_{ijA_{l-2}} = \sqrt{\frac{2(l-1)l}{(l+1)(l+2)}} \sum_{m=-l}^{l} {}^{(l-k)}S^{lm}\mathcal{Y}^{lm}_{ijA_{l-2}}. \tag{E.33e} $$

The proof then uses the definitions of the *pure-orbital vector harmonics* ($\mathbf{Y}^{l-1,lm}, \mathbf{Y}^{l,lm}, \mathbf{Y}^{l+1,lm}$) in Eqs. (E.19) and their relations with the *pure-spin vector harmonics* ($^{B}\mathbf{Y}^{lm}$, $^{E}\mathbf{Y}^{lm}$, $^{R}\mathbf{Y}^{lm}$) in Eqs. (E.13). Along the same lines, we use the definitions of the *pure-orbital tensor harmonics* ($\mathbf{T}^{2\,l-1,lm}, \mathbf{T}^{2\,l-2,lm}$) in Eqs. (E.28) and their relations with the expressions of the *pure-spin vector harmonics* ($^{L0}\mathbf{T}^{lm}$, $^{T0}\mathbf{T}^{lm}$, $^{B1}\mathbf{T}^{lm}$, $^{E1}\mathbf{T}^{lm}$, $^{B2}\mathbf{T}^{lm}$, $^{E2}\mathbf{T}^{lm}$) in Eqs. (E.29).

After tedious but straightforward algebra, we get the harmonic decomposition in Eq. (E.30). Notice that the harmonic decomposition contains all the the degrees of freedom of a spin-two symmetric tensor field, namely the pure-longitudinal and the pure-transverse spin-zero modes ($^{L0}\mathbf{T}^{lm}$, $^{T0}\mathbf{T}^{lm}$), the mixed transverse and longitudinal spin-one modes ($^{B1}\mathbf{T}^{lm}$, $^{E1}\mathbf{T}^{lm}$), and the physical transverse and traceless modes ($^{B2}\mathbf{T}^{lm}$, $^{E2}\mathbf{T}^{lm}$).

E.3.2 General residual transformations

We want to find the most general class of solutions to $\Box_\eta \xi^\mu = 0$ in terms of scalar and vector harmonics. We shall not use a Fourier transformation since linear modes in t are important solutions. Let us start with the most general vector field ξ decomposed in terms of scalar spherical harmonics Y^{lm} and pure-spin vector spherical harmonics ($^{B}\mathbf{Y}^{lm}$, $^{E}\mathbf{Y}^{lm}$, $^{R}\mathbf{Y}^{lm}$),

$$ \begin{aligned} \xi(t,r,\theta,\phi) = &\sum_{l=0}^{\infty}\sum_{m=-l}^{l}\Big(S_{lm}(t,r)\; Y^{lm}(\theta,\phi)\partial_0 + R_{lm}(t,r)\; {}^{R}Y_i^{lm}(\theta,\phi)\partial_i\Big) + \\ &+\sum_{l=1}^{\infty}\sum_{m=-l}^{l}\Big(B_{lm}(t,r)\; {}^{B}Y_i^{lm}(\theta,\phi) + E_{lm}(t,r)\; {}^{E}Y_i^{lm}(\theta,\phi)\Big)\partial_i, \end{aligned} \tag{E.34} $$

where the angular dependence is encoded in the spherical harmonics and the time and radial dependence is encoded in the coefficients of the linear combination.

For definiteness, let us study the solutions to $\Box_\eta \xi^0 = 0$ in full detail. The harmonic gauge condition amounts to the following partial differential equation for the coefficients $S_{lm}(t,r)$

$$r^2\left(-\partial_t^2 S_{lm} + \partial_r^2 S_{lm}\right) + 2r\partial_r S_{lm} - l(l+1)S_{lm} = 0, \tag{E.35}$$

where we used the property that $\mathbf{L}^2 Y^{lm} = l(l+1)Y^{lm}$. Since ∂_t is a Killing vector, we can assume the separation of variables $S_{lm}(t,r) = f_{lm}(t)g_{lm}(r)$. Then Eq. (E.35) may be written as (we drop the labels l and m for ease of notation)

$$f(t)\left[r^2\partial_r^2 g(r) + 2r\partial_r g(r) - \left(l(l+1) - \omega^2 r^2\right)g(r)\right] - r^2 g(r)\left[\partial_t^2 f(t) + \omega^2 f(t)\right] = 0, \tag{E.36}$$

and it splits into two ordinary differential equations for $f(t)$ and $g(r)$:

$$\partial_t^2 f(t) + \omega^2 f(t) = 0, \qquad r^2\partial_r^2 g(r) + 2r\partial_r g(r) - \left(l(l+1) - \omega^2 r^2\right)g(r) = 0. \tag{E.37}$$

There are two classes of solutions that are qualitatively different:

1. *Oscillatory modes* ($\omega \neq 0$). In this case the solution is a linear combination of the *spherical Bessel functions of the first and second kind*

$$S_{lm}(t,r) = e^{\pm i\omega t}\left(c_1 J_l(\omega r) + c_2 Y_l(\omega r)\right); \tag{E.38}$$

2. *Zero modes* ($\omega = 0$). In this case the solution is expressed as linear combination of 4 modes:

$$S_{lm}(t,r) = (c_1 t + c_2)r^l + (c_3 t + c_4)r^{-l-1}. \tag{E.39}$$

Outer symmetries are defined from the zero mode class alone. Moreover, the solution $\sim r^{-l-1}$ is a gauge mode which is discarded. We therefore focus our attention to the class of solutions given by the linear combination of the *regular solid scalar harmonics* $r^l Y^{lm}$

$$\xi^0 = (c_1 t + c_2)r^l Y^{lm}. \tag{E.40}$$

The coefficients B_{lm} in (E.34) obey the same constraint as in Eq. (E.35), because the vector harmonic ${}^B\mathbf{Y}^{lm}$ is an eigenvector of the operator $\mathbf{L}^2$. Hence, the coefficients B_{lm} are again given by the above form for S_{lm} and the solutions of

interest read as

$$ {}^{B}\xi_i = (c_1 t + c_2) r^l \, {}^{B}Y_i^{lm}. \tag{E.41} $$

For the electric and the radial components of the vector field (E.34), the harmonic gauge conditions are not satisfied independently. Therefore, we demand that their linear combination is a solution to the D'Alembertian equation and we find four linearly independent solutions:

$$ \mathbf{Y}_1^{lm} = \frac{c_1 t + c_2}{\sqrt{2l+1}} \frac{1}{r^{l+2}} \left(\sqrt{l} \, {}^{E}\mathbf{Y}^{lm} - \sqrt{l+1} \, {}^{R}\mathbf{Y}^{lm} \right) = \frac{c_1 t + c_2}{\sqrt{(l+1)(2l+1)}} \nabla \left(\frac{Y^{lm}}{r^{l+1}} \right), \tag{E.42a} $$

$$ \mathbf{Y}_2^{lm} = \frac{c_1 t + c_2}{\sqrt{2l+1}} \frac{1}{r^{l}} \left(\sqrt{l+1} \, {}^{E}\mathbf{Y}^{lm} + \sqrt{l} \, {}^{R}\mathbf{Y}^{lm} \right) = \frac{c_1 t + c_2}{\sqrt{l(2l+1)}} \frac{1}{r^{2l-1}} \nabla (r^l Y^{lm}), \tag{E.42b} $$

$$ \mathbf{Y}_3^{lm} = \frac{c_1 t + c_2}{\sqrt{2l+1}} r^{l-1} \left(\sqrt{l+1} \, {}^{E}\mathbf{Y}^{lm} + \sqrt{l} \, {}^{R}\mathbf{Y}^{lm} \right) = \frac{c_1 t + c_2}{\sqrt{l(2l+1)}} \nabla (r^l Y^{lm}), \tag{E.42c} $$

$$ \mathbf{Y}_4^{lm} = \frac{c_1 t + c_2}{\sqrt{2l+1}} r^{l+1} \left(\sqrt{l} \, {}^{E}\mathbf{Y}^{lm} - \sqrt{l+1} \, {}^{R}\mathbf{Y}^{lm} \right) = \frac{c_1 t + c_2}{\sqrt{(l+1)(2l+1)}} r^{2l+3} \nabla \left(\frac{Y^{lm}}{r^{l+1}} \right). \tag{E.42d} $$

Again the first two solutions are pure gauge and are discarded. The vector $\mathbf{Y}_1^{lm}$ is parallel to $\mathbf{Y}_4^{lm}$ and the vector $\mathbf{Y}_2^{lm}$ is parallel to $\mathbf{Y}_3^{lm}$. The vectors $\mathbf{Y}_1^{lm}$ and $\mathbf{Y}_3^{lm}$ are manifestly solenoidal and irrotational, because they are proportional to the gradients of solid harmonic functions. Instead, the divergence and the curl of $\mathbf{Y}_2^{lm}$ and $\mathbf{Y}_4^{lm}$ read as

$$ \nabla \cdot \mathbf{Y}_2^{lm} = -(c_1 t + c_2)(2l-1) \sqrt{\frac{l}{2l+1}} \frac{Y^{lm}}{r^{l+1}}, \qquad \nabla \times \mathbf{Y}_2^{lm} = -(c_1 t + c_2)(2l-1) \sqrt{\frac{l+1}{2l+1}} \frac{{}^{B}\mathbf{Y}^{lm}}{r^{l+1}}, \tag{E.43a} $$

$$ \nabla \cdot \mathbf{Y}_4^{lm} = -(c_1 t + c_2)(2l+3) \sqrt{\frac{l+1}{2l+1}} r^l Y^{lm}, \quad \nabla \times \mathbf{Y}_4^{lm} = (c_1 t + c_2)(2l+3) \sqrt{\frac{l}{2l+1}} r^l \, {}^{B}\mathbf{Y}^{lm}. \tag{E.43b} $$

The vector field $\boldsymbol{V}$ in the main text is indeed the time independent part of $\mathbf{Y}_4$:

$$ \mathbf{V}^{lm} = \frac{1}{\sqrt{(l+1)(2l+1)}} r^{2l+3} \nabla \left(\frac{Y^{lm}}{r^{l+1}} \right) = \frac{1}{\sqrt{2l+1}} r^{l+1} \left(\sqrt{l} \, {}^{E}\mathbf{Y}^{lm} - \sqrt{l+1} \, {}^{R}\mathbf{Y}^{lm} \right). \tag{E.44} $$

E.4 Canonical surface charges

In four-dimensional General Relativity, the infinitesimal canonical *surface charge* associated to a vector field ξ and a linearised metric $h_{\mu\nu}$ around the background

$\bar{g}_{\mu\nu}$ is given by

$$\mathbf{k}_\xi[h;\bar{g}] = \sqrt{-\bar{g}}\, k_\xi^{\mu\nu}[h;\bar{g}]\left(d^2x\right)_{\mu\nu}, \tag{E.45}$$

where $\left(d^2x\right)_{\mu\nu} = \frac{1}{4}\epsilon_{\mu\nu\alpha\beta}dx^\alpha \wedge dx^\beta$ and

$$k_\xi^{\mu\nu} = \xi^\nu\left(\bar{\nabla}^\mu h - \bar{\nabla}_\sigma h^{\mu\sigma}\right) + \xi_\sigma\bar{\nabla}^\nu h^{\mu\sigma} + \frac{1}{2}h\bar{\nabla}^\nu\xi^\mu - h^{\rho\nu}\bar{\nabla}_\rho\xi^\mu + \frac{\alpha}{2}h^{\sigma\nu}\left(\bar{\nabla}^\mu\xi_\sigma + \bar{\nabla}_\sigma\xi^\mu\right). \tag{E.46}$$

Here, the background metric is used to lower and to raise indices, *e.g.*, $h^{\mu\nu} = \bar{g}^{\mu\alpha}\bar{g}^{\nu\beta}h_{\alpha\beta}$ and $h = \bar{g}^{\mu\nu}h_{\mu\nu}$. The symbol $\bar{\nabla}_\mu$ stands for the background covariant derivative.

The corresponding linearised charges $Q_\xi[h;\bar{g}]$ associated to the vector field ξ are obtained by integrating the space-time 2-form $\mathbf{k}_\xi$ over a two-dimensional sphere S

$$Q_\xi[h;\bar{g}] = \frac{1}{8\pi G}\int_S \mathbf{k}_\xi[h;\bar{g}]. \tag{E.47}$$

The parameter α reflects the ambiguity at adding a boundary form of the form $\mathbf{E} \sim \left(d^2x\right)_{\mu\nu}(\delta g)^{\mu\alpha}\wedge(\delta g)_\alpha^{\ \nu}$ to the Lee-Wald symplectic form of Einstein gravity (Lee and Wald, 1990). For $\alpha = 0$, one has the Iyer-Wald charge (Iyer and Wald, 1994) and the Lee-Wald symplectic structure (Lee and Wald, 1990; Wald and Zoupas, 2000). For $\alpha = 1$, one has the Abbott-Deser (Abbott and Deser, 1982) or, equivalently, the Barnich-Brandt charge (Barnich and Brandt, 2002) and the invariant symplectic structure (Compère, 2007a; Barnich and Compère, 2008).

We take the background metric to be the Minkowski metric $\bar{g}_{\mu\nu} = \eta_{\mu\nu}$ and we adopt Cartesian coordinates $(t,x,y,z) = (t,x^i)$. Background covariant derivatives reduce to partial derivatives $\bar{\nabla}_\mu = \partial_\mu$. Simple algebra reduces Eq. (E.46) to the expression

$$\begin{aligned} 2k_\xi^{[0i]} = {} & \xi^i\left(\partial_j h_{0j} - \dot{h} - \dot{h}_{00}\right) + \xi^j\left(\dot{h}_{ij} - \partial_i h_{0j}\right) - \xi^0\left(\partial_i h + \partial_i h_{00} - \partial_j h_{ij}\right) + \\ & + \frac{1}{2}h\left(\partial_i\xi^0 + \dot{\xi}^i\right) + h_{00}\dot{\xi}^i + h_{0i}\dot{\xi}^0 - h_{0j}\partial_j\xi^i - h_{ij}\partial_j\xi^0 + \\ & + \frac{\alpha}{2}\left[h_{00}\left(\partial_i\xi^0 - \dot{\xi}^i\right) + h_{0j}\left(\partial_i\xi_j + \partial_j\xi_i\right) - 2h_{0i}\dot{\xi}^0 + h_{ij}\left(\partial_j\xi^0 - \dot{\xi}_j\right)\right], \end{aligned} \tag{E.48}$$

where $\xi_i = \xi^i$, but $\xi_0 = -\xi^0$. The dot stands for time derivative, *i.e.*, $\dot{h}_{\mu\nu} = \partial_0 h_{\mu\nu}$. For higher curvature theories or for a large class of matter theories (see *e.g.* Iyer and Wald, 1994; Compère, Murata, and Nishioka, 2009; Azeyanagi et al., 2009, for the explicit expression of $\mathbf{k}_\xi$).

E.4.1 Coefficients of the surface charges

The coefficients appearing in (8.26a)-(8.26b)-(8.26c) are given by

$$C_L(p,l) = -\frac{2}{(l-1)!}\sqrt{\frac{l}{l+1}}\frac{2^{p-l}}{p!}\frac{(2l-p)!}{(l-p+1)!}\times \tag{E.49a}$$
$$\times\left[\frac{\alpha}{2}(l-1)(l-p+1)+l(l-p+3)-2(p-1)+\frac{(p-1)p}{2}\left(1-\sqrt{\frac{2(l-1)}{l+2}}\right)\right],$$

$$C_K(p,l) = \frac{2}{l!}\frac{2^{p-l}}{p!}\frac{(2l-p-2)!}{(l-p+1)!}\times \tag{E.49b}$$
$$\times\left[\frac{1}{2}\frac{(2l-p+2)!}{(2l-p-2)!}-\sqrt{\frac{l(l-1)}{2(l+1)(l+2)}}p(p-1)\left[2+4l(1+2(l-p))+p(p-1)\right]\right],$$

$$C_P(p,l) = \frac{2}{l!}\frac{2^{p-l}}{p!}\frac{(2l-p-2)!}{(l-p+1)!}\left\{-\frac{l(2l-p)!}{(2l-p-2)!}+(1-\delta_{1l})\sqrt{l(l+1)}\times\right. \tag{E.49c}$$
$$\left.\times\left[2l-p(p+1)+\frac{2(l-p)}{l+1}\left[2(l^2-2l-1)-\alpha(2l+1)(l-1)\right]+p(p-1)\frac{2l+1}{l+1}\sqrt{\frac{2(l-1)}{l+2}}\right]\right\}.$$

For the sake of completeness, we write the charge associated to $\boldsymbol{V} = r^{l+1}\left(\sqrt{l}\,{}^{E}\mathbf{Y}^{lm}-\sqrt{l+1}\,{}^{R}\mathbf{Y}^{lm}\right)$. It reads as

$$8\pi G\, Q_{\boldsymbol{V}}^{lm} = \sum_{p=1}^{l+1} C_{\boldsymbol{V}}(p,l)\, r^{p+1}\,{}^{(p)}I^{lm}(u), \tag{E.50}$$

with the coefficient $C_{\boldsymbol{V}}(p,l)$ being

$$C_{\boldsymbol{V}}(p,l) = \frac{1}{l!}\frac{2^{p-l}}{(p-1)!}\frac{(2l-p-1)!}{(l-p+1)!}\times \tag{E.51}$$
$$\times\left[\sqrt{l+1}(2l-p+1)(2l-p)-(1-\delta_{1l})\sqrt{l}\left[p(p-8l-7)+4l(2l+3)+6-(2l+3)(l-p+1)\alpha\right]\right].$$

From (E.50), we clearly see that the associated charge is vanishing at spatial infinity. Moreover, the surface integral in the near zone which could in principle correspond to a multipole moment is also vanishing. Accordingly we have ignored this vector in this thesis, although it might be important in more general theories of gravity, as discussed in section 8.5.

E.4.2 Multipole charges of a harmonic gauge perturbation

The multipole charges discussed in this thesis are computed in canonical harmonic gauge. As explained in section 8.2.3, the term "canonical" refers to the extra conditions that are met by the metric configurations in addition to respecting the harmonic or de Donder gauge. Assuming asymptotically flat boundary

conditions, the canonical conditions amount to reaching mass-centred frame and reaching (8.19). The purpose of this section is to investigate whether one can relax the last condition (8.19).

To this end, we compute the variation of multipole charges Q_ξ under a variation in the metric of the form $\delta_\zeta g_{\mu\nu} = \mathscr{L}_\zeta \eta_{\mu\nu}$[1] that preserves de Donder gauge, asymptotically flat boundary conditions and the mass-centred frame but violates (8.19). The most general form of such vector is given in STF harmonics in Section VIII Eq. (8.9) of Thorne (1980), while its spherical harmonic expansion turns out to be

$$\zeta_0 = \sum_{l=0}^{\infty}\sum_{m=-l}^{l}(-1)^l\sum_{k=0}^{l}\frac{1}{2^k k!}\frac{(l+k)!}{(l-k)!}\left(\frac{1}{2}\,{}^{(l-k+1)}K^{lm}(u) - {}^{(l-k)}D^{lm}(u)\right)\frac{Y^{lm}}{r^{k+1}}, \tag{E.52a}$$

$$\begin{aligned}\zeta_i = &-\frac{1}{2}\sum_{l=0}^{\infty}\sum_{m=-l}^{l}(-1)^l\sum_{k=0}^{l}\frac{1}{2^k k!}\frac{(l+k)!}{(l-k)!}\times \\ &\times\left[\frac{{}^{(l-k)}K^{lm}(u)}{r^{k+2}}\left(\sqrt{l(l+1)}\,{}^{E}Y_i^{lm} - (k+1)\,{}^{R}Y_i^{lm}\right) - \frac{{}^{(l-k+1)}K^{lm}(u)\,{}^{R}Y_i^{lm}}{r^{k+1}}\right] + \\ &-\frac{1}{2}\sum_{l=1}^{\infty}\sum_{m=-l}^{l}(-1)^l\left[\sum_{k=0}^{l}\frac{1}{2^k k!}\frac{(l+k)!}{(l-k)!}\frac{{}^{(l-k)}N^{lm}(u)\,{}^{B}Y_i^{lm}}{r^{k+1}} + \right. \\ &\left. -\sum_{k=0}^{l-1}\frac{1}{2^k k!}\frac{(l-1+k)!}{(l-1-k)!}\frac{{}^{(l-1-k)}H^{lm}(u)}{r^{k+1}}\left({}^{E}Y_i^{lm} + \sqrt{\frac{l}{l+1}}\,{}^{R}Y_i^{lm}\right)\right].\end{aligned} \tag{E.52b}$$

The four components of the vector field ζ^μ are harmonic functions and depend upon four arbitrary functions of the retarded time u. They must satisfy the same behaviour as (8.27). We now compute the charge variation $\delta_\zeta Q_\xi = \frac{1}{8\pi G}\int_S \mathbf{k}_\xi[\mathscr{L}_\zeta\eta;\eta]$ where ξ is one of the multipole symmetries (8.9). Explicit computation shows that the charges computed at a surface S of radius r are given by

$$8\pi G\,\delta_\zeta Q_L^{lm} = (-1)^l(l-1)\sqrt{l(l+1)}\,\frac{\alpha}{8}\sum_{p=0}^{l}\frac{2^{p-l}}{p!}\frac{(2l-p)!}{(l-p)!}\,r^p\,{}^{(p+1)}N^{lm}, \tag{E.53a}$$

$$\begin{aligned}8\pi G\,\delta_\zeta Q_K^{lm} = &-(-1)^l(l-1)l\sum_{p=0}^{l}\frac{2^{p-l}}{p!}\frac{(2l-p-2)!}{(l-p-1)!}r^p\left[\frac{2l+1}{\sqrt{l(l+1)}}\,{}^{(p)}H^{lm} + {}^{(p+2)}K^{lm}\right] \\ &+ 8\pi G\,t\,\delta_\zeta Q_P^{lm},\end{aligned} \tag{E.53b}$$

$$\begin{aligned}8\pi G\,\delta_\zeta Q_P^{lm} = &(-1)^l(l-1)l\sum_{p=0}^{l}\frac{2^{p-l}}{p!}\frac{(2l-p-2)!}{(l-p-1)!}\times \\ &\times r^p\left((\alpha-2)\,{}^{(p+2)}D^{lm} + {}^{(p+3)}K^{lm} + \frac{\alpha}{2}\frac{2l+1}{\sqrt{l(l+1)}}\,{}^{(p+1)}H^{lm}\right).\end{aligned} \tag{E.53c}$$

[1] Note that $\delta_\zeta g_{\mu\nu} = \mathscr{L}_\zeta\eta_{\mu\nu} + \mathscr{L}_\zeta h_{\mu\nu}$ but the latter term is vanishing in linearised theory as both ζ and $h_{\mu\nu}$ are infinitesimal.

Now we send S to spatial infinity. As a result, all the charge variations vanish, except the mass multipole charge variation $\delta_\zeta Q_K^{lm} - t\delta_\zeta Q_P^{lm}$, due to the function H^{lm}. These gauge transformations correspond to functions $\zeta^i = \partial_i \epsilon$ with ϵ harmonic.

For the sake of completeness, the charge associated to $\mathbf{V}^{lm} = r^{l+1}\left(\sqrt{l}\ {}^E\mathbf{Y}^{lm} - \sqrt{l+1}\ {}^R\mathbf{Y}^{lm}\right)$ is given by

$$8\pi G\,\delta_\zeta Q_{\mathbf{V}}^{lm} = \frac{1}{2}(-1)^l\sqrt{l+1}\left\{\sum_{p=0}^{l+1}\frac{2^{p-l}}{p!}\frac{(2l-p+1)!}{(l-p+1)!}r^p\left[d(p,l)\ {}^{(p)}D^{lm}(u) + k(p,l)\ {}^{(p+1)}K^{lm}(u)\right] + \right.$$
$$\left. + \sum_{p=1}^{l+1}\frac{2^{p-l}}{p!}\frac{(2l-p+1)!}{(l-p+1)!}h(p,l)r^p\ {}^{(p-1)}H^{lm}(u)\right\}, \tag{E.54}$$

where

$$d(p,l) = -\frac{1}{2(2l-p+1)}\Big\{2+4l^3+2l(6-5p)+2l^2(7-2p)+p(p-3)+ \tag{E.55a}$$
$$+\alpha[2+2l^3+l^2(5-2p)+l(p^2-4p+5)+p(p-3)]\Big\},$$
$$k(p,l) = \frac{1}{2}(l+2)[2(l+1)-p], \tag{E.55b}$$
$$h(p,l) = \frac{1}{4}\sqrt{\frac{l}{l+1}}(2l+3)\left(1-\frac{\alpha}{2}\right)\frac{p(p-1)}{2l-p+1}. \tag{E.55c}$$

Bibliography

Abbott, B. P. et al. (2017a). “Multi-messenger Observations of a Binary Neutron Star Merger”. In: *Astrophys. J.* 848.2, p. L12. DOI: 10.3847/2041-8213/aa91c9. arXiv: 1710.05833 [astro-ph.HE] (cit. on p. 61).

Abbott, B. et al. (2017b). “GW170817: Observation of Gravitational Waves from a Binary Neutron Star Inspiral”. In: *Phys. Rev. Lett.* 119.16, p. 161101. DOI: 10.1103/PhysRevLett.119.161101. arXiv: 1710.05832 [gr-qc] (cit. on p. 61).

Abbott, L. and S. Deser (1982). “Stability of gravity with a cosmological constant”. In: *Nucl. Phys. B* 195, pp. 76–96. DOI: 10.1016/0550-3213(82)90049-9 (cit. on pp. 153, 212).

Abramowicz, M. A., A. Lanza, and M. J. Percival (Apr. 1997). “Accretion Disks around Kerr Black Holes: Vertical Equilibrium Revisited”. In: *Astrophys. J.* 479, pp. 179–183 (cit. on pp. 41, 52, 54, 176).

Abramowicz, M. A. and J. P. Lasota (1980). “Spin-up of black holes by thick accretion disks”. In: *Acta Astron.* 30, pp. 35–39 (cit. on p. 129).

Abramowicz, M. A., X.-M. Chen, M. Granath, and J.-P. Lasota (1996). “Advection-dominated Accretion Flows around Kerr Black Holes”. In: *Astrophys. J.* 471, pp. 762–773. DOI: 10.1086/178004. eprint: astro-ph/9607021 (cit. on pp. 41, 50, 51, 176, 177, 178).

Abramowicz, M. A., B. Czerny, J. P. Lasota, and E. Szuszkiewicz (Sept. 1988). “Slim accretion disks”. In: *Astrophys. J.* 332, pp. 646–658. DOI: 10.1086/166683 (cit. on p. 41).

Abramowicz, M. A. and P. C. Fragile (2013). “Foundations of Black Hole Accretion Disk Theory”. In: *Living Reviews in Relativity* 16.1. DOI: 10.1007/lrr-2013-1. URL: http://www.livingreviews.org/lrr-2013-1 (cit. on pp. 40, 51).

Abramowicz, M. A. et al. (2010). “Leaving the ISCO: the inner edge of a black-hole accretion disk at various luminosities”. In: *Astron. Astrophys.* 521, A15. DOI: 10.1051/0004-6361/201014467. arXiv: 1003.3887 [astro-ph.HE] (cit. on pp. 51, 128, 141).

Abramowicz, M. A. and W. Kluzniak (2001). “A Precise determination of angular momentum in the black hole candidate GRO J1655-40”. In: *Astron. Astrophys.* 374, p. L19. DOI: 10.1051/0004-6361:20010791. arXiv: astro-ph/0105077 [astro-ph] (cit. on p. 42).

Aliev, A. N. and D. V. Gal'tsov (1989a). "Exact solutions for magnetized black holes". In: *Astrophysics and Space Science* 155.2, pp. 181–192. DOI: 10.1007/BF00643854. URL: https://doi.org/10.1007/BF00643854 (cit. on p. 100).

Aliev, A. N. and D. V. Gal'tsov (1989b). "Physical interpretation of the Kerr-Newman-Ernst solutions". In: *Soviet Physics Journal* 32.10, pp. 790–795. ISSN: 1573-9228. DOI: 10.1007/BF00898308. URL: https://doi.org/10.1007/BF00898308 (cit. on p. 100).

Aliev, A. N., D. V. Gal'tsov, and A. A. Sokolov (Mar. 1980). "Rotating black hole in a strong magnetic field". In: *Soviet Physics Journal* 23, pp. 179–183. DOI: 10.1007/BF00895071 (cit. on p. 100).

Aliev, A. and D. Gal'tsov (1988). "Effective ergospheres of magnetized black holes and the Kerr-Newman-Ernst solution". In: *Zh. Eksp. Teor. Fiz* 94, pp. 15–28 (cit. on p. 100).

Aliev, A. and D. Gal'tsov (1989c). ""Magnetized" black holes". In: *Physics-Uspekhi* 32.1, pp. 75–92 (cit. on pp. 100, 109, 111).

Amsel, A. J., G. T. Horowitz, D. Marolf, and M. M. Roberts (2009). "No Dynamics in the Extremal Kerr Throat". In: *JHEP* 09, p. 044. DOI: 10.1088/1126-6708/2009/09/044. arXiv: 0906.2376 [hep-th] (cit. on pp. 16, 17).

Anninos, D. et al. (2009). "Warped AdS(3) Black Holes". In: *JHEP* 03, p. 130. DOI: 10.1088/1126-6708/2009/03/130. arXiv: 0807.3040 [hep-th] (cit. on p. 16).

Aretakis, S. (2012). "Decay of Axisymmetric Solutions of the Wave Equation on Extreme Kerr Backgrounds". In: *J. Funct. Anal.* 263, pp. 2770–2831. DOI: 10.1016/j.jfa.2012.08.015. arXiv: 1110.2006 [gr-qc] (cit. on p. 12).

Aretakis, S. (2015). "Horizon Instability of Extremal Black Holes". In: *Adv. Theor. Math. Phys.* 19, pp. 507–530. DOI: 10.4310/ATMP.2015.v19.n3.a1. arXiv: 1206.6598 [gr-qc] (cit. on p. 12).

Arnowitt, R. L., S. Deser, and C. W. Misner (1959). "Dynamical Structure and Definition of Energy in General Relativity". In: *Phys. Rev.* 116, pp. 1322–1330. DOI: 10.1103/PhysRev.116.1322 (cit. on p. 145).

Ashtekar, A. and R. O. Hansen (1978). "A unified treatment of null and spatial infinity in general relativity. I - Universal structure, asymptotic symmetries, and conserved quantities at spatial infinity". In: *J. Math. Phys.* 19, pp. 1542–1566. DOI: 10.1063/1.523863 (cit. on pp. 145, 164).

Astorino, M., G. Compère, R. Oliveri, and N. Vandevoorde (2016). "Mass of Kerr-Newman black holes in an external magnetic field". In: *Phys. Rev.* D94.2, p. 024019. DOI: 10.1103/PhysRevD.94.024019. arXiv: 1602.08110 [gr-qc] (cit. on pp. iii, 99, 101, 112, 124).

Astorino, M. (2015). "Magnetised Kerr/CFT correspondence". In: *Phys. Lett.* B751, pp. 96–106. DOI: 10.1016/j.physletb.2015.10.017. arXiv: 1508.01583 [hep-th] (cit. on pp. 101, 110, 113, 117, 122, 124).

Astorino, M. (2017). "Thermodynamics of Regular Accelerating Black Holes". In: *Phys. Rev.* D95.6, p. 064007. DOI: 10.1103/PhysRevD.95.064007. arXiv: 1612.04387 [gr-qc] (cit. on p. 117).

Ayzenberg, D. and N. Yunes (2014). "Slowly-Rotating Black Holes in Einstein-Dilaton-Gauss-Bonnet Gravity: Quadratic Order in Spin Solutions". In: *Phys. Rev.* D90. [Erratum: Phys. Rev.D91,no.6,069905(2015)], p. 044066. DOI: 10.1103/PhysRevD.91.069905,10.1103/PhysRevD.90.044066. arXiv: 1405.2133 [gr-qc] (cit. on p. 61).

Azeyanagi, T. et al. (2009). "Higher-Derivative Corrections to the Asymptotic Virasoro Symmetry of 4d Extremal Black Holes". In: *Prog. Theor. Phys.* 122, pp. 355–384. DOI: 10.1143/PTP.122.355. arXiv: 0903.4176 [hep-th] (cit. on pp. 144, 212).

Backdahl, T. (2007). "Axisymmetric stationary solutions with arbitrary multipole moments". In: *Class. Quant. Grav.* 24, pp. 2205–2215. DOI: 10.1088/0264-9381/24/9/004. arXiv: gr-qc/0612043 [gr-qc] (cit. on p. 60).

Backdahl, T. and M. Herberthson (2005). "Static axisymmetric space-times with prescribed multipole moments". In: *Class. Quant. Grav.* 22, pp. 1607–1621. DOI: 10.1088/0264-9381/22/9/009. arXiv: gr-qc/0502012 [gr-qc] (cit. on p. 60).

Baiotti, L. and L. Rezzolla (2017). "Binary neutron star mergers: a review of Einstein's richest laboratory". In: *Rept. Prog. Phys.* 80.9, p. 096901. DOI: 10.1088/1361-6633/aa67bb. arXiv: 1607.03540 [gr-qc] (cit. on p. 61).

Balbus, S. A. and J. C. B. Papaloizou (Aug. 1999). "On the Dynamical Foundations of α Disks". In: *Astrophys. J.* 521, pp. 650–658. DOI: 10.1086/307594. eprint: astro-ph/9903035 (cit. on p. 53).

Balbus, S. A. and J. F. Hawley (1991). "A powerful local shear instability in weakly magnetized disks. 1. Linear analysis. 2. Nonlinear evolution". In: *Astrophys. J.* 376, pp. 214–233. DOI: 10.1086/170270 (cit. on p. 42).

Balbus, S. A. and J. F. Hawley (1998). "Instability, turbulence, and enhanced transport in accretion disks". In: *Rev. Mod. Phys.* 70 (1), pp. 1–53. DOI: 10.1103/RevModPhys.70.1. URL: https://link.aps.org/doi/10.1103/RevModPhys.70.1 (cit. on p. 42).

Bambi, C. (2017). "Testing black hole candidates with electromagnetic radiation". In: *Rev. Mod. Phys.* 89.2, p. 025001. DOI: 10.1103/RevModPhys.89.025001. arXiv: 1509.03884 [gr-qc] (cit. on p. 141).

Banados, M., J. Silk, and S. M. West (2009). "Kerr Black Holes as Particle Accelerators to Arbitrarily High Energy". In: *Phys. Rev. Lett.* 103, p. 111102. DOI: 10.1103/PhysRevLett.103.111102. arXiv: 0909.0169 [hep-ph] (cit. on p. 12).

Banados, M., G. Barnich, G. Compère, and A. Gomberoff (2006). "Three dimensional origin of Godel spacetimes and black holes". In: *Phys. Rev.* D73, p. 044006. DOI: 10.1103/PhysRevD.73.044006. arXiv: hep-th/0512105 [hep-th] (cit. on p. 101).

Barack, L. and C. Cutler (Feb. 2007). "Using LISA extreme-mass-ratio inspiral sources to test off-Kerr deviations in the geometry of massive black holes". In: *Phys. Rev. D.* 75.4, 042003, p. 042003. DOI: 10.1103/PhysRevD.75.042003. eprint: gr-qc/0612029 (cit. on p. 60).

Bardeen, J. M. and R. V. Wagoner (1971). "Relativistic Disks. I. Uniform Rotation". In: *Astrophys. J.* 167, pp. 359–423. DOI: 10.1086/151039 (cit. on p. 12).

Bardeen, J. M. (1970). "Kerr Metric Black Holes". In: *Nature* 226, pp. 64–65. DOI: 10.1038/226064a0 (cit. on p. 12).

Bardeen, J. M., B. Carter, and S. W. Hawking (1973). "The Four laws of black hole mechanics". In: *Commun. Math. Phys.* 31, pp. 161–170. DOI: 10.1007/BF01645742 (cit. on pp. 111, 117, 118).

Bardeen, J. M. and G. T. Horowitz (1999). "The Extreme Kerr throat geometry: A Vacuum analog of $AdS_2 \times S^2$". In: *Phys. Rev.* D60, p. 104030. DOI: 10.1103/PhysRevD.60.104030. arXiv: hep-th/9905099 [hep-th] (cit. on pp. 1, 14, 16, 17).

Bardeen, J. M. and J. A. Petterson (1975). "The Lense-Thirring Effect and Accretion Disks around Kerr Black Holes". In: *Astrophys. J.* 195, p. L65. DOI: 10.1086/181711 (cit. on p. 46).

Bardeen, J. M., W. H. Press, and S. A. Teukolsky (1972). "Rotating black holes: Locally nonrotating frames, energy extraction, and scalar synchrotron radiation". In: *Astrophys. J.* 178, p. 347. DOI: 10.1086/151796 (cit. on pp. 9, 14, 17, 171, 174).

Barnich, G. and G. Compere (2005). "Generalized Smarr relation for Kerr AdS black holes from improved surface integrals". In: *Phys. Rev.* D71. [Erratum: Phys. Rev.D73,029904(2006)] p. 044016. DOI: 10.1103/PhysRevD.71.044016, 10.1103/PhysRevD.73.029904, 10.1103/PhysRevD.71.029904. arXiv: gr-qc/0412029 [gr-qc] (cit. on p. 113).

Barnich, G. and C. Troessaert (2011). "BMS charge algebra". In: *J. High Energy Phys.* 2011.12, 105. DOI: 10.1007/JHEP12(2011)105. arXiv: 1106.0213 [hep-th] (cit. on p. 145).

Barnich, G. and C. Troessaert (2010). "Symmetries of asymptotically flat 4 dimensional spacetimes at null infinity revisited". In: *Phys. Rev. Lett.* 105, 111103. DOI: 10.1103/PhysRevLett.105.111103. arXiv: 0909.2617 [gr-qc] (cit. on p. 145).

Barnich, G. (2003). "Boundary charges in gauge theories: Using Stokes theorem in the bulk". In: *Class. Quant. Grav.* 20, pp. 3685–3698. DOI: 10.1088/0264-9381/20/16/310. arXiv: hep-th/0301039 [hep-th] (cit. on p. 101).

Barnich, G. (2002). "Conserved charges in gravitational theories: Contribution from scalar fields". In: [Ann. U. Craiova Phys.12,no.III,14(2002)]. arXiv: gr-qc/0211031 [gr-qc] (cit. on p. 162).

Barnich, G. and F. Brandt (2002). "Covariant theory of asymptotic symmetries, conservation laws and central charges". In: *Nucl. Phys.* B633, pp. 3–82. DOI: 10.1016/S0550-3213(02)00251-1. arXiv: hep-th/0111246 [hep-th] (cit. on pp. 2, 101, 112, 113, 144, 153, 156, 160, 212).

Barnich, G., F. Brandt, and M. Henneaux (2000). "Local BRST cohomology in gauge theories". In: *Phys. Rept.* 338, pp. 439–569. DOI: 10.1016/S0370-1573(00)00049-1. arXiv: hep-th/0002245 [hep-th] (cit. on pp. 144, 160).

Barnich, G. and G. Compère (2005). "Conserved charges and thermodynamics of the spinning Godel black hole". In: *Phys. Rev. Lett.* 95, p. 031302. DOI: 10.1103/PhysRevLett.95.031302. arXiv: hep-th/0501102 [hep-th] (cit. on p. 101).

Barnich, G. and G. Compère (2008). "Surface charge algebra in gauge theories and thermodynamic integrability". In: *J. Math. Phys.* 49, p. 042901. DOI: 10.1063/1.2889721. arXiv: 0708.2378 [gr-qc] (cit. on pp. 2, 101, 113, 144, 153, 156, 160, 212).

Barut, A. and R. Raczka (1986). *Theory of Group Representations and Applications*. Singapore, World Scientific (1986) (cit. on p. 18).

Bauswein, A. and H. T. Janka (2012). "Measuring neutron-star properties via gravitational waves from binary mergers". In: *Phys. Rev. Lett.* 108, p. 011101. DOI: 10.1103/PhysRevLett.108.011101. arXiv: 1106.1616 [astro-ph.SR] (cit. on p. 61).

Beig, R. and W. Simon (May 1981). "On the multipole expansion for stationary space-times". In: *Proceedings of the Royal Society of London Series A* 376, pp. 333–341. DOI: 10.1098/rspa.1981.0095 (cit. on p. 60).

Beig, R. and W. Simon (Nov. 1980). "Proof of a multipole conjecture due to Geroch". In: *Communications in Mathematical Physics* 78, pp. 75–82. DOI: 10.1007/BF01941970 (cit. on p. 60).

Bekenstein, J. D. (1973). "Extraction of Energy and Charge from a Black Hole". In: *Phys. Rev. D* 7 (4), pp. 949–953. DOI: 10.1103/PhysRevD.7.949. URL: https://link.aps.org/doi/10.1103/PhysRevD.7.949 (cit. on p. 11).

Berti, E. et al. (2015). "Testing General Relativity with Present and Future Astrophysical Observations". In: *Class. Quant. Grav.* 32, p. 243001. DOI: 10.1088/0264-9381/32/24/243001. arXiv: 1501.07274 [gr-qc] (cit. on p. 61).

Beskin, V., A. Gurevich, and Y. Istomin (1993). *Physics of the Pulsar Magnetosphere*. Cambridge University Press. URL: https://books.google.be/books?id=VOZmHowe724C (cit. on p. 22).

Bisnovatyi-Kogan, G. S. and S. I. Blinnikov (July 1977). "Disk accretion onto a black hole at subcritical luminosity". In: *Astronomy and Astrophysics* 59, pp. 111–125 (cit. on p. 53).

Bičák, J. and F. Hejda (2015). "Near-horizon description of extremal magnetized stationary black holes and Meissner effect". In: *Phys. Rev.* D92.10, p. 104006. DOI: 10.1103/PhysRevD.92.104006. arXiv: 1510.01911 [gr-qc] (cit. on pp. 101, 110, 117, 122, 124).

Bičák, J. and V. Janiš (1985). "Magnetic fluxes across black holes". In: *Monthly Notices of the Royal Astronomical Society* 212.4, pp. 899–915. DOI: 10.1093/mnras/212.4.899. URL: http://dx.doi.org/10.1093/mnras/212.4.899 (cit. on p. 105).

Blanchet, L. and T. Damour (Dec. 1986). "Radiative gravitational fields in general relativity. I - General structure of the field outside the source". In: *Philosophical Transactions of the Royal Society of London Series A* 320, pp. 379–430. DOI: 10.1098/rsta.1986.0125 (cit. on pp. 60, 159).

Blanchet, L. (2014). "Gravitational Radiation from Post-Newtonian Sources and Inspiralling Compact Binaries". In: *Living Rev. Rel.* 17, p. 2. DOI: 10.12942/lrr-2014-2. arXiv: 1310.1528 [gr-qc] (cit. on pp. 62, 68, 159, 161).

Blanchet, L. (1998). "On the multipole expansion of the gravitational field". In: *Class. Quant. Grav.* 15, pp. 1971–1999. DOI: 10.1088/0264-9381/15/7/013. arXiv: gr-qc/9801101 [gr-qc] (cit. on pp. 63, 66).

Blanchet, L. (1987). "Radiative gravitational fields in general relativity. 2. Asymptotic behaviour at future null infinity". In: *Proc. Roy. Soc. Lond.* A409, pp. 383–399. DOI: 10.1098/rspa.1987.0022 (cit. on pp. 67, 68).

Blanchet, L. and T. Damour (1992). "Hereditary effects in gravitational radiation". In: *Phys. Rev.* D46, pp. 4304–4319. DOI: 10.1103/PhysRevD.46.4304 (cit. on p. 145).

Blanchet, L. and T. Damour (1986). "Radiative gravitational fields in general relativity I. general structure of the field outside the source". In: *Phil. Trans. Roy. Soc. Lond.* A320, pp. 379–430. DOI: 10.1098/rsta.1986.0125 (cit. on p. 152).

Blanchet, L., T. Damour, and B. R. Iyer (2005). "Surface-integral expressions for the multipole moments of post-Newtonian sources and the boosted Schwarzschild solution". In: *Class. Quant. Grav.* 22, pp. 155–182. DOI: 10.1088/0264-9381/22/1/011. arXiv: gr-qc/0410021 [gr-qc] (cit. on pp. 66, 157).

Blandford, R. D. and R. L. Znajek (1977). "Electromagnetic extractions of energy from Kerr black holes". In: *Mon. Not. Roy. Astron. Soc.* 179, pp. 433–456 (cit. on pp. 11, 22, 23, 35, 36).

Bondi, H. (1952). "On Spherically Symmetrical Accretion". In: *Monthly Notices of the Royal Astronomical Society* 112.2, pp. 195–204. DOI: 10.1093/mnras/112.2.195. eprint: /oup/backfile/content_public/journal/mnras/112/2/10.1093_mnras_112.2.195/2/mnras112-0195.pdf. URL: http://dx.doi.org/10.1093/mnras/112.2.195 (cit. on p. 40).

Bondi, H., M. G. J. van der Burg, and A. W. K. Metzner (Aug. 1962). "Gravitational Waves in General Relativity. VII. Waves from Axi-Symmetric Isolated Systems". In: *Proceedings of the Royal Society of London Series A* 269, pp. 21–52. DOI: 10.1098/rspa.1962.0161 (cit. on pp. 65, 145).

Bonnor, W. B. (1954). "Static Magnetic Fields in General Relativity". In: *Proceedings of the Physical Society. Section A* 67.3, p. 225. URL: http://stacks.iop.org/0370-1298/67/i=3/a=305 (cit. on p. 100).

Booth, I., M. Hunt, A. Palomo-Lozano, and H. K. Kunduri (2015). "Insights from Melvin-Kerr- Newman spacetimes". In: *Class. Quant. Grav.* 32.23, p. 235025. DOI: 10.1088/0264-9381/32/23/235025. arXiv: 1502.07388v3 [gr-qc] (cit. on pp. 101, 111, 112, 113, 116, 122, 124).

Bredberg, I., T. Hartman, W. Song, and A. Strominger (2010). "Black Hole Superradiance From Kerr/CFT". In: *JHEP* 04, p. 019. DOI: 10.1007/JHEP04(2010)019. arXiv: 0907.3477 [hep-th] (cit. on p. 15).

Bredberg, I., C. Keeler, V. Lysov, and A. Strominger (2011). "Cargese Lectures on the Kerr/CFT Correspondence". In: *Nucl. Phys. Proc. Suppl.* 216, pp. 194–210. DOI: 10.1016/j.nuclphysbps.2011.04.155. arXiv: 1103.2355 [hep-th] (cit. on p. 15).

Breitenlohner, P. and D. Z. Freedman (1982). "Positive Energy in anti-De Sitter Backgrounds and Gauged Extended Supergravity". In: *Phys. Lett.* 115B, pp. 197–201. DOI: 10.1016/0370-2693(82)90643-8 (cit. on p. 122).

Brennan, T. D., S. E. Gralla, and T. Jacobson (2013). "Exact Solutions to Force-Free Electrodynamics in Black Hole Backgrounds". In: *Class. Quant. Grav.* 30,

p. 195012. DOI: 10.1088/0264-9381/30/19/195012. arXiv: 1305.6890 [gr-qc] (cit. on pp. 23, 34, 35, 36).

Brenneman, L. (2013). "Measuring Supermassive Black Hole Spins in Active Galactic Nuclei". In: DOI: 10.1007/978-1-4614-7771-6. arXiv: 1309.6334 [astro-ph.HE] (cit. on pp. 1, 12).

Broderick, A. E. and A. Loeb (2006). "Imaging optically-thin hot spots near the black hole horizon of sgr a* at radio and near-infrared wavelengths". In: *Mon. Not. Roy. Astron. Soc.* 367, pp. 905–916. DOI: 10.1111/j.1365-2966.2006.10152.x. arXiv: astro-ph/0509237 [astro-ph] (cit. on p. 1).

Bromley, B. C., W. A. Miller, and V. I. Pariev (Jan. 1998). "The inner edge of the accretion disk around a supermassive black hole". In: *Nature* 391, 54 EP –. URL: http://dx.doi.org/10.1038/34130 (cit. on p. 141).

Burke, W. L. (1971). "Gravitational radiation damping of slowly moving systems calculated using matched asymptotic expansions." In: *Journal of Mathematical Physics* 12, pp. 401–418. DOI: 10.1063/1.1665603 (cit. on p. 66).

Caldarelli, M. M., G. Cognola, and D. Klemm (2000). "Thermodynamics of Kerr-Newman-AdS black holes and conformal field theories". In: *Class. Quant. Grav.* 17, pp. 399–420. DOI: 10.1088/0264-9381/17/2/310. arXiv: hep-th/9908022 [hep-th] (cit. on pp. 113, 117).

Campbell, W. B., J. Macek, and T. A. Morgan (1977). "Relativistic Time Dependent Multipole Analysis for Scalar, Electromagnetic, and Gravitational Fields". In: *Phys. Rev.* D15, pp. 2156–2164. DOI: 10.1103/PhysRevD.15.2156 (cit. on p. 66).

Campbell, W. B. and T. Morgan (1971). "Debye potentials for the gravitational field." In: *Physica* 53, pp. 264–288. DOI: 10.1016/0031-8914(71)90074-7 (cit. on p. 66).

Campiglia, M. and A. Laddha (2016). "Subleading soft photons and large gauge transformations". In: *JHEP* 11, p. 012. DOI: 10.1007/JHEP11(2016)012. arXiv: 1605.09677 [hep-th] (cit. on p. 146).

Cardoso, V. and L. Gualtieri (2016). "Testing the black hole no-hair hypothesis". In: *Class. Quant. Grav.* 33.17, p. 174001. DOI: 10.1088/0264-9381/33/17/174001. arXiv: 1607.03133 [gr-qc] (cit. on p. 60).

Carter, B. (1971). "Axisymmetric Black Hole Has Only Two Degrees of Freedom". In: *Phys. Rev. Lett.* 26 (6), pp. 331–333. DOI: 10.1103/PhysRevLett.26.331. URL: https://link.aps.org/doi/10.1103/PhysRevLett.26.331 (cit. on p. 100).

Carter, B. (1968). "Global Structure of the Kerr Family of Gravitational Fields". In: *Phys. Rev.* 174 (5), pp. 1559–1571. DOI: 10.1103/PhysRev.174.1559. URL: https://link.aps.org/doi/10.1103/PhysRev.174.1559 (cit. on p. 10).

Carter, B. (2009). "Republication of: Black hole equilibrium states". In: *General Relativity and Gravitation* 41.12, p. 2873. ISSN: 1572-9532. DOI: 10.1007/s10714-009-0888-5. URL: https://doi.org/10.1007/s10714-009-0888-5 (cit. on p. 104).

Carter, B. (2010). "Republication of: Black hole equilibrium states Part II. General theory of stationary black hole states". In: *General Relativity and Gravitation* 42.3, pp. 653–744. ISSN: 1572-9532. DOI: 10.1007/s10714-009-0920-9. URL: https://doi.org/10.1007/s10714-009-0920-9 (cit. on p. 104).

Carter, B. (1979). "The general theory of the mechanical, electromagnetic and thermodynamic properties of black holes". In: *General Relativity: An Einstein Centenary Survey* (cit. on pp. 23, 25).

Castro, A., A. Maloney, and A. Strominger (2010). "Hidden Conformal Symmetry of the Kerr Black Hole". In: *Phys. Rev.* D82, p. 024008. DOI: 10.1103/PhysRevD.82.024008. arXiv: 1004.0996 [hep-th] (cit. on p. 15).

Chandrasekhar, S. (July 1956). "Axisymmetric Magnetic Fields and Fluid Motions." In: *Astrophys. J.* 124, p. 232. DOI: 10.1086/146217 (cit. on p. 22).

Chandrasekhar, S. and P. C. Kendall (Sept. 1957). "On Force-Free Magnetic Fields." In: *Astrophys. J.* 126, p. 457. DOI: 10.1086/146413 (cit. on p. 22).

Chen, B. and L. C. Stein (2017). "Separating metric perturbations in near-horizon extremal Kerr". In: *Phys. Rev.* D96.6, p. 064017. DOI: 10.1103/PhysRevD.96.064017. arXiv: 1707.05319 [gr-qc] (cit. on p. 19).

Choquet-Bruhat, Y., C. DeWitt-Morette, and M. Dillard-Bleick (1982). *Analysis, Manifolds, and Physics*. Analysis, Manifolds, and Physics pt. 1. North-Holland Publishing Company. ISBN: 9780444860170 (cit. on p. 25).

Christodoulou, D. and S. Klainerman (1993). "The Global nonlinear stability of the Minkowski space". In: (cit. on pp. 145, 156).

Christodoulou, D. and R. Ruffini (1971). "Reversible transformations of a charged black hole". In: *Phys. Rev.* D4, pp. 3552–3555. DOI: 10.1103/PhysRevD.4.3552 (cit. on p. 117).

Ciesielski, A. et al. (2012). "Stability of radiation-pressure dominated disks - I. The dispersion relation for a delayed heating cosity prescription". In: *Astron. Astrophys.* 538, A148. DOI: 10.1051/0004-6361/201117478. URL: https://doi.org/10.1051/0004-6361/201117478 (cit. on p. 141).

Collins, N. A. and S. A. Hughes (2004). "Towards a formalism for mapping the space-times of massive compact objects: Bumpy black holes and their orbits".

In: *Phys. Rev.* D69, p. 124022. DOI: 10.1103/PhysRevD.69.124022. arXiv: gr-qc/0402063 [gr-qc] (cit. on pp. 60, 61).

Compère, G. (2007a). "Symmetries and conservation laws in Lagrangian gauge theories with applications to the Mechanics of black holes and to Gravity in three dimensions". PhD thesis. Bruxelles: Université libre de Bruxelles. arXiv: 0708.3153 [hep-th] (cit. on pp. 160, 212).

Compère, G. and R. Oliveri (2016). "Near-horizon Extreme Kerr Magnetospheres". In: *Phys. Rev.* D93.2. [Erratum: Phys. Rev.D93,no.6,069906(2016)], p. 024035. DOI: 10.1103/PhysRevD.93.024035. arXiv: 1509.07637 [hep-th] (cit. on pp. iii, 15, 19, 23, 71, 72, 90).

Compère, G., P. Mao, A. Seraj, and M. M. Sheikh-Jabbari (2016). "Symplectic and Killing symmetries of AdS_3 gravity: holographic vs boundary gravitons". In: *JHEP* 01, p. 080. DOI: 10.1007/JHEP01(2016)080. arXiv: 1511.06079 [hep-th] (cit. on p. 155).

Compère, G., K. Hajian, A. Seraj, and M. M. Sheikh-Jabbari (2015). "Wiggling Throat of Extremal Black Holes". In: *JHEP* 10. [JHEP10,093(2015)], p. 093. DOI: 10.1007/JHEP10(2015)093. arXiv: 1506.07181 [hep-th] (cit. on p. 155).

Compère, G. (2006). "An introduction to the mechanics of black holes". In: *2nd Modave Summer School in Theoretical Physics Modave, Belgium, August 6-12, 2006*. arXiv: gr-qc/0611129 [gr-qc] (cit. on p. 112).

Compère, G. (2007b). "Note on the First Law with p-form potentials". In: *Phys. Rev.* D75, p. 124020. DOI: 10.1103/PhysRevD.75.124020. arXiv: hep-th/0703004 [hep-th] (cit. on pp. 101, 119).

Compère, G. (2012). "The Kerr/CFT correspondence and its extensions". In: *Living Rev. Rel.* 15. [Living Rev. Rel.20,no.1,1(2017)], p. 11. DOI: 10.1007/s41114-017-0003-2. arXiv: 1203.3561 [hep-th] (cit. on pp. 15, 110).

Compere, G. and F. Dehouck (2011). "Relaxing the Parity Conditions of Asymptotically Flat Gravity". In: *Class.Quant.Grav.* 28, p. 245016. DOI: 10.1088/0264-9381/28/24/245016,10.1088/0264-9381/30/3/039501. arXiv: 1106.4045 [hep-th] (cit. on pp. 145, 163).

Compere, G., F. Dehouck, and A. Virmani (2011). "On Asymptotic Flatness and Lorentz Charges". In: *Class.Quant.Grav.* 28, p. 145007. DOI: 10.1088/0264-9381/28/14/145007. arXiv: 1103.4078 [gr-qc] (cit. on p. 164).

Compère, G. and A. Fiorucci (2017). "Asymptotically flat spacetimes with BMS_3 symmetry". In: *Class. Quant. Grav.* 34.20, p. 204002. DOI: 10.1088/1361-6382/aa8aad. arXiv: 1705.06217 [hep-th] (cit. on p. 163).

Compère, G. and J. Long (2016). "Vacua of the gravitational field". In: *JHEP* 07, p. 137. DOI: 10.1007/JHEP07(2016)137. arXiv: 1601.04958 [hep-th] (cit. on p. 146).

Compère, G., K. Murata, and T. Nishioka (2009). "Central Charges in Extreme Black Hole/CFT Correspondence". In: *JHEP* 05, p. 077. DOI: 10.1088/1126-6708/2009/05/077. arXiv: 0902.1001 [hep-th] (cit. on pp. 112, 144, 212).

Compère, G., K. Fransen, T. Hertog, and J. Long (2017). "Gravitational waves from plunges into Gargantua". In: arXiv: 1712.07130 [gr-qc] (cit. on pp. 14, 17).

Compère, G. and R. Oliveri (2017). "Self-similar accretion in thin discs around near-extremal black holes". In: *Mon. Not. Roy. Astron. Soc.* 468.4, pp. 4351–4361. DOI: 10.1093/mnras/stx748. arXiv: 1703.00022 [astro-ph.HE] (cit. on pp. iii, 15, 17, 127).

Compère, G., S. E. Gralla, and A. Lupsasca (2016). "Force-Free Foliations". In: *Phys. Rev.* D94.12, p. 124012. DOI: 10.1103/PhysRevD.94.124012. arXiv: 1606.06727 [math-ph] (cit. on pp. 24, 34).

Compère, G., R. Oliveri, and A. Seraj (2018). "Gravitational multipole moments from Noether charges". In: *JHEP* 05, p. 054. DOI: 10.1007/JHEP05(2018)054. arXiv: 1711.08806 [hep-th] (cit. on pp. iii, 143).

Conde, E. and P. Mao (2017a). "BMS Supertranslations and Not So Soft Gravitons". In: *JHEP* 05, p. 060. DOI: 10.1007/JHEP05(2017)060. arXiv: 1612.08294 [hep-th] (cit. on p. 146).

Conde, E. and P. Mao (2017b). "Remarks on asymptotic symmetries and the subleading soft photon theorem". In: *Phys. Rev.* D95.2, p. 021701. DOI: 10.1103/PhysRevD.95.021701. arXiv: 1605.09731 [hep-th] (cit. on p. 146).

Copsey, K. and G. T. Horowitz (2006). "The Role of dipole charges in black hole thermodynamics". In: *Phys. Rev.* D73, p. 024015. DOI: 10.1103/PhysRevD.73.024015. arXiv: hep-th/0505278 [hep-th] (cit. on p. 118).

Cui, W., S. N. Zhang, and W. Chen (1998). "Evidence for frame-dragging around spinning black holes in x-ray binaries". In: *Astrophys. J.* 492, p. L53. DOI: 10.1086/311092. arXiv: astro-ph/9710352 [astro-ph] (cit. on p. 42).

Dafermos, M., I. Rodnianski, and Y. Shlapentokh-Rothman (2014). "Decay for solutions of the wave equation on Kerr exterior spacetimes III: The full subextremal case |a| < M". In: arXiv: 1402.7034 [gr-qc] (cit. on p. 9).

Damour, T. and B. R. Iyer (1991). "Multipole analysis for electromagnetism and linearized gravity with irreducible cartesian tensors". In: *Phys. Rev.* D43, pp. 3259–3272. DOI: 10.1103/PhysRevD.43.3259 (cit. on p. 66).

Damour, T., A. Nagar, and L. Villain (2012). "Measurability of the tidal polarizability of neutron stars in late-inspiral gravitational-wave signals". In: *Phys. Rev.* D85,

p. 123007. DOI: 10.1103/PhysRevD.85.123007. arXiv: 1203.4352 [gr-qc] (cit. on p. 61).

Datta, B. (1988). "Recent Developments in Neutron Star Physics". In: *Fundamentals of Cosmic Physics* 12, pp. 151–239 (cit. on p. 61).

Davies, P. C. W. (1977). "Thermodynamics of Black Holes". In: *Proc. Roy. Soc. Lond.* A353, pp. 499–521. DOI: 10.1098/rspa.1977.0047 (cit. on p. 121).

Davis, S. W., C. Done, and O. M. Blaes (2006). "Testing accretion disk theory in black hole x-ray binaries". In: *Astrophys. J.* 647, pp. 525–538. DOI: 10.1086/505386. arXiv: astro-ph/0602245 [astro-ph] (cit. on p. 41).

de Cesare, M., R. Oliveri, and J. W. van Holten (2017). "Field theoretical approach to gravitational waves". In: *Fortsch. Phys.* 65.5, p. 1700012. DOI: 10.1002/prop.201700012. arXiv: 1701.07794 [gr-qc] (cit. on p. iii).

Deruelle, N. and J. Katz (2005). "On the mass of a Kerr-anti-de Sitter spacetime in D dimensions". In: *Class. Quant. Grav.* 22, pp. 421–424. DOI: 10.1088/0264-9381/22/2/013. arXiv: gr-qc/0410135 [gr-qc] (cit. on p. 113).

DeWitt, B. S. (1975). "Quantum field theory in curved spacetime". In: *Physics Reports* 19.6, pp. 295 –357. ISSN: 0370-1573. DOI: https://doi.org/10.1016/0370-1573(75)90051-4. URL: http://www.sciencedirect.com/science/article/pii/0370157375900514 (cit. on p. 17).

Dias, O. J. C., M. Godazgar, and J. E. Santos (2015). "Linear Mode Stability of the Kerr-Newman Black Hole and Its Quasinormal Modes". In: *Phys. Rev. Lett.* 114 (15), p. 151101. DOI: 10.1103/PhysRevLett.114.151101. URL: https://link.aps.org/doi/10.1103/PhysRevLett.114.151101 (cit. on p. 9).

Doeleman, S. et al. (2009). "Imaging an Event Horizon: submm-VLBI of a Super Massive Black Hole". In: *astro2010: The Astronomy and Astrophysics Decadal Survey*. Vol. 2010. Astronomy. arXiv: 0906.3899 [astro-ph.CO] (cit. on p. 1).

Doeleman, S. S. et al. (Oct. 2012). "Jet-Launching Structure Resolved Near the Supermassive Black Hole in M87". In: *Science* 338, p. 355. DOI: 10.1126/science.1224768. arXiv: 1210.6132 [astro-ph.HE] (cit. on p. 1).

Doeleman, S. et al. (2008). "Event-horizon-scale structure in the supermassive black hole candidate at the Galactic Centre". In: *Nature* 455, p. 78. DOI: 10.1038/nature07245. arXiv: 0809.2442 [astro-ph] (cit. on p. 1).

Doeleman, S. S. et al. (2009). "Methods for detecting flaring structures in Sagittarius A* with high frequency VLBI". In: *Astrophys. J.* 695, pp. 59–74. DOI: 10.1088/0004-637X/695/1/59. arXiv: 0809.3424 [astro-ph] (cit. on p. 1).

Dokuchaev, V. et al. (1987). "A black hole in a magnetic universe". In: *Zh. Eksp. Teor. Fiz* 92, pp. 1921–1935 (cit. on pp. 100, 105, 106, 111).

Eardley, D. M. et al. (1973). "Gravitational-wave observations as a tool for testing relativistic gravity". In: *Phys. Rev. Lett.* 30, pp. 884–886. DOI: 10.1103/PhysRevLett.30.884 (cit. on p. 163).

Eatough, R. P. et al. (2013). "A strong magnetic field around the supermassive black hole at the centre of the Galaxy". In: DOI: 10.1038/nature12499. arXiv: 1308.3147 [astro-ph.GA] (cit. on p. 100).

Eddington, A. (1988). *The Internal Constitution of the Stars*. Cambridge Science Classics. Cambridge University Press. ISBN: 9780521337083. URL: https://books.google.be/books?id=RjC9DpnWFbkC (cit. on p. 40).

Einstein, A. (1918). "Über Gravitationswellen". In: *Sitzungsber. Preuss. Akad. Wiss. Berlin (Math. Phys.)* 1918, pp. 154–167 (cit. on p. 68).

Ellis, G. F. R. (2009). "Relativistic cosmology". In: *Gen. Rel. Grav.* 41. [Proc. Int. Sch. Phys. Fermi47,104(1971)], pp. 581–660. DOI: 10.1007/s10714-009-0760-7 (cit. on p. 44).

Epstein, R. and R. V. Wagoner (May 1975). "Post-Newtonian generation of gravitational waves". In: *Astrophysical Journal* 197, pp. 717–723. DOI: 10.1086/153561 (cit. on p. 66).

Ernst, F. J. (1976a). "Black holes in a magnetic universe". In: *Journal of Mathematical Physics* 17.1, pp. 54–56. DOI: 10.1063/1.522781. eprint: https://doi.org/10.1063/1.522781. URL: https://doi.org/10.1063/1.522781 (cit. on p. 100).

Ernst, F. J. (1968a). "New formulation of the axially symmetric gravitational field problem". In: *Phys. Rev.* 167, pp. 1175–1179. DOI: 10.1103/PhysRev.167.1175 (cit. on p. 100).

Ernst, F. J. (1968b). "New Formulation of the Axially Symmetric Gravitational Field Problem. II". In: *Phys. Rev.* 168, pp. 1415–1417. DOI: 10.1103/PhysRev.168.1415 (cit. on p. 100).

Ernst, F. J. (1976b). "Removal of the nodal singularity of the C-metric". In: *Journal of Mathematical Physics* 17.4, pp. 515–516. DOI: 10.1063/1.522935. eprint: https://aip.scitation.org/doi/pdf/10.1063/1.522935. URL: https://aip.scitation.org/doi/abs/10.1063/1.522935 (cit. on p. 100).

Ernst, F. J. and W. J. Wild (1976). "Kerr black holes in a magnetic universe". In: *Journal of Mathematical Physics* 17.2, pp. 182–184 (cit. on p. 100).

Fabian, A. (2012). "Observational Evidence of Active Galactic Nuclei Feedback". In: *Annual Review of Astronomy and Astrophysics* 50.1, pp. 455–489. DOI: 10.1146/annurev-astro-081811-125521. URL: https://doi.org/10.1146/annurev-astro-081811-125521 (cit. on p. 22).

Falcke, H., F. Melia, and E. Agol (2000). "Viewing the shadow of the black hole at the galactic center". In: *Astrophys. J.* 528, p. L13. DOI: 10.1086/312423. arXiv: astro-ph/9912263 [astro-ph] (cit. on p. 42).

Fernández, R. and B. D. Metzger (2016). "Electromagnetic Signatures of Neutron Star Mergers in the Advanced LIGO Era". In: *Ann. Rev. Nucl. Part. Sci.* 66, pp. 23–45. DOI: 10.1146/annurev-nucl-102115-044819. arXiv: 1512.05435 [astro-ph.HE] (cit. on p. 61).

Fish, V. L. et al. (2016). "Observing and Imaging Active Galactic Nuclei with the Event Horizon Telescope". In: *Galaxies* 4.4, p. 54. DOI: 10.3390/galaxies4040054. arXiv: 1607.03034 [astro-ph.IM] (cit. on p. 42).

Fodor, G., C. Hoenselaers, and Z. Perjés (Oct. 1989). "Multipole moments of axisymmetric systems in relativity". In: *Journal of Mathematical Physics* 30, pp. 2252–2257. DOI: 10.1063/1.528551 (cit. on p. 60).

Gal'tsov, D. V. and V. I. Petukhov (Mar. 1978). "Black hole in an external magnetic field". In: *Soviet Journal of Experimental and Theoretical Physics* 47, p. 419 (cit. on p. 100).

Gammie, C. F. (Sept. 1999). "Efficiency of Magnetized Thin Accretion Disks in the Kerr Metric". In: *ApJ* 522, pp. L57–L60. DOI: 10.1086/312207. eprint: astro-ph/9906223 (cit. on p. 128).

Gammie, C. F. and R. Popham (1998). "Advection-dominated Accretion Flows in the Kerr Metric. I. Basic Equations". In: *Astrophys. J.* 498, p. 313. DOI: 10.1086/305521. arXiv: astro-ph/9705117 (cit. on pp. 41, 44, 50, 51, 176, 177).

Gammie, C. F., S. L. Shapiro, and J. C. McKinney (2004). "Black hole spin evolution". In: *Astrophys. J.* 602, pp. 312–319. DOI: 10.1086/380996. arXiv: astro-ph/0310886 [astro-ph] (cit. on p. 129).

Gao, S. (2003). "The First law of black hole mechanics in Einstein-Maxwell and Einstein-Yang-Mills theories". In: *Phys. Rev.* D68, p. 044016. DOI: 10.1103/PhysRevD.68.044016. arXiv: gr-qc/0304094 [gr-qc] (cit. on p. 117).

Geroch, R. P. (1969). "Limits of spacetimes". In: *Commun. Math. Phys.* 13, pp. 180–193. DOI: 10.1007/BF01645486 (cit. on p. 13).

Geroch, R. P. (1970). "Multipole moments. II. Curved space". In: *J. Math. Phys.* 11, pp. 2580–2588. DOI: 10.1063/1.1665427 (cit. on pp. 60, 65).

Gibbons, G. W., A. H. Mujtaba, and C. N. Pope (2013). "Ergoregions in Magnetised Black Hole Spacetimes". In: *Class. Quant. Grav.* 30.12, p. 125008. DOI: 10.1088/0264-9381/30/12/125008. arXiv: 1301.3927 [gr-qc] (cit. on pp. 101, 107, 108, 109).

Gibbons, G. W., Y. Pang, and C. N. Pope (2014). "Thermodynamics of magnetized Kerr-Newman black holes". In: *Phys. Rev.* D89.4, p. 044029. DOI: 10.1103/

PhysRevD.89.044029. arXiv: 1310.3286 [hep-th] (cit. on pp. 101, 111, 112, 113, 117, 120, 123, 124, 125).

Gibbons, G. W., M. J. Perry, and C. N. Pope (2005). "The First law of thermodynamics for Kerr-anti-de Sitter black holes". In: *Class. Quant. Grav.* 22, pp. 1503–1526. DOI: 10.1088/0264-9381/22/9/002. arXiv: hep-th/0408217 [hep-th] (cit. on p. 113).

Gold, T. (1968). "Rotating neutron stars as the origin of the pulsating radio sources". In: *Nature* 218, pp. 731–732. DOI: 10.1038/218731a0 (cit. on p. 22).

Goldreich, P. and W. H. Julian (1969). "Pulsar electrodynamics". In: *Astrophys. J.* 157, p. 869. DOI: 10.1086/150119 (cit. on p. 22).

Gou, L. et al. (2011). "The extreme spin of the black hole in Cygnus X-1". In: *Astrophys. J.* 742, 85. DOI: 10.1088/0004-637X/742/2/85. arXiv: 1106.3690 [astro-ph.HE] (cit. on pp. 1, 12).

Gou, L. et al. (2014). "Confirmation Via the Continuum-Fitting Method that the Spin of the Black Hole in Cygnus X-1 is Extreme". In: *Astrophys. J.* 790.1, p. 29. DOI: 10.1088/0004-637X/790/1/29. arXiv: 1308.4760 [astro-ph.HE] (cit. on pp. 1, 12).

Gralla, S. E., S. A. Hughes, and N. Warburton (2016). "Inspiral into Gargantua". In: *Class. Quant. Grav.* 33.15, p. 155002. DOI: 10.1088/0264-9381/33/15/155002. arXiv: 1603.01221 [gr-qc] (cit. on p. 14).

Gralla, S. E. and T. Jacobson (2014). "Spacetime approach to force-free magnetospheres". In: *Mon. Not. Roy. Astron. Soc.* 445.3, pp. 2500–2534. DOI: 10.1093/mnras/stu1690. arXiv: 1401.6159 [astro-ph.HE] (cit. on pp. 24, 25, 27, 30, 32, 33, 36, 37, 38, 93).

Gralla, S. E., A. Lupsasca, and A. Strominger (2016). "Near-horizon Kerr Magnetosphere". In: *Phys. Rev.* D93.10, p. 104041. DOI: 10.1103/PhysRevD.93.104041. arXiv: 1602.01833 [hep-th] (cit. on pp. 15, 72, 78, 79, 91, 94, 96).

Gralla, S. E., A. Lupsasca, and A. Strominger (2017). "Observational Signature of High Spin at the Event Horizon Telescope". In: DOI: 10.1093/mnras/sty039. arXiv: 1710.11112 [astro-ph.HE] (cit. on pp. 15, 17).

Gralla, S. E., A. P. Porfyriadis, and N. Warburton (2015). "Particle on the Innermost Stable Circular Orbit of a Rapidly Spinning Black Hole". In: *Phys. Rev.* D92.6, p. 064029. DOI: 10.1103/PhysRevD.92.064029. arXiv: 1506.08496 [gr-qc] (cit. on p. 14).

Gralla, S. E. and P. Zimmerman (2017). "Critical Exponents of Extremal Kerr Perturbations". In: arXiv: 1711.00855 [gr-qc] (cit. on p. 17).

Grignani, G., T. Harmark, and M. Orselli (2018). "On the existence of the Blandford-Znajek monopole for a slowly rotating Kerr black hole". In: arXiv: 1804.05846 [gr-qc] (cit. on p. 24).

Guerlebeck, N. and M. Scholtz (2017). "Meissner effect for weakly isolated horizons". In: *Phys. Rev.* D95.6, p. 064010. DOI: 10.1103/PhysRevD.95.064010. arXiv: 1702.06155 [gr-qc] (cit. on p. 106).

Guerlebeck, N. and M. Scholtz (2018). "The Meissner Effect for axially symmetric charged black holes". In: arXiv: 1802.05423 [gr-qc] (cit. on p. 106).

Guica, M., T. Hartman, W. Song, and A. Strominger (2009). "The Kerr/CFT Correspondence". In: *Phys. Rev.* D80, p. 124008. DOI: 10.1103/PhysRevD.80.124008. arXiv: 0809.4266 [hep-th] (cit. on p. 15).

Gürsel, Y. (Aug. 1983). "Multipole moments for stationary systems: The equivalence of the Geroch-Hansen formulation and the Thorne formulation". In: *General Relativity and Gravitation* 15, pp. 737–754. DOI: 10.1007/BF01031881 (cit. on p. 65).

Hadar, S. and A. P. Porfyriadis (2017). "Whirling orbits around twirling black holes from conformal symmetry". In: *JHEP* 03, p. 014. DOI: 10.1007/JHEP03(2017)014. arXiv: 1611.09834 [hep-th] (cit. on p. 14).

Hadar, S., A. P. Porfyriadis, and A. Strominger (2015). "Fast plunges into Kerr black holes". In: *JHEP* 07, p. 078. DOI: 10.1007/JHEP07(2015)078. arXiv: 1504.07650 [hep-th] (cit. on p. 15).

Hadar, S., A. P. Porfyriadis, and A. Strominger (2014). "Gravity Waves from Extreme-Mass-Ratio Plunges into Kerr Black Holes". In: *Phys. Rev.* D90.6, p. 064045. DOI: 10.1103/PhysRevD.90.064045. arXiv: 1403.2797 [hep-th] (cit. on p. 15).

Hagen, H. M. Z. (1970). "On the analyticity of stationary vacuum solutions of Einstein's equation". In: *Proceedings of the Cambridge Philosophical Society* 68, p. 199. DOI: 10.1017/S0305004100001237 (cit. on p. 67).

Hansen, R. O. (1974). "Multipole moments of stationary space-times". In: *J. Math. Phys.* 15, pp. 46–52. DOI: 10.1063/1.1666501 (cit. on pp. 60, 65).

Harrison, B. K. (1968). "New Solutions of the Einstein-Maxwell Equations from Old". In: *Journal of Mathematical Physics* 9.11, pp. 1744–1752. DOI: 10.1063/1.1664508. eprint: https://doi.org/10.1063/1.1664508. URL: https://doi.org/10.1063/1.1664508 (cit. on pp. 100, 108).

Harte, A. I. (2017). "Metric-independence of vacuum and force-free electromagnetic fields". In: *Phys. Rev. Lett.* 118.14, p. 141101. DOI: 10.1103/PhysRevLett.118.141101. arXiv: 1701.05257 [gr-qc] (cit. on p. 24).

Hartman, T., W. Song, and A. Strominger (2010). "Holographic Derivation of Kerr-Newman Scattering Amplitudes for General Charge and Spin". In: *JHEP* 03,

p. 118. DOI: 10.1007/JHEP03(2010)118. arXiv: 0908.3909 [hep-th] (cit. on p. 15).

Hawking, S. W. (1972). "Black holes in general relativity". In: *Communications in Mathematical Physics* 25.2, pp. 152–166. ISSN: 1432-0916. DOI: 10.1007/BF01877517. URL: https://doi.org/10.1007/BF01877517 (cit. on p. 100).

Hawking, S. W., M. J. Perry, and A. Strominger (2017). "Superrotation Charge and Supertranslation Hair on Black Holes". In: *JHEP* 05, p. 161. DOI: 10.1007/JHEP05(2017)161. arXiv: 1611.09175 [hep-th] (cit. on p. 163).

Henneaux, M. and C. Teitelboim (1985). "Asymptotically anti-de Sitter spaces". In: *Commun. Math. Phys.* 98, pp. 391–424. DOI: 10.1007/BF01205790 (cit. on p. 113).

Henneaux, M. and C. Troessaert (2018a). "BMS Group at Spatial Infinity: the Hamiltonian (ADM) approach". In: *JHEP* 03, p. 147. DOI: 10.1007/JHEP03(2018)147. arXiv: 1801.03718 [gr-qc] (cit. on p. 163).

Henneaux, M. and C. Troessaert (2018b). "Hamiltonian structure and asymptotic symmetries of the Einstein-Maxwell system at spatial infinity". In: arXiv: 1805.11288 [gr-qc] (cit. on p. 163).

Henneaux, M., C. Martinez, R. Troncoso, and J. Zanelli (2007). "Asymptotic behavior and Hamiltonian analysis of anti-de Sitter gravity coupled to scalar fields". In: *Annals Phys.* 322, pp. 824–848. DOI: 10.1016/j.aop.2006.05.002. arXiv: hep-th/0603185 [hep-th] (cit. on p. 122).

Herdeiro, C. and E. Radu (2015). "Construction and physical properties of Kerr black holes with scalar hair". In: *Class. Quant. Grav.* 32.14, p. 144001. DOI: 10.1088/0264-9381/32/14/144001. arXiv: 1501.04319 [gr-qc] (cit. on p. 61).

Herdeiro, C. A. R. and E. Radu (2014). "Kerr black holes with scalar hair". In: *Phys. Rev. Lett.* 112, p. 221101. DOI: 10.1103/PhysRevLett.112.221101. arXiv: 1403.2757 [gr-qc] (cit. on p. 162).

Hewish, A. et al. (1968). "Observation of a rapidly pulsating radio source". In: *Nature* 217, pp. 709–713. DOI: 10.1038/217709a0 (cit. on p. 22).

Hinderer, T., B. D. Lackey, R. N. Lang, and J. S. Read (2010). "Tidal deformability of neutron stars with realistic equations of state and their gravitational wave signatures in binary inspiral". In: *Phys. Rev.* D81, p. 123016. DOI: 10.1103/PhysRevD.81.123016. arXiv: 0911.3535 [astro-ph.HE] (cit. on p. 61).

Hirose, S., J. H. Krolik, and O. Blaes (2009). "Radiation-Dominated Disks Are Thermally Stable". In: *Astrophys. J.* 691, pp. 16–31. DOI: 10.1088/0004-637X/691/1/16. arXiv: 0809.1708 [astro-ph] (cit. on p. 53).

Hiscock, W. A. (1981). "On black holes in magnetic universes". In: *Journal of Mathematical Physics* 22.8, pp. 1828–1833 (cit. on pp. 100, 109).

Israel, W. (1986). "Third Law of Black-Hole Dynamics: A Formulation and Proof". In: *Phys. Rev. Lett.* 57 (4), pp. 397–399. DOI: 10.1103/PhysRevLett.57.397. URL: https://link.aps.org/doi/10.1103/PhysRevLett.57.397 (cit. on p. 12).

Israel, W. (1968). "Event horizons in static electrovac space-times". In: *Communications in Mathematical Physics* 8.3, pp. 245–260. ISSN: 1432-0916. DOI: 10.1007/BF01645859. URL: https://doi.org/10.1007/BF01645859 (cit. on p. 100).

Israel, W. (1967). "Event Horizons in Static Vacuum Space-Times". In: *Phys. Rev.* 164 (5), pp. 1776–1779. DOI: 10.1103/PhysRev.164.1776. URL: https://link.aps.org/doi/10.1103/PhysRev.164.1776 (cit. on p. 100).

Iyer, V. and R. M. Wald (1994). "Some properties of Noether charge and a proposal for dynamical black hole entropy". In: *Phys. Rev.* D50, pp. 846–864. DOI: 10.1103/PhysRevD.50.846. arXiv: gr-qc/9403028 [gr-qc] (cit. on pp. 2, 101, 117, 118, 144, 145, 149, 153, 156, 212).

Jacobson, T. and M. J. Rodriguez (2017). "Blandford-Znajek process in vacuo and its holographic dual". In: arXiv: 1709.10090 [hep-th] (cit. on p. 91).

Jaroszynski, M., M. A. Abramowicz, and B. Paczynski (1980). "Supercritical accretion disks around black holes". In: *Acta Astronom.* 30, pp. 1–34 (cit. on p. 41).

Johannsen, T. (2013). "Inner Accretion Disk Edges in a Kerr-Like Spacetime". In: *Phys. Rev.* D87.12, p. 124010. DOI: 10.1103/PhysRevD.87.124010. arXiv: 1304.8106 [gr-qc] (cit. on p. 141).

Johannsen, T. et al. (2016). "Testing General Relativity with the Shadow Size of Sgr A*". In: *Phys. Rev. Lett.* 116.3, p. 031101. DOI: 10.1103/PhysRevLett.116.031101. arXiv: 1512.02640 [astro-ph.GA] (cit. on p. 42).

Johnson, M. D. et al. (2015). "Resolved Magnetic-Field Structure and Variability Near the Event Horizon of Sagittarius A*". In: *Science* 350.6265, pp. 1242–1245. DOI: 10.1126/science.aac7087. arXiv: 1512.01220 [astro-ph.HE] (cit. on p. 1).

Karas, V and D Vokrouhlickỳ (1991). "On interpretation of the magnetized Kerr-Newman black hole". In: *Journal of mathematical physics* 32.3, pp. 714–716 (cit. on pp. 100, 106, 111).

Karas, V., B. Czerny, Z. Abrassart, and M. Abramowicz (2000). "A cloud model of active galactic nuclei: the iron k-alpha line diagnostics". In: *Mon. Not. Roy. Astron. Soc.* 318, p. 547. DOI: 10.1046/j.1365-8711.2000.03754.x. arXiv: astro-ph/0006187 [astro-ph] (cit. on p. 42).

Kay, B. and R. Wald (1991). "Theorems on the Uniqueness and Thermal Properties of Stationary, Nonsingular, Quasifree States on Space-Times with a Bifurcate

Killing Horizon". In: *Phys. Rep.* 207, pp. 49–136. DOI: 10.1016/0370-1573(91)90015-E (cit. on p. 17).

Kerr, R. P. (1963). "Gravitational Field of a Spinning Mass as an Example of Algebraically Special Metrics". In: *Phys. Rev. Lett.* 11 (5), pp. 237–238. DOI: 10.1103/PhysRevLett.11.237. URL: https://link.aps.org/doi/10.1103/PhysRevLett.11.237 (cit. on p. 9).

Kesden, M., G. Lockhart, and E. S. Phinney (2010). "Maximum black-hole spin from quasi-circular binary mergers". In: *Phys. Rev.* D82, p. 124045. DOI: 10.1103/PhysRevD.82.124045. arXiv: 1005.0627 [gr-qc] (cit. on p. 129).

Kim, H., C. H. Lee, and H. K. Lee (2001). "Nonvanishing magnetic flux through the slightly charged Kerr black hole". In: *Phys. Rev.* D63, p. 064037. DOI: 10.1103/PhysRevD.63.064037. arXiv: gr-qc/0011044 [gr-qc] (cit. on p. 106).

King, A. R., J. P. Lasota, and W. Kundt (1975). "Black Holes and Magnetic Fields". In: *Phys. Rev.* D12, pp. 3037–3042. DOI: 10.1103/PhysRevD.12.3037 (cit. on p. 105).

Kinoshita, S. and T. Igata (2017). "The essence of the Blandford-Znajek process". In: arXiv: 1710.09152 [gr-qc] (cit. on pp. 24, 106).

Koide, S. and T. Baba (2014). "Causal extraction of black hole rotational energy by various kinds of electromagnetic fields". In: *Astrophys. J.* 792, p. 88. DOI: 10.1088/0004-637X/792/2/88. arXiv: 1407.7088 [astro-ph.HE] (cit. on p. 37).

Komissarov, S. S. (2009). "Blandford-Znajek mechanism versus Penrose process". In: *J. Korean Phys. Soc.* 54, pp. 2503–2512. DOI: 10.3938/jkps.54.2503. arXiv: 0804.1912 [astro-ph] (cit. on p. 37).

Komissarov, S. S. (2004). "Electrodynamics of black hole magnetospheres". In: *Mon. Not. Roy. Astron. Soc.* 350, p. 407. DOI: 10.1111/j.1365-2966.2004.07446.x. arXiv: astro-ph/0402403 [astro-ph] (cit. on p. 96).

Koratkar, A. and O. Blaes (Jan. 1999). "The Ultraviolet and Optical Continuum Emission in Active Galactic Nuclei: The Status of Accretion Disks". In: *PASP* 111, pp. 1–30. DOI: 10.1086/316294 (cit. on p. 128).

Krolik, J. H. (Apr. 1999). "Magnetized Accretion inside the Marginally Stable Orbit around a Black Hole". In: *ApJ* 515, pp. L73–L76. DOI: 10.1086/311979. eprint: astro-ph/9902267 (cit. on p. 128).

Krolik, J. H. and J. F. Hawley (2002). "Where is the inner edge of an accretion disk around a black hole?" In: *Astrophys. J.* 573, p. 754. DOI: 10.1086/340760. arXiv: astro-ph/0203289 [astro-ph] (cit. on p. 141).

Kundu, P. (June 1981a). “Multipole expansion of stationary asymptotically flat vacuum metrics in general relativity”. In: *Journal of Mathematical Physics* 22, pp. 1236–1242. DOI: 10.1063/1.525047 (cit. on p. 60).

Kundu, P. (Sept. 1981b). “On the analyticity of stationary gravitational fields at spatial infinity”. In: *Journal of Mathematical Physics* 22, pp. 2006–2011. DOI: 10.1063/1.525148 (cit. on p. 60).

Kunduri, H. K. and J. Lucietti (2013). “Classification of near-horizon geometries of extremal black holes”. In: *Living Rev. Rel.* 16, p. 8. DOI: 10.12942/lrr-2013-8. arXiv: 1306.2517 [hep-th] (cit. on p. 101).

Kunduri, H., J. Lucietti, and H. Reall (2007). “Near-horizon symmetries of extremal black holes”. In: *Class. Quantum Grav.* 24, pp. 4169–4190. DOI: 10.1088/0264-9381/24/16/012. arXiv: 0705.4214 [hep-th] (cit. on p. 16).

Laarakkers, W. G. and E. Poisson (Feb. 1999). “Quadrupole Moments of Rotating Neutron Stars”. In: *Astrophys. J.* 512, pp. 282–287. DOI: 10.1086/306732. eprint: gr-qc/9709033 (cit. on p. 61).

Lackey, B. D. et al. (2012). “Extracting equation of state parameters from black hole-neutron star mergers. I. Nonspinning black holes”. In: *Phys. Rev.* D85, p. 044061. DOI: 10.1103/PhysRevD.85.044061. arXiv: 1109.3402 [astro-ph.HE] (cit. on p. 61).

Lasota, J.-P. (2016). “Black Hole Accretion Discs”. In: *Astrophysics of Black Holes: From Fundamental Aspects to Latest Developments*. Ed. by C. Bambi. Vol. 440. Astrophysics and Space Science Library, p. 1. DOI: 10.1007/978-3-662-52859-4_1 (cit. on p. 46).

Lasota, J. P. et al. (2014). “Extracting black-hole rotational energy: The generalized Penrose process”. In: *Phys. Rev.* D89.2, p. 024041. DOI: 10.1103/PhysRevD.89.024041. arXiv: 1310.7499 [gr-qc] (cit. on p. 37).

Lasota, J. (1994). “Slim Accretion Discs”. In: *Theory of Accretion Disks?2*. Springer Netherlands, pp. 341–349 (cit. on p. 178).

Lattimer, J. M. (2012). “The nuclear equation of state and neutron star masses”. In: *Ann. Rev. Nucl. Part. Sci.* 62, pp. 485–515. DOI: 10.1146/annurev-nucl-102711-095018. arXiv: 1305.3510 [nucl-th] (cit. on p. 61).

Lee, J. and R. Wald (1990). “Local symmetries and constraints”. In: *J. Math. Phys.* 31, pp. 725–743. DOI: 10.1063/1.528801 (cit. on pp. 145, 160, 212).

Lewandowski, J. and T. Pawlowski (2003). “Extremal isolated horizons: A Local uniqueness theorem”. In: *Class. Quant. Grav.* 20, pp. 587–606. DOI: 10.1088/0264-9381/20/4/303. arXiv: gr-qc/0208032 [gr-qc] (cit. on p. 101).

Li, H. and J. Wang (2017). "Expanded solutions of force-free electrodynamics on general Kerr black holes". In: *Phys. Rev.* D96.2, p. 023014. DOI: 10.1103/PhysRevD.96.023014. arXiv: 1705.08757 [astro-ph.HE] (cit. on p. 24).

Li, H., C. Yu, J. Wang, and Z. Xu (2015). "Force-free magnetosphere on near-horizon geometry of near-extreme Kerr black holes". In: *Phys. Rev.* D92.2, p. 023009. DOI: 10.1103/PhysRevD.92.023009. arXiv: 1403.6959 [gr-qc] (cit. on p. 72).

Li, L.-X. (Mar. 2002). "Accretion Disk Torqued by a Black Hole". In: *Astrophys. J.* 567, pp. 463–476. DOI: 10.1086/338486. eprint: astro-ph/0012469 (cit. on pp. 41, 129, 131).

Li, L.-X. (Apr. 2000). "Extracting Energy from a Black Hole through Its Disk". In: *ApJ* 533, pp. L115–L118. DOI: 10.1086/312616. eprint: astro-ph/0002004 (cit. on p. 128).

Li, L.-X., E. R. Zimmerman, R. Narayan, and J. E. McClintock (2005). "Multi-temperature blackbody spectrum of a thin accretion disk around a Kerr black hole: Model computations and comparison with observations". In: *Astrophys. J. Suppl.* 157, pp. 335–370. DOI: 10.1086/428089. arXiv: astro-ph/0411583 [astro-ph] (cit. on p. 128).

Lightman, A. P. and D. M. Eardley (Jan. 1974). "Black Holes in Binary Systems: Instability of Disk Accretion". In: *The Astrophysical Journal Letters* 187, p. L1. DOI: 10.1086/181377 (cit. on pp. 41, 42, 53, 140).

Lupsasca, A., A. P. Porfyriadis, and Y. Shi (2018). "Critical Emission from a High-Spin Black Hole". In: *Phys. Rev.* D97.6, p. 064017. DOI: 10.1103/PhysRevD.97.064017. arXiv: 1712.10182 [gr-qc] (cit. on pp. 15, 17).

Lupsasca, A. and M. J. Rodriguez (2015). "Exact Solutions for Extreme Black Hole Magnetospheres". In: *JHEP* 07, p. 090. DOI: 10.1007/JHEP07(2015)090. arXiv: 1412.4124 [hep-th] (cit. on pp. 15, 19, 23, 72, 83, 84, 87, 95, 184, 186, 187, 189, 190).

Lupsasca, A., M. J. Rodriguez, and A. Strominger (2014). "Force-Free Electrodynamics around Extreme Kerr Black Holes". In: *JHEP* 12, p. 185. DOI: 10.1007/JHEP12(2014)185. arXiv: 1406.4133 [hep-th] (cit. on pp. 15, 19, 23, 72).

Lüst, R. and A. Schlüter (Jan. 1954). "Kraftfreie Magnetfelder". In: *Zeitschrift fur Astrophysik* 34, p. 263 (cit. on p. 22).

Lynden-Bell, D. (1969). "Galactic nuclei as collapsed old quasars". In: *Nature* 223, p. 690. DOI: 10.1038/223690a0 (cit. on p. 40).

Lyutikov, M. (2011). "Electromagnetic power of merging and collapsing compact objects". In: *Phys. Rev.* D83, p. 124035. DOI: 10.1103/PhysRevD.83.124035. arXiv: 1104.1091 [astro-ph.HE] (cit. on pp. 23, 36).

MacDonald, D. and K. S. Thorne (1982). "Black-hole electrodynamics - an absolute-space/universal-time formulation". In: *Mon. Not. Roy. Astron. Soc.* 198, pp. 345–383 (cit. on pp. 35, 37).

Mann, R. B., D. Marolf, and A. Virmani (2006). "Covariant Counterterms and Conserved Charges in Asymptotically Flat Spacetimes". In: *Class. Quant. Grav.* 23, pp. 6357–6378. DOI: 10.1088/0264-9381/23/22/017. arXiv: gr-qc/0607041 [gr-qc] (cit. on p. 164).

Mann, R. B., D. Marolf, R. McNees, and A. Virmani (2008). "On the Stress Tensor for Asymptotically Flat Gravity". In: *Class. Quant. Grav.* 25, p. 225019. DOI: 10.1088/0264-9381/25/22/225019. arXiv: 0804.2079 [hep-th] (cit. on p. 164).

Mao, P. and J.-B. Wu (2017). "Note on asymptotic symmetries and soft gluon theorems". In: arXiv: 1704.05740 [hep-th] (cit. on p. 146).

Marchand, T., L. Blanchet, and G. Faye (2016). "Gravitational-wave tail effects to quartic non-linear order". In: *Class. Quant. Grav.* 33.24, p. 244003. DOI: 10.1088/0264-9381/33/24/244003. arXiv: 1607.07601 [gr-qc] (cit. on p. 159).

Maselli, A. et al. (2015). "Testing Gravity with Quasi Periodic Oscillations from accreting Black Holes: the Case of the Einstein-Dilaton-Gauss-Bonnet Theory". In: *Astrophys. J.* 801.2, p. 115. DOI: 10.1088/0004-637X/801/2/115. arXiv: 1412.3473 [astro-ph.HE] (cit. on p. 141).

Mathews, J. (1962). "Gravitational Multipole Radiation". In: *Journal of the Society for Industrial and Applied Mathematics* 10.4, pp. 768–780. DOI: 10.1137/0110059. eprint: https://doi.org/10.1137/0110059. URL: https://doi.org/10.1137/0110059 (cit. on p. 67).

McClintock, J. E., R. Narayan, and J. F. Steiner (2014). "Black Hole Spin via Continuum Fitting and the Role of Spin in Powering Transient Jets". In: *Space Sci. Rev.* 183, pp. 295–322. DOI: 10.1007/s11214-013-0003-9. arXiv: 1303.1583 [astro-ph.HE] (cit. on p. 128).

McClintock, J. E. et al. (2006). "The Spin of the Near-Extreme Kerr Black Hole GRS 1915+105". In: *Astrophys. J.* 652, pp. 518–539. DOI: 10.1086/508457. arXiv: astro-ph/0606076 [astro-ph] (cit. on pp. 1, 12, 41).

McKinney, J. C., A. Tchekhovskoy, and R. D. Blandford (2012). "General Relativistic Magnetohydrodynamic Simulations of Magnetically Choked Accretion Flows around Black Holes". In: *Mon. Not. Roy. Astron. Soc.* 423, p. 3083. DOI: 10.1111/j.1365-2966.2012.21074.x. arXiv: 1201.4163 [astro-ph.HE] (cit. on p. 22).

Meissner, W. and R. Ochsenfeld (1933). "Ein neuer Effekt bei Eintritt der Supraleitfähigkeit". In: *Naturwissenschaften* 21.44, pp. 787–788. ISSN: 1432-1904. DOI:

10.1007/BF01504252. URL: https://doi.org/10.1007/BF01504252 (cit. on p. 105).

Melvin, M. A. (1964). "Pure magnetic and electric geons". In: *Physics Letters* 8.1, pp. 65–68 (cit. on p. 100).

Menon, G. (2015). "Force-free Currents and the Newman-Penrose Tetrad of a Kerr Black Hole: Exact Local Solutions". In: *Phys. Rev.* D92.2, p. 024054. DOI: 10.1103/PhysRevD.92.024054. arXiv: 1505.08172 [gr-qc] (cit. on pp. 23, 33).

Menon, G. and C. D. Dermer (2007). "A class of exact solution to the blandford-znajek process". In: *Gen. Rel. Grav.* 39, pp. 785–794. DOI: 10.1007/s10714-007-0418-2. arXiv: astro-ph/0511661 [astro-ph] (cit. on pp. 23, 33).

Menon, G. and C. D. Dermer (2005). "Analytic solutions to the constraint equation for a force-free magnetosphere around a kerr black hole". In: *Astrophys. J.* 635, pp. 1197–1202. DOI: 10.1086/497631. arXiv: astro-ph/0509130 [astro-ph] (cit. on pp. 23, 33).

Menon, G. and C. D. Dermer (2011). "Jet Formation in the magnetospheres of supermassive black holes: analytic solutions describing energy loss through Blandford-Znajek processes". In: *Mon. Not. Roy. Astron. Soc.* 417, p. 1098. DOI: 10.1111/j.1365-2966.2011.19327.x. arXiv: 1105.4139 [astro-ph.HE] (cit. on pp. 23, 33).

Michel, F. C. (Feb. 1973). "Rotating Magnetosphere: a Simple Relativistic Model". In: *Astrophys. J.* 180, pp. 207–226. DOI: 10.1086/151956 (cit. on pp. 22, 23, 35).

Michel, F. C. (1982). "Theory of pulsar magnetospheres". In: *Rev. Mod. Phys.* 54, pp. 1–66. DOI: 10.1103/RevModPhys.54.1 (cit. on p. 22).

Miller, J. M. et al. (2013). "NuSTAR Spectroscopy of GRS 1915+105: Disk Reflection, Spin, and Connections to Jets". In: *The Astrophysical Journal Letters* 775.2, p. L45. URL: http://stacks.iop.org/2041-8205/775/i=2/a=L45 (cit. on pp. 129, 136).

Miller, J. M., A. C. Fabian, and M. C. Miller (2004). "A Comparison of intermediate mass black hole candidate ULXs and stellar-mass black holes". In: *Astrophys. J.* 614, pp. L117–L120. DOI: 10.1086/425316. arXiv: astro-ph/0406656 [astro-ph] (cit. on p. 41).

Mirbabayi, M. and M. Simonović (2016). "Weinberg Soft Theorems from Weinberg Adiabatic Modes". In: arXiv: 1602.05196 [hep-th] (cit. on p. 146).

Mishra, B., P. C. Fragile, L. C. Johnson, and W. Kluźniak (2016). "Three-dimensional, global, radiative GRMHD simulations of a thermally unstable disc". In: *Mon. Not. Roy. Astron. Soc.* 463.4, pp. 3437–3448. DOI: 10.1093/mnras/stw2245. arXiv: 1603.04082 [astro-ph.HE] (cit. on p. 141).

Misner, C. W. (1972). "Interpretation of Gravitational-Wave Observations". In: *Phys. Rev. Lett.* 28 (15), pp. 994–997. DOI: 10.1103/PhysRevLett.28.994. URL: https://link.aps.org/doi/10.1103/PhysRevLett.28.994 (cit. on p. 11).

Misner, C. W., K. S. Thorne, and J. A. Wheeler (1973). *Gravitation*. San Francisco: W. H. Freeman. ISBN: 9780716703440 (cit. on pp. 64, 67).

Moeen Moghaddas, M. (2016). "Bulk viscosity of accretion disks around non rotating black holes". In: *Astrophysics and Space Science* 362.1, p. 14. DOI: 10.1007/s10509-016-2992-9. URL: https://doi.org/10.1007/s10509-016-2992-9 (cit. on p. 45).

Noble, S. C., J. H. Krolik, and J. F. Hawley (Mar. 2010). "Dependence of Inner Accretion Disk Stress on Parameters: The Schwarzschild Case". In: *ApJ* 711, pp. 959–973. DOI: 10.1088/0004-637X/711/2/959. arXiv: 1001.4809 [astro-ph.HE] (cit. on p. 128).

Novikov, I. D. and K. S. Thorne (1973). "Astrophysics of Black Holes". In: *Black Holes*. Ed. by C. DeWitt and B. S. DeWitt. New York: Gordon and Breach, pp. 343–450 (cit. on pp. 41, 45, 46, 47, 52, 129, 172, 174).

Ogilvie, G. I. (Apr. 2003). "On the dynamics of magnetorotational turbulent stresses". In: *Mon. Not. Roy. Astron. Soc.* 340, pp. 969–982. DOI: 10.1046/j.1365-8711.2003.06359.x. eprint: astro-ph/0212442 (cit. on p. 53).

Ohsuga, K., S. Mineshige, M. Mori, and Y. Kato (June 2009). "Global Radiation-Magnetohydrodynamic Simulations of Black-Hole Accretion Flow and Outflow: Unified Model of Three States". In: *Publications of the Astronomical Society of Japan* 61, pp. L7–L11. DOI: 10.1093/pasj/61.3.L7. arXiv: 0903.5364 [astro-ph.HE] (cit. on p. 53).

Ottewill, A. and E. Winstanley (2000a). "Divergence of a quantum thermal state on Kerr space-time". In: *Phys. Lett. A* 273, pp. 149–152. DOI: 10.1016/S0375-9601(00)00487-4. arXiv: gr-qc/0005108 [gr-qc] (cit. on p. 17).

Ottewill, A. and E. Winstanley (2000b). "The Renormalized stress tensor in Kerr space-time: general results". In: *Phys. Rev. D* 62, 084018. DOI: 10.1103/PhysRevD.62.084018. arXiv: gr-qc/0004022 [gr-qc] (cit. on p. 17).

Pacini, F. (July 1968). "Rotating Neutron Stars, Pulsars and Supernova Remnants". In: *Nature* 219, p. 145. URL: http://dx.doi.org/10.1038/219145a0 (cit. on p. 22).

Paczynski, B. and M. A. Abramowicz (Feb. 1982). "A model of a thick disk with equatorial accretion". In: *Astrophys. J.* 253, pp. 897–907. DOI: 10.1086/159689 (cit. on p. 41).

Paczyński, B. and P. J. Wiita (Aug. 1980). "Thick accretion disks and supercritical luminosities". In: *Astron. Astrophys.* 88, pp. 23–31 (cit. on p. 41).

Page, D. N. and K. S. Thorne (1974). "Disk-Accretion onto a Black Hole. I. Time-Averaged Structure of Accretion Disk". In: *Astrophys. J.* 191, pp. 499–506. DOI: 10.1086/152990 (cit. on pp. 41, 45, 46, 54, 173).

Pan, Z. and C. Yu (2015a). "Analytic Properties of Force-free Jets in the Kerr Spacetime – I". In: *Astrophys. J.* 812.1, p. 57. DOI: 10.1088/0004-637X/812/1/57. arXiv: 1504.04864 [astro-ph.HE] (cit. on p. 24).

Pan, Z. and C. Yu (2016). "Analytic Properties of Force-free Jets in the Kerr Spacetime – II". In: *Astrophys. J.* 816.2, p. 77. DOI: 10.3847/0004-637X/816/2/77. arXiv: 1511.07925 [astro-ph.HE] (cit. on p. 24).

Pan, Z. and C. Yu (2015b). "Fourth-order split monopole perturbation solutions to the Blandford-Znajek mechanism". In: *Phys. Rev.* D91.6, p. 064067. DOI: 10.1103/PhysRevD.91.064067. arXiv: 1503.05248 [astro-ph.HE] (cit. on p. 24).

Pan, Z., C. Yu, and L. Huang (2017). "Analytic properties of force-free jets in the Kerr spacetime – III: uniform field solution". In: *Astrophys. J.* 836.2, p. 193. DOI: 10.3847/1538-4357/aa5c36. arXiv: 1702.00513 [astro-ph.HE] (cit. on p. 24).

Papaloizou, J. and J. E. Pringle (Nov. 1977). "Tidal torques on accretion discs in close binary systems". In: *Mon. Not. Roy. Astron. Soc* 181, pp. 441–454. DOI: 10.1093/mnras/181.3.441 (cit. on p. 45).

Papapetrou, A. (1966). "Champs gravitationnels stationnaires a symetrie axiale". In: *Ann. Inst. H. Poincare Phys. Theor.* 4, pp. 83–105 (cit. on p. 102).

Peitz, J. and S. Appl (1997). "Viscous accretion discs around rotating black holes". In: *Mon. Not. Roy. Astron. Soc.* 286, p. 681. DOI: 10.1093/mnras/286.3.681. arXiv: astro-ph/9612205 [astro-ph] (cit. on pp. 44, 50, 51, 178).

Penna, R. F. (2015). "Black hole jet power from impedance matching". In: *Phys. Rev.* D92.8, p. 084017. DOI: 10.1103/PhysRevD.92.084017. arXiv: 1504.00360 [astro-ph.HE] (cit. on p. 38).

Penna, R. F. (2014a). "Black hole Meissner effect and Blandford-Znajek jets". In: *Phys. Rev.* D89.10, p. 104057. DOI: 10.1103/PhysRevD.89.104057. arXiv: 1403.0938 [astro-ph.HE] (cit. on p. 106).

Penna, R. F. (2014b). "Black hole Meissner effect and entanglement". In: *Phys. Rev.* D90.4, p. 043003. DOI: 10.1103/PhysRevD.90.043003. arXiv: 1406.2976 [hep-th] (cit. on p. 106).

Penna, R. F., R. Narayan, and A. Sadowski (2013). "General Relativistic Magnetohydrodynamic Simulations of Blandford-Znajek Jets and the Membrane Paradigm". In: *Mon. Not. Roy. Astron. Soc.* 436, p. 3741. DOI: 10.1093/mnras/stt1860. arXiv: 1307.4752 [astro-ph.HE] (cit. on p. 22).

Penna, R. F., A. Sadowski, and J. C. McKinney (2012). "Thin Disk Theory with a Non-Zero Torque Boundary Condition and Comparisons with Simulations". In: *Mon. Not. Roy. Astron. Soc.* 420, p. 684. DOI: 10.1111/j.1365-2966.2011.20084.x. arXiv: 1110.6556 [astro-ph.HE] (cit. on pp. 51, 54, 128, 130, 131, 140, 172).

Penrose, R. (1969). "Gravitational Collapse: the Role of General Relativity". In: *Nuovo Cimento Rivista Serie* 1 (cit. on p. 10).

Penrose, R. and R. M. Floyd (1971). "Extraction of rotational energy from a black hole". In: *Nature* 229, pp. 177–179 (cit. on p. 11).

Pessah, M. E., C.-k. Chan, and D. Psaltis (2006). "Local Model for Angular-Momentum Transport in Accretion Disks Driven by the Magnetorotational Instability". In: *Phys. Rev. Lett.* 97 (22), p. 221103. DOI: 10.1103/PhysRevLett.97.221103. URL: http://link.aps.org/doi/10.1103/PhysRevLett.97.221103 (cit. on p. 53).

Poisson, E. and C. Will (2014). *Gravity: Newtonian, Post-Newtonian, Relativistic*. Cambridge University Press (cit. on p. 60).

Poisson, E. (1998). "Gravitational waves from inspiraling compact binaries: The Quadrupole moment term". In: *Phys. Rev.* D57, pp. 5287–5290. DOI: 10.1103/PhysRevD.57.5287. arXiv: gr-qc/9709032 [gr-qc] (cit. on p. 61).

Porfyriadis, A. P., Y. Shi, and A. Strominger (2017). "Photon Emission Near Extreme Kerr Black Holes". In: *Phys. Rev.* D95.6, p. 064009. DOI: 10.1103/PhysRevD.95.064009. arXiv: 1607.06028 [gr-qc] (cit. on p. 15).

Porfyriadis, A. P. and A. Strominger (2014). "Gravity waves from the Kerr/CFT correspondence". In: *Phys. Rev.* D90.4, p. 044038. DOI: 10.1103/PhysRevD.90.044038. arXiv: 1401.3746 [hep-th] (cit. on p. 15).

Regge, T. and C. Teitelboim (1974). "Role of surface integrals in the Hamiltonian formulation of general relativity". In: *Ann. Phys. (N.Y.)* 88, pp. 286–318. DOI: 10.1016/0003-4916(74)90404-7 (cit. on pp. 2, 101, 113, 145, 153, 156).

Reid, M. J. et al. (2014). "A Parallax Distance to the Microquasar GRS 1915+105 and a Revised Estimate of its Black Hole Mass". In: *Astrophys. J.* 796, p. 2. DOI: 10.1088/0004-637X/796/1/2. arXiv: 1409.2453 [astro-ph.GA] (cit. on pp. 129, 136).

Reynolds, C. S. (2014). "Measuring Black Hole Spin using X-ray Reflection Spectroscopy". In: *Space Sci. Rev.* 183.1-4, pp. 277–294. DOI: 10.1007/s11214-013-0006-6. arXiv: 1302.3260 [astro-ph.HE] (cit. on pp. 1, 12).

Reynolds, C. S. and A. C. Fabian (2008). "Broad iron K-alpha emission lines as a diagnostic of black hole spin". In: *Astrophys. J.* 675, p. 1048. DOI: 10.1086/527344. arXiv: 0711.4158 [astro-ph] (cit. on p. 42).

Riffert, H. and H. Herold (1995). "Relativistic Accretion Disk Structure Revisited". In: *Astrophys. J.* 450, p. 508. DOI: 10.1086/176161 (cit. on p. 41).

Robinson, D. C. (1974). "Classification of black holes with electromagnetic fields". In: *Phys. Rev. D* 10 (2), pp. 458–460. DOI: 10.1103/PhysRevD.10.458. URL: https://link.aps.org/doi/10.1103/PhysRevD.10.458 (cit. on p. 100).

Rogatko, M. (2002). "Physical process version of the first law of thermodynamics for black holes in Einstein-Maxwell axion dilaton gravity". In: *Class. Quant. Grav.* 19, pp. 3821–3827. DOI: 10.1088/0264-9381/19/14/320. arXiv: hep-th/0207147 [hep-th] (cit. on p. 117).

Ross, J., H. N. Latter, and J. Guilet (2016). "The stress-pressure relationship in simulations of MRI-induced turbulence". In: *Mon. Not. Roy. Astron. Soc.* 455.1, pp. 526–539. DOI: 10.1093/mnras/stv2286. arXiv: 1510.01214 [astro-ph.HE] (cit. on p. 53).

Ruiz, M., C. Palenzuela, F. Galeazzi, and C. Bona (2012). "The Role of the ergosphere in the Blandford-Znajek process". In: *Mon. Not. Roy. Astron. Soc.* 423, pp. 1300–1308. DOI: 10.1111/j.1365-2966.2012.20950.x. arXiv: 1203.4125 [gr-qc] (cit. on pp. 37, 106).

Ryan, F. D. (Aug. 1997). "Accuracy of estimating the multipole moments of a massive body from the gravitational waves of a binary inspiral". In: *Phys. Rev. D.* 56, pp. 1845–1855. DOI: 10.1103/PhysRevD.56.1845 (cit. on p. 60).

Sachs, R. K. (1961). "Gravitational waves in general relativity. 6. The outgoing radiation condition". In: *Proc. Roy. Soc. Lond.* A264, pp. 309–338. DOI: 10.1098/rspa.1961.0202 (cit. on p. 68).

Sachs, R. K. (Oct. 1962). "Gravitational Waves in General Relativity. VIII. Waves in Asymptotically Flat Space-Time". In: *Proceedings of the Royal Society of London Series A* 270, pp. 103–126. DOI: 10.1098/rspa.1962.0206 (cit. on pp. 65, 145).

Sakimoto, P. J. and F. V. Coroniti (July 1981). "Accretion disk models for QSOs and active galactic nuclei - The role of magnetic viscosity". In: *Astrophys. J.* 247, pp. 19–31. DOI: 10.1086/159005 (cit. on p. 53).

Salgado, M., S. Bonazzola, E. Gourgoulhon, and P. Haensel (Nov. 1994). "High precision rotating netron star models 1: Analysis of neutron star properties". In: *Astronomy and Astrophysics* 291, pp. 155–170 (cit. on p. 61).

Sądowski, A. et al. (Aug. 2011). "Spinning up black holes with super-critical accretion flows". In: *A & A* 532, A41, A41. DOI: 10.1051/0004-6361/201116702. arXiv: 1102.2456 [astro-ph.HE] (cit. on p. 129).

Schmidt, M. (Mar. 1963). "3C 273 : A Star-Like Object with Large Red-Shift". In: *Nature* 197, pp. 1040+. DOI: 10.1038/1971040a0. URL: http://dx.doi.org/10.1038/1971040a0 (cit. on pp. 22, 40).

Seraj, A. (2016). "Multipole charge conservation and implications on electromagnetic radiation". In: arXiv: 1610.02870 [hep-th] (cit. on pp. 145, 146).

Seraj, A. and D. Van den Bleeken (2017). "Strolling along gauge theory vacua". In: *JHEP* 08, p. 127. DOI: 10.1007/JHEP08(2017)127. arXiv: 1707.00006 [hep-th] (cit. on p. 150).

Shafee, R. et al. (2006). "Estimating the spin of stellar-mass black holes via spectral fitting of the x-ray continuum". In: *Astrophys. J.* 636, pp. L113–L116. DOI: 10.1086/498938. arXiv: astro-ph/0508302 [astro-ph] (cit. on p. 41).

Shakura, N. I. and R. A. Sunyaev (June 1976). "A theory of the instability of disk accretion on to black holes and the variability of binary X-ray sources, galactic nuclei and quasars". In: *Mon. Not. Roy. Astron. Soc.* 175, pp. 613–632. DOI: 10.1093/mnras/175.3.613 (cit. on pp. 42, 141).

Shakura, N. I. and R. A. Sunyaev (1973). "Black holes in binary systems. Observational appearance". In: *Astron. Astrophys.* 24, pp. 337–355 (cit. on pp. 41, 46, 47, 53).

Shibazaki, N. and R. Hoshi (1975). "Structure and Stability of Accretion-Disk around a Black-Hole". In: *Progress of Theoretical Physics* 54.3, pp. 706–718. DOI: 10.1143/PTP.54.706. URL: http://dx.doi.org/10.1143/PTP.54.706 (cit. on pp. 42, 140).

Simon, W. and R. Beig (1983). "The multipole structure of stationary space-times". In: *Journal of Mathematical Physics* 24.5, pp. 1163–1171. DOI: 10.1063/1.525846. eprint: https://doi.org/10.1063/1.525846. URL: https://doi.org/10.1063/1.525846 (cit. on p. 60).

Strominger, A. (2013). "On BMS Invariance of Gravitational Scattering". In: arXiv: 1312.2229 [hep-th] (cit. on pp. 145, 163).

Takahashi, R. (2004). "Shapes and positions of black hole shadows in accretion disks and spin parameters of black holes". In: *J. Korean Phys. Soc.* 45. [Astrophys. J.611,996(2004)], S1808–S1812. DOI: 10.1086/422403. arXiv: astro-ph/0405099 [astro-ph] (cit. on p. 42).

Tanabe, K. and S. Nagataki (2008). "Extended monopole solution of the Blandford-Znajek mechanism: Higher order terms for a Kerr parameter". In: *Phys. Rev.* D78, p. 024004. DOI: 10.1103/PhysRevD.78.024004. arXiv: 0802.0908 [astro-ph] (cit. on p. 24).

Tchekhovskoy, A., R. Narayan, and J. C. McKinney (2011). "Efficient Generation of Jets from Magnetically Arrested Accretion on a Rapidly Spinning Black Hole". In: *Mon. Not. Roy. Astron. Soc.* 418, pp. L79–L83. DOI: 10.1111/j.1745-3933.2011.01147.x. arXiv: 1108.0412 [astro-ph.HE] (cit. on p. 22).

Thorne, K. S. (July 1974). "Disk-Accretion onto a Black Hole. II. Evolution of the Hole". In: *Astrophys. J.* 191, pp. 507–520. DOI: 10.1086/152991 (cit. on pp. 12, 129, 131, 135).

Thorne, K. S. (1980). "Multipole Expansions of Gravitational Radiation". In: *Rev. Mod. Phys.* 52, pp. 299–339. DOI: 10.1103/RevModPhys.52.299 (cit. on pp. 59, 60, 61, 63, 65, 66, 67, 68, 150, 151, 152, 154, 157, 201, 202, 203, 204, 205, 207, 208, 214).

Thorne, K. S., R. H. Price, and D. A. Macdonald, eds. (1986). *Black holes: the membrane paradigm*. ISBN: 9780300037708 (cit. on pp. 37, 38).

Török, G., Abramowicz, M. A., Klu´zniak, W., and Stuchlík, Z. (2005). "The orbital resonance model for twin peak kHz quasi periodic oscillations in microquasars". In: *Astron. Astrophys.* 436.1, pp. 1–8. DOI: 10.1051/0004-6361:20047115. URL: https://doi.org/10.1051/0004-6361:20047115 (cit. on p. 42).

Townsend, P. K. (1997). "Black holes: Lecture notes". In: arXiv: gr-qc/9707012 [gr-qc] (cit. on p. 120).

Troessaert, C. (2018). "The BMS4 algebra at spatial infinity". In: *Class. Quant. Grav.* 35.7, p. 074003. DOI: 10.1088/1361-6382/aaae22. arXiv: 1704.06223 [hep-th] (cit. on pp. 145, 163).

Uchida, T. (1997a). "Theory of force-free electromagnetic fields. I. General theory". In: *Phys. Rev. E* 56 (2), pp. 2181–2197. DOI: 10.1103/PhysRevE.56.2181. URL: https://link.aps.org/doi/10.1103/PhysRevE.56.2181 (cit. on pp. 24, 25, 27).

Uchida, T. (1997b). "Theory of force-free electromagnetic fields. II. Configuration with symmetry". In: *Phys. Rev. E* 56 (2), pp. 2198–2212. DOI: 10.1103/PhysRevE.56.2198. URL: https://link.aps.org/doi/10.1103/PhysRevE.56.2198 (cit. on pp. 24, 27, 28).

Virmani, A. (2012). "Supertranslations and Holographic Stress Tensor". In: *J. High Energy Phys.* 2012.02, 024. DOI: 10.1007/JHEP02(2012)024. arXiv: 1112.2146 [hep-th] (cit. on pp. 145, 163).

Wald, R. (1993). "Black hole entropy is Noether charge". In: *Phys. Rev.* 48, R3427–R3431. DOI: 10.1103/PhysRevD.48.R3427. arXiv: gr-qc/9307038 (cit. on pp. 144, 160).

Wald, R. M. (1974). "Black hole in a uniform magnetic field". In: *Phys. Rev.* D10, pp. 1680–1685. DOI: 10.1103/PhysRevD.10.1680 (cit. on pp. 100, 102, 124).

Wald, R. M. (1984). *General Relativity*. Chicago, USA: Chicago Univ. Pr. DOI: 10.7208/chicago/9780226870373.001.0001 (cit. on p. 29).

Wald, R. M. and A. Zoupas (2000). "A General definition of 'conserved quantities' in general relativity and other theories of gravity". In: *Phys. Rev.* D61, p. 084027.

DOI: 10.1103/PhysRevD.61.084027. arXiv: gr-qc/9911095 [gr-qc] (cit. on pp. 160, 212).

Whiting, B. F. (1989). "Mode Stability of the Kerr Black Hole". In: *J. Math. Phys.* 30, p. 1301. DOI: 10.1063/1.528308 (cit. on p. 9).

Yagi, K. and N. Yunes (2017). "Approximate Universal Relations among Tidal Parameters for Neutron Star Binaries". In: *Class. Quant. Grav.* 34.1, p. 015006. DOI: 10.1088/1361-6382/34/1/015006. arXiv: 1608.06187 [gr-qc] (cit. on p. 61).

Yagi, K., N. Yunes, and T. Tanaka (2012). "Slowly Rotating Black Holes in Dynamical Chern-Simons Gravity: Deformation Quadratic in the Spin". In: *Phys. Rev.* D86. [Erratum: Phys. Rev.D89,049902(2014)], p. 044037. DOI: 10.1103/PhysRevD.89.049902,10.1103/PhysRevD.86.044037. arXiv: 1206.6130 [gr-qc] (cit. on p. 61).

Yagi, K. et al. (2014). "Why I-Love-Q: Explaining why universality emerges in compact objects". In: *Phys. Rev.* D90.6, p. 063010. DOI: 10.1103/PhysRevD.90.063010. arXiv: 1406.7587 [gr-qc] (cit. on p. 61).

Zel'Dovich, Y. B. (Aug. 1971). "Generation of Waves by a Rotating Body". In: *ZhETF Pisma Redaktsiiu* 14, p. 270 (cit. on p. 11).

Zhang, F., H. Yang, and L. Lehner (2014). "Towards an understanding of the force-free magnetosphere of rapidly spinning black holes". In: *Phys. Rev.* D90.12, p. 124009. DOI: 10.1103/PhysRevD.90.124009. arXiv: 1409.0345 [astro-ph.HE] (cit. on pp. 15, 23, 72, 89, 183, 189, 194).

Zhang, H. et al. (2017). "Testing Einstein-dilaton-Gauss-Bonnet gravity with the reflection spectrum of accreting black holes". In: *Phys. Rev.* D95.10, p. 104043. DOI: 10.1103/PhysRevD.95.104043. arXiv: 1704.04426 [gr-qc] (cit. on p. 141).

Znajek, R. L. (1977). "Black hole electrodynamics and the Carter tetrad". In: *Monthly Notices of the Royal Astronomical Society* 179.3, pp. 457–472. DOI: 10.1093/mnras/179.3.457. URL: http://dx.doi.org/10.1093/mnras/179.3.457 (cit. on pp. 35, 37).